

ON THE OVERSTRAINING OF THICK-WALLED  
CYLINDERS UNDER INTERNAL FLUID PRESSURE  
AND UNDER INTERFERENCE FIT PRESSURE

by

MONTGOMERIE CHRISTIE STEELE

(B. Sc., M. Sc., A. R. T. C., A. M. I. Mech. E.)

THESIS

Submitted for the Degree of  
Doctor of Philosophy in Engineering  
in the  
UNIVERSITY OF GLASGOW, 1951.

ProQuest Number: 13838397

All rights reserved

INFORMATION TO ALL USERS

The quality of this reproduction is dependent upon the quality of the copy submitted.

In the unlikely event that the author did not send a complete manuscript and there are missing pages, these will be noted. Also, if material had to be removed, a note will indicate the deletion.



ProQuest 13838397

Published by ProQuest LLC (2019). Copyright of the Dissertation is held by the Author.

All rights reserved.

This work is protected against unauthorized copying under Title 17, United States Code  
Microform Edition © ProQuest LLC.

ProQuest LLC.  
789 East Eisenhower Parkway  
P.O. Box 1346  
Ann Arbor, MI 48106 – 1346

## SUMMARY

The thesis is divided into three parts. The first part presents a general and historical introduction to the subject and a critical review of previous theoretical investigations on thick-walled cylinders under internal fluid pressure and under interference fit pressure. Part II contains the author's experimental work on cylinders under internal fluid pressure. A review of previous experiments is also included. Thirdly, the author presents his theoretical and experimental work on ring and plug interference fit assemblies. This section is also preceded by a review of work performed by other experimenters in the field. Finally appendices are attached which contain information of interest to the work yet unsuitable for submission in the main body of the text.

Analytical and experimental work is restricted to ring and solid plug specimens, for which the ratio of outside diameter to bore is 2. An open-end condition and an idealised flat-topped tensile stress-strain graph are assumed in the theories. Specimens are of mild steel material.

### Part I. Introductory and General

#### 1. Explanatory and Historical

Interference fit practice is reviewed from the middle of the nineteenth century to the present day. It is shown that there is a need for fundamental research work for application to more rational design procedures. An outline is given of the course such a scheme of research should follow. A brief review follows of the extent of theoretical and experimental work on thick-walled cylinders under internal fluid pressure and under interference fit pressure.

#### 2. Features of Theory

A condensed précis of the assumptions associated with inelastic analysis is presented. The conditions to be satisfied for the solution of a thick-walled cylinder under uniform internal pressure are enunciated. A general comparison of

other thick-walled cylinder investigations is made from which three theories are selected to form the nucleus of a more detailed and critical review.

### 3. Critical Review of Thick-walled Cylinder Theories

The theories of Nadai-Steele, (Nadai's theory modified by the author) Sopwith, and MacGregor, Coffin, and Fisher form the nucleus of the review. They are all of the Total Strain type. A comparison of the stresses and strains derived from the first two theories shows the effect of neglecting the compressibility of the elastic component of strain in the plastic material. Discontinuities arise in some of the stresses and strains at the elastic-plastic boundary but the effect on the measurable quantities, bore and outside diameter circumferential strains, is not serious. Comparison of Sopwith, and MacGregor, Coffin, and Fisher shows the effect of different theories of failure, namely, the maximum shear stress and the maximum shear strain energy theories. Stresses and strains are appreciably different and experimental observations at either the bore or the outside diameter should indicate clearly which theory of failure the material is following.

The theories of Cook, Macrae, and Morrison and Shepherd are reviewed. Cook's classical treatment of the counterpart of upper and lower yield point in a tension test is discussed fully. The author derives two curves, of internal pressure against outside diameter circumferential strain, by assuming two extreme variations in the shear stress distribution across the wall of the cylinder. It is shown that Cook's experimental results lie between the curves and that considerable licence is given the theorist if he once accepts the phenomenon of upper and lower yield points to hold in the overstraining of a thick-walled cylinder. Macrae's theory is based on experimental observations. It bears little resemblance to the others, yet predicts bore and outside circumferential strains in close agreement with the more correct theory of Sopwith.

The derivation of an internal pressure-outside diameter circumferential strain curve presented by Morrison and Shepherd is discussed. Their method is shown to be suitable for closed-ended cylinders but not so accurate for open-ended ones.

#### 4. Review of Interference Fit Theories

The customary elastic analysis of interference fits based on Lame's is derived. Reference is given to charts derived by Baugher to facilitate the designer's use of Lame's theory. Rankin examined the effect of shaft extensions on the theoretical elastic interface pressure between a ring and an infinitely long shaft. The effect is negligible if the ratio ring length to shaft diameter is greater than one-half. Friction at the interface due to differential straining on cooling in shrink fitted assemblies was treated elastically by Goodier. A summary of his work is presented but no quantitative effects are obtained for a practical assembly. Frictional forces tend to increase the interface pressure and the hoop stress at the bore of the outer member.

### Part II. Thick-walled Cylinders under Internal Fluid Pressure

#### 1. Work of Previous Experimenters

The work of Macrae on open-ended cylinders of gun steel and Cook on closed-ended cylinders of mild steel is reviewed. Their apparatus, techniques, and specimen treatment are carefully examined to serve as a guide for the author's experimental work. The results of outside diameter circumferential measurements of Macrae and Cook, on 2:1 ratio cylinders, are compared with the theories of Sopwith and MacGregor, Coffin, and Fisher. Macrae's results agree well with the former theory which is based on a maximum shear stress flow condition. The type of yielding which mild steel characterises gives rise to results not wholly in agreement with Sopwith. Cook explains the discrepancies by introducing the counterpart of upper and lower yield points in a tension test.

The author concludes that it is essential to measure the actual strains existing at the bores of mild steel thick-walled cylinders in order to further examine the effects registered at the outside diameter. No published work of this nature is known to the author.

## 2. Author's Investigations

A technique is developed to measure bore strains. An apparatus is designed to apply internal pressures to "open-ended" thick-walled cylinders. In principle, a fluid is confined inside the test cylinder and compressed by means of a piston and loading machine. Test cylinders are 3 inches bore, 6 inches outside diameter, and 8 inches long. The fluid pressure extends over 93.75 % of the cylinder length.

Bore circumferential strains are recorded by specially applied electrical resistance gauges in a bakelite matrix. Outside diameter circumferential and axial strains are measured by the conventional paper-backed resistance gauges. Readings of pressure are noted on a carefully calibrated Bourdon gauge. Results are presented for bore circumferential and outside diameter circumferential and axial strains up to pressures causing the cylinder wall to be fully yielded.

## 3. Discussion of the Author's Experimental Results

It is shown that ambiguous interpretations are possible for outside diameter observations if a knowledge of the bore strain behaviour is not known. This is attributed to the characteristic wedge-shaped yielding of mild steel, which differs from the rotationally symmetric boundaries assumed by theory. The effect is to stiffen the outside diameter against deflection until a wedge region of overstrained material breaks through the outer elastic hoop.

The bore strain recordings reveal that initial yielding commences at a value of internal pressure predicted theoretically using the maximum shear stress

theory of failure. There is no evidence of an upper and lower yield point. Experiment agrees well with Sopwith's theoretical curve based on the maximum shear stress theory of failure.

There is a time effect at the high pressures which is considered to be of practical importance. Strains creep by 5 to 10 % in 15 minutes under constant pressure after yielding is well advanced into the cylinder wall. It may be serious in some members such as interference fits in which the interface pressure and hence the holding ability is dependent on the bore deflection of the scantling.

### Part III. Thick-walled Cylinders under Interference Fit Pressure

#### 1. Work of Previous Experimenters

The work of Russell and of Werth on parallel force fit assemblies of varying fit allowance is examined. It is shown that push out loads to destroy the grip bear a characteristic relationship to the fit allowance variable due to the deleterious effect of the entry forces. The author presents a new interpretation of Russell's results based on an interference fit theory using Sopwith's thick-walled cylinder analysis. It is shown that the optimum value of fit allowance is associated with considerable overstrain in the ring (54 % for the case examined) and not with an elastic theory of failure as proposed by Russell. At this optimum value of fit allowance the interface pressure is only 82.5 % of the maximum elastic interface pressure calculated by neglecting entry forces.

The work of several investigators is presented to examine the effect of variables on the coefficient of friction at the interface. Among these Russell, Werth, Association of Manufacturers of Chilled Car Wheels of America, Sawin, Baugher, and Wilmore have made contributions. There is one notable feature in all the works, namely, that there are large variations in the coefficients of friction for apparently standardised conditions. This is attributed to the

complex nature of the friction phenomenon and the difficulty of standardising operative variables.

## 2. Author's Investigations

Work is presented on theoretical and experimental analyses of shrink fit assemblies. The major variable is fit allowance. A theory is derived using Sopwith's thick-walled cylinder analysis. The latter is selected in view of the good agreement shown with experiment on mild steel cylinders under internal fluid pressure. Four theoretical graphs are constructed relating interface pressure, outside diameter circumferential strain, outside diameter residual strain, and bore residual strain to the fit allowance.

Experimental work on three independent series of specimens is presented. Two of these series have lubricated (sperm oil) mating surfaces and one series is assembled chemically dry and free from film. Measurement techniques and fitting and stripping operations are given in full. Non-dimensional plots are used in recording the strain results. This reduces the number of graphs and aids in the comparison of the different series. Results for outside diameter change on fitting and outside diameter residual change and bore residual change on dis-assembly, are recorded. In addition, axial push out loads are given and residual fit allowances computed.

## 3. Discussion of Author's Experimental Results

There are shown to be discrepancies with the interference fit theory. These are due to second order effects which are operative under certain conditions. For example, axial friction at the interface of a shrink fit assembly is operative if the members are assembled with the mating surfaces chemically dry and free from film; this effect is considered negligible, however, if the surfaces are machined and well lubricated. Approximate theories are presented

to indicate the magnitude of the axial friction effect.

An analysis is presented to allow for variations in Young's modulus and the yield shear stress with temperature. It is shown, using a curve of conservative values of these variations, that the residual strain measurements are particularly sensitive to this effect.

The axial push out load variable, on the stress and strain distributions, is discussed with reference to experimental work recorded in Appendix B. The effect is shown to be small.

Of more practical significance is the creep of bore deflections at the higher fit allowances. No actual measurement of this creep is observed in interference fits but it is shown that considerable decreases in interface pressure and alterations to the strain variables are possible for the magnitude of creep recorded in the investigations of Part II.

A comparison of Russell's work and the author's shows that the interface pressure for optimum fit allowance (i.e. the maximum interface pressure) in shrink fits is almost twice that for force fits. This is due to the more deleterious effect of the latter method of assembly.

An accurate prediction of holding ability for the lubricated specimens is hampered by the variable nature of the coefficients of friction. Little difference is shown in coefficients of friction for honed and ground mating surfaces. Four superfinished specimens, however, give comparatively low values which is in contradiction to previous beliefs. The first slip load for the "dry" specimens is much smaller than the maximum load which is obtained after a movement of from  $1/32$  to  $1/16$  inch and is governed by the ultimate shearing strength of the material.

CONTENTS

	<u>Page No.</u>
Title Page . . . . .	
Summary . . . . .	(i)
Contents . . . . .	(viii)
Acknowledgements . . . . .	(xii)
List of Symbols . . . . .	(xiii)

---

PART I. INTRODUCTORY AND GENERAL

I. <u>EXPLANATORY AND HISTORICAL</u> . . . . .	1
1. Historical Review of Interference Fit Practice	
2. Necessity for and Nature of Research Work	
3. Extent of Theoretical and Experimental Work on Thick-walled Cylinders	
4. Extent of Theoretical and Experimental Work on Interference Fit Assemblies	
II. <u>FEATURES OF THEORY</u> . . . . .	11
1. Assumptions Associated with Inelastic Analysis	
2. Conditions to be Satisfied for Theoretical Solution of the Thick-walled Cylinder	
3. General Comparison of Theoretical Investigations	
III. <u>CRITICAL REVIEW OF THICK-WALLED CYLINDER THEORIES</u> . . . . .	21
1. Analysis - Complete Solution - NADAI-STEINLE	
2. Analysis - Summary Solution - SOPWITH	
3. Analysis - Summary Solution - MACGREGOR, COFFIN, and FISHER	

4. Comparison with Respect to Compressibility - NADAI-

STEELE and SOPWITH

5. Comparison with Respect to Theory of Failure - SOPWITH

and MACGREGOR, COFFIN and FISHER

6. Analysis (Summary) and Discussion - COOK

7. Analysis (Summary) and Discussion - MACRAE

8. Analysis (Summary) and Discussion - MORRISON and

SHEPHERD

IV. REVIEW OF INTERFERENCE FIT THEORIES . . . . . 60

1. Customary Elastic Analysis Based on LAME<sup>1</sup>

2. Elastic Analysis - Shaft Protrusion - RANKIN

3. Elastic Analysis - Frictional Effect - GOODIER

V. SUMMARY OF THEORETICAL TREATMENTS . . . . . 66

1. Relating to Thick-walled Cylinders

2. Relating to Interference Fits

---

PART II. THICK-WALLED CYLINDERS UNDER INTERNAL FLUID PRESSURE

I. WORK OF PREVIOUS EXPERIMENTERS . . . . . 68

1. Experimental Techniques and Specimens - MACRAE, COOK

2. Results (MACRAE) and Discussion

3. Results (COOK) and Discussion

4. Conclusions from Work of Previous Experimenters

II. AUTHOR'S INVESTIGATIONS . . . . . 84

1. Apparatus

2. Measuring Devices

- 3. Specimens
- 4. Test Procedure
- 5. Test Results
- III. DISCUSSION OF AUTHOR'S EXPERIMENTAL RESULTS . . . . . 109
  - 1. Outside Diameter Circumferential Strains
  - 2. Bore Circumferential Strains
  - 3. Axial Strains
  - 4. Circumferential Variations in Strains
  - 5. Time Effects - Creep
- IV. CONCLUSIONS . . . . . 114
  - 1. Advantages of Measuring Bore Strains
  - 2. Inelastic Characteristics Exhibited by Mild Steel
  - 3. Creep

---

PART III. THICK-WALLED CYLINDERS UNDER INTERFERENCE FIT PRESSURE

- I. WORK OF PREVIOUS EXPERIMENTERS . . . . . 115
  - 1. The Variable Fit-allowance - RUSSELL, WERTH
  - 2. The Variable Coefficient of Friction - RUSSELL, WERTH,  
ASSOCIATION OF MANUFACTURERS OF CHILLED CAR WHEELS OF  
AMERICA, SAWIN, BAUGHER, MACGILL
  - 3. Conclusions from Work of Previous Experimenters
- II. AUTHOR'S INVESTIGATIONS . . . . . 132
  - 1. Theory
  - 2. Specimens
  - 3. Measuring Devices

- 4. Test Procedure
- 5. Experimental Results

III. DISCUSSION OF AUTHOR'S EXPERIMENTAL RESULTS . . . . . 153

- 1. Axial Friction at the Interface
- 2. Variation in Elastic Constants Due to Temperature
- 3. Axial Load Effect
- 4. Time Effect - Creep
- 5. Analysis of Strain Observations
- 6. Analysis of Axial Holding Ability of Grip

IV. CONCLUSIONS . . . . . 177

- 1. Agreement of Theory with Experiment
- 2. Author's Interpretation of Russell's Experiments
- 3. Coefficient of Friction
- 4. Maximum Interface Pressures - Shrink and Force Fits

---

APPENDICES

- A. Preliminary Investigation of Pressure Effect on Electrical Strain Gauges
- B. Effects of Axial Dis-assembly Force
- C. Quantitative Measurements of Surface Finish and Lubricant
- D. Bibliography

ACKNOWLEDGEMENTS

The majority of this work was carried out in the laboratories of the Civil and Mechanical Engineering Department of the Royal Technical College, Glasgow, under the sponsorship of the British Shipbuilding Research Association. The thick-walled cylinder investigation was completed in the Department of Theoretical and Applied Mechanics of the University of Illinois, U. S. A.

The writer wishes to express his thanks to the above named institutions for provision of working facilities; and to Professors A. S. T. Thomson, D. Sc., Ph. D., A. R. T. C., M. I. Mech. E., and A. W. Scott, B. Sc., Ph. D., A. R. T. C., M. I. Mech. E. of the Royal Technical College, and Professors F. B. Seely, M. S., and J. O. Smith, M. S. of the University of Illinois for their generous support of the researches.

List of Symbols

General

$\epsilon$	Principal strain
$\epsilon_e$	Elastic part of principal strain
$\epsilon_p$	Plastic part of principal strain
$\sigma$	Principal stress
$e$	Strain deviator
$S$	Stress deviator

N.B. Subscripts 1, 2, 3, refer to principal directions; '.' refers to derivative with respect to time.

Cylinders

Stresses and strains are as defined above with subscripts,  $\theta$ ,  $r$ , and  $z$  to denote principal directions (circumferential, radial, and axial, respectively).

$P$	Internal or interface pressure
$\sigma_e$	Yield stress in tension
$s = \sigma_e/2$	"Yield shear stress" in tension. Applies to lower value of yield shear stress when discussing upper and lower yield points.
$s'$	Upper yield shear stress in tension
$F$	Axial dis-assembly force
$F_A$	Axial friction force
$T$	Temperature; torque to destroy grip
$r_0; d$	Internal radius; diameter
$r = y r_0$	Variable radius
$r_n = n r_0$	Radius of plastic-elastic interface

$r_1 = k r_0 ; D$	Outside radius; diameter
$L$	Length of interference fit ring
$\Delta$	Total fit allowance (Mils) -- 1 Mil = 0.001 inches
$\Delta'$	Fit allowance per inch bore diameter $\frac{\text{Mils}}{\text{Ins}}$
$\delta\Delta'; \delta L_p; \delta L_R$	Small change in $\Delta'$ ; plug length; ring length
$u_o/d$	Outside diameter deflection
$u_R$	Permanent deflection of bore
$E ; G ; K$	Modulus of: - elasticity; rigidity; compressibility
$\mu$	Poisson's ratio
$\alpha$	Coefficient of linear expansion
$\bar{\mu}$	Coefficient of friction
$\beta$	Function of cylinder radius
$\varphi$	$= \frac{1}{3} \left[ \frac{\partial u}{\partial r} - \frac{u}{r} \right]$ where 'u' is extension of a radius
$a$	Sopwith's function dependent on end condition of cylinder
$W_1, W_2, W_3, W_5$	Sopwith's tabulated functions of $\left(\frac{y}{R}\right)^2$
$\lambda$ and $d\lambda$	Functions used to describe plastic flow

A few symbols are defined in the text for convenience.

PART I

INTRODUCTORY AND GENERAL

## I. EXPLANATORY AND HISTORICAL

### 1. Historical Review of Interference Fit Practice

Force and shrink fitting have an early origin. In the stone-age, wooden shafts were force fitted in the heads of primitive axe-weapons. The shrinking of an iron rim on a wooden wheel assisted in the economic maintenance of horse drawn carriages and dates back as far as the historic Roman chariots. Yet another illustration lies in the heavy iron strengthening rings shrunk on to the earliest cannons (15th century). An excellent example of this may be seen on the famous "Mons Meg" now situated in the grounds of Edinburgh castle.

These cases of interference fitting are of historic interest only, and one must proceed to the middle of the nineteenth century to find a bearing on present day problems. The steam engine was then becoming a commercial proposition and emphasis was placed on its economical manufacture. It was found to be cheaper to build-up certain large parts which previously had been forged or cast. In addition, the ease with which worn or fractured pieces could be replaced gave the fabricated component an indefinite life. The most important of these parts were undoubtedly locomotive and marine crankshafts. Owing to the size of the latter there was no alternative to fabrication and it will be convenient to refer to a marine crankshaft, when tracing variations in practice from 1850 to the present day. Progress affected other cases of interference fitting in a similar way.

It was common practice to include a key or dowel with a built up assembly which transmitted a torque. These were considered necessary should the grip loosen. The dowel served its purpose in so far as it remained in position but springing of the grip caused by driving the dowel detracted from the efficiency of the assembly.

Crankshafts failed by loosening of one of the pins in the web. Grips were strong enough to cope with normal bending and torque actions and failure was

caused, in the early stages, by the addition of abnormal bending moments. These were due to machining errors, lack of stiffness in frames and misalignment and their effects could be serious. Improvements in machining and fitting were made over years of close experience and failures were uncommon in the period just before the Great War.

The advent of the Diesel Engine introduced changes in engineering methods. Little previous experience was at the disposal of Diesel designers and the need for information on many problems was evident. One of these was the built-up crankshaft which had to be designed to suit a set of heavier load conditions from those in the steam engine. Shop methods were considered inadequate. The problem passed to qualified men in design offices. Rational treatment was not possible owing to a lack of fundamental data but the difficulties and the importance of overcoming them quickly, were now known in the correct circles. The vital need for information as to the best practice for interference fits attracted the attention of several men both in this country and in the U.S.A.

Experiments on model fit assemblies immediately following the war confirmed the belief that the holding ability of a grip could cope with normal service torques. Keys and dowels were discarded and a new emphasis was thus placed on grip quality. This alteration in practice took place 25 to 30 years ago and its inception was undoubtedly hastened by a renaissance which may be attributed to the introduction of the Diesel Engine. It was realised that fit surface finish and lubricant had a bearing on grip quality but practice varied between firms. Some firms used a rough finish with a certain shrinkage and others a smooth finish with a comparatively low fit allowance. Little attention was paid to the film condition of the surfaces.

Loosening of the grips was still the failure characteristic and the numbers tended to increase as the Diesel Engine was made larger and more powerful. The after end of a marine engine crankshaft transmits the full engine torque, and

failure of this component is a troublesome feature to the present day.

Research investigations over the past 20 years have had their effect on modern practice. These have been carried out on model rings and plugs with parallel force fits and results obtained have also been applied to the design of shrinkage assemblies. It is generally realized now that a smooth finish gives a better grip. Commercial justification can be found in the wet scrape finish used on crank pins and journal studs. Tests, using different lubricants on the fit surfaces, showed that variations of grip strength amounting to 500 % were possible. This information assists in the selection of suitable lubricants for force fits. Shrink fits, however, are always assembled "shop dry". The latter term implies the wiping of wet surfaces with a handy piece of waste, which gives rise to a lubricant film of doubtful properties. The major factor in design is the value of fit allowance. This depends on the ratio of metal thickness to bore diameter and to some extent on the shape of the scantling. Variations on the fit allowance amounting to 100 %, are common for similar jobs fabricated by different firms. For a metal thickness equal to half the bore diameter, average values are 1 and 1-1/2 mils/inch bore diameter for steam and diesel crankshaft practice, respectively.

## 2. Necessity for and Nature of Research Work

A comparison of engineering practices before and after the establishment of the Diesel Engine leads to interesting conclusions. The older design methods were based on a close experience of the performance of individual parts. In this, the shop foreman played an important role, and it is even doubtful whether the chief draughtsman held his confidence. New design methods, however, are based on the results of research plus experience and are controlled by a specially qualified staff attached to the drawing office. This is a superior arrangement from which fundamental data are correlated and applied to rational rather than empirical design.

There is a dearth of fundamental data required for the design of interference fit assemblies. It is necessary to base the design of new built-up parts on past experience which has limited application. Assemblies ultimately operate successfully, but only after a period of costly development. Previous investigations have been tests rather than research and use of information is limited by its qualitative nature. A research scheme should envisage as its ultimate aim the accumulation of data from which rational design based on quantitative information may be practised. For example, if a variable is examined, an attempt should be made to obtain a relation with an easily measured physical quantity. In some cases this is a difficult proposition.

Failure of an interference fit assembly may occur by either, slipping of the fit surfaces, or overstressing, resulting in fracture of one of the members. For rational design it is essential to possess a knowledge of (i) the initial fit stresses, (ii) the coefficient of friction of the mating surfaces, and (iii) the service loads. The effects of service loads superposed on the initial fit stresses and strains are extremely complex. These loads are frequently cyclic and the fatigue properties of the materials of the members must be considered.

A scheme of research must include: -

(i) An experimental and theoretical analysis of the stresses and strains produced by initial fitting. The variable is fit allowance. The range of values should utilise fully the strength of the outer member. This will include fit allowances which produce overstraining.

(ii) The determination of coefficients of friction. Two approaches are open. Firstly, by defining the variable qualitatively; for example, ground and machined surface finishes are considered qualitative terms. Secondly, by relation to a quantitative variable; for example, surface finish may be defined as some function of the depth of the surface microimperfections and their pitch. Instruments are available to measure these physical quantities.

The latter approach is considered fundamental. It requires a comparatively large amount of data before each variable may be correctly related to its significant group of physical quantities. The accumulation and interpretation of data from several investigations is necessary for a solution. Thus, although the individual investigation resorts to qualitative comparisons, because of lack of data, the recording of significant physical quantities will have a use when sufficient information is amassed.

The qualitative approach provides information of a more limited application. It is a policy which gives a comparatively quick solution and as such is widely commended by industry.

In some of the experimental work of this thesis qualitative comparisons are made, but related physical quantities have also been recorded in the belief, as expressed above, that a more rational basis for comparison may be finally achieved.

(iii) The effects of service loads. Little is known regarding these effects due to the difficulties of both experimental and theoretical analysis. All interference fit assemblies today have, as a basis for their design, past experience with a similar type of assembly. Occasionally significant factors are disregarded and failure of the original assemblies results. By suitable juggling with dimensions this may be overcome and the particular assembly, subject to the particular service loads, functions satisfactorily. Little information is gathered concerning the design of a new assembly which must necessarily travel the same paths of costly development.

It is apparent that the effects of service loads should be examined to cover two factors. Firstly, the resultant conditions of stress and strain existing in the assembly. It should be noted that the superposition of stresses due to a service load presents difficulties when initial interference fit stresses are high enough to cause overstrain of the outer member. Resultant deflections

at the interface may relieve the interface pressure to such an extent that loosening of the grip ensues. The second effect requiring investigation lies in the change in coefficient of friction brought about by "fretting" at the interface. For example, it is well known that marine crankshafts "breathe" under operating loads, and wear at the interface may well detract from the efficiency of the assembly.

The foregoing is regarded as three essential steps to be taken chronologically in a research investigation of interference fit assemblies. This thesis presents data pertaining to (i) and (ii). It is intended that a satisfactory basis be established to continue investigation on the more difficult problem outlined in (iii).

In the author's experimental work, specimens conform to ring and plug shapes. This simplification reduces the complexities of mathematical analysis and experimental interpretation.

Factors influencing the initial stresses and strains in interference fit assemblies include (i) fit allowance, (ii) ratio of ring outside diameter to bore ( $k$ ), (iii) ratio of length to bore ( $L/d$ ), (iv) material, (v) machining errors -- taper, out-of-roundness, (vi) position of plug relative to ring, (vii) mating surface condition -- dry, lubricated, and (viii) assembly method -- force, shrink, expansion. In the author's experimental work certain of these variables are standardized.  $k = 2$ ;  $L/d = 11/12$ ; material is mild steel -- stress-strain diagram of the form shown in Fig. 1; plug and ring are the same length. It is considered that machining errors are adequately controlled.

The major variable is fit allowance. Particular attention is directed towards overstrained assemblies. Specimens are shrink fitted and separated by axial force. Dry and lubricated surface conditions are examined.

The restriction on variables is great. It is believed, however, that the

results are fundamental and may be applied to assemblies of different dimension ratios. A modification to theory is necessary for strain hardening materials.

The correct relationship between ring bore strain and interface pressure is essential in the development of a theory for overstressed interference fit assemblies. A review of the allied subject of thick-walled cylinders under internal fluid pressure provides no information on the experimental measurement of bore strains. The approach to the interference fit problem is thus made through the medium of a fundamental investigation of mild steel (no strain hardening) thick-walled cylinders under internal fluid pressure.

### 3. Extent of Theoretical and Experimental Investigations on Thick-Walled Cylinders

A solution requires computation of all stresses and strains in terms of applied load or loads for the particular boundary conditions, which are:

- (i) Internal boundary -- uniform pressure, 'P'
- (ii) External boundary -- uniform pressure, zero
- (iii) Axial boundary -- either (a) Axial strain zero ( $\epsilon_z = 0$ )
  - (b) Closed ends ( $\int_1^k \sigma_z y dy = \frac{P}{2}$ )
  - (c) Open ends ( $\int_1^k \sigma_z y dy = 0$ )

The first two boundary conditions are common to all the theories which are reviewed in a later section. Axial boundary provides a difference. It is overcome by adapting all the theories to an open-end condition which is operative in the experimental work of Parts II and III of the thesis.

The stresses and strains in an all elastic thick-walled cylinder under internal fluid pressure are given by the well-known theory of Lamé'.<sup>(39)<sup>+</sup></sup>

<sup>+</sup> Numbers in parenthesis refer to bibliography.

Frequently, however, the applied load is so great as to cause the material immediately surrounding the bore, and for some depth into the wall to exceed the elastic limit. This results in a cylinder partly plastic and partly elastic.

A knowledge of the stresses and strains existing in such a member has immense practical significance. The design of pressure vessels for strength and gun-tubes for "dimension stabilized" bores are probably the most important. Heavy interference fit assemblies are in the same class and a necessity for the closer design of such units instigated the more basic research, under consideration in Part II of the thesis.

Theoreticians have an interest in the partly plastic thick-walled cylinder since the plastic strains are comparable in magnitude to the elastic ones. Earlier theories, viz. those of Nadai,<sup>(29)</sup> Cook<sup>(9)</sup> and Macrae<sup>(25)</sup> neglected this fact, and their solutions, are not rigorously correct. Recently the thick-walled cylinder was used to compare the plastic flow theories of Prandtl-Reuss and Hencky.<sup>(17)</sup>

A theoretical review of work published by the many investigators is hampered by inconsistencies in the axial boundary condition chosen. For instance, there is no solution to the writer's knowledge of the cylinder with open ends, making use of the Prandtl-Reuss plastic stress-strain law. There is, however, a solution for zero axial strain, which is a condition not found in practice. Nadai also uses an end restraint to give zero axial strain, whereas Sopwith,<sup>(41)</sup> and Macgregor, Coffin, and Fisher<sup>(24)</sup> revert to the more practical open or closed ended cylinders.

In reviewing past theories, a policy is adopted of narrowing down the range of work. This is necessitated by the large amount of computation involved in effecting a comparison using a standard set of conditions. Thus, although a theory is presented incorporating say Nadai's basic assumptions, an alteration in boundary conditions and/or theory of failure would make the theory one not

compatible with the original. A new title to the theory is then given combining the names of the originator and the modifier.

It is found from a close study of the various approaches that three theories may be effectively used to illustrate two of the basic differences, viz. compressibility of the plastic material and flow condition. The particular set of conditions chosen for this purpose are: -

- (1) Open - ends
- (2) 2 : 1 ratio of outside diameter to bore (k)
- (3) Material exhibiting no strain-hardening in the strain ranges considered.

Previous experimental work is limited to a measurement of outside diameter strains (circumferential and axial). Overstrain initiates at and propagates from the bore. Theories have been checked from measurements recorded at a region remote from these highly stressed layers and there is some doubt as to the validity of conclusions concerning their strain behaviour. This is especially true of mild steel cylinders which yield in such a way that theories based on a homogeneous material structure have doubtful application. It is considered essential to measure the actual strains occurring at the bore of overstrained thick-walled cylinders.

#### 4. Extent of Theoretical and Experimental Work on Interference Fit Assemblies

A review of previous investigations is intended primarily to serve as a guide in the design and interpretation of the fundamental theoretical and experimental work of the thesis. Consequently, it is restricted to investigations which bear a direct interest to that phase of the problem under consideration.

Previous theoretical analyses are restricted to elastic treatments. The most common, due to Lamé',<sup>(39)</sup> is briefly reviewed. Rankin<sup>(51)</sup> applied the methods of the theory of elasticity to investigate the effects of a short ring shrunk on to a relatively long shaft. His results provide useful information.

Goodier, <sup>(14)</sup> also by the theory of elasticity, examined the frictional effects in shrink fits. A brief review is of interest to the experimental section on shrink fits.

Russell's <sup>(33)</sup> classical experiments on parallel force fits are analysed in detail. His claim that overstraining of the outer member provides no additional holding ability is refuted on the basis of a theoretical analysis which is presented in Part III of the thesis.

The results of several isolated investigations are grouped and reviewed to establish qualitatively the effects of significant variables on the apparent coefficient of friction. It is found that little constructive criticism is possible here, and the review reduces to a presentation of facts.

## II. FEATURES OF THEORY

### 1. Assumptions Associated with Inelastic Analysis

There are certain conventional assumptions associated with inelastic analysis which can be used in the development of equations to replace the elastic stress-strain relationships.

(i) Total Strain = elastic strain + plastic strain.

$$\epsilon = \epsilon_e + \epsilon_p \quad \text{----- (1)}$$

In some problems in plasticity, the plastic strains are large compared to the elastic ones and the latter may be ignored with little effect on the accuracy of the theory. In thick-walled cylinders this simplification is not true and both elastic and plastic strains should be accounted for.

(ii) Compressibility of Inelastic Material is due to Elastic Component of Strain Only.

$$\epsilon_1 + \epsilon_2 + \epsilon_3 = \frac{1 - 2\mu}{E} (\sigma_1 + \sigma_2 + \sigma_3) \quad \text{----- (2)}$$

This is sometimes stated in the form:

$$(\epsilon_p)_1 + (\epsilon_p)_2 + (\epsilon_p)_3 = 0 \quad \text{----- (3)}$$

which means that the plastic components of strain do not contribute to volume change.

If the elastic component of strain is ignored then the material is said to be incompressible. If it is included the inelastic material is compressible according to Eq. 2. As previously stated, neglect of this compressibility is only possible where plastic strains are large compared to elastic ones.

(iii) Plastic Stress-Strain Laws

Three laws are used to replace the well-known Hooke's law associated with elastic theory. They were developed by St. Venant, Hencky and Reuss.<sup>(15)</sup> St. Venant does not allow for elastic strains and hence his law may be discarded in

this thesis. Dr. Reuss crystallised previous work on the subject by Prandtl and their law is generally referred to under the dual name Prandtl-Reuss. Their law is essentially that of St. Venant with elastic strains included.

(a) Hencky Stress-Strain Law

This law connects stress with strain and in its original form was stated as: -

$$(\text{Strain deviator tensor}) = \frac{1 + \lambda}{2G} \cdot (\text{Stress deviator tensor}) \quad \text{----- (4)}$$

where ' $\lambda$ ' is some function of the rate of deformation.

Which means: -

$$S_1 : S_2 : S_3 = e_1 : e_2 : e_3$$

$$\text{or } \frac{S_1}{e_1} = \frac{S_2}{e_2} = \frac{S_3}{e_3} \quad \text{----- (5)}$$

Consider,  $\frac{S_1}{e_1} = \frac{S_2}{e_2}$  or  $\frac{S_1 - S_2}{S_2} = \frac{e_1 - e_2}{e_2}$

$$\frac{S_2}{e_2} = \frac{S_1 - S_2}{e_1 - e_2} = \frac{\sigma_1 - \sigma - \sigma_2 + \sigma}{\epsilon_1 - \epsilon - \epsilon_2 + \epsilon} = \frac{\sigma_1 - \sigma_2}{\epsilon_1 - \epsilon_2}$$

Hence Eq. 5 reduces to: -

$$\frac{\sigma_1 - \sigma_2}{\epsilon_1 - \epsilon_2} = \frac{\sigma_2 - \sigma_3}{\epsilon_2 - \epsilon_3} = \frac{\sigma_3 - \sigma_1}{\epsilon_3 - \epsilon_1} \quad \text{----- (6)}$$

Eq. 6 expresses mathematically the common plasticity relationship used in the "Total Strain" or "Deformation" type of theory.

(b) Prandtl-Reuss Stress-Strain Law

This law connects stress with velocity strain rather than with strain as in the latter case. In its original form it was stated as: -

$$\dot{\epsilon}_1 - \dot{\epsilon} = \frac{1}{2G} (\dot{\sigma}_1 - \dot{\sigma}) + \lambda(\sigma_1 - \sigma) \quad \text{----- (7)}$$

+ 2 similar eqs.

where  $\lambda$  is a function of the rate of deformation.

It has been shown by Hill, Lee and Tupper<sup>(16)</sup> that use of the time derivative in the above equation is an unnecessary restriction and it is more usual to associate the derivatives with a characteristic parameter of plastic flow. In the thick cylinder case this is usually 'n', the radius of the plastic ring.

Thus Eq. 7 may be rewritten: -

$$2G \frac{\partial e_1}{\partial n} = \frac{\partial S_1}{\partial n} + \lambda S_1 \quad \text{----- (8)}$$

+ 2 similar eqs.

This is the equation used by Hodge and White<sup>(17)</sup> of Brown University, U.S.A.

An inspection of Eqs. 7 and 8 indicates that the first and second terms of the right hand sides are proportional to the elastic and plastic strains respectively. If the plastic component only is considered it is seen that: -

$$\frac{\partial(e_p)_1}{S_1} = \frac{\partial(e_p)_2}{S_2} = \frac{\partial(e_p)_3}{S_3} \quad \text{----- (9)}$$

which reduces as in the Hencky Stress-Strain law to: -

$$\frac{d(\epsilon_1 - \epsilon_2)_p}{\sigma_1 - \sigma_2} = \frac{d(\epsilon_2 - \epsilon_3)_p}{\sigma_2 - \sigma_3} = \frac{d(\epsilon_3 - \epsilon_1)_p}{\sigma_3 - \sigma_1} \quad \text{--- (10)}$$

This is the law used by Hill, Lee and Tupper,<sup>(16)</sup> who claim that it has an experimental basis established by Taylor and Quinney. It is associated with the "Incremental Strain" or "Flow" theory.

If the elastic component of Eq. 8 is similarly treated and added to Eq. 10 it can be shown that from Prandtl-Reuss's law: -

$$\frac{d(\epsilon_1 - \epsilon_2)}{\sigma_1 - \sigma_2} = \frac{d(\epsilon_2 - \epsilon_3)}{\sigma_2 - \sigma_3} = \frac{d(\epsilon_3 - \epsilon_1)}{\sigma_3 - \sigma_1} \quad \text{----- (11)}$$

Sopwith<sup>(41)</sup> pointed out that if the ratios of the principal stresses were constant, then

$$\frac{d(\epsilon_1 - \epsilon_2)}{d(\epsilon_2 - \epsilon_3)} = \frac{(\epsilon_1 - \epsilon_2)}{(\epsilon_2 - \epsilon_3)}$$

Hence, Eq. 11 may be rewritten: -

$$\frac{\epsilon_1 - \epsilon_2}{\sigma_1 - \sigma_2} = \frac{\epsilon_2 - \epsilon_3}{\sigma_2 - \sigma_3} = \frac{\epsilon_3 - \epsilon_1}{\sigma_3 - \sigma_1} \quad \text{which is the same as the Hencky}$$

law.

It has been shown by Taylor<sup>(41)</sup> that where the ratios of the principal stresses are not constant as in the case of the thick cylinders, the adoption of the Hencky hypothesis implies the assumption that the instantaneous state of stress determines the instantaneous state of total strain and not as it should be of incremental strain.

Eqs. 1, 2, and 6 are each seen to satisfy equations of the type: -

$$\begin{aligned} E \epsilon_1 &= \sigma_1 - \mu (\sigma_2 + \sigma_3) + \lambda \left[ \sigma_1 - \frac{1}{2} (\sigma_2 + \sigma_3) \right] \\ E \epsilon_2 &= \sigma_2 - \mu (\sigma_3 + \sigma_1) + \lambda \left[ \sigma_2 - \frac{1}{2} (\sigma_3 + \sigma_1) \right] \quad \text{----- (12)} \\ E \epsilon_3 &= \sigma_3 - \mu (\sigma_1 + \sigma_2) + \lambda \left[ \sigma_3 - \frac{1}{2} (\sigma_1 + \sigma_2) \right] \end{aligned}$$

Eqs. 1, 2, and 10 are each seen to satisfy equations of the type: -

$$\begin{aligned} E d\epsilon_1 &= d\sigma_1 - \mu d(\sigma_2 + \sigma_3) + d\lambda \left[ \sigma_1 - \frac{1}{2} (\sigma_2 + \sigma_3) \right] \\ E d\epsilon_2 &= d\sigma_2 - \mu d(\sigma_3 + \sigma_1) + d\lambda \left[ \sigma_2 - \frac{1}{2} (\sigma_3 + \sigma_1) \right] \quad \text{---- (13)} \\ E d\epsilon_3 &= d\sigma_3 - \mu d(\sigma_1 + \sigma_2) + d\lambda \left[ \sigma_3 - \frac{1}{2} (\sigma_1 + \sigma_2) \right] \end{aligned}$$

$\lambda$  and  $d\lambda$  are equal 0, for no plastic flow.

$\lambda$  is a function of the radius for any stage in the progression of plastic flow.

Eqs. 12 or 13 replace the corresponding elastic equations deduced from Hooke's law.

#### (iv) Flow Conditions - No Strain Hardening

The stresses in the plastic domain are further governed by a flow condition. When a certain function of the stresses reaches a maximum as determined from a simple laboratory test (usually a tension test), inelastic action occurs

and the limiting value of the function is maintained in the inelastic region. These functions are usually referred to as "Theories of Failure", and the two of interest in this work are the Maximum Shear Stress, and Maximum Distortion Energy theories. The latter is often called after its originator Von Mises, the former after Tresca.

Mathematically, these may be stated as: -

$$(\sigma_1 - \sigma_3) = 2s \quad \text{----- (14)}$$

where  $(\sigma_1 - \sigma_3)$  is the greatest numerical stress difference and 's' is the shear stress at yield in a tension test;

$$\text{and } (\sigma_1 - \sigma_2)^2 + (\sigma_2 - \sigma_3)^2 + (\sigma_3 - \sigma_1)^2 = 2\sigma_e^2, \quad \text{----- (15)}$$

where  $\sigma_e = \text{Yield in tension} = 2s$ .

## 2. Conditions to be Satisfied for Theoretical Solution of the Thick-Walled Cylinder

The following conditions should be fulfilled for a solution of the thick-walled cylinder problem.

### (i) Stress Equilibrium

$$\sigma_\theta = \frac{\partial}{\partial y} \cdot (y\sigma_r) \quad \text{----- (16)}$$

### (ii) Strain Compatibility

The mathematical formulation of the condition for strain compatibility may be obtained from the expressions for hoop and radial strain, viz.

$$\epsilon_r = \frac{\partial u}{\partial r} \quad \text{and} \quad \epsilon_\theta = \frac{u}{r} \quad \text{----- (17)}$$

Hence,

$$\epsilon_r = \frac{\partial}{\partial r} (\epsilon_\theta \cdot r)$$

$$\text{or, } \epsilon_r = \frac{\partial}{\partial y} (y \cdot \epsilon_\theta) \quad \text{----- (18)}$$

### (iii) Boundary Conditions

$$\sigma_r = -P \quad \text{when} \quad y = 1$$

$$\sigma_r = 0 \quad \text{when} \quad y = k.$$

Either (a)  $\epsilon_z = 0$

or (b)  $\int_1^k \sigma_z y dy = 0$ , (open-ended cylinder) ----- (19)

or (c)  $\int_1^k \sigma_z y dy = \frac{P}{2}$ , (closed-ended cylinder).

(iv) Plane Sections to remain plane

This condition is satisfied if the cylinder is sufficiently long compared to its diameter and means that,

$$\epsilon_z = \text{constant} \quad \text{-----} \quad (20)$$

(v) All strains to be continuous across elastic-plastic interface

If the stress-strain diagram from a tension test of the material is continuous then the above condition can be extended to the stresses also.

(vi) The Plastic Stress-Strain Relations

Either 
$$\frac{\epsilon_\theta - \epsilon_r}{\sigma_\theta - \sigma_r} = \frac{\epsilon_r - \epsilon_z}{\sigma_r - \sigma_z} = \frac{\epsilon_z - \epsilon_\theta}{\sigma_z - \sigma_\theta} \quad \text{-----} \quad (21)$$

or 
$$\frac{d(\epsilon_\theta - \epsilon_r)}{\sigma_\theta - \sigma_r} = \frac{d(\epsilon_r - \epsilon_z)}{\sigma_r - \sigma_z} = \frac{d(\epsilon_z - \epsilon_\theta)}{\sigma_z - \sigma_\theta} \quad \text{-----} \quad (22)$$

(vii) Compressibility of plastic material

Either  $\epsilon_\theta + \epsilon_r + \epsilon_z = 0$ , (incompressible) ----- (23)

or  $\epsilon_\theta + \epsilon_r + \epsilon_z = \frac{1-2\mu}{E} (\sigma_\theta + \sigma_r + \sigma_z)$ , (compressible) ---- (24)

(viii) Criterion of plastic flow for the material of the cylinder

No positive statement can be made regarding the correct criterion but in this thesis the maximum shear stress and distortion energy theories will be used exclusively. Use is made of either,

$$(\sigma_\theta - \sigma_r) = 2s \quad \text{-----} \quad (25)$$

$$\text{or } (\sigma_{\theta} - \sigma_r)^2 + (\sigma_{\theta} - \sigma_z)^2 + (\sigma_r - \sigma_z)^2 = 2 \sigma_e^2 \quad \text{--- (26)}$$

### 3. General Comparison of Theoretical Investigations

Table I lists the investigators and relative differences of seven thick-walled cylinder theories. It can be seen from the variety of conditions that a straight forward comparison of the results of these investigations would merely disguise the individual effects. For example in order to compare the work of Nadai (No. 1 in the table) to the work of most of the others, it is convenient to change the flow law and axial boundary to the Tresca hypothesis and open ends respectively. This will be apparent later and as the solutions and the majority of the work is different from that given by Nadai, the theory will be referred to under the joint name of Nadai-Steele.

It is well known that solutions Nos. 6 and 7 are the most rigorously correct. Use of the Tresca hypothesis in (6) and zero axial strain in both of them, considerably simplifies the mathematics. Even so, a numerical method requiring much time, is necessary for a solution. Introduction of the open end condition along with Von Mises' flow law complicates the equations and to the writer's knowledge is not solved. The open-ended cylinder is more common in practice and is a condition adopted in the experimental work of this thesis. A theoretical investigation was made, therefore, to examine the practicability of a solution combining the Prandtl-Reuss law, compressibility, Von Mises' flow condition and open ends. It requires the solution of the following four simultaneous partial differential equations: -

$$\frac{\partial e}{\partial r} - \frac{\partial \varphi}{\partial r} = \frac{2\varphi}{r} \quad \text{----- (a)}$$

No.	Investigator	Plastic Stress-Strain Law	$\Sigma$ Princ. Strains	Flow Condition	Axial Condition	Bibliography Ref. No.
1	Nadai	Hencky	0	Von Mises	$\epsilon_z = 0$	29
2	Cook	Hencky	0	Tresca	Dependent on experiment measurements on closed-ended cylinders	9
3	Macrae	Indeterminate	Indeterminate	Tresca	Open and Closed ends	25
4	Sopwith	Hencky	$\frac{1-2\mu}{E}(\sigma_\theta + \sigma_r + \sigma_z)$	Tresca	Open and Closed ends	41
5	Macgregor, Coffin and Fisher	Hencky	$\frac{(1-2\mu)}{E}(\sigma_\theta + \sigma_r + \sigma_z)$	Von Mises	Open-ends	24
6	Hill, Lee, and Tupper	Prandtl-Reuss	$\frac{(1-2\mu)}{E}(\sigma_\theta + \sigma_r + \sigma_z)$	Tresca	$\epsilon_z = 0$	16
7	Hodge and White	Prandtl-Reuss and Hencky	$\frac{(1-2\mu)}{E}(\sigma_\theta + \sigma_r + \sigma_z)$	Von Mises	$\epsilon_z = 0$	17

TABLE I. Variations in Basic Assumptions Used by Previous Thick-walled Cylinder Investigators.

$$\begin{aligned} \frac{\partial S_r}{\partial r_n} + \frac{\partial e}{\partial r_n} \left[ \frac{G}{4K^2} \left\{ 3S_r \sqrt{4K^2 - 3S_r^2} - 4K^2 + 3S_r^2 \right\} \right] \\ - \frac{\partial \varphi}{\partial r_n} \left[ \frac{3G}{4K^2} \left\{ S_r \sqrt{4K^2 - 3S_r^2} + 4K^2 - 3S_r^2 \right\} \right] \\ - \frac{\partial \epsilon_z}{\partial r_n} \left[ \frac{G}{2K^2} \left\{ 2S_r \sqrt{4K^2 - 3S_r^2} - 4K^2 + 3S_r^2 \right\} \right] = 0 \quad \text{--- (b)} \end{aligned}$$

$$\frac{\partial S_r}{\partial r} + 3K \frac{\partial e}{\partial r} = \frac{-3}{2} S_r + \frac{1}{2} \sqrt{4K^2 - 3S_r^2} \quad \text{----- (c)}$$

$$\begin{aligned} \frac{(r_1^2 - r_n^2)}{2} \left[ E \epsilon_z + \frac{2\mu C E \epsilon_z}{\left( c^2 - \frac{3r_1^2}{4} \right) r_n} + \frac{2\mu}{\left( c^2 - \frac{3r_1^2}{4} \right) r_n} \right] \\ \sqrt{3K^2 c^2 + 3E^2 \epsilon_z^2 \frac{r_1^4}{r_n^4} - \frac{9K^2 r_1^4}{r_n^4}} = \int_{r_0}^{r_n} \left( \frac{1}{2} S_r \right. \\ \left. + \frac{1}{2} \sqrt{4K^2 - 3S_r^2} - 3K e \right) r dr \quad \text{----- (d)} \end{aligned}$$

where  $e$ ,  $\varphi$ ,  $S_r$ ,  $\epsilon_z$  are dependent variables defined in nomenclature, and ' $r$ ', ' $r_n$ ' are independent variables.

It is possible that Eq. (d) could be simplified by an assumption based on experimental observation. There would still remain a gigantic task in establishing finite difference equations for a solution. Hodge and White's equations are the same as the first three with  $\epsilon_z$  put to 0. This excludes the whole expression beginning  $\frac{\partial \epsilon_z}{\partial r_n}$ . The derivation of Eqs. a, b, c, and d follows the steps employed by Hodge and White <sup>(17)</sup> in their solution for  $\epsilon_z = 0$ . It is also noted that integration takes place with respect to two variables and hence all previous elastic-plastic states must be considered. This, of course, is not a disadvantage when a complete solution for a range of pressures is desired.

Hodge and White compared solutions in which the stress-strain laws of Hencky and Prandtl-Reuss were used and all other conditions standardized. (See

Table I, No. (7).) Their results show for the particular problem chosen -- plane strain with rotational symmetry -- that no measurable differences exist when graphical plots of stress and strain are made. It is reasonable to deduce that the conclusion should be extended to open-ended cylinders. It is decided, therefore, to avoid the more correct incremental strain law in favor of the deformation or Hencky law.

### III. CRITICAL REVIEW OF THICK-WALLED CYLINDER THEORIES

The effect of (a) compressibility and (b) theory of failure are examined for the following standard set of conditions: -

- (i) Hencky Stress-Strain law.
- (ii) No strain-hardening in the plastic range. Tensile test graph for material is of the form shown in Fig. 1.
- (iii) Open-ends.
- (iv)  $k = 2$ .
- (v) Stress distributions across wall of cylinder plotted for  $n = 1.5$ , i.e. plastic flow half-way through wall.

The examination is made by reference to three theories viz. (a) Nadai-Steele, (b) Sepwith, (c) MacGregor, Coffin and Fisher. The first one may be deduced from the more general theory given by Cook in reference 9, but differences in the derivation of the equations warrant its presentation in full.

#### 1. Analysis - Complete Solution - NADAI-STEELE

Theory is based on,

$$\epsilon_{\theta} + \epsilon_r + \epsilon_z = 0 \quad (\text{Incompressibility}) \quad \text{-----} \quad (27)$$

$$\frac{\epsilon_{\theta} - \epsilon_r}{\sigma_{\theta} - \sigma_r} = \frac{\epsilon_r - \epsilon_z}{\sigma_r - \sigma_z} = \frac{\epsilon_z - \epsilon_{\theta}}{\sigma_z - \sigma_{\theta}} = 3\beta \quad \text{-----} \quad (28)$$

(Hencky Plastic Stress-Strain Law)

where  $\beta$  is a function of radius only for a given stage in the plastic flow.

$$\sigma_{\theta} - \sigma_r = 2s \quad (\text{Tresca shear hypothesis}) \quad \text{-----} \quad (29)$$

The elastic outer shell and plastic inner core (see Fig. 2) will be considered separately and boundary conditions chosen to satisfy the whole cylinder.

In the elastic domain ( $n < y < k$ ), the well-known theory of Lamé<sup>1</sup>, gives: -

$$\sigma_r = A + \frac{B}{y^2}$$

and

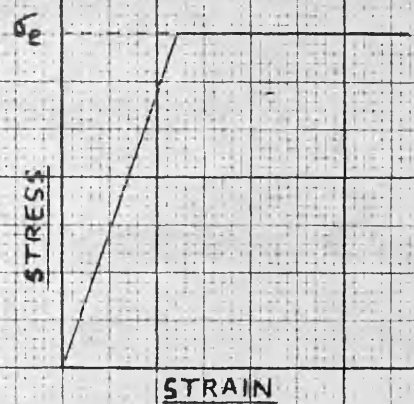


FIG. 1 - IDEALISED TENSILE STRESS-STRAIN DIAGRAM.

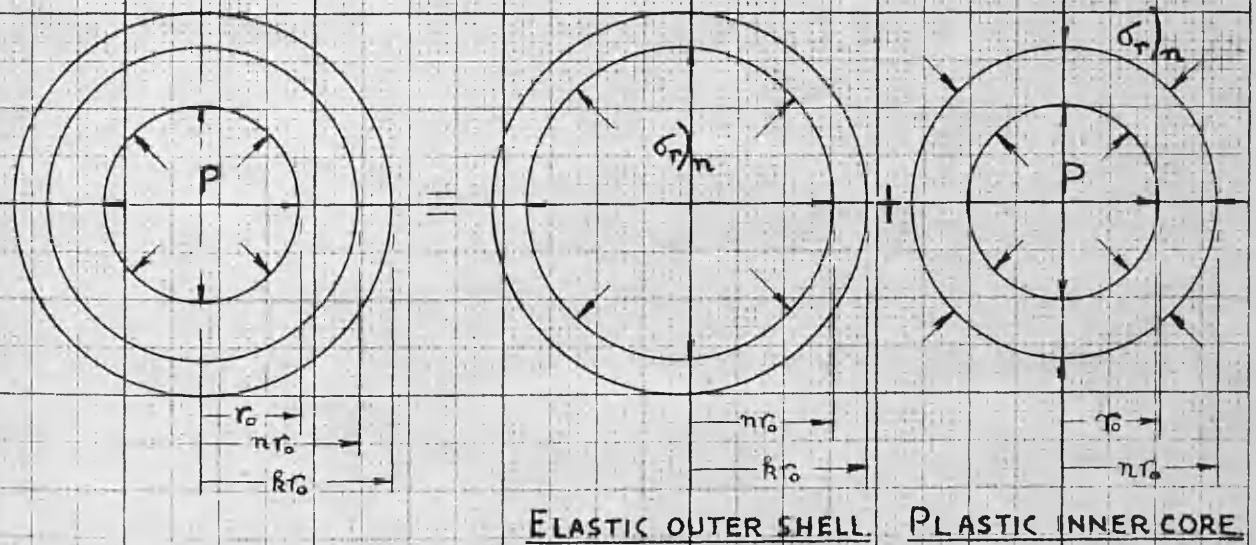


FIG. 2 - ELASTIC AND PLASTIC DOMAINS IN AN OVERSTRAINED CYLINDER.

$$\sigma_{\theta} = A - \frac{B}{y^2} \quad \text{----- (30)}$$

In the plastic domain ( $1 < y < n$ ),

$$y \frac{\partial \sigma_r}{\partial y} = \sigma_{\theta} - \sigma_r = 2s \quad (\text{From Eqs. 16 and 25}).$$

Hence,

$$\begin{aligned} \sigma_r &= 2s \log y + C, \\ \sigma_{\theta} &= 2s \log y + 2s + C \end{aligned} \quad \text{----- (31)}$$

Constants A, B, and C are obtained from the boundary conditions: -

- (i)  $\sigma_r = 0$  at  $y = k$ ,
- (ii)  $\sigma_r$  continuous at elastic-plastic boundary,
- (iii)  $\sigma_{\theta}$  continuous at elastic-plastic boundary,

and equations become: -

Elastic Domain ( $n < y < k$ )

$$\sigma_r = \frac{n^2 s}{k^2} - \frac{n^2 s}{y^2} \quad \text{----- (32)}$$

$$\sigma_{\theta} = \frac{n^2 s}{y^2} + \frac{n^2 s}{y^2}$$

Plastic Domain ( $1 < y < n$ )

$$\sigma_r = s \left[ \log \left( \frac{y}{n} \right)^2 - \frac{(k^2 - n^2)}{k^2} \right] \quad \text{----- (33)}$$

$$\sigma_{\theta} = s \left[ \log \left( \frac{y}{n} \right)^2 + \frac{(k^2 + n^2)}{k^2} \right]$$

Putting  $\sigma_r = -P$  at  $y = 1$  gives the internal pressure as a function of 'n',

$$P = s \left[ \log n^2 + \frac{(k^2 - n^2)}{k^2} \right] \quad \text{----- (34)}$$

It should be observed at this stage that in the development of the above equations, constant maximum shear stress in the plastic range, is the only assumption involving the nature of plastic flow. The derivation of expressions for  $\sigma_r$  and the principal strains in the plastic domain introduces the other conditions associated with inelastic action. The following holds for the region  $1 < y < n$ .

From Eqs. (27) and (28)

$$\epsilon_{\theta} = 3\beta s - \epsilon_z/2$$

$$\epsilon_r = -3\beta s - \epsilon_z/2$$

and substituting for  $\epsilon_{\theta}$  and  $\epsilon_r$  in compatibility Eq. (18),

$$\frac{d\beta}{\beta} = -2 \frac{dy}{y} \quad \text{is obtained.}$$

and on integration,

$$\log \beta = -2 \log y + C.$$

The value of  $\beta$  at  $y = n$  determines  $C$ .

At  $y = n$ ,

$$\beta = \frac{1}{3} \frac{(\epsilon_{\theta} - \epsilon_r)}{(\sigma_{\theta} - \sigma_r)} = \frac{1}{3} \frac{\frac{1}{E} (1 + \mu) (\sigma_{\theta} - \sigma_r)}{(\sigma_{\theta} - \sigma_r)} = \frac{1 + \mu}{3E}$$

Hence

$$\beta = \frac{(1 + \mu)}{3E} \cdot \frac{n^2}{y^2} \quad \text{----- (35)}$$

and

$$\epsilon_{\theta} = \frac{(1 + \mu)}{E} \cdot s \frac{n^2}{y^2} - \epsilon_z/2 \quad \text{----- (36)}$$

$$\epsilon_r = \frac{-(1 + \mu)}{E} \cdot s \frac{n^2}{y^2} - \epsilon_z/2 \quad \text{----- (37)}$$

From (28), 
$$\sigma_z = \frac{\epsilon_z}{3\beta} - \frac{\epsilon_{\theta}}{3\beta} + \sigma_{\theta}$$

and on substitution for  $\epsilon_{\theta}$  and  $\sigma_{\theta}$  from (36) and (33) respectively,

$$\sigma_z = \frac{3Ey^2}{2(1 + \mu)n^2} \cdot \epsilon_z + s \left[ \log \left( \frac{y}{n} \right)^2 + \frac{n^2}{k^2} \right] \quad \text{----- (38)}$$

Eq. (38) gives  $\sigma_z$  in terms of  $\epsilon_z$ , and  $\epsilon_z$  is determined by applying the axial boundary conditions. The appropriate one (open ends) from Eq. 19 is

$$\int_1^k \sigma_z y dy = 0$$

$$\text{or } \int_1^n \sigma_z y dy + \int_n^k \sigma_z y dy = 0$$

(Plastic Domain) (Elastic Domain)

$\sigma_z$  in the elastic domain may also be expressed in terms of  $\epsilon_z$ , according to the usual elastic equations.

$$\sigma_z = E \epsilon_z + \frac{2 \mu n^2 s}{k^2} \quad \text{----- (39)}$$

The axial strain is, of course, constant across the whole wall. (Plane sections remain plane.)

$$\int_1^n \left[ \frac{3E}{2(1+\mu)} \frac{y^2}{n^2} \epsilon_z + s \left\{ \log \left( \frac{y}{n} \right)^2 + \frac{n^2}{y^2} \right\} \right] y dy$$

$$+ \int_n^k \left[ E \epsilon_z + \frac{2 \mu n^2 s}{k^2} \right] y dy = 0.$$

From which,

$$\epsilon_z = \frac{-s \left[ \frac{(k^2 - n^2)}{k^2} \{ 2 \mu n^2 - n^2 + 1 \} + \log n^2 \right]}{E \left[ \frac{3}{4} \frac{(n^4 - 1)}{(1 + \mu)n^2} + k^2 - n^2 \right]} \quad \text{----- (40)}$$

It is seen that the solution could be used for closed-ended cylinders on inserting the appropriate condition from Eq. 19.

From the above analysis, stresses and strains at all radii in the cylinder may be calculated for any stage in the plastic flow from,  $1 < n < k$ . The strains of most interest are those at the bore and the outside diameter. Expression for bore strain is found from Eq. 36 by putting  $y = 1$  and inserting the value of  $\epsilon_z$  from Eq. 40. Outside diametral strain is obtained by insertion of the correct values of  $\sigma_\theta$  and  $\sigma_z$  in the elastic equation.

$$\epsilon_{\theta \text{ o/d}} = \frac{1}{E} \left[ \sigma_{\theta \text{ o/d}} - \mu \sigma_z \text{ o/d} \right]$$

Summarizing, the pertinent equations are: -

ELASTIC DOMAIN ( $n < y < k$ )

$$\sigma_r = \frac{n^2 s}{k^2} - \frac{n^2 s}{y^2}$$

$$\sigma_\theta = \frac{n^2 s}{k^2} + \frac{n^2 s}{y^2}$$

$$\sigma_z = E \epsilon_z + \frac{2 \mu n^2 s}{k^2}$$

$$\epsilon_{\theta} \text{ o/d} = \frac{s}{E} \left[ \frac{2n^2}{k^2} (1 - \mu^2) - \mu \cdot \frac{E \epsilon_z}{s} \right] \quad \text{--- (41)}$$

PLASTIC DOMAIN ( $1 < y < n$ )

$$\sigma_r = s \left[ \log \left( \frac{y}{n} \right)^2 - \frac{(k^2 - n^2)}{k^2} \right]$$

$$\sigma_\theta = s \left[ \log \left( \frac{y}{n} \right)^2 + \frac{(k^2 + n^2)}{k^2} \right]$$

$$\sigma_z = \frac{3 E \epsilon_z}{2 (1 + \mu) n^2} \cdot y^2 + s \left[ \log \left( \frac{y}{n} \right)^2 + \frac{n^2}{k^2} \right]$$

$$\epsilon_{\theta} \text{ bore} = \frac{s}{E} \left[ (1 + \mu) n^2 - \frac{1}{2} \frac{E \epsilon_z}{s} \right] \quad \text{----- (42)}$$

where  $\epsilon_z$  = constant for any value of 'n', and given by,

$$\epsilon_z = - \frac{s}{E} \left[ \frac{\frac{(k^2 - n^2)}{k^2} \{ 2 \mu n^2 - n^2 + 1 \} + \log n^2}{\frac{3}{4} \frac{(n^4 - 1)}{(1 + \mu) n^2} + k^2 - n^2} \right]$$

2. Analysis - Summary Solution - SOPWITH

Sopwith's theory differs from the previous one, only in that the material in the plastic domain is compressible according to the equation,

$$\epsilon_\theta + \epsilon_r + \epsilon_z = \frac{(1 - 2\mu)}{E} (\sigma_\theta + \sigma_r + \sigma_z).$$

This condition, although more exact, introduces a complexity into the

analysis. A simple differential equation in ' $\beta$ ' and ' $y$ ' may not be derived. If an attempt is made to find ' $\beta$ ' in the same way as the previous solution, a differential equation of the following form results: -

$$\frac{d\beta}{dy} + \frac{C\beta^3 + F_1(y)\beta^2 + F_2(y)\beta + F_3(y)}{F_4(y)\beta^2 + F_5(y)\beta + F_6(y)} = 0.$$

Most of the functions of ' $y$ ' contain natural logarithms. The solution to such an equation would be a lengthy procedure, involving numerical methods.

Sopwith's theory consists of close approximations and devices, to utilize the complex results obtained from an equation similar to the one above. By suitable substitutions at an early stage in his theory, he reduces complexities to a minimum. The differential equation he solves is in closed form and contains hyperbolic tangents. To present expressions for stresses and strains in a reasonably simple form, functions of the variables ' $y$ ' and ' $n$ ' are introduced. Tables giving the values of these functions for particular radii and stage in the plastic flow are given in reference 41. A complete derivation of this theory may also be found in this reference.

Sopwith's pertinent equations are, in the terminology of this thesis: -

ELASTIC DOMAIN ( $n < y < k$ )

$$\sigma_r = \frac{n^2 s}{k^2} - \frac{n^2 s}{y^2}$$

$$\sigma_\theta = \frac{n^2 s}{k^2} + \frac{n^2 s}{y^2}$$

$$\sigma_z = E \epsilon_z + \frac{2 \mu n^2 s}{k^2}$$

$$\epsilon_\theta \text{ o/d} = \frac{s}{E} \left[ (1 - 2\mu) \left\{ \frac{n^2}{k^2} + 2\mu a \right\} + \frac{(1 + \mu) n^2}{k^2} \right] \quad \text{---- (43)}$$

PLASTIC DOMAIN ( $1 < y < n$ )

$$\sigma_r = s \left[ \log \left( \frac{y}{n} \right)^2 - \frac{(k^2 - n^2)}{k^2} \right]$$

$$\sigma_\theta = s \left[ \log \left( \frac{y}{n} \right)^2 + \frac{(k^2 + n^2)}{k^2} \right]$$

$$\sigma_z = s \left[ \frac{n^2}{k^2} - 2 W_2 - 2 a W_3 \right] \quad \text{----- (44)}$$

$$\epsilon_{\theta \text{ bore}} = \frac{s}{E} \cdot (1 - 2\mu) \left[ \frac{n^2}{k^2} + W_5 + a W_1 \right] \quad \text{----- (45)}$$

and  $\epsilon_z = \text{constant}$  for any value of 'n', and given by,

$$\epsilon_z = \frac{s}{E} \left[ (1 - 2\mu) \frac{n^2}{k^2} - 2 (1 - 2\mu) a \right] \quad \text{----- (46)}$$

N.B. Functions of 'W' are tabulated for particular values of 'y' and 'n'. In the expression for  $\epsilon_{\theta \text{ bore}}$ , for example, the correct values for 'W<sub>1</sub>' and 'W<sub>5</sub>' and also 'a' pertaining to specific 'y' and 'n' variables, must be inserted.

The above equations give the stresses and strains at all radii of the cylinder for any stage in the progression of plastic flow. Speed of computation for plotting graphs depends on the amount of interpolation necessary in using the tables of functions. Values of functions of 'N', which are functions of 'W' (see reference), not given in the tables, were found using 3-point Lagrangian interpolation, for the particular selection of parameters chosen here. Linear interpolation sufficed for odd values of the 'W' functions.

Sopwith's solution is more complex than Nadai-Steele's. It has been simplified, however, by using the Tresca hypothesis in the plastic domain.

### 3. Analysis - Summary Solution - MACGREGOR, COFFIN, and FISHER.

MacGregor, Coffin and Fisher have given a solution in which the distortion-energy theory of failure is used instead of the maximum shear theory as in the

previous article. This is the only important difference from (2). The basic assumptions are recapitulated: -

$$\epsilon_{\theta} + \epsilon_r + \epsilon_z = \frac{(1 - 2\mu)}{E} (\sigma_{\theta} + \sigma_r + \sigma_z)$$

$$\frac{\epsilon_{\theta} - \epsilon_r}{\sigma_{\theta} - \sigma_r} = \frac{\epsilon_r - \epsilon_z}{\sigma_r - \sigma_z} = \frac{\epsilon_z - \epsilon_{\theta}}{\sigma_z - \sigma_{\theta}}$$

$$(\sigma_{\theta} - \sigma_r)^2 + (\sigma_r - \sigma_z)^2 + (\sigma_z - \sigma_{\theta})^2 = 2\sigma_0^2.$$

The mathematical procedure utilizes a numerical calculation by successive approximations, using Lagrangian integration.

One other assumption is used in the general theory to make use of an arbitrary stress-strain curve. This may be stated in the form: -

"There is a unique relationship between the effective stress and the effective strain." These terms are defined mathematically as: -

$$\sigma = \frac{\sqrt{2}}{2} \sqrt{(\sigma_{\theta} - \sigma_r)^2 + (\sigma_r - \sigma_z)^2 + (\sigma_z - \sigma_{\theta})^2}$$

and,

$$\epsilon = \frac{\sqrt{2}}{3} \sqrt{(\epsilon_{\theta} - \epsilon_r)^2 + (\epsilon_r - \epsilon_z)^2 + (\epsilon_z - \epsilon_{\theta})^2}$$

The stress definition is, of course, a statement of the distortion-energy expression.

Experience indicates that for a given material and values of ' $\epsilon$ ' less than about 0.2, the plot of ' $\sigma$ ' versus ' $\epsilon$ ' is independent of the nature of the deformation. For such values of ' $\epsilon$ ', the relationship between ' $\sigma$ ' and ' $\epsilon$ ' can therefore be determined from a tension test, and will hold for all possible states of combined stress producing plastic flow. Assumption assumes the relationship,  $\sigma = f(\epsilon)$  as determined from a tension test, to hold also for the plastic deformation of a thick-walled cylinder.

A detailed treatment of this theory may be found in reference 24. The

derived equations are complex and must be solved simultaneously. In the following form, they may be solved for any boundary condition and for any arbitrary stress-strain curve: -

$$\begin{aligned} \sigma_r' &= \sigma_\theta - \sigma_r \\ \sigma_\theta' &= \frac{[(w_1 - w_2) a_z^2 + w_1 a_r a_\theta] \varphi_2 + (w_2^2 - w_1^2) \varphi_1}{(\text{Den})} \cdot (\sigma_\theta - \sigma_r) \\ \sigma_z' &= \frac{(a_r - a_\theta) (a_z w_1 + a_\theta w_2) \varphi_2 \cdot (\sigma_\theta - \sigma_r)}{(\text{Den})} \quad \text{----- (47)} \\ \lambda' &= \frac{(w_1^2 - w_2^2) (a_\theta - a_r) \varphi_2}{(\text{Den})} \cdot (\sigma_\theta - \sigma_r) \end{aligned}$$

Where (Den) = - [(a\_\theta^2 + a\_z^2) w\_1 + 2 a\_\theta a\_z w\_2] \varphi\_2 + (w\_1^2 - w\_2^2) \varphi\_1

$$\varphi_1 = \frac{4m}{9} (w_1 + w_2) (a_r^2 + a_\theta^2 + a_z^2)$$

$$\varphi_2 = \frac{4m}{9} (w_1 + w_2)^2 - 1$$

$$m = \frac{1}{E^2} \cdot \frac{\sigma}{\epsilon} \cdot \frac{d\sigma}{d\epsilon}$$

$$w_1 = 1 + \lambda$$

$$w_2 = \mu + \lambda/2$$

$$a_r = \sigma_r - \frac{1}{2} (\sigma_\theta + \sigma_z)$$

$$a_\theta = \sigma_\theta - \frac{1}{2} (\sigma_z + \sigma_r)$$

$$a_z = \sigma_z - \frac{1}{2} (\sigma_r + \sigma_\theta)$$

The (') refers to derivative with respect to a variable, x = log\_e \frac{\gamma}{n} .

The particular conditions associated with this review may now be inserted for the solution of these equations. The idealized stress-strain relationship shown in Fig. 1 is used and it can readily be shown that: -

(i) For elastic region

$$\sigma = \frac{3E}{2(1+\mu)} \cdot \epsilon$$

and (ii) For plastic region

$$m = \frac{1}{E^2} \cdot \frac{\sigma}{\epsilon} \cdot \frac{d\sigma}{d\epsilon} = 0 \quad (\text{Since plastic portion of curve is horizontal})$$

Hence in elastic domain

$$\sigma_r' = \sigma_\theta - \sigma_r$$

$$\sigma_\theta' = -(\sigma_\theta - \sigma_r)$$

$$\sigma_z' = 0$$

$$\lambda' = 0$$

which integrate directly into the well-known Lamé' equations, on changing the variable 'x' to the variable 'r', viz: -

$$\sigma_r = A - \frac{B}{r^2}$$

$$\sigma_\theta = A + \frac{B}{r^2}$$

----- (48)

$$\sigma_z = \text{const.}$$

In the plastic domain, equations reduce to: -

$$\sigma_r' = \sigma_\theta - \sigma_r$$

$$\sigma_\theta' = \frac{(w_2 - w_1) a_z^2 - w_1 a_r a_\theta}{(\text{Den})} \cdot (\sigma_\theta - \sigma_r)$$

$$\sigma_z' = \frac{(a_\theta - a_r) (a_z w_1 + a_\theta w_2)}{(\text{Den})} \cdot (\sigma_\theta - \sigma_r)$$

$$\lambda' = \frac{(w_2^2 - w_1^2) (a_\theta - a_r)}{(\text{Den})} \cdot (\sigma_\theta - \sigma_r)$$

where  $(\text{Den}) = (a_\theta^2 + a_z^2) w_1 + 2a_\theta a_z w_2$

and  $w_1$ ,  $w_2$ ,  $a_r$ ,  $a_\theta$ , and  $a_z$  are as defined before.

This system of equations can be solved numerically for  $\sigma_r$ ,  $\sigma_\theta$ ,  $\sigma_z$  and  $\lambda$  as functions of  $x = \log_e \frac{y}{n}$ .

The boundary conditions to be satisfied by the solution for the stresses in the plastic region are: -

(i)  $\lambda = 0$  at  $x = 0$  (i.e. at  $r = r_n$ )

(ii)  $\sigma_r$ ,  $\sigma_\theta$ , and  $\sigma_z$  in the plastic region at  $x = 0$

are equal to the corresponding stresses in the elastic portion of the cylinder at  $x = 0$ , the plastic-elastic boundary. Here also  $\sigma$  must equal  $\sigma_e$ .

(iii) End load on tube =  $2 \pi r_o^2 \int_1^k \sigma_z y dy = 0$ .

Tables of  $\frac{\sigma_r}{\sigma_e}$ ,  $\frac{\sigma_\theta}{\sigma_e}$ ,  $\frac{\sigma_z}{\sigma_e}$  and  $\lambda$  were computed by MacGregor for various values of  $k$ ,  $k/n$  and  $x = \log_e \frac{y}{n}$ . These are listed in a United States Naval Report.<sup>(43)</sup>

The computations involved in preparing these tables are considerable.

The stresses in the elastic region of partially yielded tubes have not been tabulated, as they are easily derivable from the state of stress at plastic-elastic boundary. Solving for constants A, B, and C of Eq. 48, the following solutions are found: -

$$\frac{\sigma_r}{\sigma_e} = \frac{1}{2} \left[ \frac{\sigma_r}{\sigma_e} \frac{n}{n} + \frac{\sigma_\theta}{\sigma_e} \frac{n}{n} \right] \left\{ 1 - \left( \frac{k}{y} \right)^2 \right\}$$

$$\frac{\sigma_\theta}{\sigma_e} = \frac{1}{2} \left[ \frac{\sigma_r}{\sigma_e} \frac{n}{n} + \frac{\sigma_\theta}{\sigma_e} \frac{n}{n} \right] \left\{ 1 + \left( \frac{k}{y} \right)^2 \right\}$$

$$\frac{\sigma_z}{\sigma_e} = \frac{\sigma_z}{\sigma_e} \frac{n}{n}$$

Where a value of 'x' or 'k/n' for a particular 'k' is not listed in the tables, Lagrangian Interpolation formula must be used. Three-point is sufficient when

interpolating with respect to 'x', but five-point is necessary for interpolation with respect to 'k/n'. In the graphs prepared for comparison purposes a value of 'n' making plastic flow half-way through the wall is selected. This gives a ratio of  $k/n = 1.3333$ , which is not given in the tables. Plotting of the graphs is therefore a laborious procedure.

Figs. 3-7 shows plots, for the three theories, of: -

- (i)  $\sigma_r/s$  versus radius for configuration  $n = 1.5$
- (ii)  $\sigma_\theta/s$  versus radius for configuration  $n = 1.5$
- (iii)  $\sigma_z/s$  versus radius for configuration  $n = 1.5$
- (iv)  $P/s$  versus  $\frac{E \epsilon_\theta}{s} \frac{o/d}{s}$  from values of  $P/s$  rising from zero to fully plastic.
- (v)  $P/s$  versus  $\frac{E \epsilon_\theta}{s} \frac{\text{bore}}{s}$  from values of  $P/s$  rising from zero to fully plastic, respectively.

#### 4. Comparison with Respect to Compressibility - NADAI-STEELE and SOPWITH

The theories of Nadai-Steele and Sopwith are used to compare the effect of neglecting compressibility of the plastic material. Figs. 3-5 inclusive show plots of the stresses existing in a partially plastic thick-walled tube, when plastic flow is assumed to have progressed half-way through the wall.

Fig. 3 and 4 indicate that there is no difference between both the radial and hoop stresses. They are, of course, plotted from the same equations, and they are independent of the effect of compressibility. It should be noted that this is only the case when the maximum shear stress condition is used, since the equilibrium equation can be integrated directly. If a theory of failure incorporating all three principal stresses is supposed, the radial and hoop stresses would not be independent of the compressibility effect, at least, for open-ended cylinders.

A study of Fig. 5 illustrates one of the main issues arising out of the

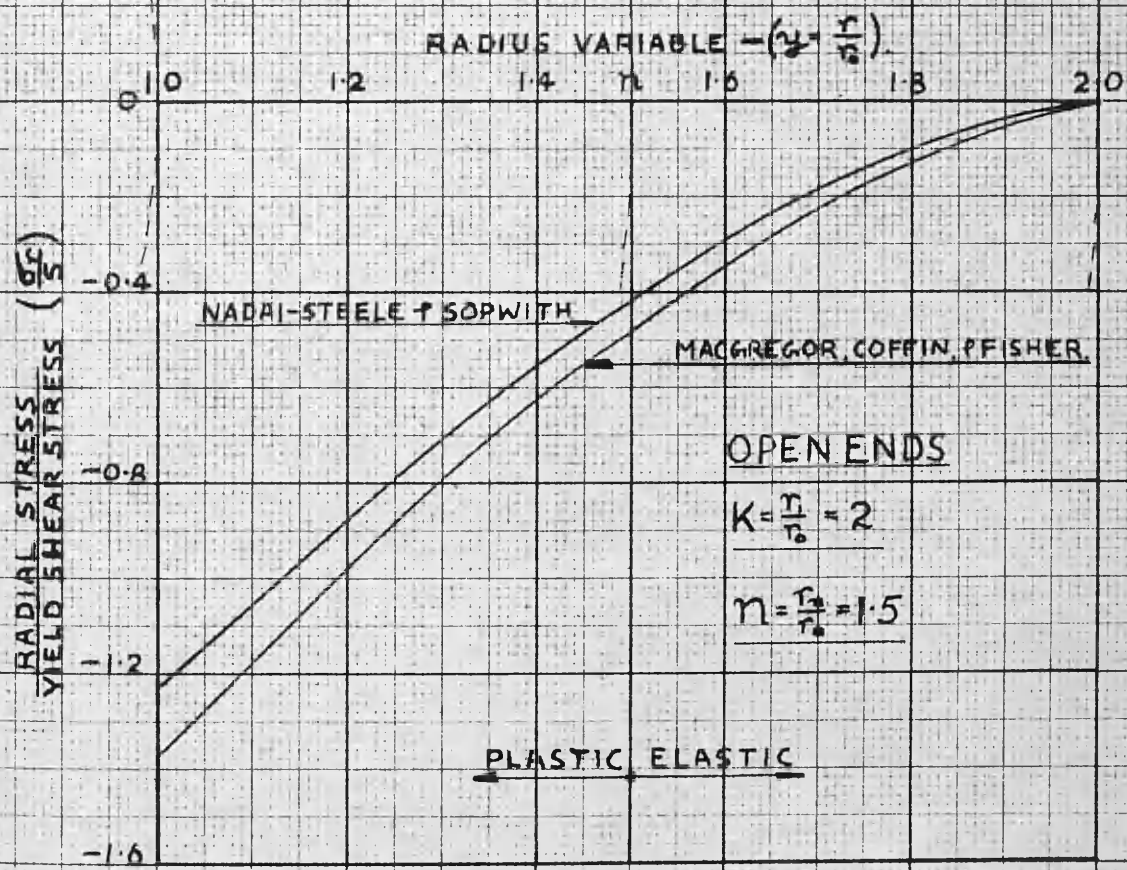


FIG. 3- RADIAL STRESS DISTRIBUTIONS IN A PARTIALLY OVERSTRAINED CYLINDER ACCORDING TO:-

- (i) NADAI- STEELE.
- (ii) SOPWITH,
- (iii) MACGREGOR, COFFIN, & FISHER.

NO. 34 20 BYZEBEN GRAPH PAPER 20 X 20 PER INCH

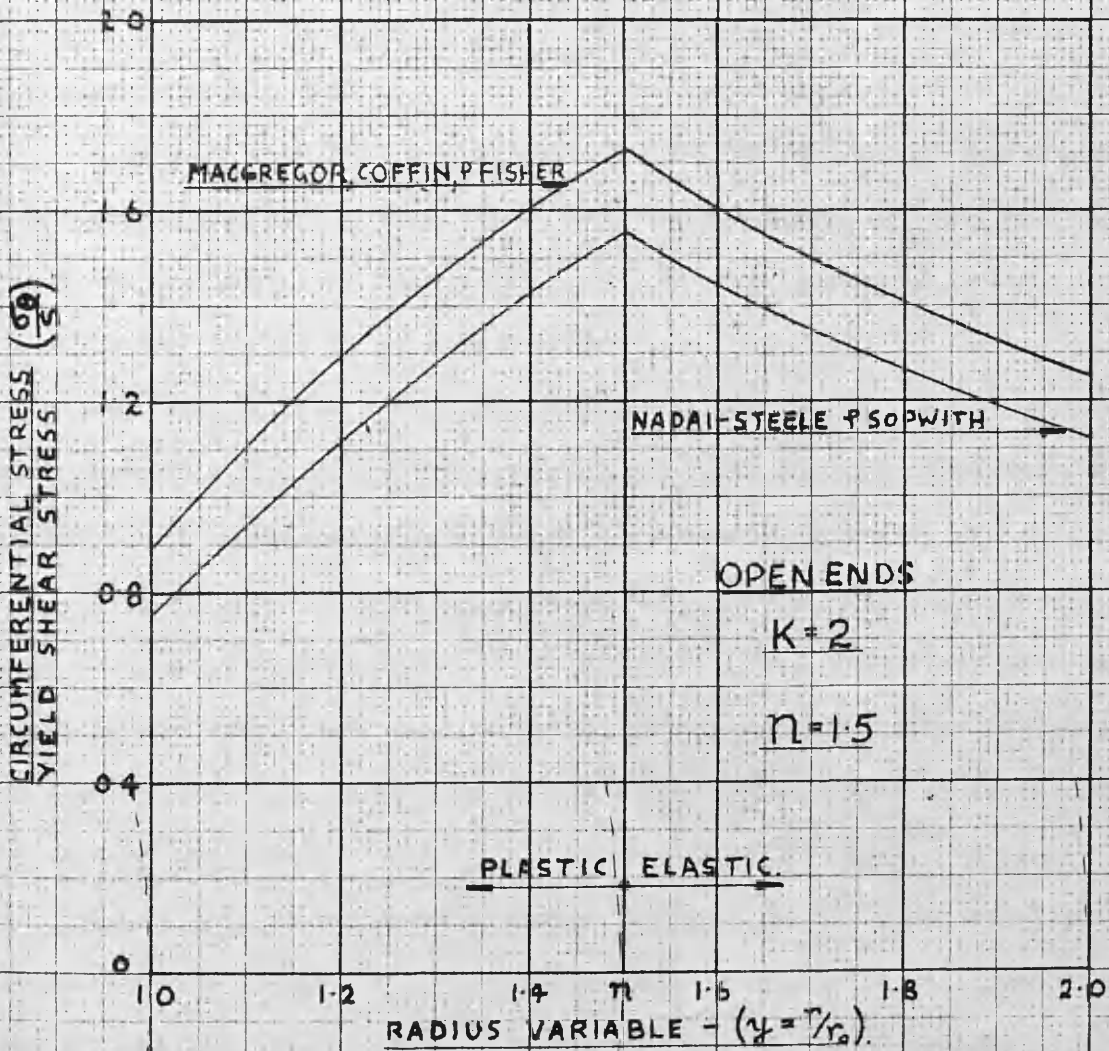


FIG. 4-CIRCUMFERENTIAL STRESS DISTRIBUTIONS IN A PARTIALLY OVERSTRAINED CYLINDER ACCORDING TO:-  
 (i) NADAI-STEEL,  
 (ii) SOPWITH  
 (iii) MACGREGOR, COFFIN, & FISHER.

comparison. A condition exists at the plastic-elastic boundary, for Nadai-Steels's theory, in which  $\epsilon_{\theta} + \epsilon_r + \epsilon_z = 0$  is satisfied on the plastic side and  $\epsilon_{\theta} + \epsilon_r + \epsilon_z = \frac{(1 - 2\nu)}{E} (\sigma_{\theta} + \sigma_r + \sigma_z)$  on the elastic. The result of making both of these conditions valid is the discontinuity in  $\sigma_z$ . Sopwith's curve does not show such a deviation since the value of the sum of the three principal strains is the same in both regions.

It is seen from Fig. 6 that plots of internal pressure against outside diametral strain are almost identical. This would suggest that any differences occurring in the plastic domain due to the varying assumption produce little effect on the changes in outside diameters.

Measurable difference in the changes of internal diameter, however, is apparent -- see Fig. 7. It is accentuated by a discontinuity at the end of the elastic curve in Nadai-Steels's theory, due to the assumption of incompressibility.

It is of interest that experimental work on thick cylinders has been confined to outside surface measurements and theoretical deductions made as to the bore behavior under load. The preceding curves serve to emphasize the necessity for experimental measurements at the bore where the effects of overstrain may be more accurately gauged.

Theoretical reasoning establishes inclusion of the compressibility of the material in the plastic domain. In so doing, however, the solution is made more complex, and some doubt arises as to whether the increased complexity is warranted by the small differences in result. It may be that a design procedure could be based on the simpler approach, but a comparison of this type is a necessary preliminary to such a step.

##### 5. Comparison with Respect to Theory of Failure - SOPWITH and MACGREGOR, COFFIN and FISHER

This comparison differs from the previous one in that either the Tresca or

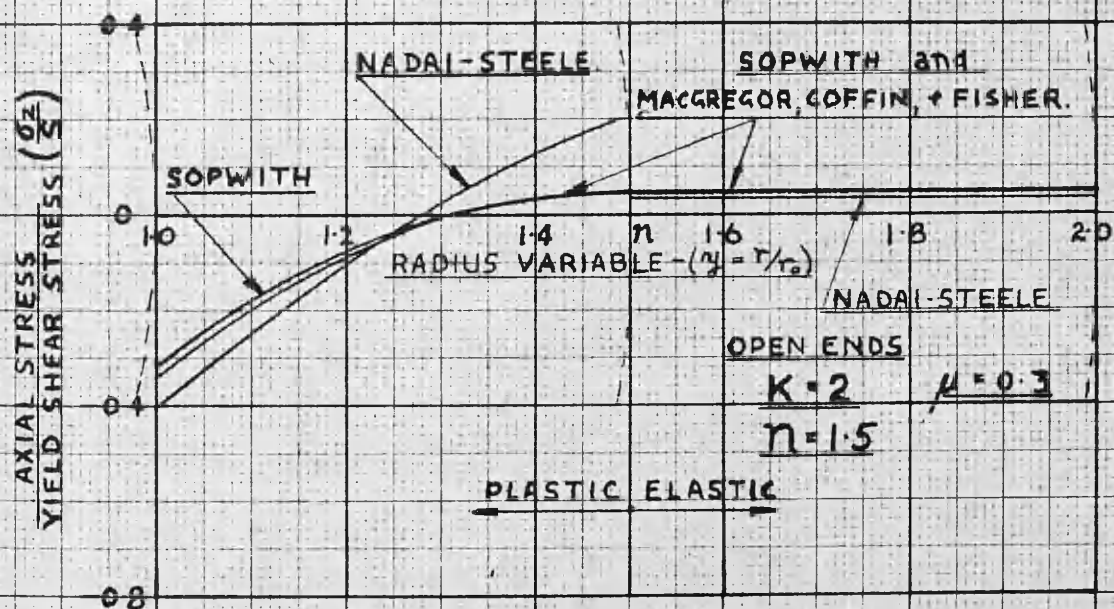


FIG. 5 - AXIAL STRESS DISTRIBUTIONS IN A PARTIALLY OVERSTRAINED CYLINDER ACCORDING TO:-

- (i) NADAI-STEEL,
- (ii) SOPWITH,
- (iii) MACGREGOR, COFFIN, & FISHER.

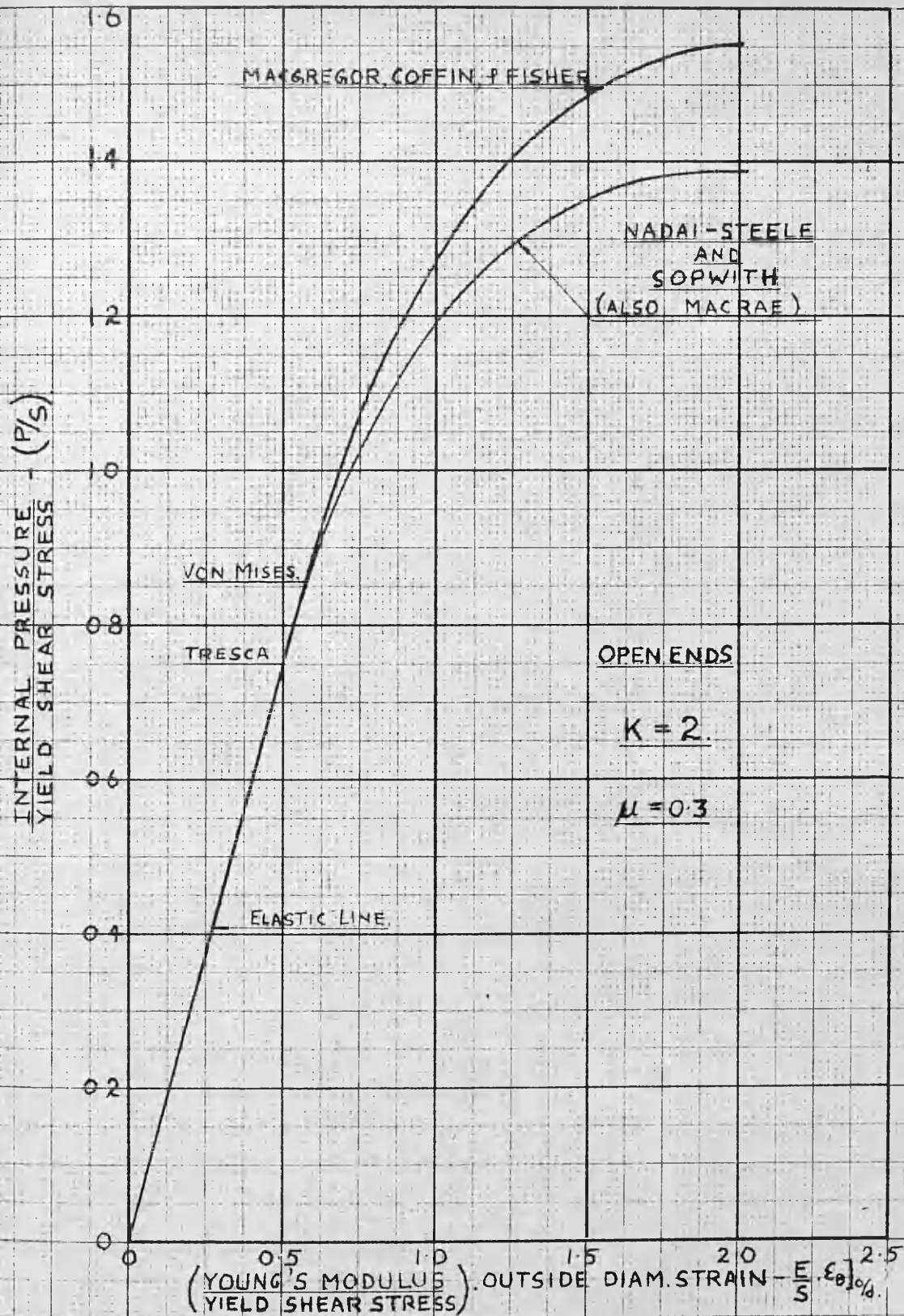


FIG. 6 - OUTSIDE DIAMETRAL STRAINS, UP TO FULLY PLASTIC CONDITION, ( $n=2$ ), IN A PARTIALLY OVERSTRAINED CYLINDER, ACCORDING TO:-

- (i) NADAI-STEEL
- (ii) SOPWITH
- (iii) MACGREGOR, COFFIN, & FISHER.

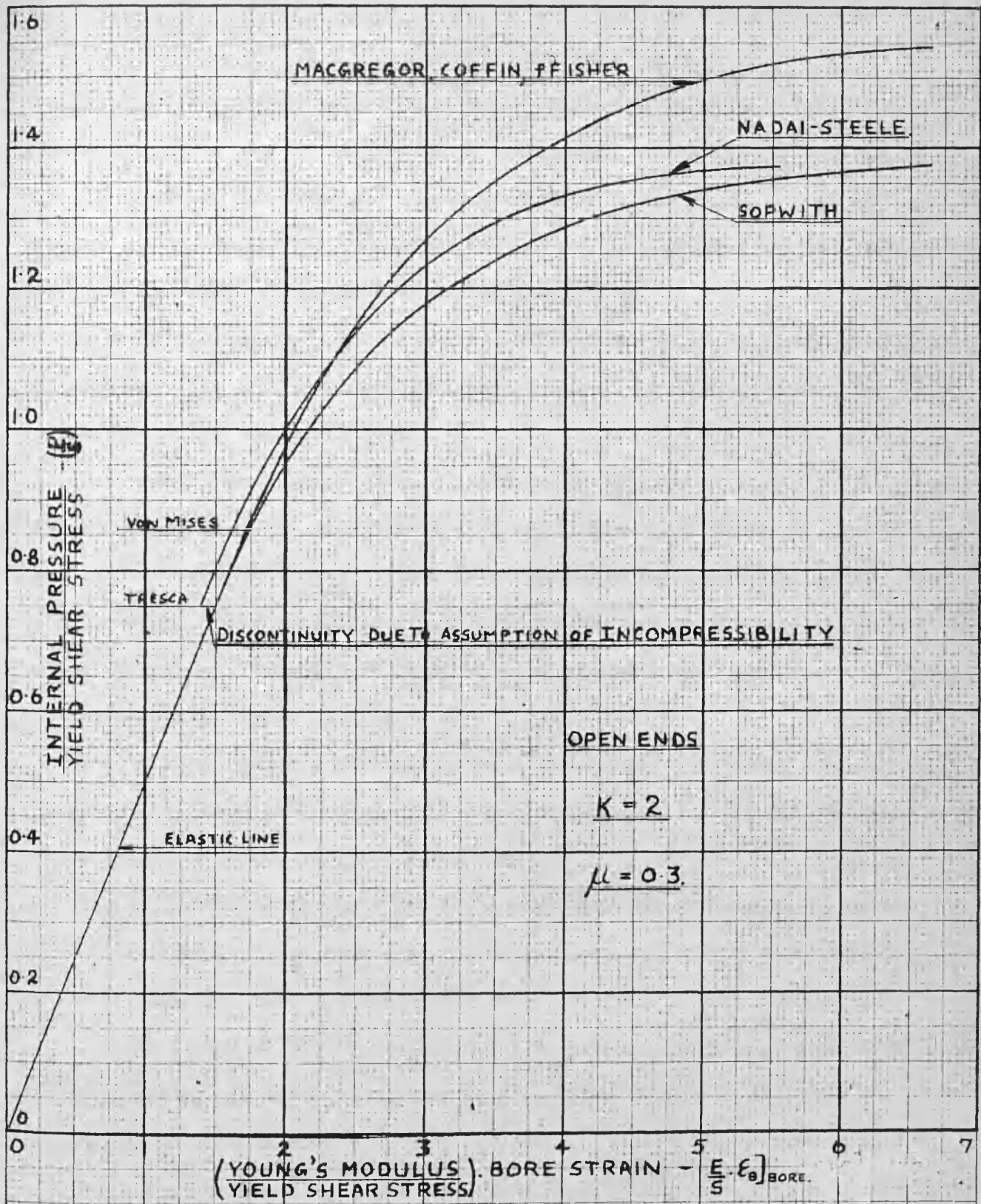


FIG. 7 - BORE STRAINS, UP TO FULLY PLASTIC CONDITION, ( $\mu=2$ ) IN A PARTIALLY OVERSTRAINED CYLINDER ACCORDING TO:-

- (i) NADAI- STEELE,
- (ii) SOPWITH,
- (iii) MACGREGOR, COFFIN, FISHER.

the Von Mises Theory may be the correct one, depending on the material under consideration. Theories of failure are so established that a general one holding for all materials and under all stress conditions is not known. It is not the purpose of this comparison, therefore, to say one is right and the other wrong, but rather to state the cause and discuss the effect.

A study of Figs. 3-7, will show that differences in the theories of Sopwith and MacGregor are considerable. This may be taken as primarily due to the varying assumption in flow conditions.

The radial stress graph (Fig. 3) records an increase of 15 % in the bore pressure required to produce plastic flow half-way through the wall, when using the distortion-energy theory. Even larger increases are seen (Fig. 4) for the hoop stresses. These differences may be traced in part to the stresses at initial yielding. The cylinder remains elastic under higher stresses when the distortion-energy theory is used.

Fig. 5 shows little difference between the two plots of axial stress. In the elastic domain the constant axial stresses are almost identical, and only a slight deviation exists in the plastic region.

The strain graphs, Figs. 6 and 7, clearly show the differences in measurable quantities. Both outside diametral strain and bore strain graphs are of the same shape and they bear a quantitative relationship of the same sense.

Sopwith discussed the limitations of his analysis and gave an approximate method of making his solution satisfy the Von Mises' theory of failure. In the terminology of this thesis,

$$(\sigma_{\theta} - \sigma_r) = 2s \quad \text{----- (a)}$$

$$\sigma_{\theta} + \sigma_r - 2\sigma_z = 2s W_3 \{ \log W + a \} = 2s Z \quad \text{----- (b)}$$

From which,

$$\sigma_{\theta} - \sigma_z = s (1 + Z) \quad \text{----- (c)}$$

$$\sigma_z - \sigma_r = s(1 - Z) \quad \text{----- (d)}$$

(a), (c) and (d) can now be substituted in the equation

$$(\sigma_\theta - \sigma_r)^2 + (\sigma_\theta - \sigma_z)^2 + (\sigma_z - \sigma_r)^2 = 2\sigma_0^2$$

to give

$$\sigma_0 = s\sqrt{3 + Z^2}$$

If 'Z' is constant then the Von Mises' condition is satisfied and the value of 's' used in Sopwith's equations would be  $\frac{2}{\sqrt{3 + Z^2}}$  s. Any variation in 'Z' shows a corresponding variation of this stress which depends on its constancy for integration of the equilibrium equation.

For cylinders with closed ends, the maximum variation of this stress is only 1 % and if a mean value is used, only a small error is introduced. An approximation of this sort is not sound for the open-ended cylinder under consideration. Values of 'Z' vary from .09 at the bore to .95 at the outer boundary when the cylinder is fully plastic. Corresponding values of stress are from 1.15s to 1.01s, a difference of approximately 15 %. Any attempt to extend Sopwith's analysis to cover that of MacGregor's has therefore been discarded for open-ended cylinders.

Some practical features may be noticed about the strain graphs. If measurements are made on a test cylinder, the question arises whether the observations will disclose initial yielding and the subsequent flow condition the material obeys. An examination of the theoretical graphs in the region of primary elastic breakdown indicates that changes in slope are small and that it would be difficult to determine the first deviation from linearity. The tests must be in a more advanced stage, say half the wall plastic, before a concrete opinion could be ventured as to the law the material of the cylinder were following.

The above three theories form the nucleus of the review on thick cylinders. The work of some other investigators may be compared with them.

## 6. Summary Analysis and Discussion - COOK

Cook has presented a valuable contribution to the study of mild steel thick cylinders. His theory is dependent on experimental results for its final solution. The basic assumptions are the same as those of Nadai-Steele, viz: -

$$\epsilon_{\theta} + \epsilon_r + \epsilon_z = 0,$$

$$\frac{\epsilon_{\theta} - \epsilon_r}{\sigma_{\theta} - \sigma_r} = \frac{\epsilon_r - \epsilon_z}{\sigma_r - \sigma_z} = \frac{\epsilon_z - \epsilon_{\theta}}{\sigma_z - \sigma_{\theta}},$$

and the variation exists in the treatment of Tresca's theory of failure.

Mild steel cylinders were used in his experiments and, as a consequence, the controversial upper and lower yield points introduced. If 's' and 's'' refer to the upper and lower shear stress respectively, then normally the shear stress distribution across the wall of an overstrained cylinder would be as shown in Fig. 8.

Using the same approach as in the Nadai-Steele theory, only allowing for the new shear stress conditions, it can easily be shown that the internal pressure is given by,

$$P = s \log_e n^2 + s' \frac{(k^2 - n^2)}{k^2} \quad \text{----- (49)}$$

It was soundly reasoned by Cook that the value of 's' would be that given by the lower limit in a simple tension test. Because of the unpredictable nature of the upper limit, however, it was considered unwise to attach a value to 's''. Eq. 49 thus contains two variables, 's'' and 'n', on which the internal pressure depends. It is solved with the help of experimental observations.

The following two equations may be easily deduced: -

$$s' = \sigma_{\theta} \frac{o/d}{n^2} \cdot \frac{k^2}{n^2} \quad \text{----- (50)}$$

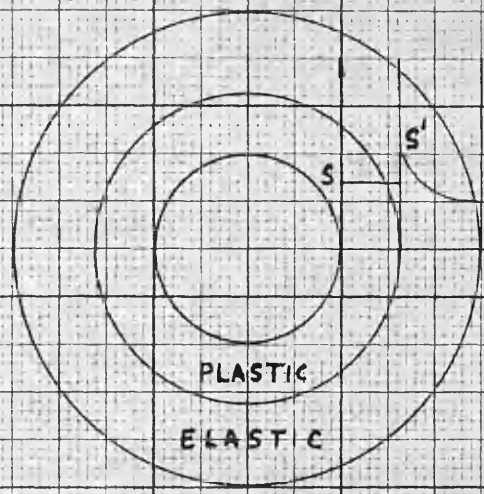


FIG. 8 - CONVENTIONAL SHEAR STRESS IN AN OVERSTRAINED CYLINDER OF A MATERIAL SHOWING UPPER & LOWER YIELD POINTS.

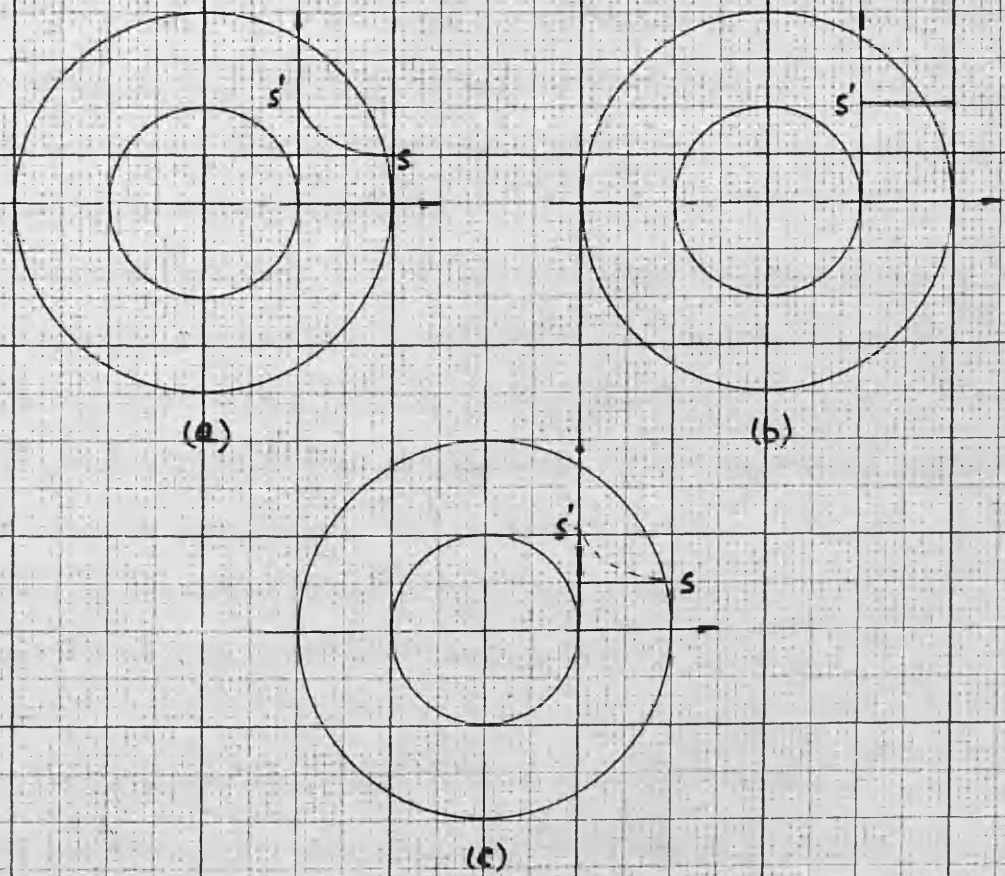


FIG. 9 - EXPERIMENTAL AND ASSUMED EXTREME SHEAR STRESS DISTRIBUTIONS TO CAUSE YIELDING OF ELASTIC MATERIAL AS ELASTIC-PLASTIC BOUNDARY PROGRESSES THROUGHOUT WALL OF CYLINDER

$$s = \frac{1}{\log_e n^2} \left[ P - \sigma_{\theta} \frac{o}{d} \cdot \frac{(k^2 - n^2)}{2n^2} \right] \quad \text{----- (51)}$$

To these may be added a third equation necessary for the computation of axial stresses in the plastic domain: -

$$\sigma_z = s \left[ \log_e y^2 + \beta y^2 + 1 \right] - P \quad \text{----- (52)}$$

where,

$$\beta = \frac{3 \left\{ \sigma_z \frac{o}{d} - \mu \sigma_{\theta} \frac{o}{d} \right\}}{n^2 \left\{ \sigma_{\theta} \frac{o}{d} + \sigma_z \frac{o}{d} \right\} \cdot (1 - 2\mu) + k \sigma_{\theta} \frac{o}{d} \cdot (1 + \mu)}$$

An examination of Eqs. 50, 51, and 52, shows that they are in terms of three measurable quantities, viz: -  $P$ ,  $\sigma_{\theta} \frac{o}{d}$ , and  $\sigma_z \frac{o}{d}$ . Substitution of these experimental values in the theoretical equations determines 's', and 'n', and  $\sigma_z$  in the plastic region. Knowing these three quantities, all the remaining stresses and strains may be computed.

Cook's results show that 's' is not a constant as supposed but varies with 'n'. This variation may be found by using his experimental results and Eqs. 49 and 50. Its approximate form is shown in Fig. 9(s).

This observation has further corroboration in work previously performed by Cook, (6) in which he examined the initial elastic breakdown of: -

- (i) Cylinders of the same bore and varying wall thickness.
- (ii) Cylinders of the same wall thickness and varying bore.

He showed that,

- (i) Initial yield shear stress was independent of wall thickness.
- (ii) Initial yield shear stress varied with bore diameter, becoming less as the bore size increased.

A qualitative argument may be used to justify these results. It is visualized that as initial elastic breakdown approaches, a number of plastic wedges,

which occupy a small volume of material, yet relieve a comparatively large amount of strain because of their ductility, are formed. At some stage in the formation of these, an integrated effect is noticed on an overall dimension, usually the outside diameter, and "yield" is said to take place. Local yielding may have taken place under a particular shear stress but general yielding would give the impression of a higher shear stress being required to cause an initial observable breakdown. In effect, what should be stated, is that a pressure 'P' is built up higher than a fictitious pressure 'P'' say, which theoretically would cause orderly yielding to take place, if there were no possible self-adjustment within the material. The difference in pressures, (P-P') is only a measure of the capacity of the material, by virtue of its ductility, to stave off any serious yielding. The upper shear stress, or what is equivalent to an upper shear stress, is not an actual stress existing in the material, but to simplify analysis, may be considered so. Cook shows that this fictitious shear stress varies with 'n' or bore, becoming smaller as 'n' or, in effect the bore, increases. Thus, using the above argument, the capacity of the material to withstand progression of plastic front diminishes as the plastic domain increases. According to Cook, the drop in resistance is sharp after initial yielding, Fig. 9(s).

It should be kept in mind that Cook's experiments were performed on cylinders of small bore (0.375 ins. for  $k = 2$ ) and there is a distinct possibility that this effect would not be noticed in larger cylinders. It is worthwhile studying the effect of a variation in 's' ', however, on the graphs presented in the basic review. This will be done by choosing the two extreme variations of 's' ' and assuming that any intermediate variation such as that given by Cook's experimental results, will produce effects which may be interpolated.

Figs. 9(t) and (c) define the extreme variations in 's' '. Mathematically, these may be stated: -

$$(i) \bar{s} = s' , 1 < y < k.$$

$$(ii) \bar{s} = s' , y = 1 ; \bar{s} = s , 1 < y < k.$$

If ' $\bar{P}$ ' is initial elastic breakdown pressure at the bore, then,

$$\bar{P} = \bar{s} \left( 1 - \frac{1}{k^2} \right). \quad \text{----- (53)}$$

$$\bar{P} = s \log_e n^2 + \bar{s} \left( 1 - \frac{n^2}{k^2} \right) \quad \text{----- (54)}$$

Both of these equations are valid at initial breakdown. Hence

$$\bar{s} \left( 1 - \frac{1}{k^2} \right) = s \log_e n^2 + \bar{s} \left( 1 - \frac{n^2}{k^2} \right) \quad \text{where } \bar{s} = s' \text{ in case (i) and } \bar{s} = s \text{ in case (ii).}$$

CASE (i)  $n = 1$ , satisfies equation.

CASE (ii)  $n > 1$ , satisfies equation. This means that initial breakdown produces a finite depth of the plastic domain, before yielding is arrested. It takes place under constant pressure and gives rise to a discontinuity when plots of internal pressure against circumferential strain are made. Cook, actually showed such discontinuities in his experiment results but did not discuss the reason for their existence. It may be reasoned that if this effect is noticed by measurement of outside diametral strains, a more accurate explanation may be forthcoming if bore strains could be measured.

The conventional curves are drawn for a particular ratio of  $s'/s = 1.65$ . This is selected from Cook's experimental results. The purpose of constructing these curves is merely to show the effects, if such shear stress variations were to exist. The ratio  $s'/s$  could be arbitrarily chosen, the closer the ratio being to 1, the smaller the effect.

Proceeding as in Nadai-Steele's theory, the equations become,

ELASTIC DOMAIN  $n < y < k$

$$\sigma_r = \frac{\bar{s} n^2}{k^2} - \frac{\bar{s} n^2}{y^2} \quad \text{----- (55)}$$

$$\sigma_\theta = \frac{\bar{s} n^2}{k^2} + \frac{\bar{s} n^2}{y^2} \quad \text{----- (56)}$$

$$\sigma_z = E \epsilon_z + \frac{2 \mu n^2 \bar{s}}{k^2} \quad \text{----- (57)}$$

$$\epsilon_{\theta \text{ o/d}} = \frac{s}{E} \left[ \frac{2n^2}{k^2} \cdot \frac{\bar{s}}{s} - \frac{2\mu n^2 \bar{s}}{k^2 s} - \frac{\mu E \epsilon_z}{s} \right] \quad \text{----- (58)}$$

PLASTIC DOMAIN  $1 < y < n$

$$\sigma_r = s \log \left( \frac{y}{n} \right)^2 + \frac{\bar{s} n^2}{k^2} - \bar{s} \quad \text{----- (59)}$$

$$\sigma_\theta = s \log \left( \frac{y}{n} \right)^2 - \frac{\bar{s} (k^2 - n^2)}{k^2} + 2\bar{s} \quad \text{----- (60)}$$

$$\sigma_z = \frac{3 E \epsilon_z}{2(1 + \mu) n^2} \cdot \frac{s}{s} \cdot y^2 + s \left[ \log \left( \frac{y}{n} \right)^2 + 1 \right] - \bar{s} \cdot \frac{(k^2 - n^2)}{k^2} \quad \text{----- (61)}$$

$$\epsilon_{\theta \text{ bore}} = \frac{s}{E} \left[ (1 + \mu) n^2 \cdot \frac{\bar{s}}{s} - \frac{1}{2} \frac{E \epsilon_z}{s} \right] \quad \text{----- (62)}$$

and  $\epsilon_z = \text{constant}$  for any one value of 'n', and given by

$$\epsilon_z = - \frac{s}{E} \left[ \frac{\log n^2 + \frac{\bar{s} (k^2 - n^2)}{s k^2} \{ 2\mu n^2 - n^2 + 1 \}}{\frac{3}{4} \cdot \frac{(n^4 - 1) s}{(1 + \mu) n^2 s} + k^2 - n^2} \right] \quad \text{----- (63)}$$

Figs. 10-14 inclusive, clearly show the effects of the two assumptions regarding the value of  $\bar{s}$ . It can be seen that, if the theorist once accepts a possible variation in  $\bar{s}$ , say intermediate of those chosen, he has considerable licence in fitting his curves to any experimental data. An extension of this

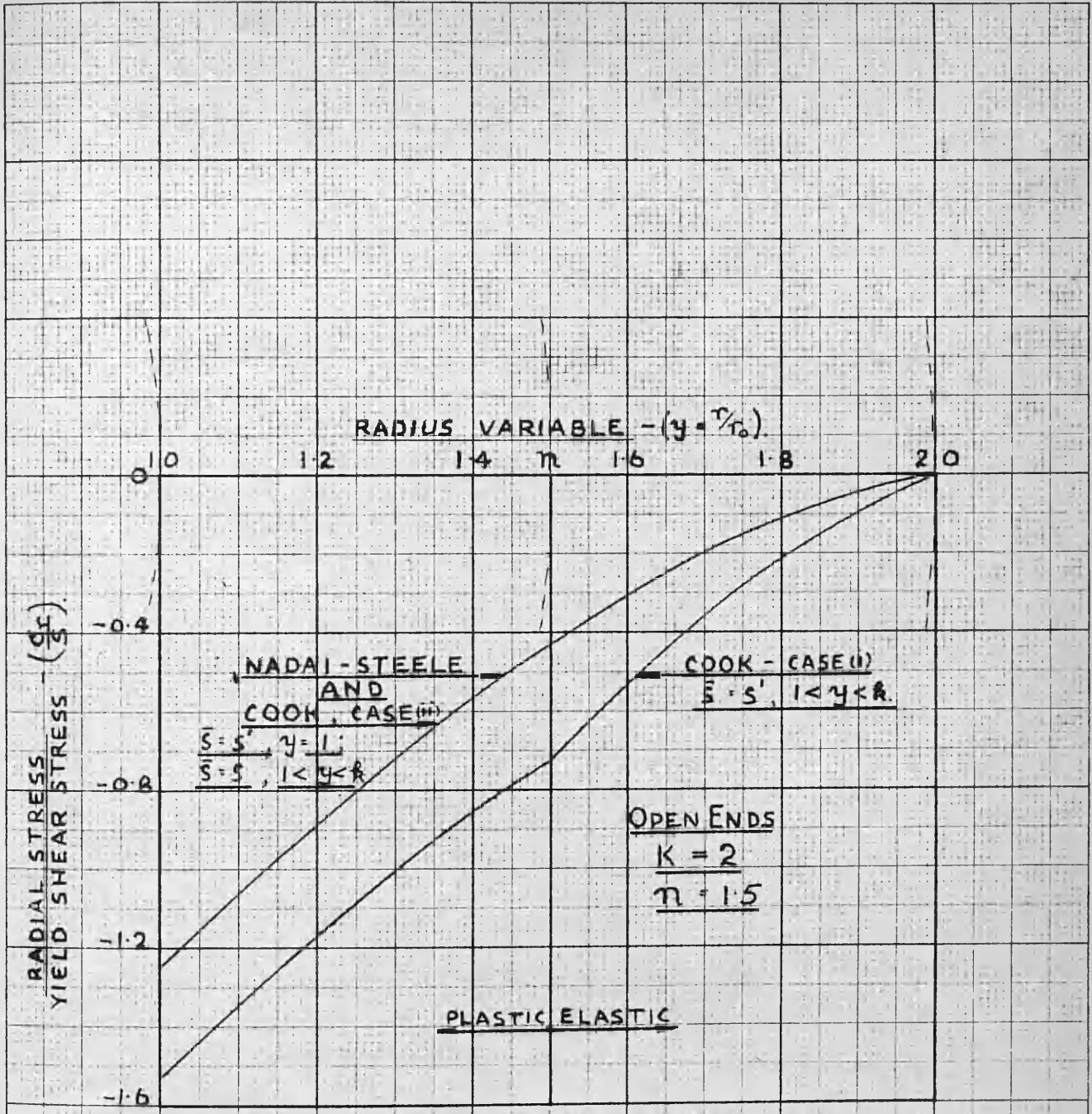


FIG. 10 COMPARISON WITH RADIAL STRESSES DUE NADAI-STEEL OF THOSE OBTAINED BY ASSUMING EXTREME ELASTIC BOUNDARY SHEAR STRESS VARIATIONS DISCUSSED UNDER COOK'S THEORY.

NO. 345 20 DOTTEN GRAPH PAPER 20 X 20 PER IN.

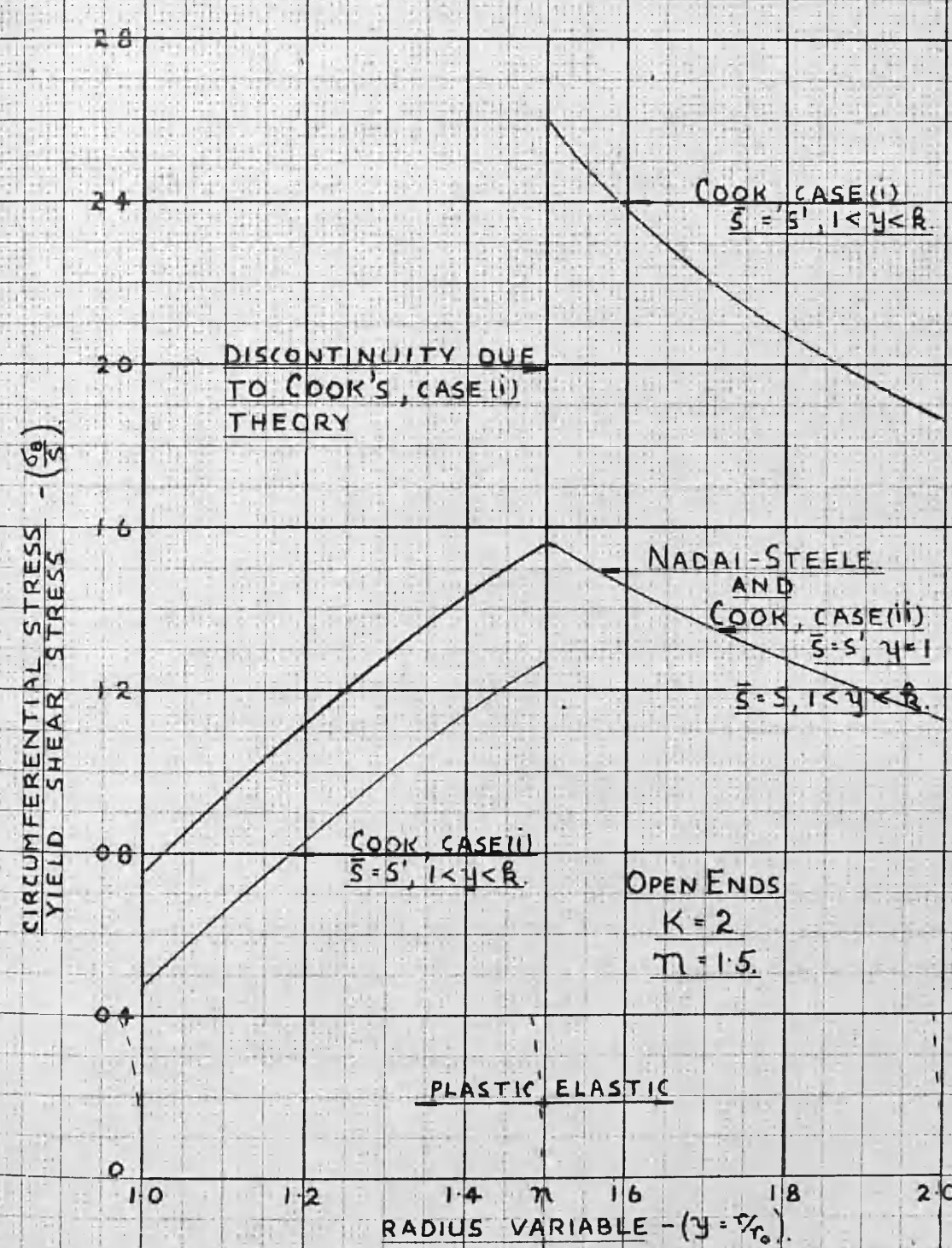


FIG. 11 - COMPARISON WITH CIRCUMFERENTIAL STRESSES DUE NADAI-STEELE OF THOSE OBTAINED BY ASSUMING EXTREME ELASTIC BOUNDARY SHEAR STRESS VARIATIONS DISCUSSED UNDER COOK'S THEORY.

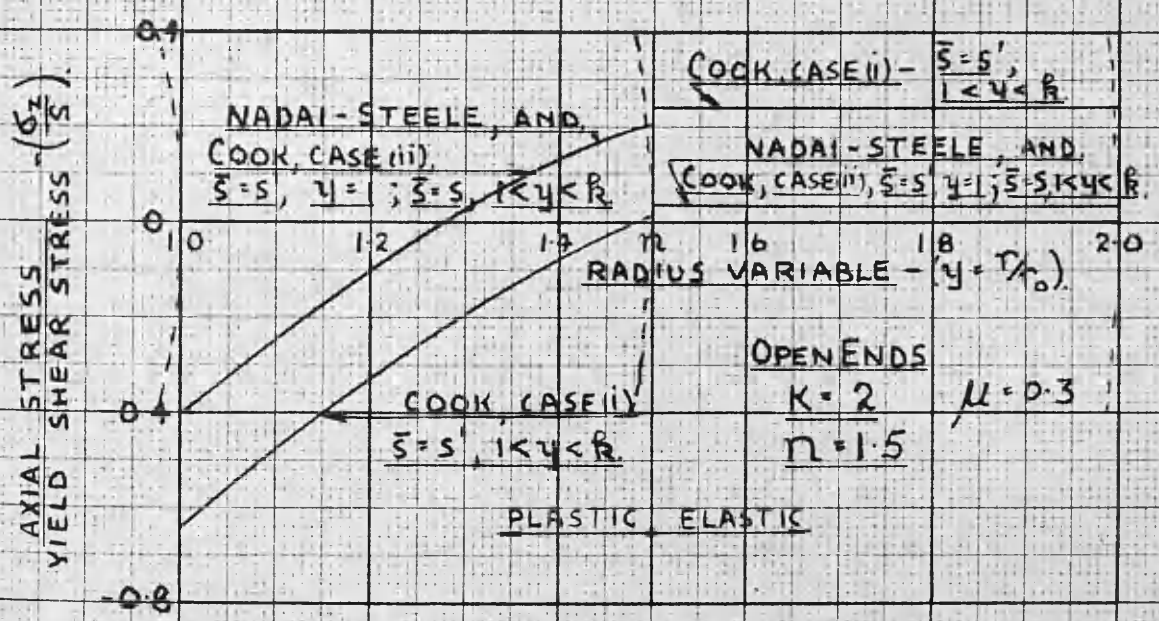


FIG. 12 - COMPARISON WITH AXIAL STRESSES DUE NADAI-STEELE OF THOSE OBTAINED BY ASSUMING EXTREME ELASTIC BOUNDARY SHEAR-STRESS VARIATIONS DISCUSSED UNDER COOK'S THEORY.

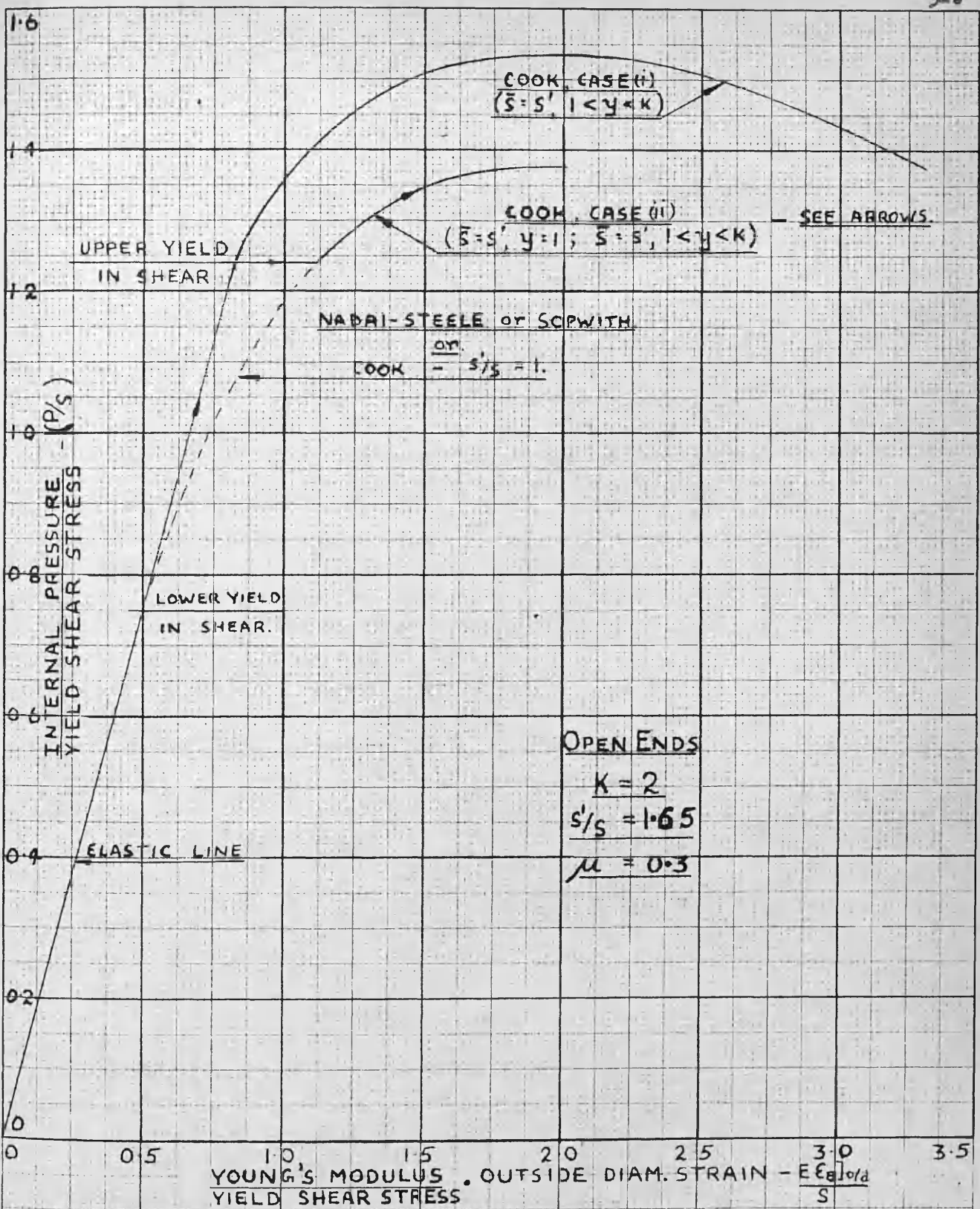


FIG.13-OUTSIDE DIAMETRAL STRAINS, UP TO FULLY PLASTIC CONDITION. ( $n=2$ ) ASSUMING TWO EXTREMES IN VARIATION OF YIELD SHEAR STRESS AT PLASTIC-ELASTIC BOUNDARY.

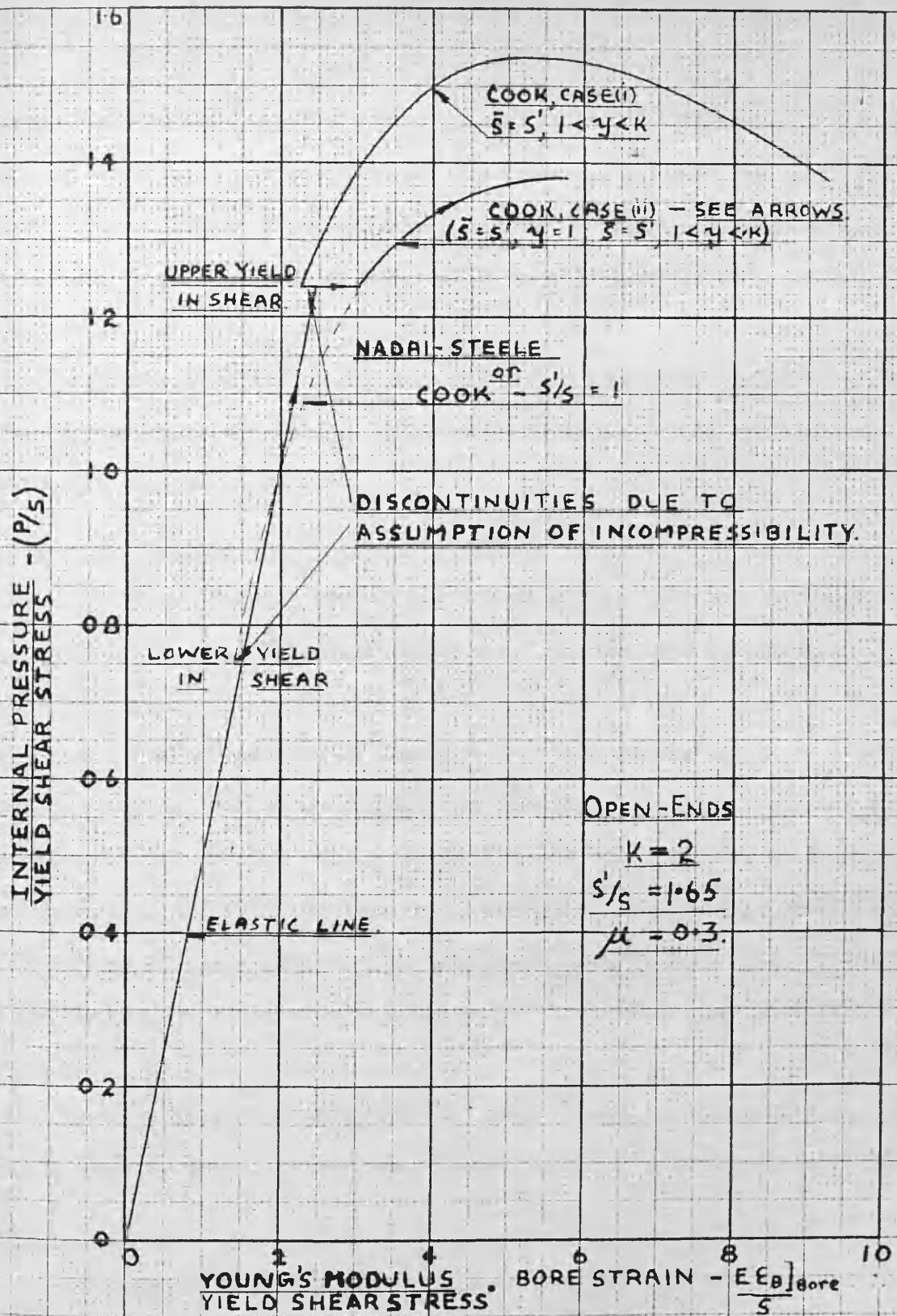


FIG. 14 BORE STRAINS, UP TO FULLY PLASTIC CONDITION, ( $n=2$ ), ASSUMING TWO EXTREMES IN VARIATION OF YIELD SHEAR STRESS AT PLASTIC-ELASTIC BOUNDARY.

idea to Sopwith's more correct theory, would provide a flexible theory extremely difficult to disprove experimentally (by measuring outside strains), and on theoretical grounds. If measurements of plastic-elastic boundaries could be made during tests, more conclusive data would be available for the corroboration of assumptions.

Cook suggested that axial stresses are approximately arithmetic means of the other two principal stresses. This refers to closed-ended cylinders and is not applicable to open-ended ones.

## 7. Summary Analysis and Discussion - MACRAE

In 1930 the British War Office published work performed by Major Macrae of the Royal Artillery. This book referred to certain observations made from numerous fundamental experiments performed in an attempt to further understand the nature of stresses and strains set up in the autofrettaging process. Credit must be given to the author not only for the presentation of valuable experimental data, but for the unique way in which he utilized it. He furnished designers with a "drill" for the future design of autofrettaged cylinders. His theory bears little resemblance to the others, and is based largely on experiment. It is, indeed, worthwhile to briefly record the methods used in this ingenious treatise.

Macrae's theory uses the maximum shear stress failure condition. Reference will be made to the diagram of overtension followed by overcompression of Fig. 15.

### Initial Stresses

The problem is treated in two dimensions. Eqs. 32 and 33 of Nadai-Steele's theory apply. No mention of axial stresses occurring in an overstrained cylinder with open ends is made, and in computation of strains, they are ignored.

### Initial Strains

Some definitions are necessary.

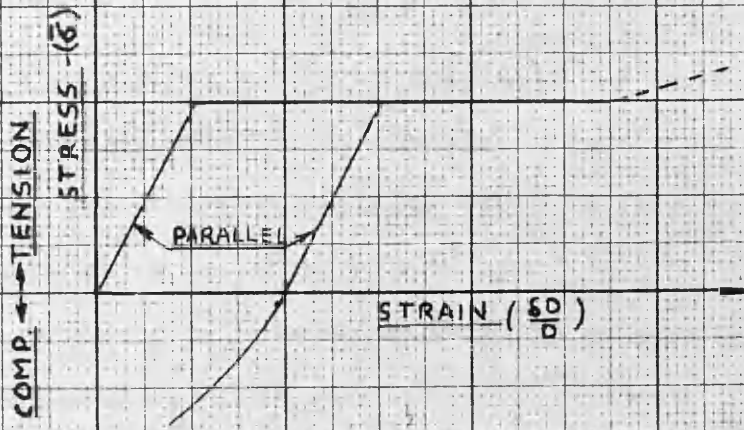


FIG. 15 - TENSILE TEST DIAGRAM USED BY MACRAE IN RELATING CYLINDER VALUES TO TEST-PIECE VALUES.

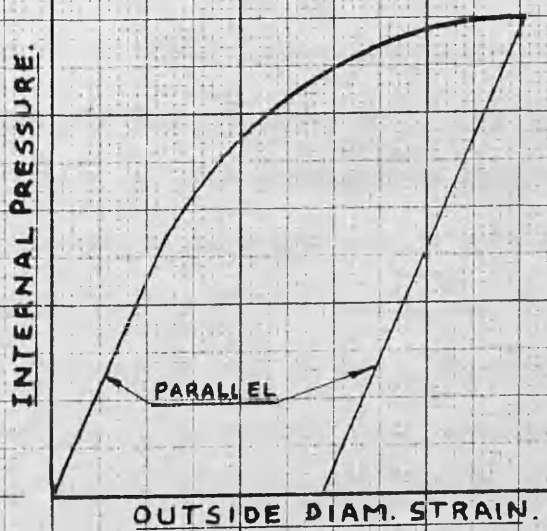


FIG. 16 - MACRAE'S LOADING AND UNLOADING CURVES, SHOWING ELASTIC RELEASE OF STRAIN.

NO. 3140 50 BREZDEN GRAPH PAPER 20 X 30 PER INCH ENGINE DESIGN CO.

Equivalent "Simple Stress" is defined by

$$\bar{\sigma} = (\sigma_{\theta} - \sigma_r) \quad \text{----- (a)}$$

where  $\bar{\sigma}$  refers to tension or compression test piece stress.

Equivalent "Simple Strain",  $\frac{\delta D}{D}$ , is defined as the tension or compression test piece strain, corresponding to the test piece stress.

These stresses and strains do not occur in the cylinder but are used to calculate those existing in the cylinder.

Macrae made some remarkable assumptions for the calculation of cylinder strains. They are listed as follows: -

(i)  $\frac{\delta D}{D}$  is inversely proportional to the square of the diameter.

This is an assumption which is difficult to prove or disprove. As far as the writer can see, there is no general basis for it.

(ii) Removal of Pressure is accompanied by elastic release of cylinder strains.

There is experimental corroboration (See Fig. 16) of this statement for the outside diameter. It is doubtful whether this is the case for all diameters.

(iii) Residual cylinder strains  $\frac{\delta d}{d}$  are equal to residual test piece strains.

This is derived from (a), the experimental observation that the length of a cylinder after the release of bore pressure is practically the same as the length before the application of bore pressure, and (b) the conservation of volume. The latter statement seems to be used loosely. It appears that a conservation of volume takes place between (a) a cylinder free from stress and (b) the same cylinder on release of bore pressure which is not free from stress. Zero change in volume can take place in a material which deforms plastically only, but not where any elastic strains are present. It is not even used here as Nadai used it i.e. neglect of elastic strains in the plastic region.

The above assumptions lay the foundation for the following equations: -

Cylinder strain under pressure P = residual cylinder strain + cylinder elastic release of strain

$$\text{or } \epsilon_{\theta} = \frac{\delta d}{d} + \frac{\sigma_{\theta} - \mu \sigma_r}{E} \quad \text{--- (b)}$$

where  $\sigma_{\theta}$  and  $\sigma_r$  are values of stresses due to bore pressure 'P' when cylinder is considered elastic.

Also Test piece strain = residual test piece strain + release of test piece strain

$$\text{or } \frac{\delta D}{D} = \frac{\delta d}{d} + \frac{(\sigma_{\theta} - \sigma_r)}{E} \quad \text{--- (c)}$$

From Eqs. (b) and (c),

$$\epsilon_{\theta} = \frac{\delta D}{D} + \frac{(1 - \mu) \sigma_r}{E} \quad \text{----- (d)}$$

N.B.  $\sigma_r$  may be expressed in terms of 'P' and hence cylinder strain can be found from test-piece strain and 'P'.

Equations are: -

ELASTIC DOMAIN  $n < y < k$

$$\sigma_r = \frac{n^2 s}{k^2} - \frac{n^2 s}{y^2}$$

$$\sigma_{\theta} = \frac{n^2 s}{k^2} + \frac{n^2 s}{y^2}$$

$$\sigma_z = 0 \quad \text{----- (64)}$$

$$\epsilon_{\theta} \text{ o/d} = \frac{s}{E} \cdot \frac{2n^2}{k^2} \quad \text{----- (65)}$$

PLASTIC DOMAIN  $1 < y < n$

$$\sigma_r = s \left[ \log \left( \frac{y}{n} \right) - \frac{(k^2 - n^2)}{k^2} \right]$$

$$\sigma_{\theta} = s \left[ \log \left( \frac{y}{n} \right) + \frac{(k^2 + n^2)}{k^2} \right]$$

$$\sigma_z = 0$$

$$\epsilon_{\theta \text{ bore}} = \frac{s}{E} \left[ 2 n^2 - (1 - \mu) \left( \log n^2 + \frac{k^2 - n^2}{k^2} \right) \right] \quad \text{-- (66)}$$

Fig. 17 shows the bore strain graph plotted from Macrae's theory and compared with Sopwith's. Although Macrae in his presentation lacks a sound theoretical approach, this curve adheres closely to that of Sopwith's. Plots of outside diametral strain are identical.

### 8. Summary Analysis and Discussion - MORRISON and SHEPHERD

A review would not be complete without some reference to an analysis given by Morrison and Shepherd<sup>(26)</sup> in a recent paper. Their method requires: --

- (i) Shear Stress-Shear Strain relationship for a material.
- (ii) Assumption that the maximum shear strain throughout the wall of the cylinder is inversely proportional to the square of the radius. This is of course true for an elastic cylinder, but not strictly so after yield has taken place.

Equilibrium condition gives,

$$r \cdot \frac{\partial \sigma_r}{\partial r} = \sigma_{\theta} - \sigma_r = 2s$$

Hence,  $\sigma_r = 2 \int \frac{1}{r} \cdot s \cdot dr$  taken between limits of 'r' at the external and internal surfaces.

It is seen that the method is limited to a relation between outside diametral strain and internal pressure. Morrison<sup>(26)</sup> states, "For any given external expansion the shear strain, and hence from the known  $q = f(\gamma)$ , the shear stress, at each radius, are evaluated."  $q = f(\gamma)$  is the known shear stress-shear strain relationship. An examination of Morrison's statement produces restrictions inherent in the method. Consider the outside diameter strains: --

$$E \epsilon_{\theta} = \sigma_{\theta} - \mu \sigma_z$$

$$E \epsilon_r = -\mu (\sigma_{\theta} + \sigma_z)$$

$$E \epsilon_z = \sigma_z - \mu \sigma_{\theta}$$

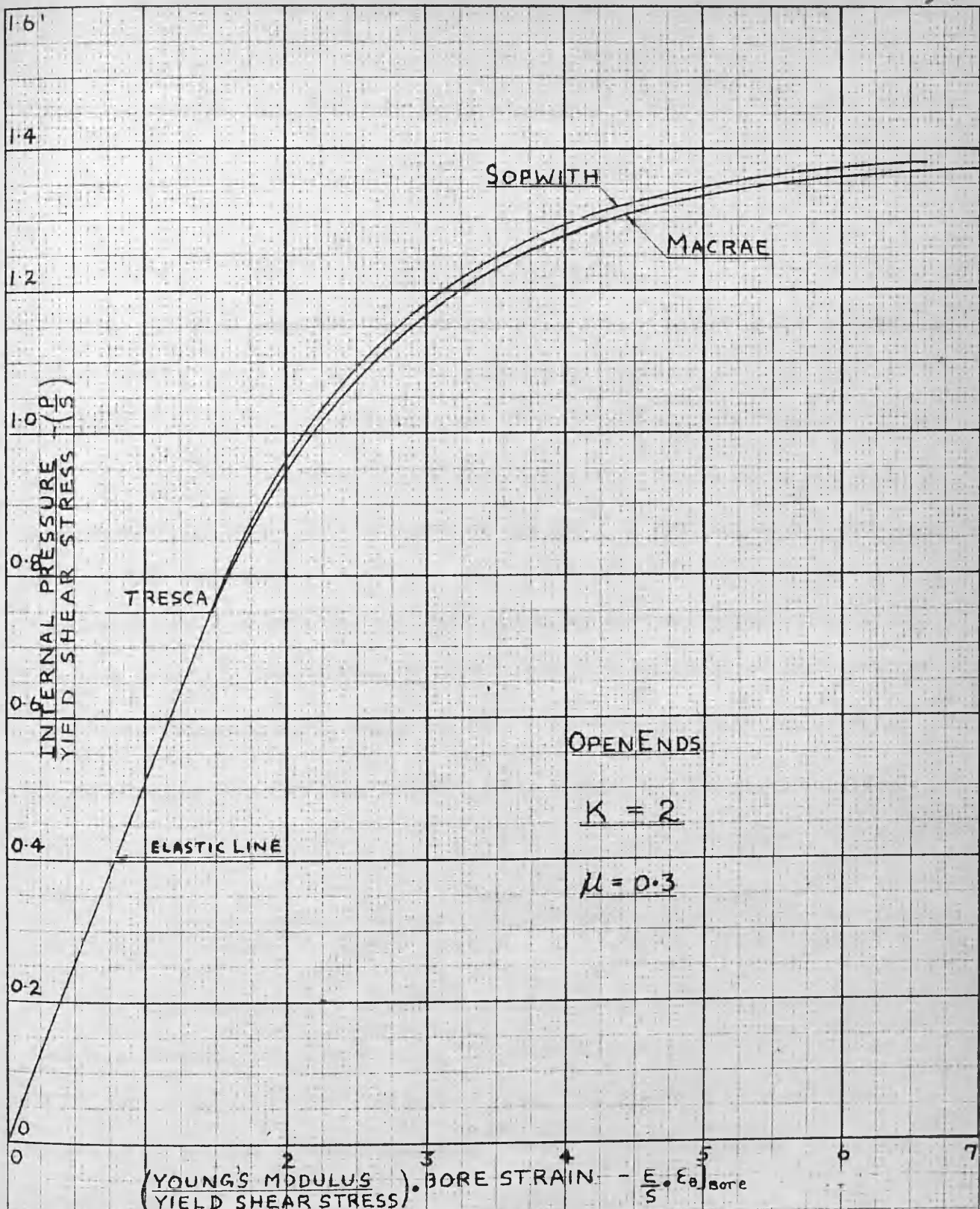


FIG.17 - BORE STRAINS, UP TO FULLY PLASTIC CONDITION, ( $n=2$ ), IN A PARTIALLY OVERSTRAINED CYLINDER ACCORDING TO:-

- (i) SOPWITH,
- (ii) MACRAE

From which, the maximum shear-strain is given by

$$(\epsilon_{\theta} - \epsilon_r) = \frac{(1 + \mu)}{E} [E \epsilon_{\theta} + \mu \sigma_z] \quad \text{----- (67)}$$

or

$$(\epsilon_{\theta} - \epsilon_r) = \frac{1}{(1 - \mu)} [\epsilon_{\theta} + \mu \epsilon_z] \quad \text{----- (68)}$$

Eqs. 67 and 68 show that the maximum shear strain cannot be deduced directly from an assumed value of  $\epsilon_{\theta}$  without reference to  $\sigma_z$  or  $\epsilon_z$ .

If  $\epsilon_z = 0$  or if a closed-ended cylinder is assumed, then relation

$(\epsilon_{\theta} - \epsilon_r) = \frac{\epsilon_{\theta}}{(1 - \mu)}$  would be sufficiently accurate. Errors would be larger in an open-ended cylinder, however, and the one merit of applying such a theory, would be its simplicity.

Sopwith made an interesting investigation of Morrison's basic assumption, viz.  $(\epsilon_{\theta} - \epsilon_r) r^2 = \text{constant}$ . He showed that this condition is tantamount to  $\frac{(3 - W_3) W}{W_3}$  being constant, where the 'W's' refer to his functions of  $(y/n)^2$ .

The calculations are confined to the plastic domain, and are shown tabulated below.

$(y/n)^2$	1	0.8	0.6	0.4	0.2
$(\epsilon_{\theta} - \epsilon_r)$	6.00	6.46	6.96	7.50	7.91 (accuracy $\pm .05$ )

This wide variation in an assumed constant does not detract much from certain solutions. If, for example, the shear stress-shear strain relation has a flat top as in the review's idealized case, then an error in shear strain would not affect the corresponding shear stress which is contained under the integral sign.

#### IV. REVIEW OF INTERFERENCE FIT THEORIES

##### 1. Customary Elastic Analysis based on LAME'

It is assumed that a constant pressure exists at the interface and that the elements are the same length. The theory is restricted to assemblies whose fit allowances do not cause overstraining of the ring. The problem is one of plane stress ( $\sigma_z = 0$ ). Assuming an interface pressure  $P$  to exist, the stresses and strains in the ring are given by: -

$$\sigma_r = \frac{P}{(k^2 - 1)} \left[ 1 - \frac{k^2}{y^2} \right] \quad \text{-----} \quad (69)$$

$$\sigma_\theta = \frac{P}{(k^2 - 1)} \left[ 1 + \frac{k^2}{y^2} \right] \quad \text{-----} \quad (70)$$

$$\epsilon_\theta = \frac{P}{E (k^2 - 1)} \left[ (1 - \mu) + (1 + \mu) \frac{k^2}{y^2} \right] \quad \text{----} \quad (71)$$

$$\epsilon_\theta \text{ o/d} = \frac{2P}{E (k^2 - 1)} \quad \text{-----} \quad (72)$$

$$\epsilon_\theta \text{ bore} = \frac{P}{E (k^2 - 1)} \left[ (1 - \mu) + (1 + \mu) k^2 \right] \quad \text{----} \quad (73)$$

The stresses and strains in a solid cylinder subjected to a pressure of magnitude  $P$  are given by: -

$$\sigma_r = \sigma_\theta = -P \quad \text{-----} \quad (74)$$

$$\epsilon_\theta = -\frac{P}{E} (1 - \mu) \quad \text{-----} \quad (75)$$

It is conditional that the unit bore extension of the ring added to the unit contraction of the plug realises the fit allowance per unit of bore diameter.

$$\text{Thus } \Delta' = \frac{P}{E(k^2 - 1)} \left[ (1 - \mu) + (1 + \mu)k^2 \right] + \frac{P}{E}(1 - \mu)$$

$$\text{or } \Delta' = \frac{2P}{E} \frac{k^2}{(k^2 - 1)} \quad \text{----- (76)}$$

Eq. 76 reduces the interference fit problem to one involving the solution of two thick-walled cylinders.

It has been assumed in this treatment that the material of the plug and ring (and hence the values of Young's modulus and Poisson's ratio) is the same. Frequently, a cast-iron hub is pressed or shrunk on to a steel shaft and correct account of the differences in material constants must be made. Baugher gives design charts based on the above equations with allowance for difference in material constants. His charts relate (i) the maximum tensile stress and (ii) the interface pressure to the fit allowance for  $1.052 < k < \infty$ .

## 2. Elastic Analysis - Shaft Protrusion - RANKIN (31)

Frequently, a ring of short axial length is shrunk or pressed on to a shaft whose length is so much greater than the length of the ring that for theoretical purposes it may be considered infinite (Fig. 18a). Assuming the pressure between the ring and the shaft to be constant, Rankin shows by methods of the theory of elasticity, that the average strain of the solid shaft is given by: -

$$e_0 = \frac{(1 - \mu) P}{CE} \quad \text{where } C \text{ is a factor which depends on the}$$

ratio  $L/d$ . As  $L/d$  becomes large, 'C' becomes asymptotic at the value 1. It is worthwhile to examine the percentage increase in interface pressure over that calculated by Lamé' for various values of  $L/d$ . Combining the average strain of the shaft with the average strain of the ring bore (Eq. 75) and equating to the fit allowance per inch shaft diameter, it is seen that,

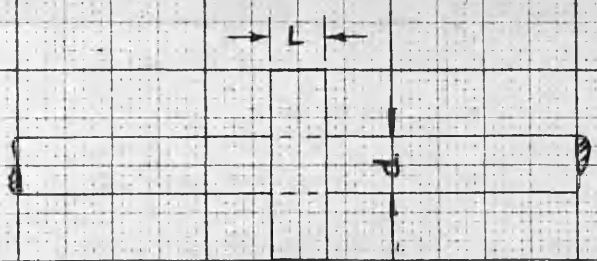


FIG. 18a - SHRINK FIT WITH LONG SHAFT COMPARED TO RING LENGTH.

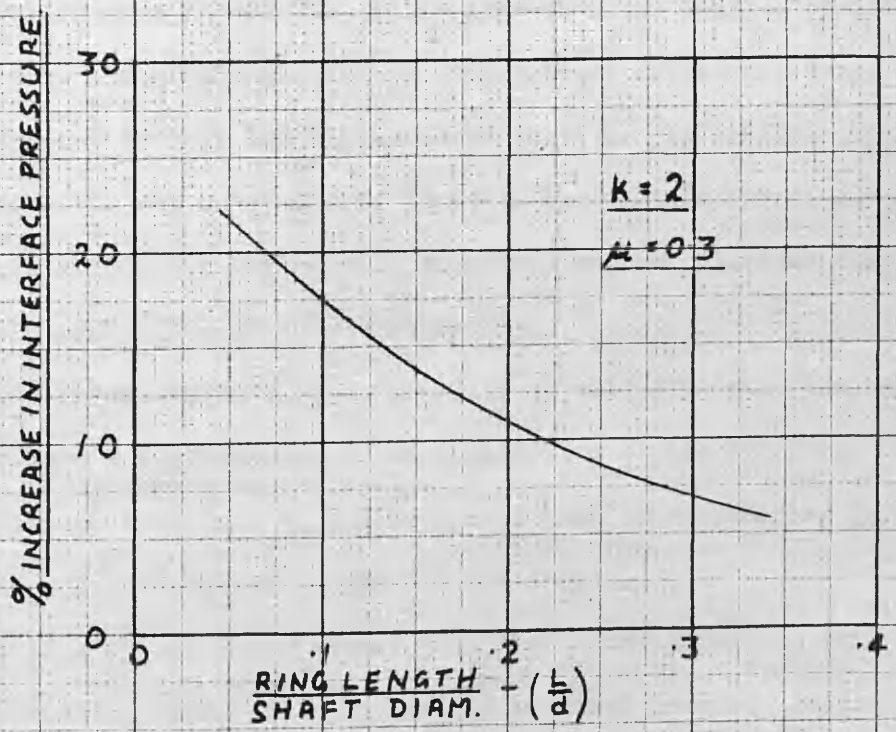


FIG. 18b - PERCENTAGE INCREASE IN INTERFACE PRESSURE DUE SHAFT EXTENSIONS

NE 140 20 DIETZGEN GRAPH PAPER 50 X 25 1/2 MCH 1-1-1

$$P = \frac{E \Delta^0}{\frac{1 - \mu}{C} + \frac{(1 - \mu) + (1 + \mu) k^2}{k^2 - 1}} \quad \text{----- (77)}$$

Eq. 77 reduces to Eq. 76 when  $C = 1$ .

From Eqs. 76 and 77, Fig. 18b may be constructed. Values of 'C' in Rankin's paper are only given up to L/d ratios of 1/3.

It is seen that Lamé's theory has an appreciable error for small values of L/d. A typically proportioned crank web has an L/d ratio of .625 (Lloyd's rules) and in general, values are even higher than this. For example, in the experimental assemblies of this thesis  $L/d = .921 \left( \frac{11}{12} \right)$ . It may be concluded that the effects of shaft extensions are only significant for values of L/d less than  $\frac{1}{2}$ .

### 3. Elastic Analysis - Frictional Effect - GOODIER<sup>(14)</sup>

In the cooling of a shrink fit, it is apparent that besides pressure due to radial contraction, there will also occur longitudinal frictional drag, directed, on the cold component towards the middle cross section. In addition, since under the interface pressure the outer member tends to contract longitudinally and the inner one extend, frictional forces will be set up at the interface because of the nature of the strainings in the members.

Goodier has presented an elastic analysis of this problem. The assumptions introduced to obtain a solution limit the application of his analysis. The qualitative effect of tractions at the interface will be of interest in discussing experimental results presented later in the thesis.

The conditions of analysis require that the assembly must be long compared to the diameter and the shaft and ring must be of equal length. Goodier shows that, for the part of the assembly removed from the ends, the effect of friction, sufficiently great to prevent slip, is to increase the interface pressure to a "plane strain" ( $\epsilon_x = 0$ ) value from the normally calculated one in which "plane

stress" ( $\sigma_z = 0$ ) is assumed. In a steel assembly this amounts to a 40 % increase in interface pressure. At the ends the friction sets up a local disturbance and Goodier found difficulty in completing his analysis for the end regions. By assuming an infinitely large outer diameter for the ring and a solid shaft a solution may be obtained using Love's treatment of a similar problem.

Fig. 19 shows the effects of the disturbance at the ends for an infinite outer cylinder and solid shaft. By plotting  $\tau_{rz}/\sigma_r$  values of coefficient of friction are obtained for the condition and it is seen that 1.27 is the maximum value for no slip. In a practical assembly it is unlikely that the friction value will be as high as 1.27. Consequently, the effects will be modified. It is of interest to note that although the interface pressure falls at the end of the cylinder the tensile circumferential stress in the outer member increases to twice its normal value.

For practical purposes it may be concluded that friction of the normal amount will tend to increase the interface pressure and hence all the dependent stresses. In addition, at the ends, the hoop stress in the outer member will increase more than the amount simply corresponding to the interface pressure rise.

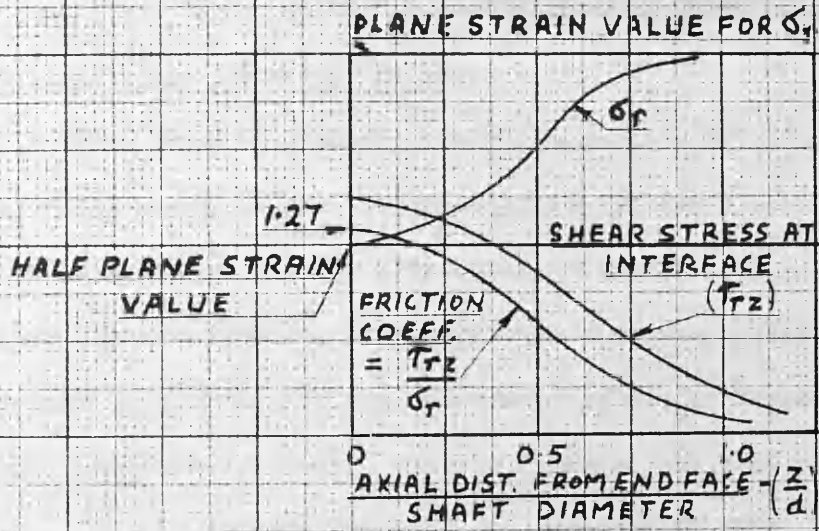


FIG. 19 a. - CONTACT PRESSURE AND FRICTIONAL DRAG AT THE ENDS OF GOODIER'S CYLINDER

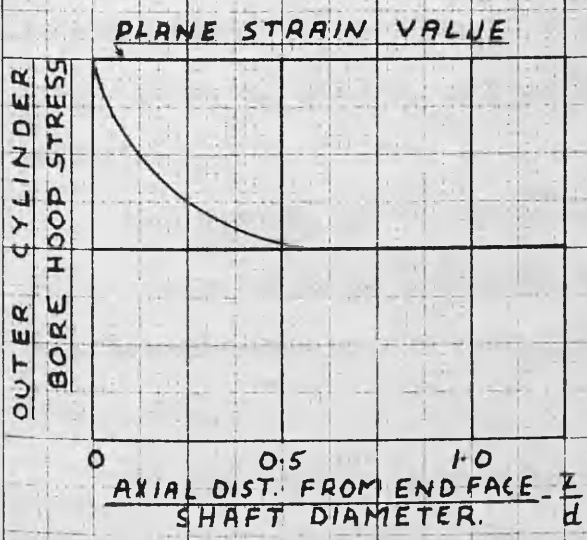


FIG. 19 b. - OUTER CYLINDER (TENSILE) BORE CIRCUM. STRESS

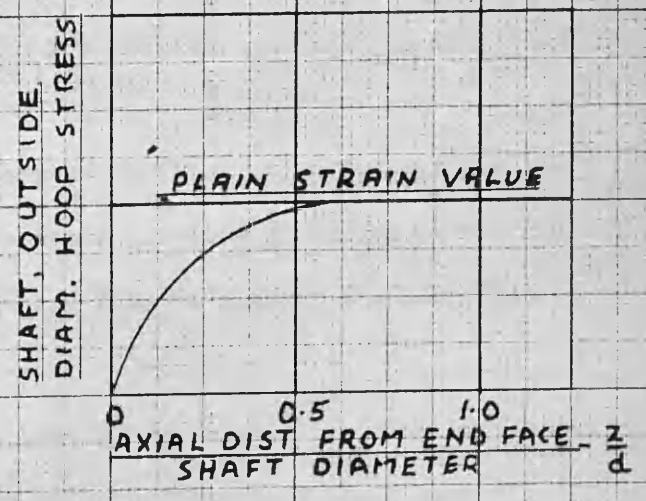


FIG. 19 c. - SHAFT (COMP.) OUTSIDE DIAM. CIRCUM. STRESS

## V. SUMMARY OF THEORETICAL TREATMENTS

### 1. Relating to Thick-walled Cylinders

(i) In an elastic-plastic problem, such as a thick-walled cylinder under internal fluid pressure, the compressibility of the elastic component of strain in the plastic region must be considered. Otherwise, discontinuities exist in certain of the stresses and strains at the elastic-plastic interface. The effects of ignoring the compressibility, however, are not so serious on the two measurable quantities, namely, outside diameter and bore circumferential deflections. It can be seen from Fig. 6, for example, that the graphs of internal pressure against outside diameter circumferential strain, for the Nadai-Steele and Sopwith theories, are coincident.

(ii) In the case of the thick-walled cylinder subjected to internal fluid pressure only, the Total Strain plastic stress-strain law may replace the more correct Incremental law without great loss in accuracy.

(iii) MacGregor, Coffin, and Fisher (Total strain and compressibility) provide an adequate solution for materials which obey the maximum shear strain energy theory of failure. All gun steels are probably governed by this flow condition.

(iv) Sopwith, (Total strain and compressibility) using the maximum shear stress theory of failure, presents an accurate solution in closed form. His work is applicable to mild steel cylinders. This is clearly shown in Part II of this thesis.

(v) Cook (Total strain and incompressibility) treats the flow condition which commences at an upper shear stress and continues at a lower one. The theory provides an excellent flexible framework for the fitting of experimental results.

## 2. Relating to Interference Fits

(i) There is the need for an interference fit analysis to include overstraining in the scantlings. Lame's theory is restricted to elastic strains.

(ii) Rankin's elastic analysis of shrink fits with protruding shafts shows the effect of the shaft extension on the interface pressure to be negligible if  $L/d > \frac{1}{2}$ . In the author's experimental work of Part III,  $L/d = \frac{11}{12}$ .

(iii) Goodier's analysis of frictional forces at the interface in a shrink fit assembly provides information of a qualitative nature. The tendency of the frictional forces is to increase the interface pressure and the hoop stress in the hollow member. It is unlikely that this effect will be large when the coefficient of friction is small, e.g. when surfaces are machined and well lubricated.

PART II

THICK-WALLED CYLINDERS UNDER INTERNAL FLUID PRESSURE

## I. WORK OF PREVIOUS EXPERIMENTERS

### 1. Experimental Techniques and Specimens - MACRAE, COOK

Table II is constructed to compare the techniques employed by Macrae and Cook.

#### (i) Application of Fluid Pressure

Fig. 20 shows Macrae's arrangement for applying internal pressure to a test cylinder. It consists of compressing fluid trapped in the cylinder by means of a hydraulic press. The arrangement approximates to open-end conditions, in which the only axial restraint is due to friction at the packings.

Cook favours the use of an intensifier which he designed to hold the load for the high pressures. It could, of course, be used on cylinders which have either open or closed ends.

The former method is probably the simpler of the two. The prevailing factor in a decision as to their relative merits would be the sensitivity of the pressure control. No mention of this is made by either of the investigators, but it is probable that Cook's intensifier would more accurately control the application of pressure.

#### (ii) Fluid Pressure Medium

Macrae made some preliminary tests to aid in the selection of a suitable pressure medium. A fluid with the following properties is desirable: -

- (a) High compression modulus
- (b) No undue increase in viscosity at high pressure
- (c) No corrosive action on the metal surfaces

It was shown that glycerine and castor oil are the most suitable. If used in temperatures near 0° C, glycerine will crystallize at pressures above 105,000 lbs./in.<sup>2</sup> A mixture of 10 % water and 90 % glycerine may be used for the higher pressures.

TABLE II

<u>Ref. No. in Text</u>	<u>Experimental Techniques</u>	<u>INVESTIGATORS</u>	
		<u>Macrae</u> (25)	<u>Cook</u> (9)
(i)	<u>Application of Fluid Pressure</u>	Hydraulic Press and Plungers see Fig. 20	Intensifier
(ii)	<u>Fluid Pressure Medium</u>	Commercial Glycerine	<u>Either</u> (a) Pure Glycerine or (b) Castor Oil
(iii)	<u>Seals</u>	See Fig. 20 (Open-Ends)	Cylinder Ends Screwed and Caps Fitted. (Closed-Ends)
(iv)	<u>Pressure Measurement</u>	See Fig. 22	Specially Constructed Bourdon Gauge
(v)	<u>Outside Diametral Strain Measurement</u>	Micrometer (Gauge Diam. 6")	Specially Designed Extensometer See Fig. 25 (Gauge Diam. 5/4")

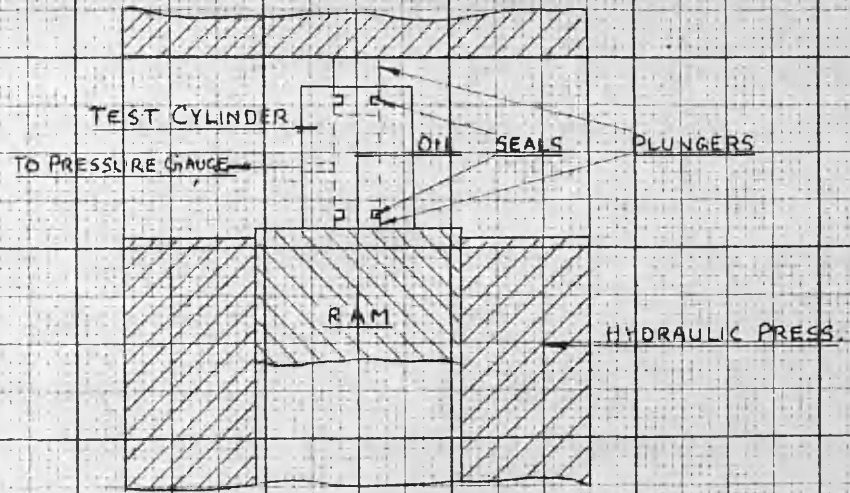


FIG 20-MACRAE'S ARRANGEMENT FOR APPLYING INTERNAL PRESSURE TO A THICK-WALLED CYLINDER

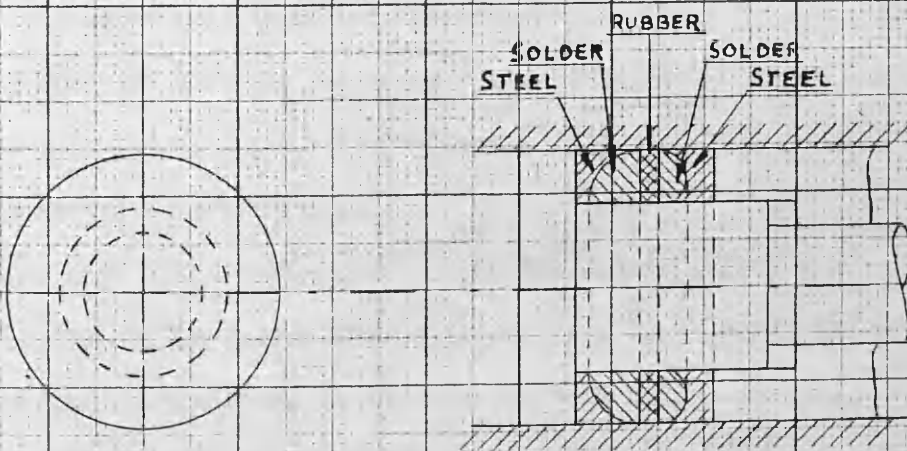


FIG 21-MACRAE'S SEAL USED ON PLUNGERS

### (iii) Seals

The seals on the plungers in Macrae's apparatus are the type shown in Fig. 21. They are complicated to construct and may introduce an excess of axial friction.

The closed ends of Cook's cylinders are screwed and capped. No sealing difficulties arise in this case.

### (iv) Pressure Measurement

The gauge used by Macrae was designed in the Royal Arsenal and its principle may be seen from Figs. 22 (a) and (b). Fluid from the cylinder enters a chamber A in the block. A suitably designed plunger B transmits a load (proportional to pressure) through a system of knife-edged supported levers, to a spring balance. A pointer moves over a circular dial on the balance to record pressure when the instrument is calibrated. Calibration is performed by removing the plug F and inserting another plunger similar to B. The new plunger is connected through stirrups to an accurate beam-type weighing machine held in a vertical position by a pulley arrangement (Fig. 22(b)). Macrae does not discuss the accuracy of this instrument.

Cook used a specially constructed Bourdon Gauge, in which the pivots are mounted on jewels to reduce friction. Calibration, before and after each test, is a necessary precaution. A dead-weight calibrator was used. Cook points out that in high pressure gauges of this type, elastic hysteresis effects may be appreciable. Hence, readings will be accurate for pressure changes in the same direction as the calibration run, but will be high for the reverse direction. The gauge used on tests recorded a maximum pressure of 20 tons/in.<sup>2</sup> (44,800 lbs./in.<sup>2</sup>) and read correctly to  $\pm .01$  tons/in.<sup>2</sup> ( $\pm 22 \cdot 4$  lbs./in.<sup>2</sup>).

It is apparent that Cook's method of measuring pressure is much simpler and probably more accurate. The Bourdon gauge, however, is limited to pressures of

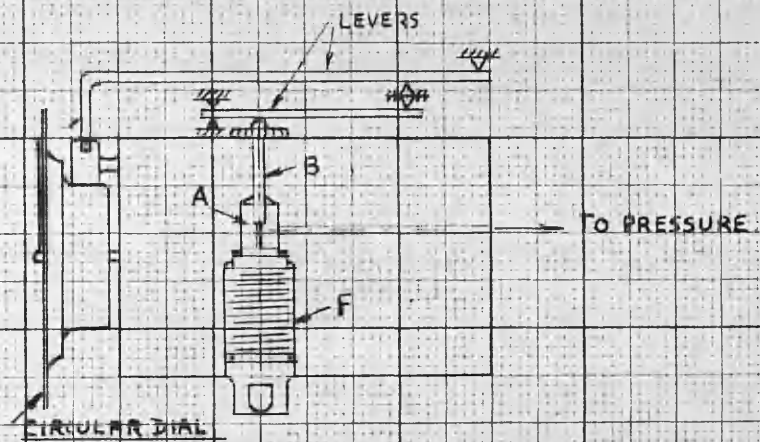


FIG 22(a) SCHEMATIC ARRANGEMENT SHOWING THE PRINCIPLE OF MACRAE'S PRESSURE GAUGE.

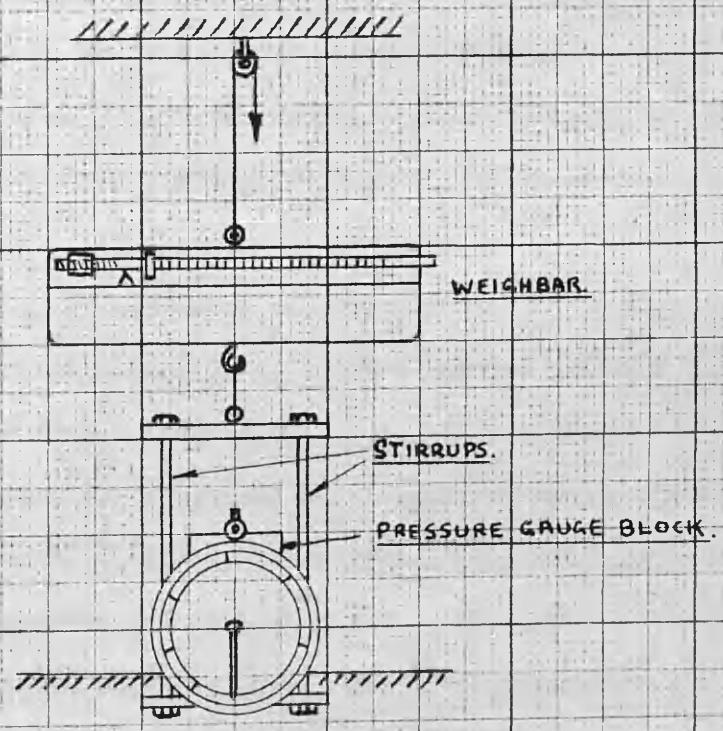


FIG 22(b) CALIBRATOR RIG FOR MACRAE'S GAUGE

the order of 50,000 lbs./in.<sup>2</sup> Macrae's instrument, on the other hand, may be used for higher pressures and inconvenience and inaccuracy are compensated by the larger range.

Bridgman measures pressures by a method which is both convenient and accurate. In principle, the change in resistance of a coil of wire with pressure is utilized. It is customary to use manganin wire which gives a linear relation between the two variables. High-pressure physicists use this method exclusively, but calibration of the wire presents a problem, when suitable apparatus is not available.

#### (v) Outside Diametral Strain Measurements

Macrae employed skilled men to use micrometers for the measurement of outside diameter changes. They exercised the utmost caution by using height blocks and scribing lines on the cylinder surface, to insure that measurements were made at the same places.

Cook's instrument (Fig. 23) deserves special mention. It consists of a pair of diametral extensometers (A and B) so constructed and arranged that the frame of one passes through that of the other, thus enabling them to be located in the same plane. A combination of optical and mechanical levers permits a change of the order of  $0.5 \times 10^{-6}$  inch to be observed. The axial extensometer shown at C is arranged to measure the extension over 2-1/4 inches. In the figure, the upper and lower attachments only are shown, but the construction is sufficiently obvious.

A comparison of the accuracy of the two methods is shown in Table III. They are both compared with the electrical strain-gauge which is used in tests presented later in this thesis. It is seen that Cook's measurements are the most reliable and that electrical strain-gauge measurements are close to accuracies obtained by the careful use of a micrometer.

TABLE III

Method of Strain Measurement	Micrometer (Macrae)	Extensometer (Cook)	Electrical Strain Gauge
Diameter on which measurements are made (inches)	6	.75	----
Accuracy of Gauge (% Strain)	.0017	.000067	.0020

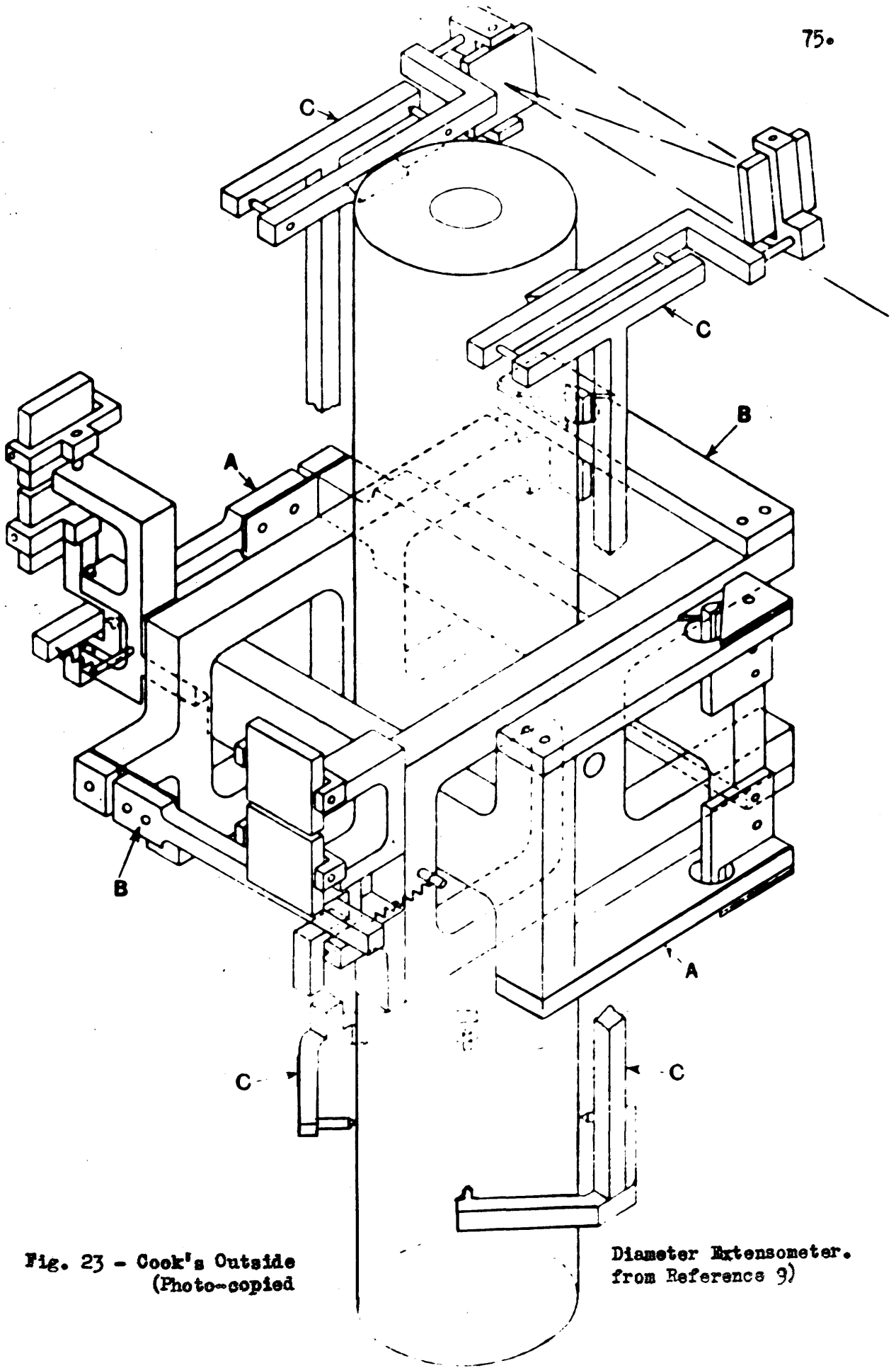


Fig. 23 - Cook's Outside  
(Photo-copied

Diameter Extensometer.  
from Reference 9)

It has been found necessary to measure changes in dimension across at least two diameters at right angles to each other. Cook points out that measurements across a single diameter are sufficient if all the material is elastic. When, however, overstrain begins at the internal surface, the symmetry is usually disturbed so that different diameters extend by unequal amounts. He states that variations at the external surface are quasi-elliptical in shape, although of extremely small eccentricity, and the average diametral extension is obtained with sufficient accuracy as the means of measurements made on a pair of diameters at right angles to each other and in the same plane.

In carrying out a test, Cook allowed ten minutes between each observation to observe or allow for any creep. He experienced difficulty in controlling the pressure within sufficiently close limits in some cases. Macrae examined the effect of creep at the high pressures and showed it to be negligible. His tests were performed on cylinders of gun steel.

#### (vi) Specimens

Care must be exercised in the design and preparation of specimens. The effect of the ends will influence diametral extensions if the length does not exceed a certain minimum. This, according to Cook, is somewhat less than three diameters. No definite limiting ratio of length to diameter is known, however, since the need to restrict the length has not been apparent where outside diametral changes only are measured. If bore strains are to be gauged, the accessibility of the central bore surface will control the length of the cylinder and may reduce the  $L/d$  ratio to a questionable value. Figs. 24 (a) and (b) show the type of specimen used by Macrae and Cook respectively.

Macrae's cylinders were machined from a gun-steel forging, manufactured and treated to pass a service specification. Tensile tests were made of several test pieces cut tangentially from discs parted off one or both ends of the forging. In

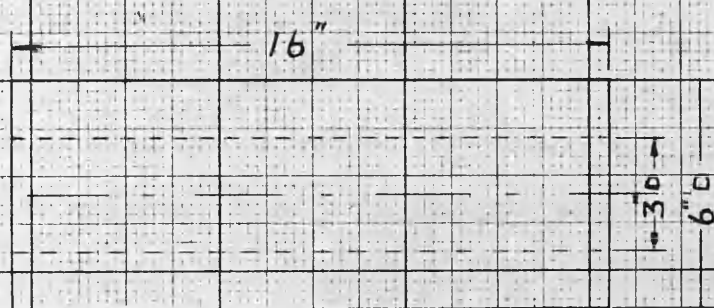
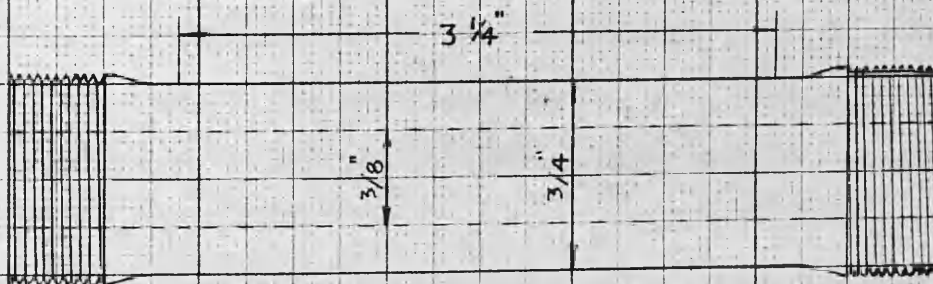
(a) MACRAE(b) COOK

FIG. 24 - SPECIMENS USED BY MACRAE AND COOK

the machining and subsequent treatment of specimens, he was merely assimilating material specifications of gun barrels in service. Cook, however, prepared his specimens in a more scientific manner. He placed emphasis on: -

- (i) Concentricity of external and internal surfaces.
- (ii) Bores free from scratches and tool marks.
- (iii) Normalization of material (in vacuo) after machining.

It is of interest to examine the necessity for such precautions. Cook's specimens were small compared to Macrae's, and possible scale effect would seriously detract from the value of his observations. Further reference is made to this under "Results". Cook, also, cut tensile test pieces from the bar material between the center and the outside diametral surface, so as to coincide in position, as far as possible, with that of the material in the cylinders.

## 2. Results (MACRAE) and Discussion

In Fig. 25 results for three cylinders ( $k = 2$ ) are compared with the open-end theories examined in the first part of this review. Two of the cylinders were tested for a low autofrettage pressure and experimental points do not cover the full range of the curves. The nickel gun steel results, however, are taken from a test proceeding to 6 % strain at the bore. Three facts are significant from a study of Fig. 25: -

- (a) Close agreement with elastic theory in all cases. This shows the dependability of his method of testing and measurements of pressure and strain, if elastic theory is assumed to be correct.
- (b) In the overstrained region, observations may follow either the upper or lower curve, depending on the material used. Points for the nickel-chromium - molybdenum steel would seem to favour Von Mises' flow condition, although conclusive evidence is not forthcoming owing to the limited range of the results. The other two steels definitely favour the curve constructed on the maximum shear

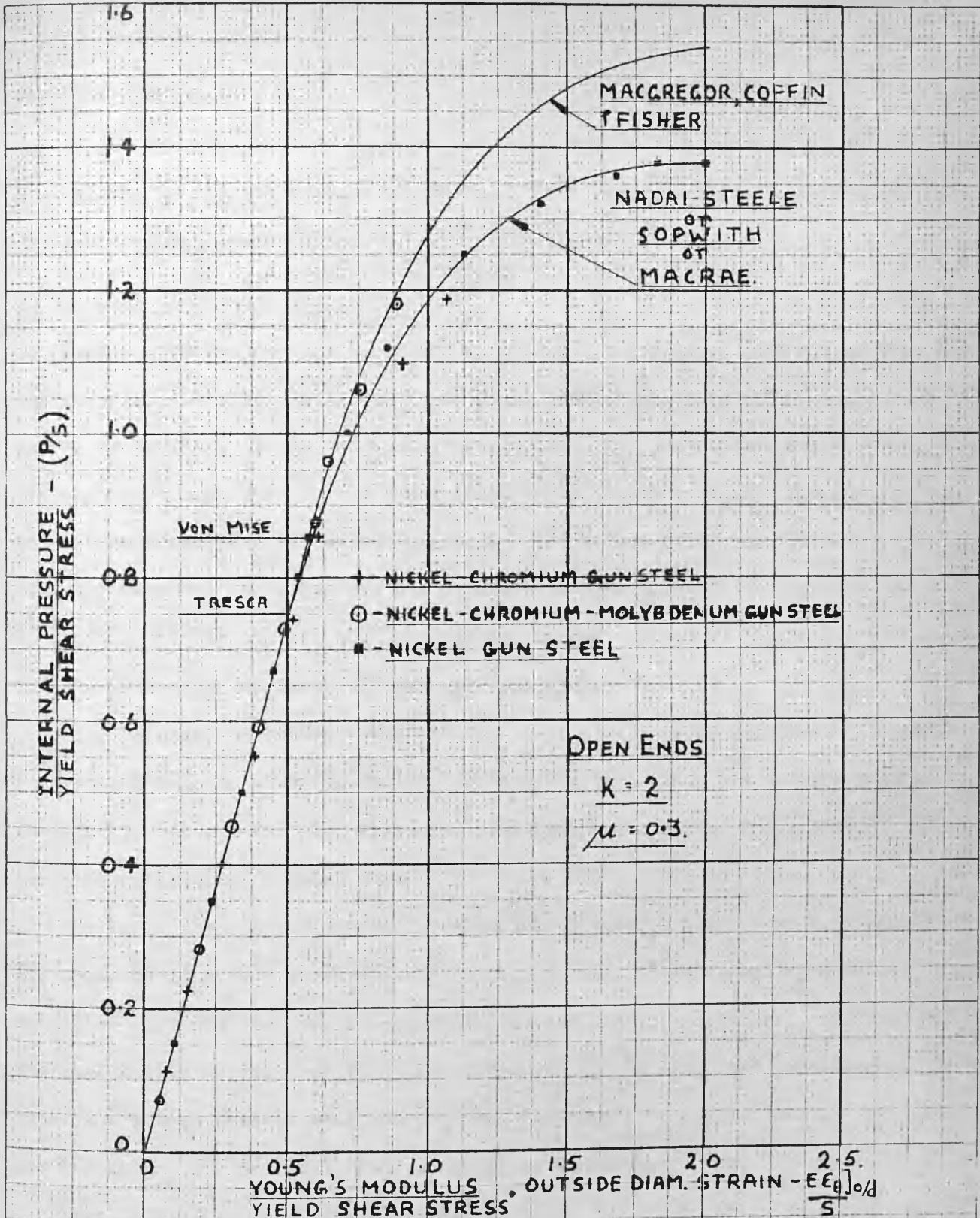


FIG. 25-MACRAE'S EXPERIMENTAL RESULTS COMPARED WITH THEORIES USING FLOW CONDITIONS OF:-

- (i) MAXIMUM SHEAR STRESS,
- (ii) MAXIMUM DISTORTION ENERGY.

stress hypothesis.

(c) It was shown by these investigations that release of bore pressure is accompanied by elastic release of strains. This fact simplifies calculations for residual stresses and strains.

### 3. Results (COOK) and Discussion

Cook's experiments were performed on mild-steel cylinders with closed ends and the material exhibited upper and lower yield points when carefully prepared and tested in tension. It is seen from results (Fig. 26) that this phenomenon has its counterpart in the two and three dimensional stress problem. The results will be analyzed from two points of view: - (a) by accepting the existence of such a phenomenon and repeating the arguments in the theoretical approach (Part I, section III (6)) to fit the experimental curve, and (b) by discussing reasons for the phenomenon in terms of the specimens used.

Fig. 26 shows in dotted lines the two theoretical curves constructed from the theoretical outline given in Part I, section III (6). They are not the same as in Fig. 13, but are for the closed-end condition and a value of  $\bar{s}/s$  of 1.52. This ratio is obtained as follows: -

The lower shear stress value is taken from a tension test to be 8.55 tons/in.<sup>2</sup> The upper shear stress in the tension test, however, is dependent on several variables which may not be reproduced in the testing of a cylinder. In fact, if the qualitative argument of Part I, section III (6) is used, the relationship between  $\bar{s}$ 's from tensile test and cylinder test would be obscure and at this stage the two values may be considered as having no connection. Thus, the value of  $\bar{s}$  is obtained from cylinder test results and is 13 tons/in.<sup>2</sup> It is recalled that  $\bar{s}$ , the elastic breakdown shear stress at the elastic-plastic boundary, may be considered a variable as the plastic front is propagated. The dotted line curves of Fig. 26 refer to the two extreme variations of  $\bar{s}$  discussed in Part I, section III

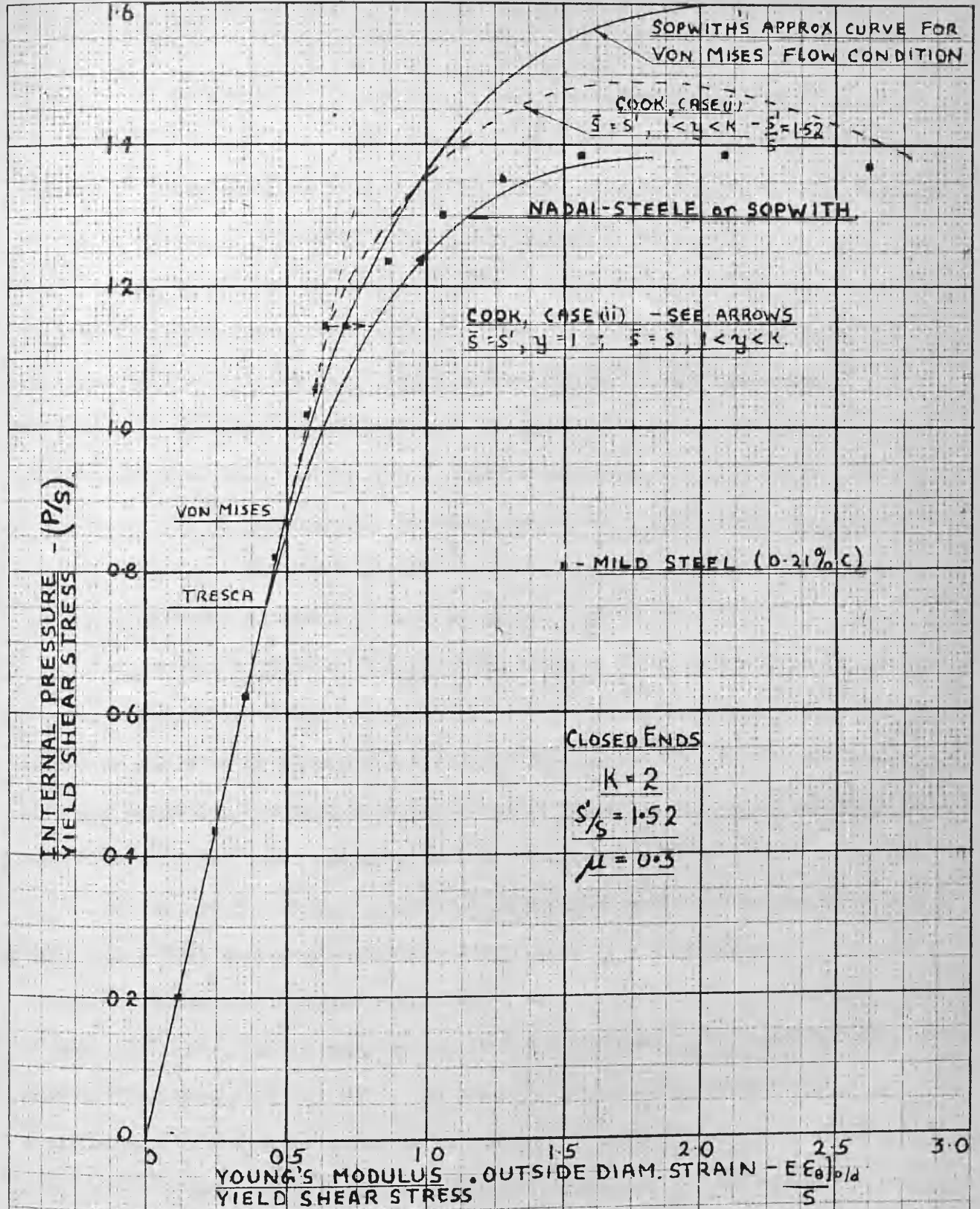


FIG.26-COOK'S EXPERIMENTAL RESULTS COMPARED WITH THEORIES USING FLOW CONDITIONS OF (i) MAXIMUM SHEAR STRESS AND (ii) MAXIMUM DISTORTION ENERGY AND (iii) ASSUMING TWO EXTREMES IN VARIATION OF YIELD SHEAR STRESS AT PLASTIC-ELASTIC BOUNDARY.

(6). It is obvious from results that intelligent selection of the  $\bar{s}$  variable could fit the experimental curve closely. This variable will conform more to Fig. 9 (c) variation than to Fig. 9 (b). Cook actually found  $\bar{s}$  to vary approximately according to the dotted line shown in Fig. 9 (c).

It would be radical to attempt to link Cook's results for initial stages of plastic flow with the curve constructed from the distortion energy theory of failure. A closeness to it is recognized at one point, but the value of  $\bar{s}$  is dependent on an effect which is random in character and the equivalence to a certain value of shear stress is the simpler approach. It is possible that in the future, the phenomenon will be accounted for on a statistical basis where the several effects of wedges, randomly orientated in space, will be integrated and explained in terms of average stresses in the principal directions.

A further examination of the specimens used by Cook, will assist in accounting for the results of his experiments. It is considered unlikely that the upper and lower yield point characteristic would be observed if the cylinder bores had not been carefully machined with consequent elimination of tool scratches. Also, such fine finishes would not be practical on say Macrae's cylinders, which had bore diameters of 3 inches. In general, a cylinder used in practice would not have such a fine surface finish and test results on mild steel cylinders under the more practical conditions would more likely conform to the theoretical curve of Sopwith. Thus, in the preparation of Cook's specimens, the scale effect variable has been reduced, but a new one, the counterpart of upper and lower shear stress in a tension test, is introduced. The deviation of experimental points from Sopwith's curve could be likened to an experimental error.

This does not detract from the value of the experimental results which are clearly the most accurate and important in this field.

#### 4. Conclusions from Work of Previous Experimenters.

(i) Relating to Experimental Techniques

(a) Strain measurements should be made across at least two diameters at right angles to one another and in the same plane.

(b) A carefully calibrated Bourdon Gauge is suitable for measuring pressures up to 50,000 lbs./in.<sup>2</sup> Beyond this, an electrical resistance gauge of the type used by Bridgman is the most feasible.

(ii) Relating to Experimental Results

(a) Macrae's results agree well with Sopwith's theory which is based on a maximum shear stress flow condition.

(b) The type of yielding which mild steel characterises, gives rise to outside diameter deflections not wholly in agreement with Sopwith. Cook explains the discrepancies by introducing the counterpart of upper and lower yield points in a tension test.

(c) It is essential to measure the actual strains existing at the bores of mild steel thick-walled cylinders in order to further examine the effects registered at the outside diameter.

## II. AUTHOR'S INVESTIGATIONS

### 1. Apparatus

The apparatus is designed to apply internal fluid pressures to "open-ended" thick-walled cylinders. In principle a fluid is confined inside the test cylinder and compressed by means of a plunger and loading machine.

Fig. 27 shows the assembled arrangement in section. It consists of a central core A which fits inside the test cylinder. A is built in two parts connected by a screw thread. This enables the core to be fitted without interference to gauges on the inside of the cylinder. Synthetic rubber O-ring seals at B and C prevent leakage at the ends. A plunger operates in the hole D and connecting holes E and F allows the system to be filled with a fluid. A load on the plunger compresses the fluid which transmits a pressure to the insides of the test cylinder. An O-ring seal G on the plunger and a Neoprene washer H at the screw-thread ensure a leakage free system. J is a pressure gauge pipe connection. At K, two of eight units (2 per flat) are shown. They are set in the core to convey electrical leads from strain gauges used on the test cylinder. The load is transmitted from a compression machine to the plunger via a spherical head L.

The pressure gauge pipe connection is shown in detail in Fig. 28. It makes use of the "unsupported area" principle originated by Bridgman.

Fig. 29 shows in detail the method of removing electrical leads from the fluid pressure. The units were designed and manufactured in the work shops of the Theoretical and Applied Mechanics Department of the University of Illinois. They operated with complete success. Previously, commercially sold glow plugs for model diesel engines had been used but they proved unreliable.

Given a sufficiently strong test cylinder failure of the apparatus will probably be governed by the O-ring seals. The writer has successfully used these

**Fig. 27 - SECTIONAL ARRANGEMENT OF PRESSURE APPARATUS.**

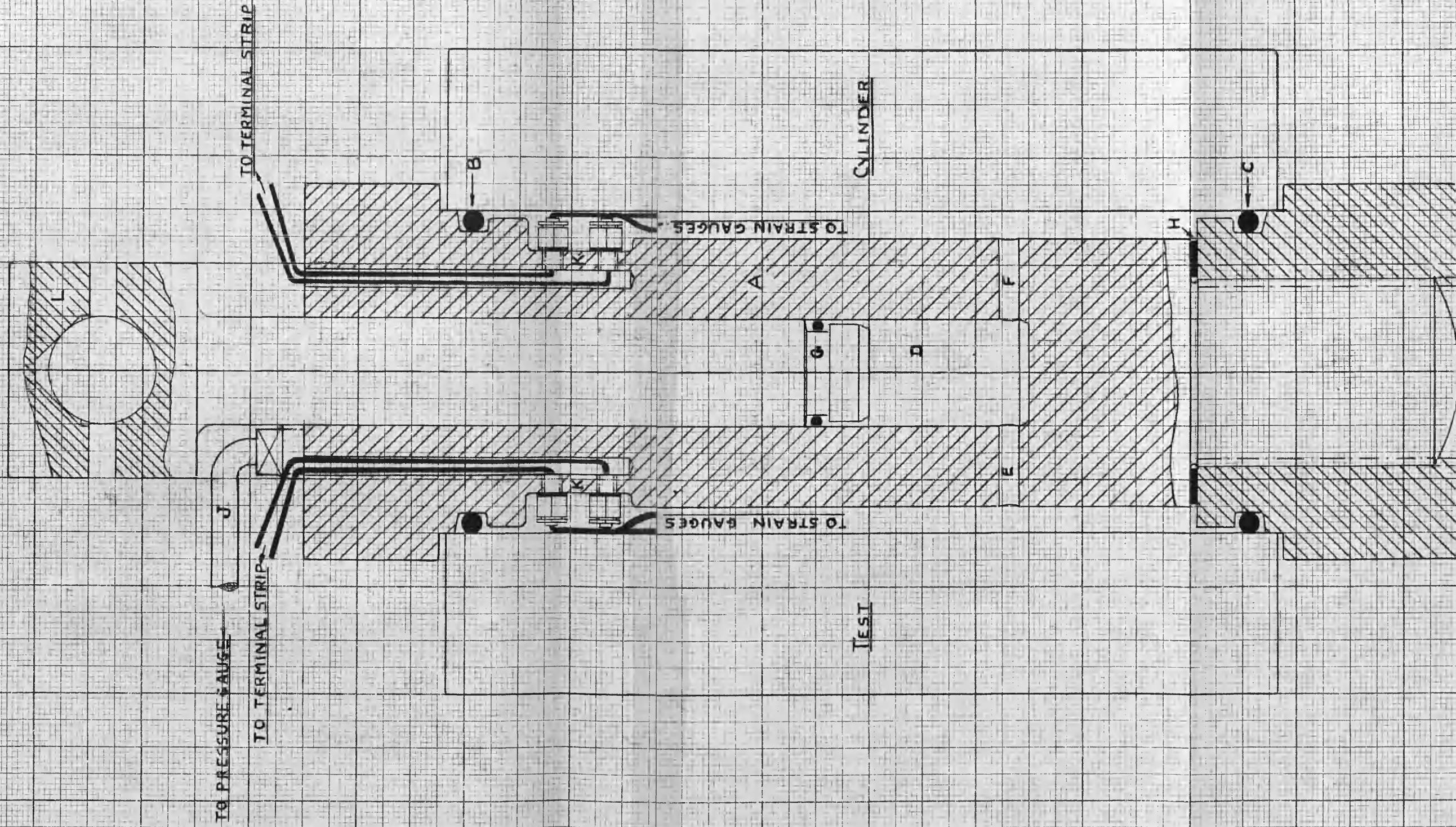


FIG 27. SECTIONAL ARRANGEMENT OF PRESSURE APPARATUS.  
(FULL SIZE)

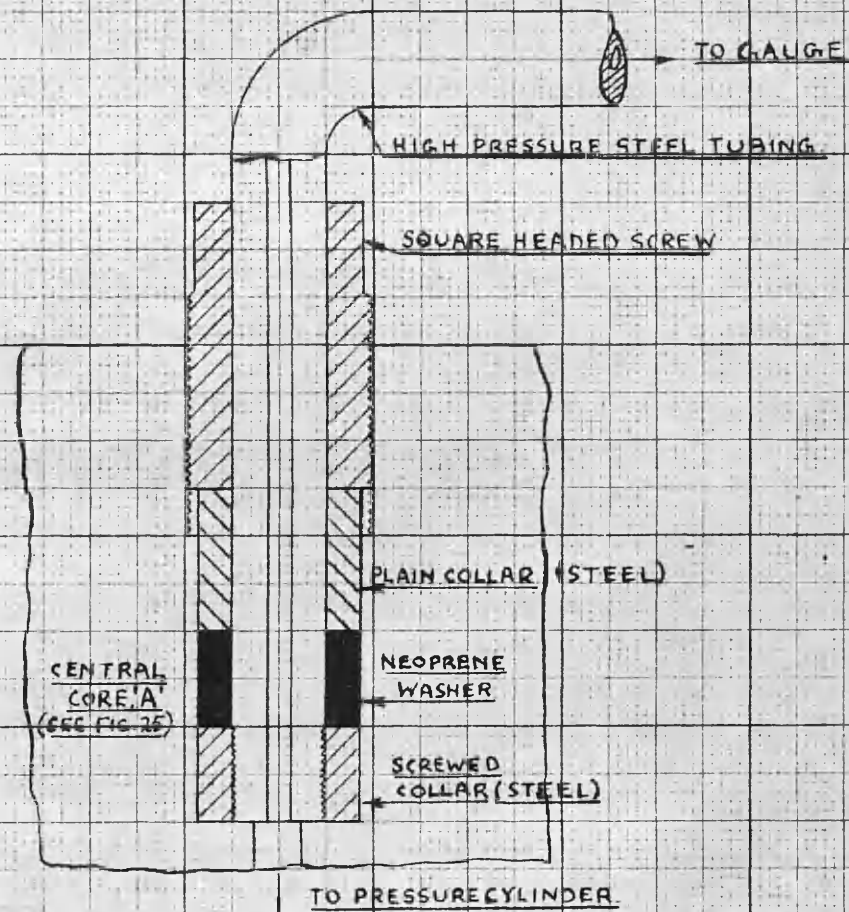


FIG. 28 - DETAIL OF PRESSURE GAUGE PIPE CONNECTIONS  
(TWICE FULL SIZE)

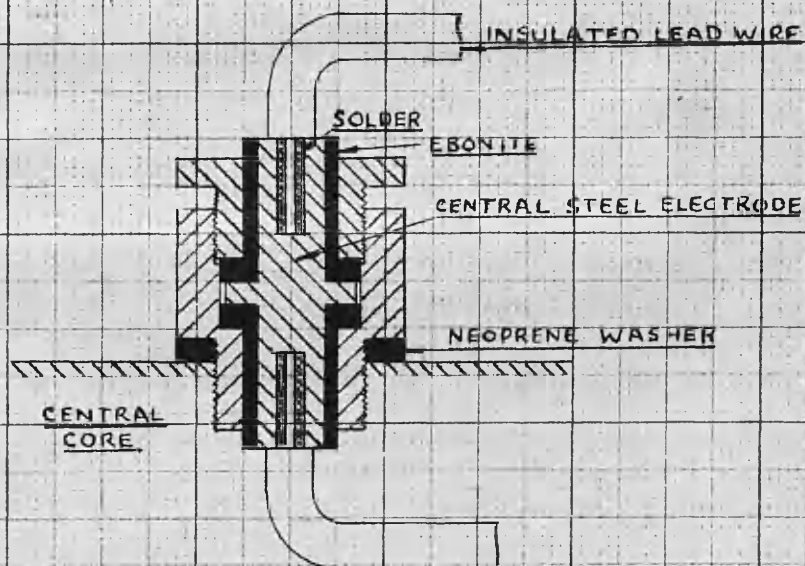


FIG. 29 - DETAIL OF UNIT FOR REMOVING ELECTRICAL LEADS  
FROM CYLINDER - (FOUR TIMES FULL SIZE)

seals up to 25,000 lbs./in.<sup>2</sup> The radial gap is kept as small as possible to prevent extrusion. The core is designed for strength to withstand a pressure of 80,000 lbs./in.<sup>2</sup>

The compressibility of the fluid -- transformer oil -- controls the travel of the plunger. The plunger diameter is fixed by strength considerations in the core and its length determined to provide sufficient travel to reach a pressure of 80,000 lbs./in.<sup>2</sup>

The core is machined from a medium carbon steel which is oil quenched at 1500° F after rough machining. Subsequently, the part is soaked at 300° F for 3 hours.

The placing of the pressure gauge tapping at the highest point in the core simplifies the filling of the system with fluid. It is advisable to bleed both ends of the pressure gauge pipe when the system is under a small pressure. If the system is now topped up the equipment is ready for use.

It is seen that the test cylinder moves axially against a slight amount of friction at the O-rings. The open-ended condition of testing is closely assimilated. The ratio of cylinder length under pressure to total cylinder length is as high as .9375.

Figs. 30 and 31 show photographs of the apparatus before and after assembly.

## 2. Measuring Devices

### (1) Fluid Pressure

A 25,000 lbs./in.<sup>2</sup> Bourdon gauge measures pressure. Its smallest division reads 100 lbs./in.<sup>2</sup> and an estimation correct to 20 lbs./in.<sup>2</sup> may be made.

The gauge is calibrated against a dead weight calibrator of standard principle. The latter was built to a specification issued by the M.I.T. and its accuracy is adequate.



Fig. 30 -- THICK-WALLED CYLINDER APPARATUS -- BEFORE ASSEMBLY.



Fig. 31 - THICK-WALLED CYLINDER APPARATUS - AFTER ASSEMBLY.

The calibration curve is shown in Fig. 32. One was made before and after a test but no difference is observed.

(ii) Strains

Electrical resistance type strain gauges are employed to measure strain. A standard Young's A.C. bridge circuit records strains in microinches per inch.

Gauges affixed on the outside of the cylinder, Fig. 33, are of the paper backed type of one inch gauge length. Standard procedure for mounting is observed.

It is found that paper backed gauges do not stand up to the high fluid pressures used in the test. Consequently bakelite gauges are employed to measure bore strain. Care is exercised in their mounting but no protection is given them from the fluid. Four are used, placed around the central circumference  $90^\circ$  apart, Fig. 33. Gauge lengths are  $1/4$  inch.

The technique in applying the bakelite gauges and also the effect of pressure on them has been studied in some preliminary work to be found in appendix A. This work consists of mounting gauges on rectangular strips and placing them in the fluid under pressure. Of the total recorded strain part is assumed due to pressure and part to the straining of the strip. The latter is calculated theoretically and hence the effect of pressure deduced. It is seen to vary slightly among gauges though in all cases a linear relationship with pressure is recorded up to the highest pressure of 25,000 lbs./in.<sup>2</sup> A 2:1 ratio mild steel cylinder is likely to be fully plastic at this pressure so the following plan is adopted: - The effect of pressure on gauges affixed to the bore of the cylinder is deduced by accepting Lamé's elastic line. Effects due to pressures causing plastic flow are found by extrapolation. This is considered safe because of the linear results of the preliminary tests.

The technique of mounting the gauges will be given in detail.

(a) Preparation of Surface

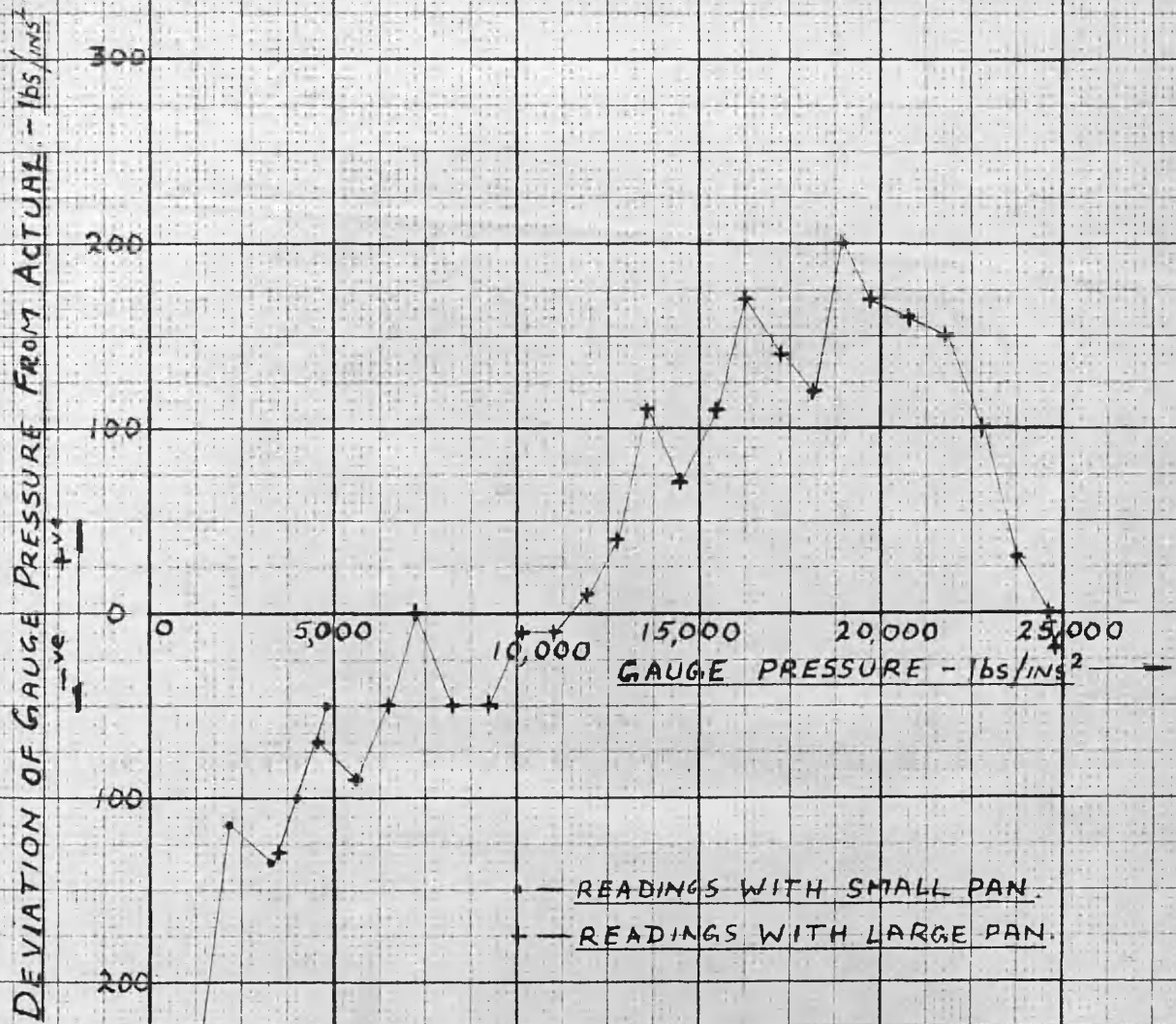


FIG. 32 — PRESSURE GAUGE CALIBRATION CURVE.

## CYLINDER

BORE - 3 INCHES

OUTSIDE DIAM. - 6 INCHES

LENGTH - 8 INCHES.

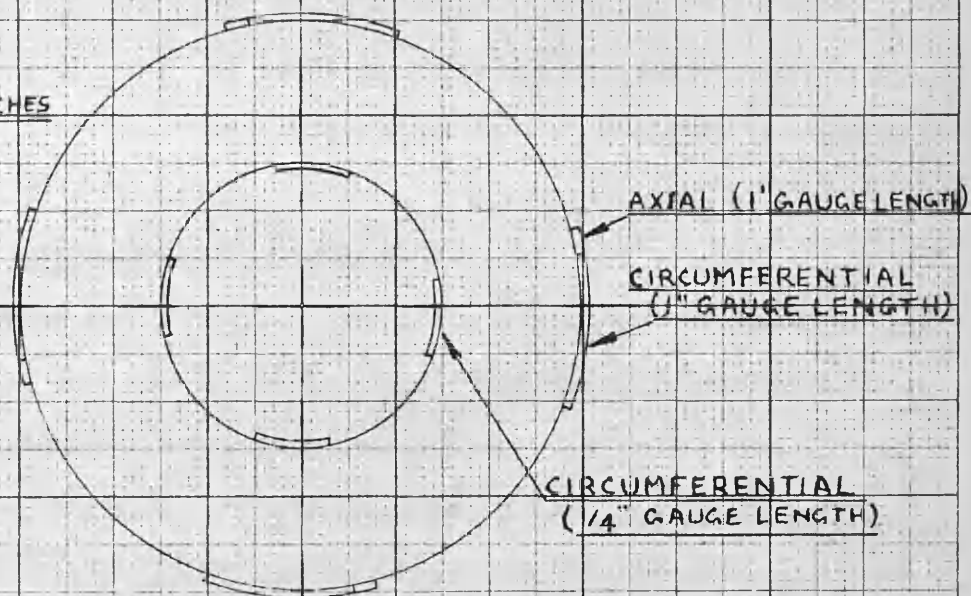


FIG. 33 - TEST CYLINDER SHOWING GAUGE LOCATIONS  
(HALF FULL SIZE)

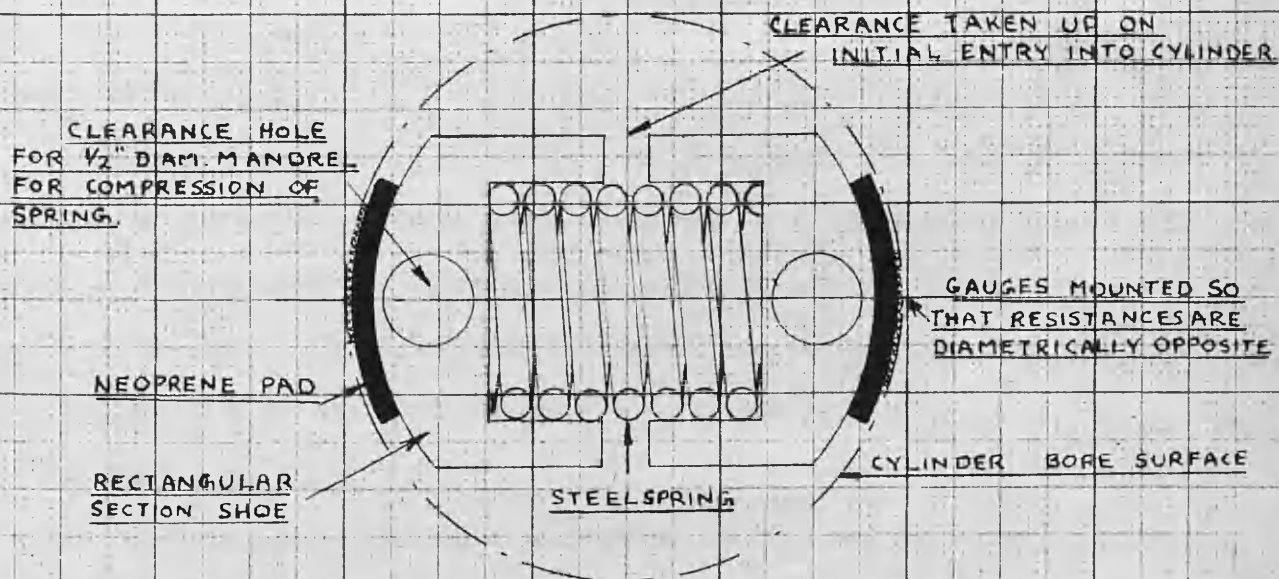


FIG. 34 - SYMMETRICAL SECTION (PERP. TO CYLINDER AXIS)  
OF SPRING DEVICE FOR THE MOUNTING AND  
CURING OF BAKELITE GAUGES (FULL SIZE)

All scale or rust removed and the surface roughened with medium grade emery paper. The surface is then carefully cleaned with acetone or alcohol to remove all possible traces of grease or oil.

(b) Preparation of gauges prior to mounting

In the curing sequence for bakelite gauges it is necessary to exert a uniform pressure on the gauge of from 100 to 200 lbs./in.<sup>2</sup> The spring loaded device shown in Fig. 34 is designed for this purpose and it is also useful in positioning the gauges in the cylinder. It is seen that gauges suitably positioned on the shoes of the spring loaded device can be mounted diametrically opposite in any desired location on the cylinder.

(c) Mounting of the gauges

Immediately prior to mounting, the metal surface and the gauge bonding surface are thoroughly cleaned with acetone or alcohol. Both surfaces are then thoroughly but thinly coated with a bakelite cement produced by the Baldwin Locomotive Company.

The spring loaded device is now compressed by means of a lever arrangement and slipped inside the cylinder. The shoes can be accurately positioned with regard to the cylinder and hence the gauges may be located in any desired location on the cylinder. Release of the levers mounts the gauge with the uniform pressure supplied by the spring holding them in place.

(d) Curing Treatment

The complete arrangement is placed inside an oven and subjected to baking of (i) One hour at 140° F; (ii) Two hours at 175° F; (iii) Two hours at 250° F. The cylinder is allowed to cool before removing the spring load.

The bakelite gauges are now firmly bonded and it is even found to be difficult to cut pieces off with a knife.

3. Specimens

The size of the specimen is shown in Fig. 33. The bore is 3 inches diameter and the length is restricted by the accessibility of the central section for the application of strain gauges.

The material is mild steel and the specimen is rough machined from a hot-rolled billet, annealed at  $1650^{\circ} F$  and cooled in the furnace, then finish machined to size.

Tensile tests of the material are made on three samples cut out from the billet circumferentially as shown in Fig. 35. In position the specimens correspond to the bore layers of the test cylinders. They are given the same annealing treatment. Twin Huggenberger extensometers, mounted diametrically opposite on the tensile specimens determine the values of Young's modulus. An ordinary dial gauge extensometer suffices to determine the yield points. Table IV gives the average material constants.

#### 4. Test Procedure

One bridge unit records the strains for the outside gauges and one for the bore gauges.

Readings of strain were noted at every 1000 lbs./in.<sup>2</sup> pressure increment until the plastic region was reached when increments were reduced to 500 lbs./in.<sup>2</sup>. Every pressure was held for 15 minutes. Where creep was evident readings were taken at 5 minute intervals. In one instance, at 17,000 lbs./in.<sup>2</sup>, the time interval was extended to 30 minutes to more fully study the effect of creep.

Zero readings for the outside gauges only were recorded on release of pressure. The bore gauges had been strained to destruction.

#### 5. Experimental Results

Figs. 36, 37 and 38 show the variations with pressure of outside diameter circumferential strain, bore circumferential strain and outside diameter axial

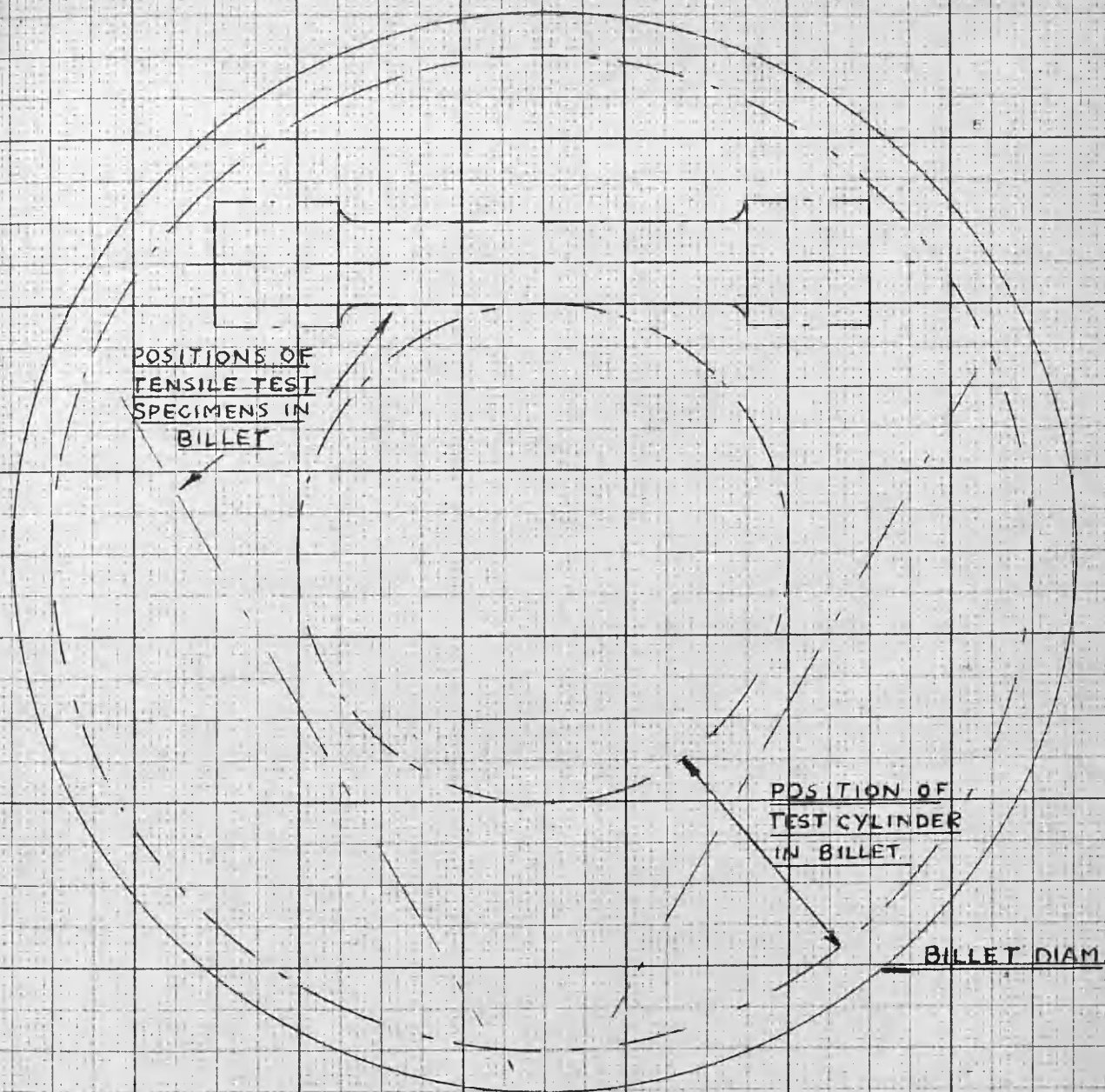


FIG. 35 - POSITION OF TENSILE TEST SPECIMENS CUT FROM BILLET. (FULL SIZE).

YIELD STRESS (2S)	25,000 lbs/IN <sup>2</sup>
ULTIMATE STRESS	55,500 lbs/IN <sup>2</sup>
YOUNG'S MODULUS (E)	28.97 X 10 <sup>6</sup> lbs/IN <sup>2</sup>
% REDUCTION IN AREA	45.4
% ELONGATION	29.7

TABLE IV - AVERAGE MATERIAL PROPERTIES OF TEST CYLINDER.

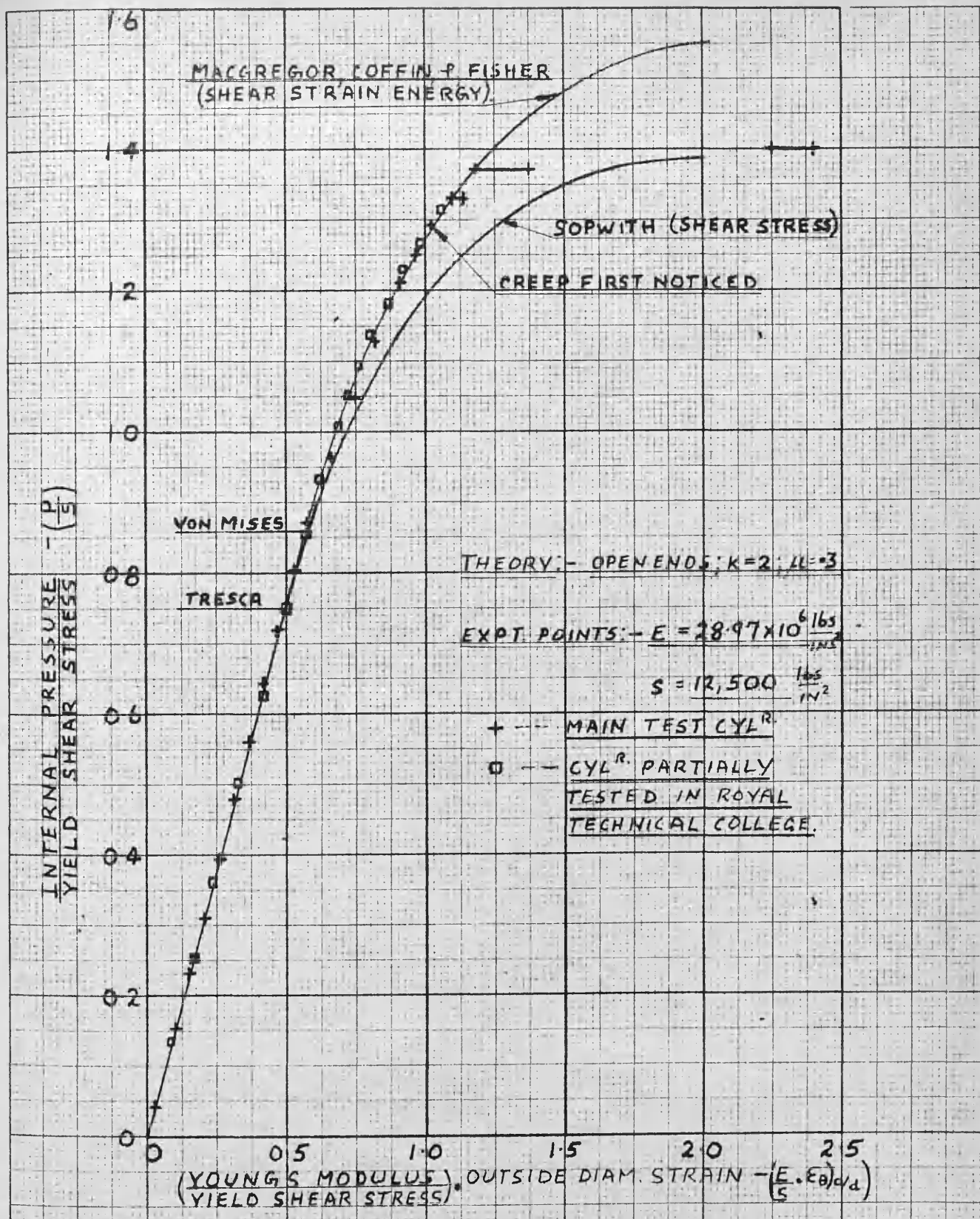


FIG. 36 - OUTSIDE DIAMETER CIRCUMFERENTIAL STRAINS

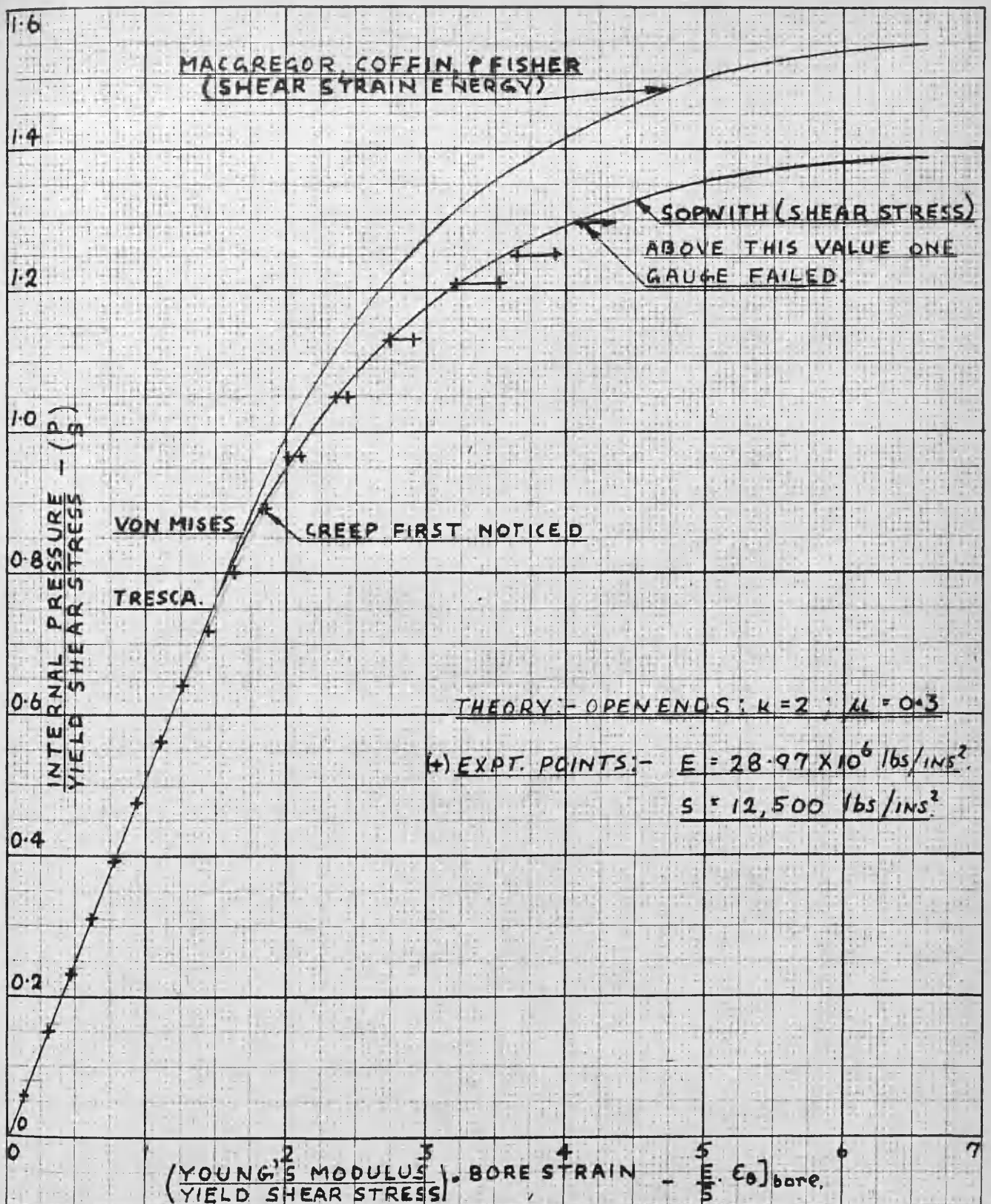


FIG. 3.7. — BORE CIRCUMFERENTIAL STRAINS.

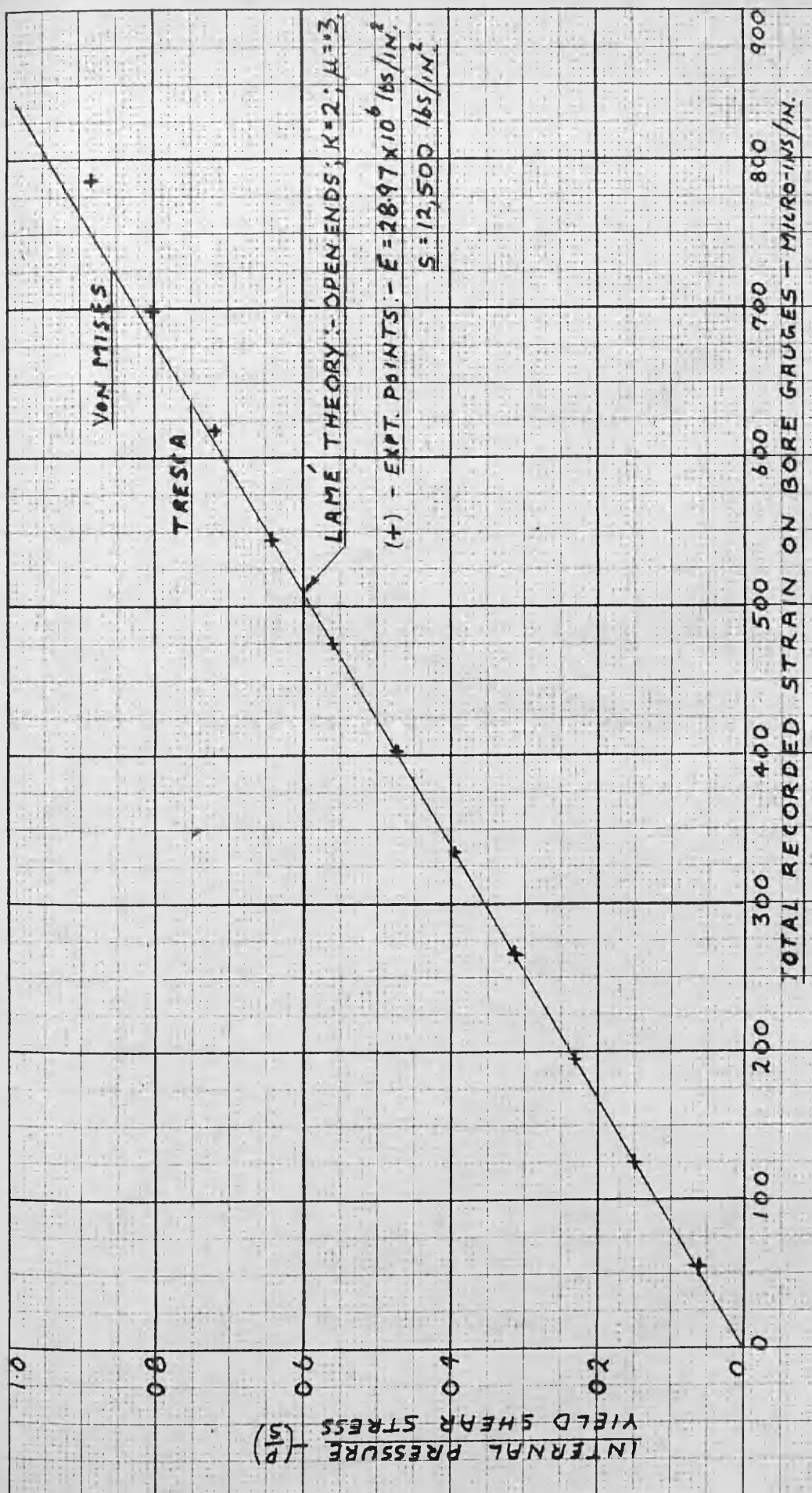


FIG. 37a. - BORE CIRCUMFERENTIAL STRAINS IN ELASTIC REGION; ESTIMATION OF PRESSURE EFFECT ON GAUGES.

NO. 1410 25 OLEFIN DRIFT PAPER 30 X 50 1/2 X 1 1/2

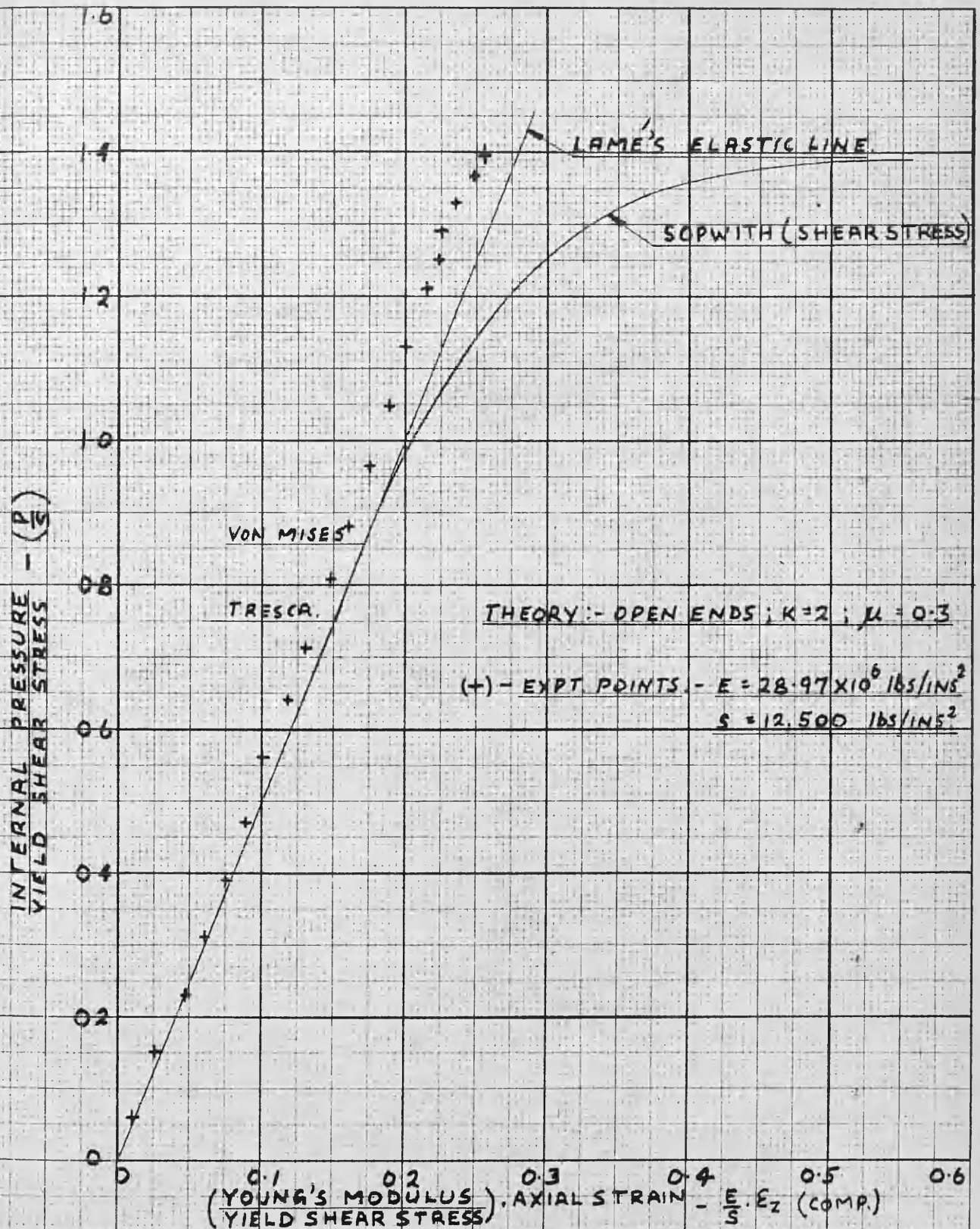


FIG. 38 — OUTSIDE DIAMETER AXIAL STRAINS.

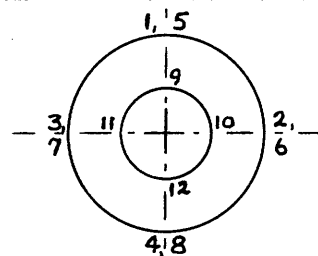
strain, respectively. Theoretical curves are shown by full lines and experimental data by points. Fig. 37a shows the elastic portion of Fig. 37 to an enlarged scale.

Table V is drawn up to illustrate the variation in a circumferential direction of the strain gauge readings for the above three variables.

Figs. 39 (a, b, c, and d) and 40 (a, b, and c) show the effect of time, for various steady pressures, on outside diameter circumferential strain and bore circumferential strain, respectively. Creep was not noticeable in the axial gauges, and on one of the bore gauges.

Gauge Press. in 1000 lbs/in <sup>2</sup>	Outside Diam. Circum. Strain -Microinches per Inch + <sup>ve</sup> (Tensile)				Bore Circum. Strain -Microinches per Inch + <sup>ve</sup> (Tensile)				Outside Axial Strain -Microinches per Inch + <sup>ve</sup> (Compressive)			
	1	2	3	4	9	10	11	12	5	6	7	8
1	19	19	21	17	58	47	56	59	4	2	6	4
2	42	43	44	41	132	121	125	130	10	11	13	12
3	64	65	66	63	198	191	193	198	16	16	21	20
4	85	88	92	86	273	257	262	269	25	23	26	25
5	110	111	114	110	346	330	334	337	30	30	34	30
6	133	134	136	134	416	396	401	404	39	35	41	36
7	155	158	158	158	489	464	473	475	45	42	44	43
8	180	180	183	179	562	533	541	546	49	49	50	51
9	202	204	205	203	638	601	606	619	57	55	58	55
10	228	229	233	229	727	678	684	704	65	64	63	61
11	254	257	257	258	828	759	761	791	70	68	70	68
12	283	285	287	287	-	-	-	-	74	73	78	77
13	318	325	319	322	1038	962	892	1104	80	78	79	81
14	343	358	353	355	1345	1107	935	1329	90	83	83	87
15	371	395	385	384	1745	1259	985	1559	97	87	89	94
15.5	387	417	407	396	1985	1437	1020	1862	101	89	91	101
16	415	430	437	416	2211	1697	1089	2072	106	91	88	102
16.5	471	446	476	436	2481	1893	-	2337	121	91	80	112
17	534	480	548	475	2828	2196	-	2642	128	94	76	124
17.5	894	918	720	1351	-	-	-	4769	198	46	-27	218

TABLE V - VARIATION CIRCUMFERENTIALLY OF STRAINS  
MEASURED IN THICK-WALLED CYLINDER.



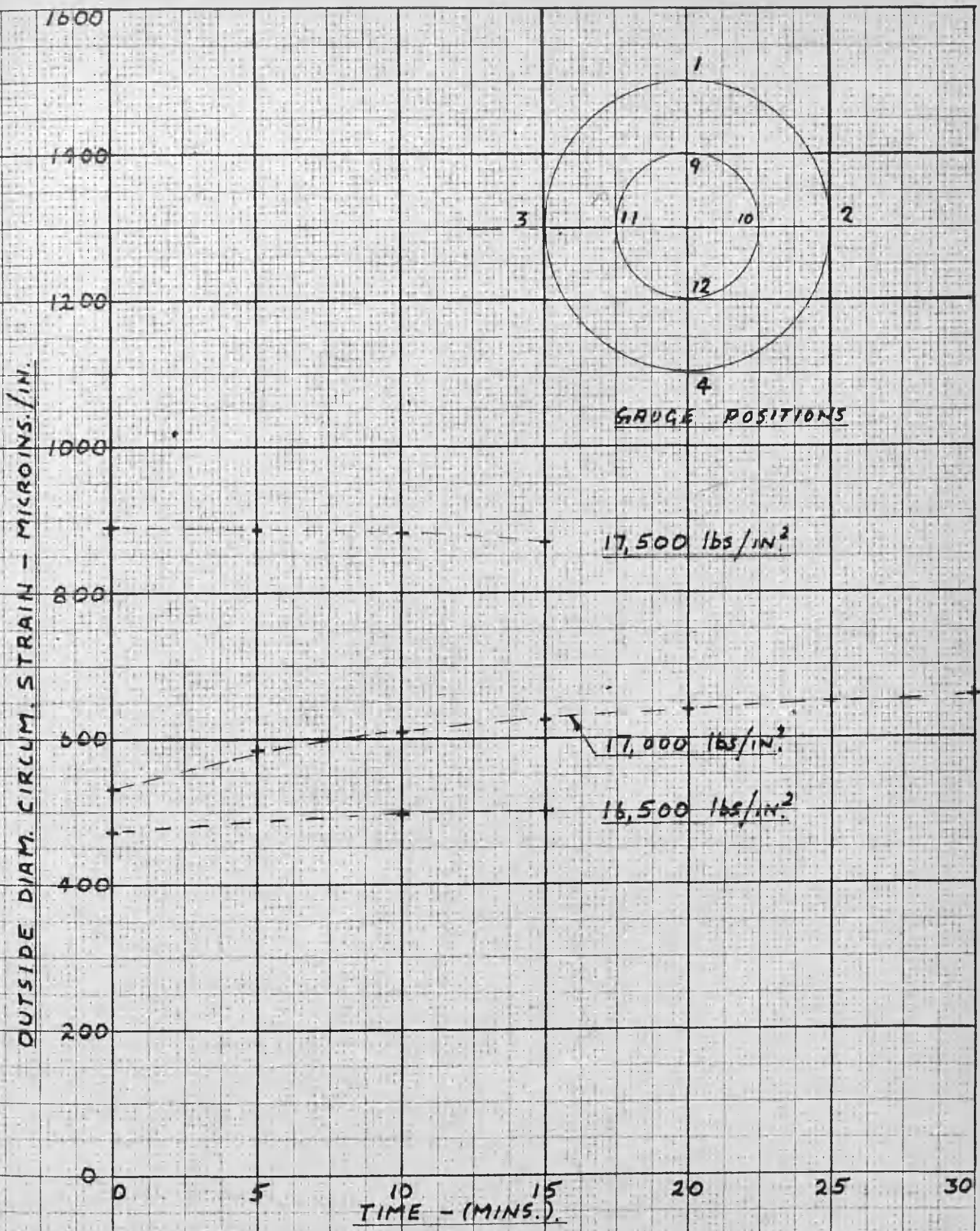


FIG. 39 a. — NO. 1 GAUGE CREEP FOR VARIOUS PRESSURES.

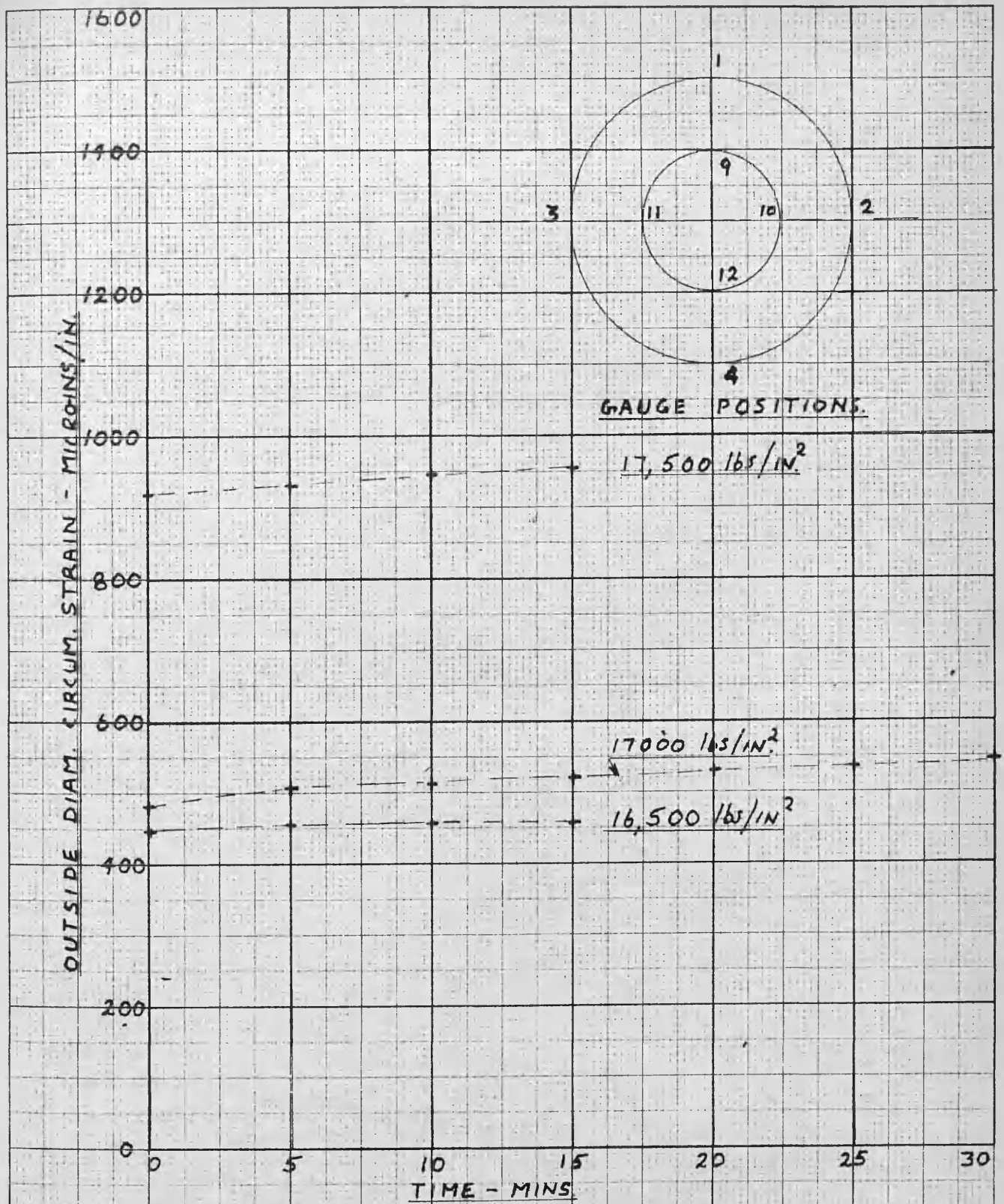


FIG. 39 b. - No. 2 GAUGE CREEP FOR VARIOUS PRESSURES.

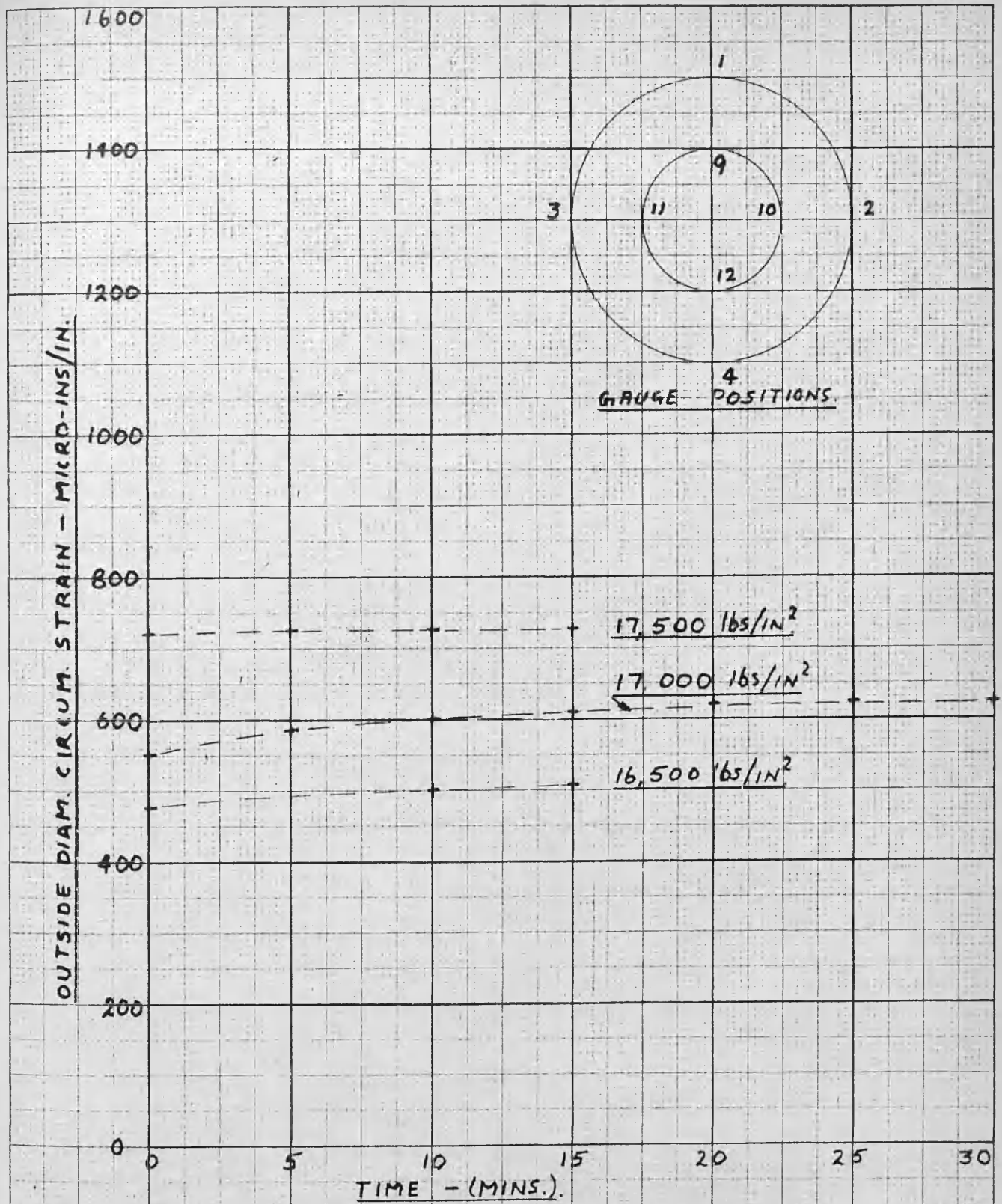


FIG. 39c - No. 3 GAUGE CREEP FOR VARIOUS PRESSURES.

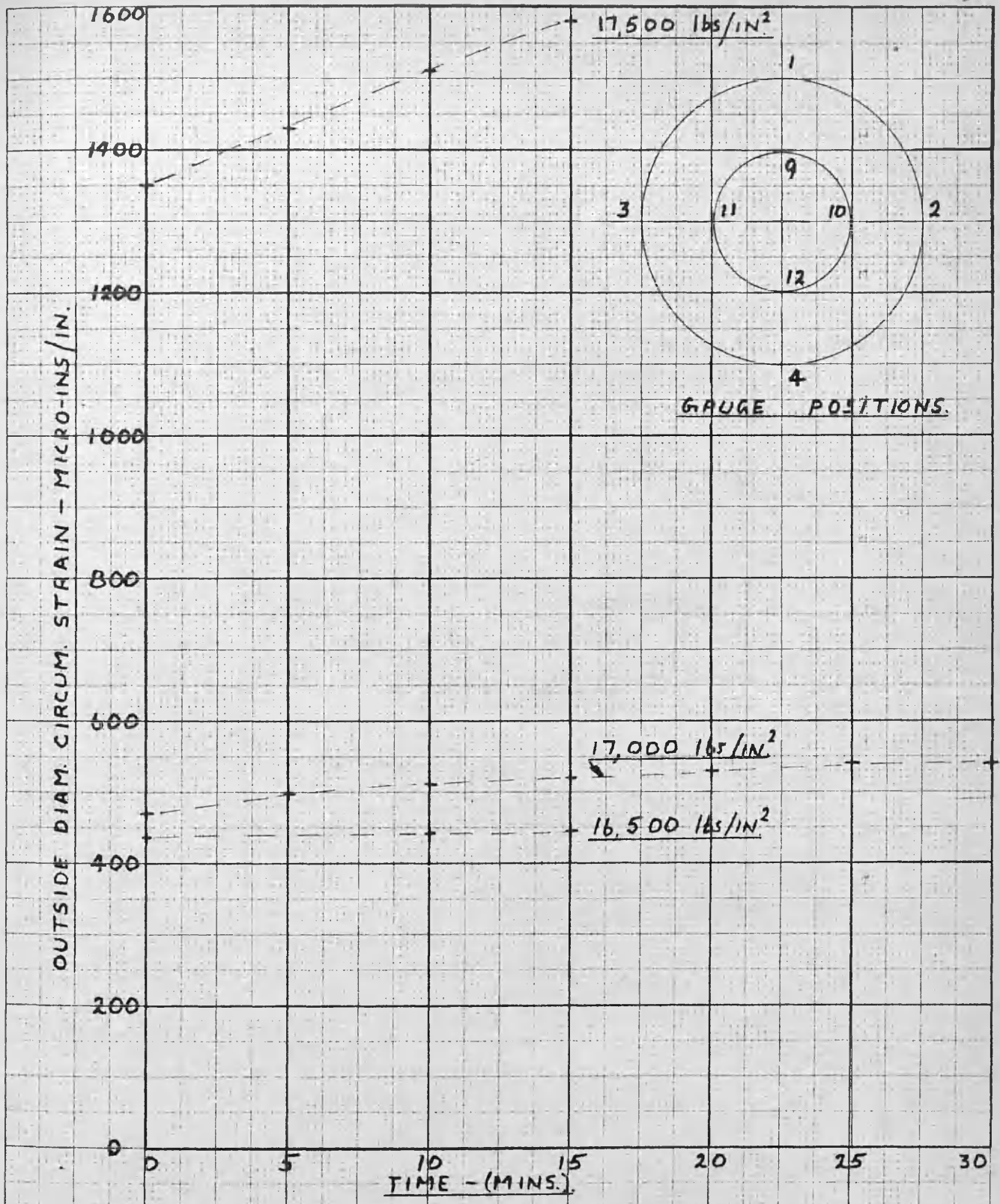


FIG. 39 d - No. 4 GAUGE CREEP FOR VARIOUS PRESSURES.

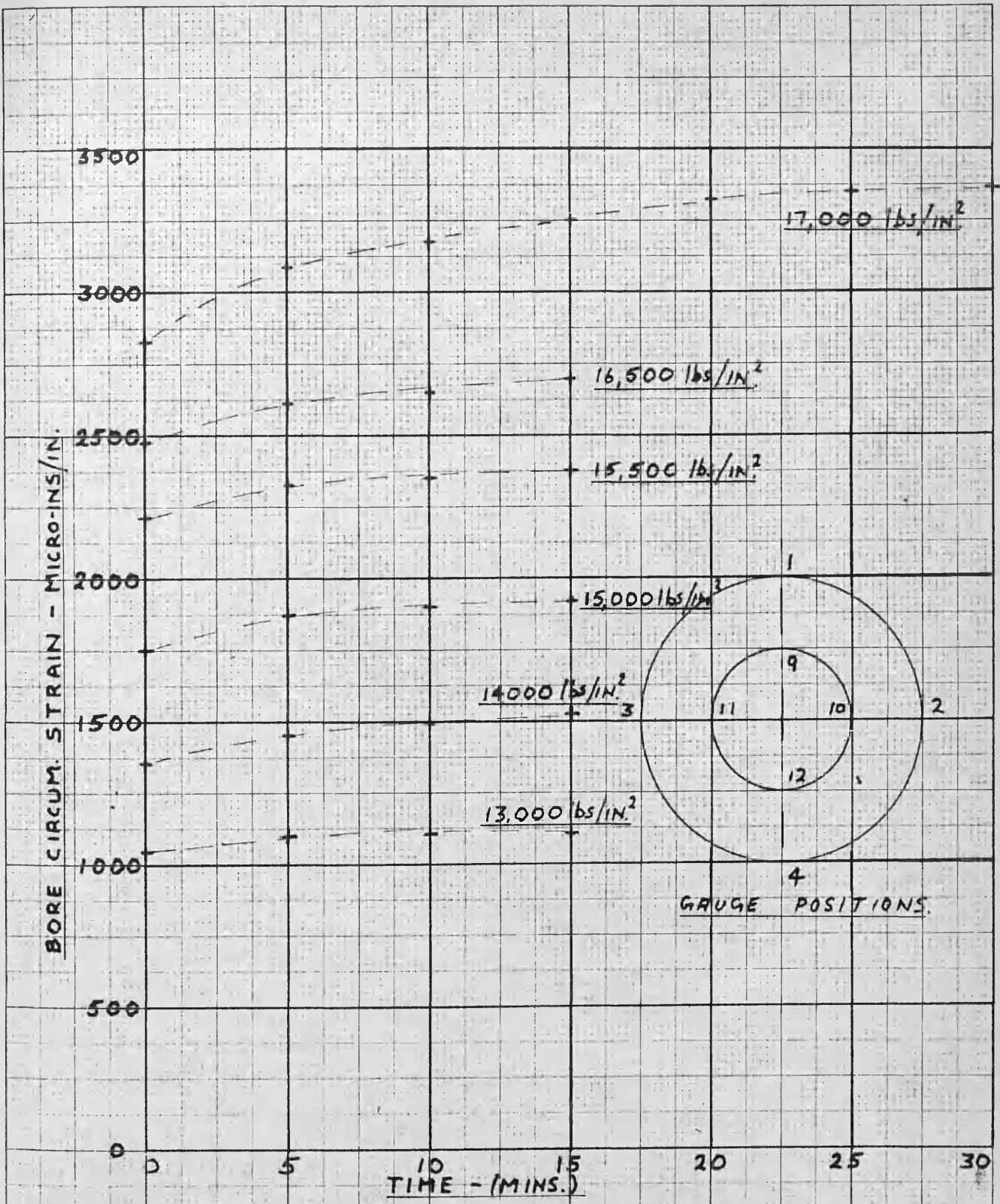


FIG. 40 a. - No. 9 GAUGE CREEP FOR VARIOUS PRESSURES.

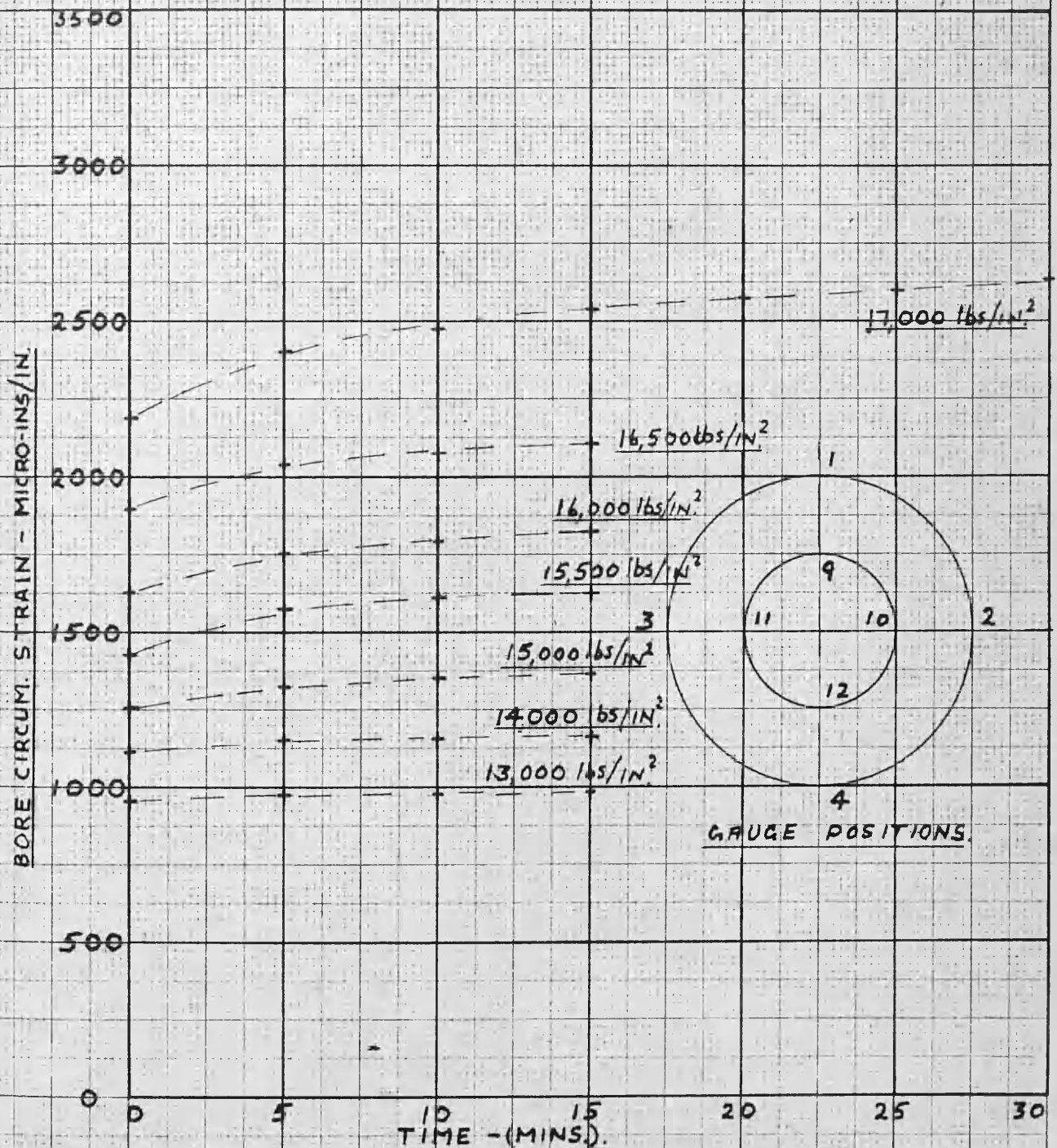


FIG. 40b — No. 10 GAUGE CREEP FOR VARIOUS PRESSURES.

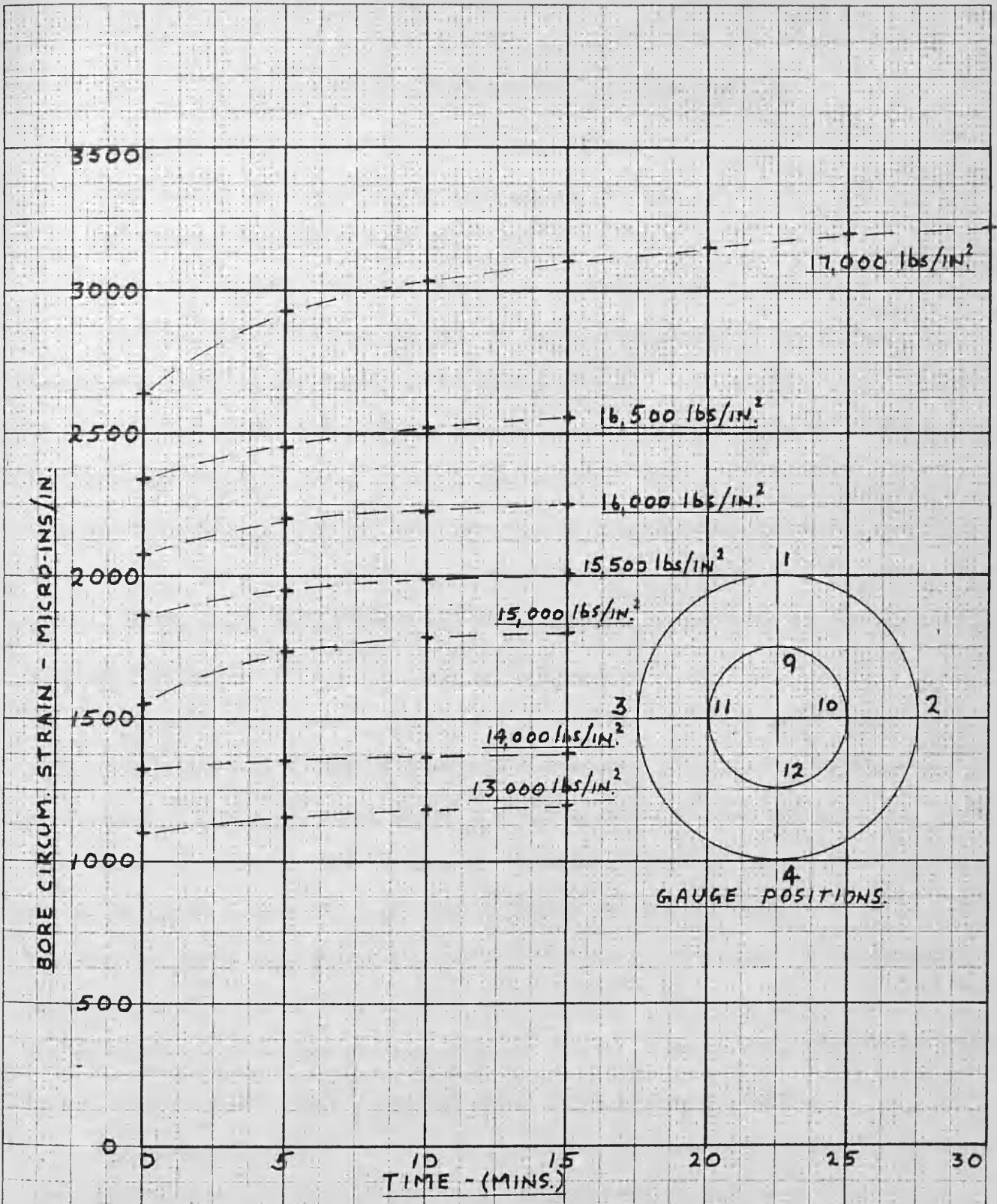


FIG. 40 c. — No. 12 GAUGE CREEP FOR VARIOUS PRESSURES.

### III. DISCUSSION OF AUTHOR'S EXPERIMENTAL RESULTS

#### 1. Outside Diameter Circumferential Strains. (Fig. 36)

Four factors emerge from a cursory glance at Fig. 36.

(i) Lamé' theory is verified.

(ii) The pressure at which overstrain commences is not evident.

(iii) The fully plastic pressure is in accordance with a theory based on the maximum shear stress theory of failure.

(iv) The points intermediate between elastic line and fully plastic condition do not lie on a curve based on maximum shear stress. It is difficult in view of (iii) above to suggest that they lie on a theoretical curve predicted using the Von Mises' flow condition. Rather should it be said that the points do not lie on the shear stress curve and it is fortuitous that they lie on the one based on Von Mises.

It is seen that interpretation of the results shown in Fig. 36 would necessarily resort to a certain amount of undesirable conjecture. Guidance may be obtained from Fig. 37 which shows internal pressure plotted against bore circumferential strain. Two factors are immediately noticed here. Firstly, overstrain begins at a pressure predicted by Tresca and not Von Mises. Secondly, the bore strains agree tolerably well with a theoretical curve based on the maximum shear stress theory of failure. With this additional information an explanation may be suggested as to why the experimental outside diameter circumferential strain points lie off the theoretical curve based on maximum shear.

The cylinder material is mild steel. It is well known that this material has a characteristic manner of yielding. Wedges form in regions of overstrain but little is known of their number or size. Since the material is ductile, it is reasonable to suggest that overstrain at the bore can be relieved easily by the wedges without necessarily transferring much additional load to the elastic

outer shell. Indeed with carefully prepared specimens such as those used by Professor Cook there is no change in the slope from the original elastic line and there would appear to be a fictitiously high shear stress existing at the bore. This was discussed more fully in the review.

It is suggested that due to the manner of yielding characteristic of mild steel that initial stages of overstrain can take place at the bore of a thick-walled cylinder without affecting the outside diametral strains as much as theory predicts. The theory of course is based on a more ordered type of yielding. As the wedge type yielding progresses towards the outside its effect is more and more apparent on the outside strains until on final break through of one or more of the wedges the theoretically predicted stiffness is attained.

Experimental data from a mild steel cylinder tested in the laboratories of the Royal Technical College, Glasgow are also shown on Fig. 36. The points are seen to compare favourably with the others, but the cylinder was not tested to the fully plastic condition. Outside diameter circumferential strains only were measured.

## 2. Bore Circumferential Strains (Fig. 37)

The technique of measuring bore strains consisted firstly of deducing the effect of pressure on the bakelite gauges. Fig. 37a was plotted for this purpose but it can be seen that experimental points agree exactly with Lamé's elastic line and hence the inference would be that the gauges are not affected by pressure. This fact simplifies matters considerably.

Reasonably close agreement is noticed between the experimental data and Sopwith's theoretical curve based on maximum shear stress theory of failure.

It should be noticed that nowhere on Fig. 37 do the experimental points fall near the curve deduced from Von Mises flow condition. This is considered important especially in view of the outside diameter results.

Creep of the inelastic bore strains under constant pressures is recorded. It tends to displace the points to the right of the maximum shear stress flow curve. The possibility of slow creep in overstrained mild steel material cannot be ruled out from the present results.

There is no evidence of an upper and lower value for the maximum shear stress. Overstrain commences at an internal pressure which is theoretically deduced using the yield shear stress taken from the tension tests.

### 3. Axial Strains (Fig. 38)

In the all elastic range the experimental points lie on a line slightly removed from the theoretical. This is not a serious discrepancy and may be attributed to a small tensile axial stress set up by friction at the packings. Its effect is negligible in the circumferential direction.

According to theory the magnitude of the axial strain should increase at a greater rate after overstraining begins. This is not borne out by the experimental data. An explanation may be traced to the strains measured in the circumferential direction.

Outside diameter axial strains are given by: -

$$E \epsilon_z = \sigma_z - \mu \sigma_\theta \quad \text{----- (a)}$$

and outside diameter circumferential strains by: -

$$E \epsilon_\theta = \sigma_\theta - \mu \sigma_z \quad \text{----- (b)}$$

It is apparent from Eqs. (a) and (b) that if  $E \epsilon_\theta$  (experimental) is small compared to theory, then  $E \epsilon_z$  (experimental) will also be less than its corresponding theoretical value. The outside circumferential strain finally increases rapidly yet no average increase is recorded in the axial direction. This may mean that the four axial gauges are not sufficient to give a true picture of average strain.

From Table V it is seen that at the fully plastic value of internal pressure,

a compressive axial strain of 218 microinches per inch exists at one point on the circumference and  $90^\circ$  removed a tensile axial strain of 27 microinches per inch is to be found. It would seem that the test cylinder has been subjected to a stress system producing strains not compatible with preconceived ideas.

#### 4. Circumferential Variations in Strains

Table V is drawn up to show the circumferential variation in the strains. The position of the gauges relative to one another are shown along side the table.

It is seen that variations among gauges when the cylinder is elastic is very small. As overstrain progresses the variations in gauge readings increases. Serious differences however are not apparent until close to the fully plastic value of internal pressure. It would appear that a wedge or region of overstrain reaches the outside diameter close to gauge no. 4.

Cook discusses the variation in outside diametral extensions of thick-walled cylinders brought about by overstrained regions disturbing the symmetry. He maintains that the outside takes an elliptical shape and that it is only necessary to measure extensions across two diameters at right angles in order to obtain a mean. It is not possible to say what shape the outside finally becomes in the cylinder under test but it would appear to be complex. The four gauges show up dramatically the asymmetrical nature of the straining.

Since wide variations circumferentially have been noticed among gauges the question arises as to whether four gauges to measure any one variable will give a statistical mean. The problem is peculiar to a material like mild steel which yields so that two adjacent regions vary in strain. This is being studied by the Theoretical and Applied Mechanics Department at the University of Illinois using mild steel beams and electrical strain gauges of varying gauge lengths. It is found advisable to use gauges of large gauge length (4 to 6 inches) or a large number of smaller gauge length ( $1/4$  inch or thereabouts) in order to obtain a

statistical mean. From their tests it is considered reasonable to use 4-1/4 inch gauge length gauges on the inside surface of the cylinder which has an available circumferential length of 3π inches. It would be advisable however to use as many gauges as is practical.

In some previous work performed by the writer the mean of the four outside gauges gave a figure comparable to the mean of two mechanical gauges placed at right angles to one another. This check was used as evidence that four circumferential and four axial electrical gauges of 1 inch gauge length could adequately cope with the measurement problem on the outside of the cylinder.

#### 5. Time Effects - Creep

At the higher pressures there is evidence of the circumferential strains creeping during the 15 minutes each pressure is held constant. Readings of strain are then taken at 5 minute intervals and Figs. 39 (a, b, c, and d) and 40 (a, b, and c) show their variation. Creep is first noticed in the bore strains at a pressure of 11,000 lbs./in.<sup>2</sup> The amount is small but as the pressures increase the creep becomes important. The results show that after 15 minute intervals the creep rate is comparatively slow. This would indicate that the time interval between readings is adequate. It is possible, however, that a slow creep might show measurable changes in bore strain over a period of hours or weeks or years. The answer to this particular problem is one of urgent necessity to industry before it will place any faith in the plastic design of mild steel members.

Creep is not apparent in the outside diameter circumferential gauges until a pressure as high as 16,000 lbs./in.<sup>2</sup> It would seem that the outside strains are not sensitive to changes in bore strain. This fact will be discussed more fully in the section on Interference Fits.

#### IV. CONCLUSIONS

##### 1. Advantages of Measuring Bore Strains

The measurement of bore strains has revealed: -

(i) Initial yielding starts at a value of the internal pressure predicted theoretically using the maximum shear stress (Tresca) theory of failure. There is no evidence in bore measurements of an upper and lower yield point.

(ii) Experiment agrees well with Sopwith's theoretical curve based on the maximum shear stress theory of failure.

##### 2. Inelastic Characteristics Exhibited by Mild Steel

The type of yielding of the mild steel material is such as to produce asymmetry in the member. Also, in the early stages of overstrain the mechanism of yielding is such that the elastic outer shell is not so seriously loaded as theory predicts. This fact is also shown by Cook's results and he attributed it to the existence of an upper and lower yield point in the material. Cook did not measure bore strains so it is not known if the upper and lower limit phenomenon was present at the bore.

Macrae's results on gun steels showed strict adherence to the maximum shear stress curve for outside diameter strains. The wedge-type of yielding does not occur in gun steels.

##### 3. Creep

There is a time effect which requires more investigation. It may be serious in some members such as interference fits in which the interface pressure and hence the holding ability is dependent on the bore deflections of the scantling.

PART III

THICK-WALLED CYLINDERS UNDER INTERFERENCE FIT PRESSURE

I. WORK OF PREVIOUS EXPERIMENTERS1. The Variable Fit-Allowance - Force Fits - RUSSELL, (53) WERTH (13)(1) Russell

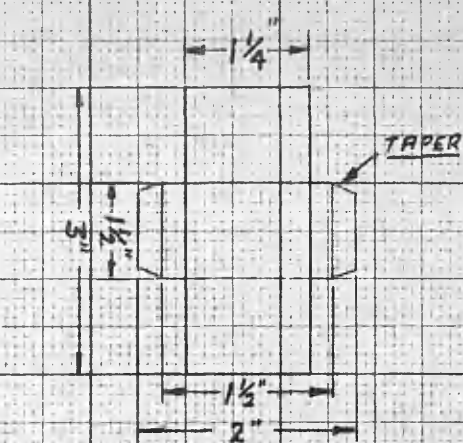
Russell carried out tests on simple ring and plug specimens of varying fit allowances. He recorded (a) the outside diameter deflection after entry of the plug ( $u_{o/d}$ ), (b) the bore permanent set ( $u_R$ ) after disassembly, (c) the pressing on and withdrawing loads.

The magnitude of the fit allowances varied from zero to values causing complete overstrain of the ring. Specimen details and pertinent conditions of test are shown in Fig. 41. It should be noted that the plugs are of hard steel and thus no overstraining is produced in them. The ring material is mild steel for which a tension test gives a well defined yield point.

The holding ability of an assembly is measured by the axial load necessary to destroy the grip. Load-fit allowance curves have the characteristic shape shown in Fig. 42. It is seen that the optimum value of fit allowance with respect to maximum holding ability is  $\Delta_A$ . Russell associated this value with an all-elastic assembly and claims that overstraining of the ring provides no increase in holding ability. It is the main purpose of the review to refute this claim. It will be shown that the percentage of the wall of the ring overstrained for the optimum value of fit allowance is as high as 54 %.

The author's analysis of Russell's results makes use of a theory presented on pages 132-135. It is based on Sopwith's theory for thick-walled cylinders. This was shown in the first part of the thesis to agree with experiment for mild steel cylinders.

Fig. 43 shows the mean of Russell's strain measurements compared with theoretically deduced curves. It is noticed (a) that the bore permanent sets indicate an interface pressure much higher than theory is operative and (b) the



$$E = 3500 \text{ TONS/IN}^2$$

$$S = 5.1 \text{ TONS/IN}^2$$

### RING:-

MATERIAL - MILD STEEL

BORE SURFACE - "WELL GROUND & FINISHED"

BORE MEASUREMENT - PIN-GAUGE - TRAVEL METHOD.

O/D MEASUREMENT - NEWALL MACHINE

### PLUG:-

MATERIAL - HARD STEEL.

SURFACE - "WELL GROUND & FINISHED"

MEASUREMENT - NEWALL MACHINE.

LUBRICANT - "PREPARED GRAPHITE"

RANGE OF FITS -  $0 < \Delta' < 3\frac{1}{2}$  MILS/IN.

FIG. 41 - DETAILS OF RUSSELL'S SPECIMENS.

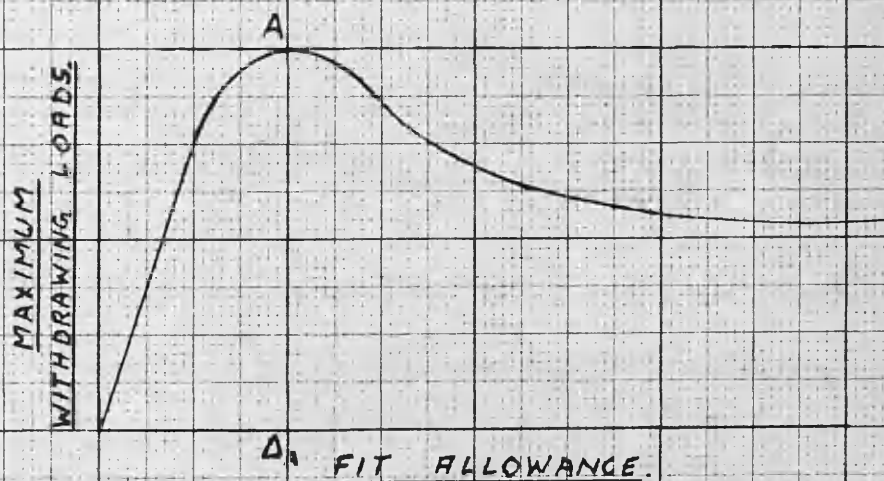


FIG. 42 - CHARACTERISTIC SHAPE OF MAXIMUM WITHDRAWING LOAD - FIT ALLOWANCE CURVE FOR FORCE FITS.

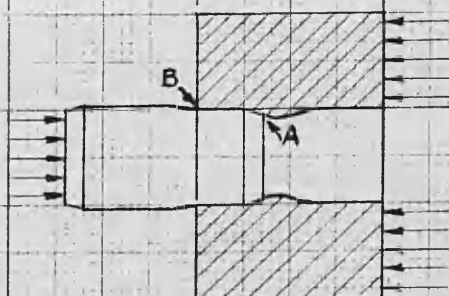


FIG. 44 - DAMAGING EFFECTS OF ENTRY LOADS IN FORCE FITS.

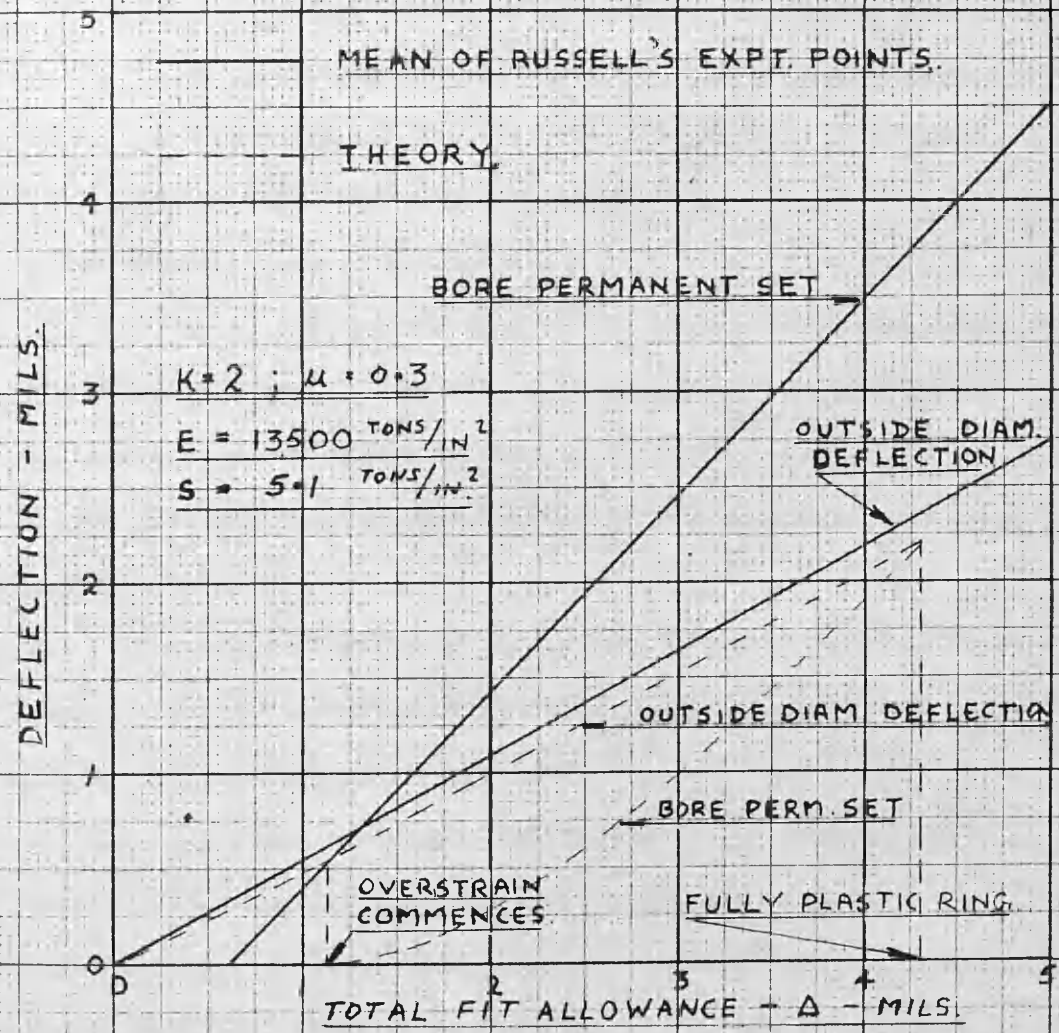


FIG. 43 - MEAN OF RUSSELL'S EXPERIMENTAL STRAIN RESULTS.

outside diameter deflections show only slight difference from theory. It is believed that this is due to the existence of high pressures at A on entry (at B also to a lesser extent), Fig. 44. Thus every section of the ring is subjected to a higher pressure than that predicted by theory. If the ring remains elastic under this higher pressure then the final value will closely correspond to normal theory. If the ring is overstrained on entry, however, a sequence of loading followed by partial unloading results. It can be shown that the shape of the load-fit allowance curve supports this supposition.

The assumptions are as follows: -

(a) Assembly by forcing the plug in the ring produces pressures not accounted for by ordinary methods of analysis, e.g. at points A and B (Fig. 44).

(b) A close approximation to the maximum effective pressure on entry is obtained from the experimental measurements of bore permanent set, when correctly interpreted by theory.

(c) A close approximation to the average pressure existing in an assembly on completion of the fit is given by the experimental measurements of outside diameter change, when correctly interpreted by theory.

(d) The most severe pressure effects are due to entry of the plug and not disassembly. This enables the history of straining to be deduced. Firstly, effective pressures given by bore permanent set readings are produced at the interface. Secondly, these pressures fall to the values predicted from outside diameter changes. Elastic release of strains is assumed.

Fig. 45 shows theoretical curves for outside diameter change and bore permanent set plotted against the interface pressure. Table VI shows experimental strain values taken from Russell's results. Values for initiation and completion of overstrain in the ring are found from a mean curve drawn through the experimental points.

Total Fit ( $\Delta$ ) (Mils)	Outside Diameter Deflection (Mils)	Bore Permanent Set (Mils)
0.62	0.36	Zero
0.82	0.50	0.16
1.00	0.72	0.48
1.40	0.81	0.56
2.00	1.18	1.42
2.74	1.56	2.21

TABLE VI - RUSSELL'S EXPERIMENTAL DATA - FORCE FITS

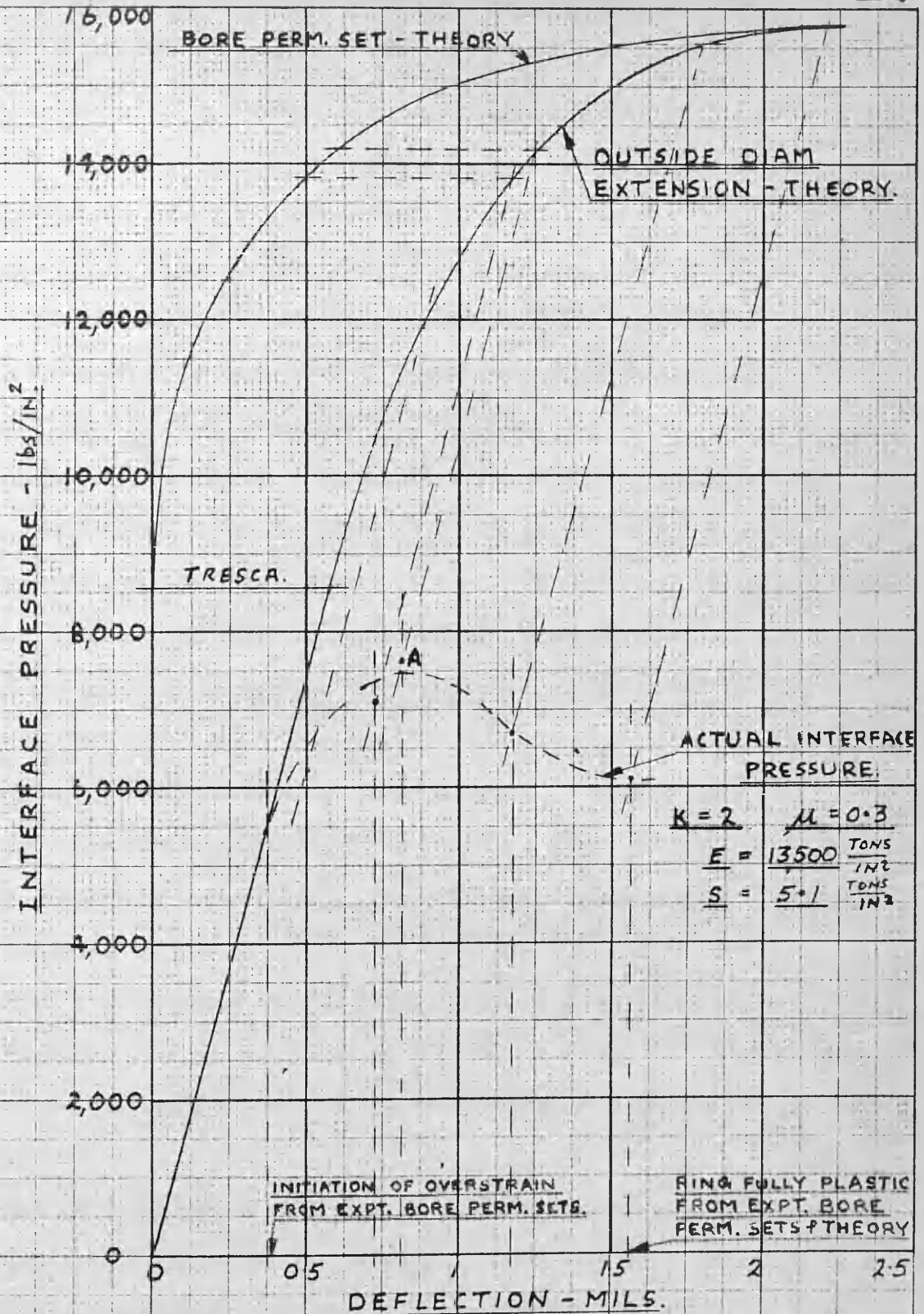


FIG. 45 - CURVE OF ACTUAL INTERFACE PRESSURE OBTAINED FROM THEORY AND RUSSELL'S EXPT. RESULTS.

From the analysis the actual interface pressure for  $\Delta = 1$  mil. is 7100 lbs./in.<sup>2</sup> The sequence of operations leading to this deduction is as follows: -

- (a) From Table VI,  $\Delta = 1$  mil gives  $U_R = .48$  mils.
- (b) From Fig. 45,  $U_R = .48$  mils gives  $P = 13,850$  lbs./in.<sup>2</sup>
- (c) From Fig. 45 and  $P = 13,850$  lbs./in.<sup>2</sup> is obtained the value of outside diameter change corresponding to the maximum effective pressure.
- (d) From Table VI,  $\Delta = 1$  mil gives  $U_{o/d} = .72$  mils.
- (e) From Fig. 45, by elastic release of strain point A is located which gives the actual interface pressure in the assembly (7,100 lb./in.<sup>2</sup>).

This process is repeated for all the values in Table VI and the dotted curve in Fig. 44 is obtained. This may be replotted to a base of total fit and compared with the axial loads to destroy the grip. This is shown in Fig. 46. The shapes are very similar.

From Fig. 45, it is seen that the maximum interface pressure obtainable in this series of force fits is 82.5 % of the maximum elastic interface pressure calculated by neglecting entry forces. The efficiency is drastically reduced by this method of assembly.

The optimum fit allowance for his force fits is  $\Delta = 1.3$  mils. The experimental bore permanent set corresponding to this is 0.7 mils. For this value of permanent set the ring wall may be shown theoretically to be 54 % overstrained. (See Fig. 65)

The effect of entry forces will necessarily be dependent on friction conditions and may not be assumed to be a function of fit allowance only. It is thought that this interpretation of force fit theory and experiment will dispel the current belief that overstraining of the outer member is to be avoided. It is of interest that the optimum fit-allowance from Russell's experiments and the one predicted from Lamé' and the strain-energy theory of failure are close.

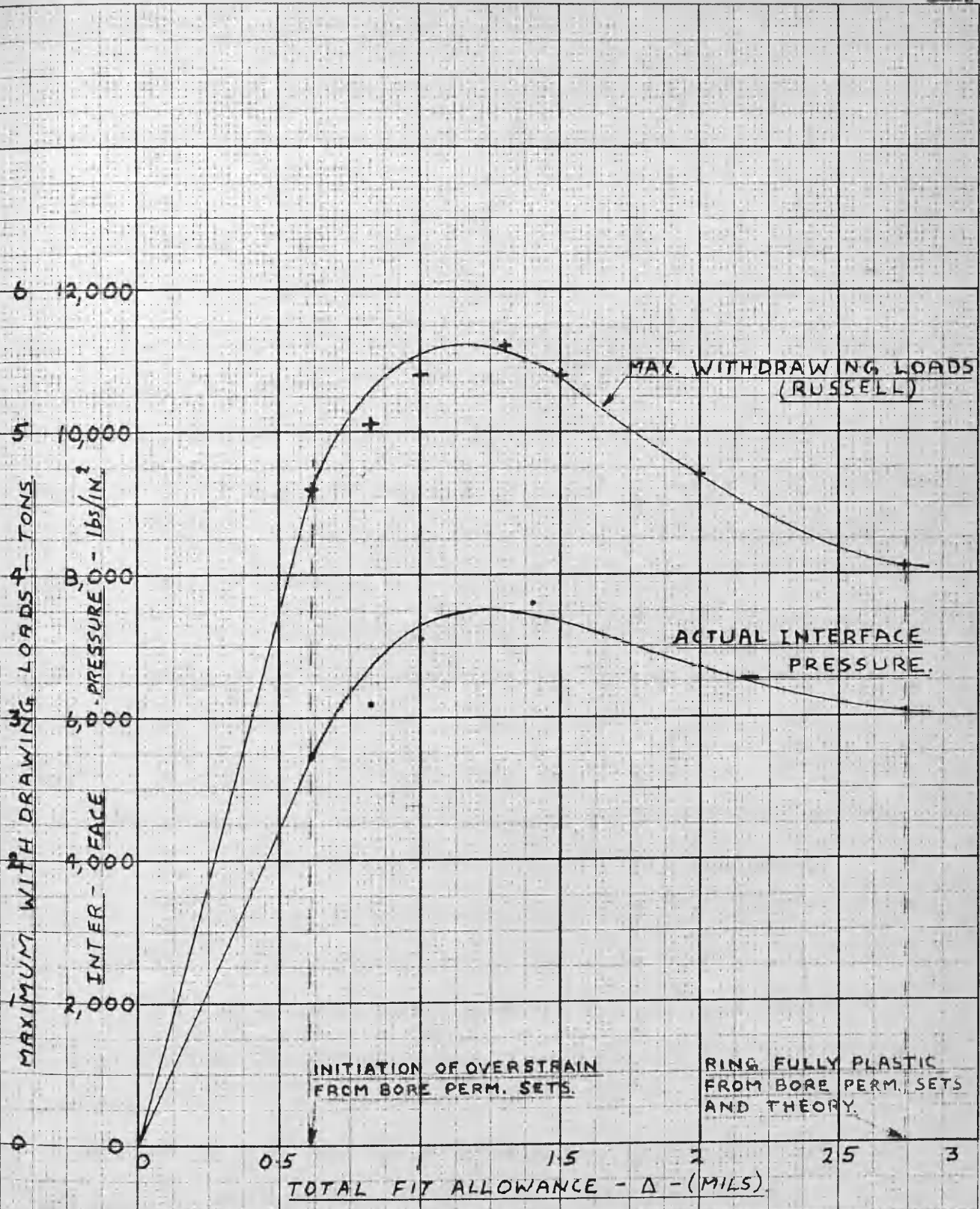


FIG. 46 - SIMILARITY BETWEEN RUSSELL'S EXPT. LOADS AND ACTUAL INTERFACE PRESSURES DEDUCED IN FIG. 45.

These are the grounds for Russell's interpretation, which can be easily disproved by referring to the bore permanent set measurements.

(ii) Werth

Werth carried out load tests on parallel force fits varying in magnitude up to 40 mils per inch bore diameter. He used excessive fits (for a 2:1 ratio ring) and the practical worth of his results must be restricted to the lower values of fit allowance.

The specimens are of simple ring and plug shape ( $d = .704$  inches;  $L = 1.395$  inches) and both plug and ring material are a good low carbon steel (yield point 51,800 lbs./in.<sup>2</sup>). Results from specimens of ring ratio approximately 2:1 are considered here for comparison with Russell's work.

Werth's work was originally published in a German book which the writer was unable to obtain either in Britain or America. The source of information is an article in the Transactions of the American Society of Mechanical Engineers. Fig. 47 is reproduced from this reference. The fit allowance scale is so small that an incorrect interpretation can be made of the results in the practical range of fit allowances. It would appear from Fig. 46 that linearity of load with fit allowance can be expected up to a value of 3 mils per inch bore diameter. This is not so and if Werth's individual points for withdrawing loads are plotted to a larger abscissae scale a shape of curve similar to Russell's is obtained (see Fig. 48). Fit allowances up to 13 mils per inch bore diameter are considered.

From Fig. 46 it is seen that withdrawing loads are higher than press-on loads -- in the practical range of the graph. This is in accordance with the majority of observations. Russell, however, in the results already discussed records press-on loads which are the same as his withdrawing loads. The reason for the difference is not obvious but could probably be explained in terms of

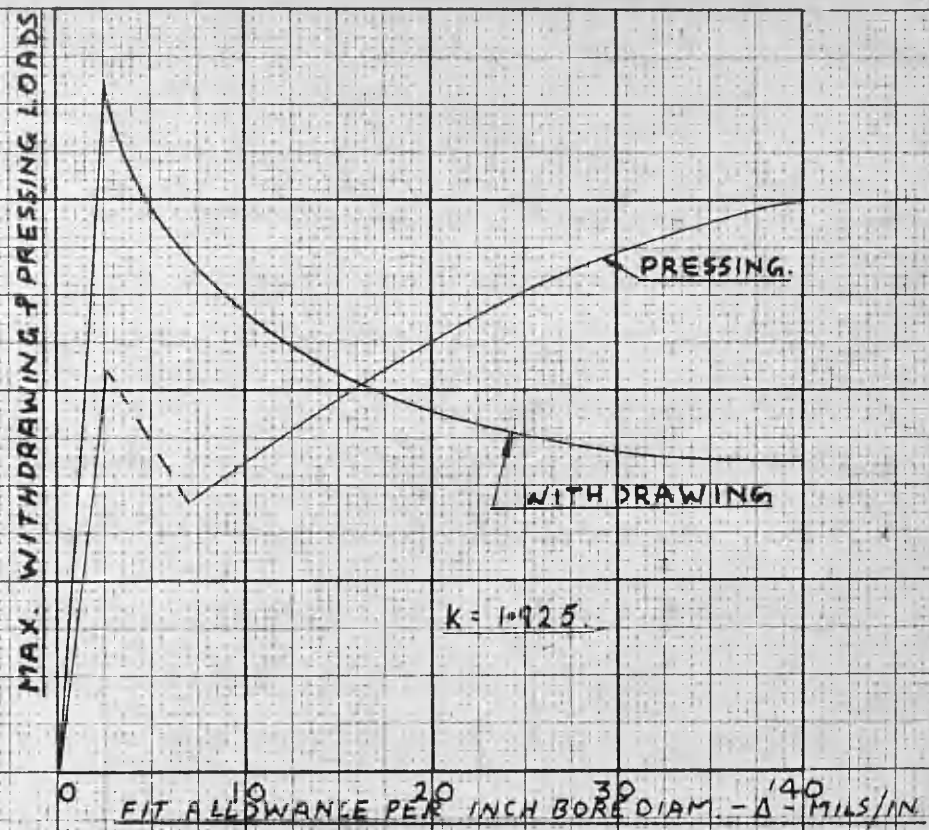


FIG. 47 - WERTH'S LOAD-FIT ALLOWANCE CURVES.

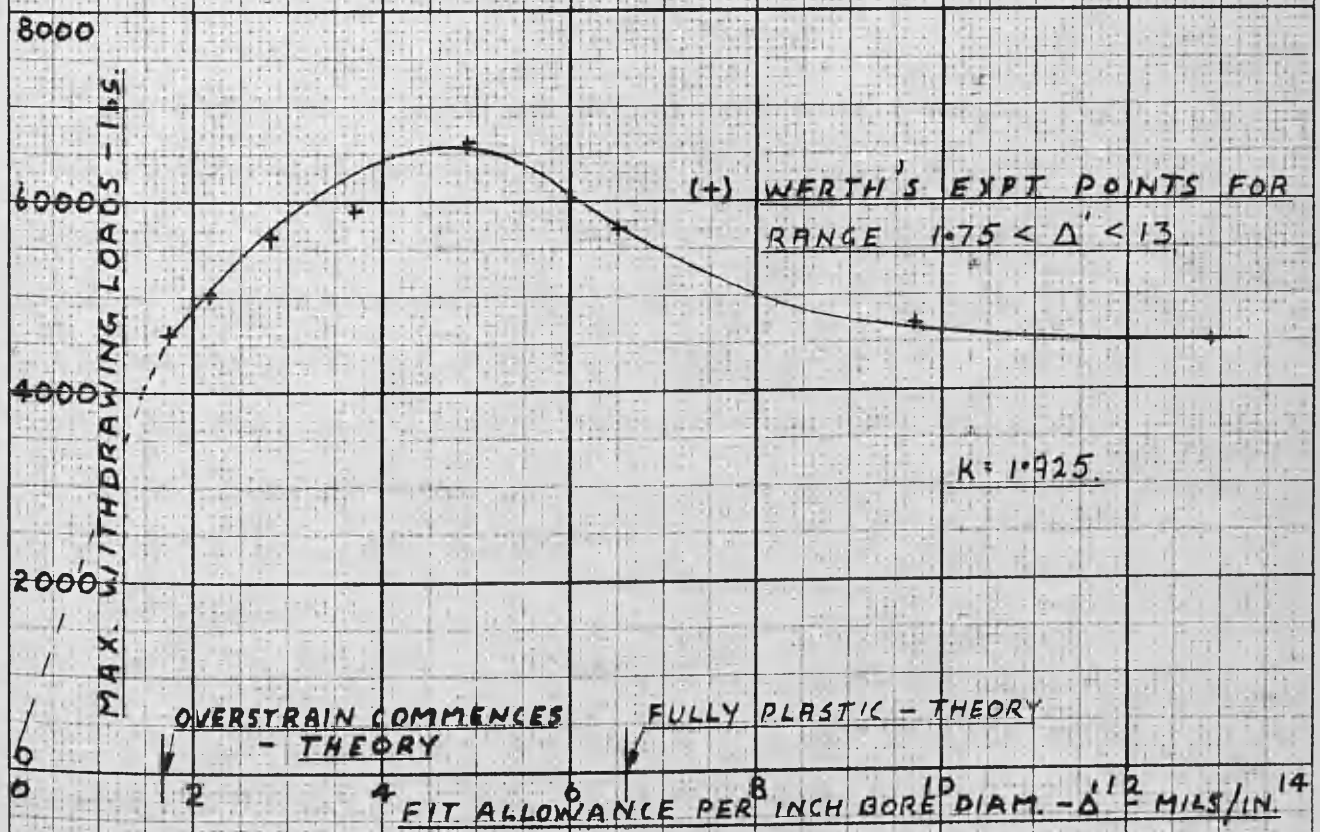


FIG. 48 - WERTH'S LOAD-FIT ALLOWANCE CURVE FOR WITHDRAWING TO A LARGER SCALE - RANGE  $1.75 < \Delta' < 13$ .

surface finish and lubricant conditions at the interfaces.

Fig. 48 indicates the characteristic load-fit allowance curve. No points are given below 1.75 mils per inch bore diameter but the shape of the curve is obvious in the lower range. Theoretical values for initiation and completion of overstrain in the ring are marked. It can be seen that they agree in position, relative to the characteristic curve, with Russell's results. No strain data is available to check the shape of Werth's load-fit allowance curve.

2. The Variable, Coefficient of Friction - RUSSELL, WERTH, ASSOCIATION OF MANUFACTURERS OF CHILLED CAR WHEELS OF AMERICA, SAWIN, BAUGHER, MACGILL

The axial load to press-on or press off an interference fit assembly is given by,

$$F = \bar{\mu} \pi d L P \quad \text{-----} \quad (78)$$

The torque to destroy a grip is given by,

$$T = \bar{\mu} \pi d^2 L P/2 \quad \text{-----} \quad (79)$$

The computation of  $\bar{\mu}$  requires the experimental determination of either  $F$  or  $T$  and the theoretical interface pressure. Lamé' has always been used for the latter purpose and it is apparent that only in limited cases will the theoretical interface pressure correspond with the actual one. Russell, for instance, bases his values for coefficient of friction on the press-on loads. It is certain, in view of the first part of the review, that the values will all be high. The failure to account for actual conditions in most cases renders the coefficients of friction of comparative use only.

(1) Lubricant

Russell<sup>(34), (35), (36)</sup> found a variation in grip strength amounting to 300 % for specimens force fitted with different oils on the mating surfaces but otherwise identical. In general, a mineral oil gives the strongest grip. A fatty oil such as sperm or rape oil produces a weak grip.

Werth<sup>(19)</sup> showed similar results using machine oil, rape oil and tallow. His figures are erratic but in general the strength of grips are in the order named with machine oil the strongest. Press-off loads are always higher than press-on loads.

The Association of Manufacturers of Chilled Car Wheels of America,<sup>(19)</sup> experimented to find the effect of varying the amount of white lead in a base of boiled linseed oil. Their conclusions tally with Russell and Werth in that "oiliness" provides lower coefficients of friction.

#### (ii) Surface Generation

Three factors are operative, viz. (a) degree of smoothness of surface (surface finish), (b) out-of-roundness, and (c) taper. Taper has not been examined to the writer's knowledge.

Russell<sup>(34)</sup> attempted an investigation of out-of-roundness. It consisted of push out load tests on simple ring and plug shape specimens. The rings had grooves cut in them. By varying the width of the grooves, the possible area of contact was varied among specimens. He showed that the axial loads decrease with decrease in area of contact. It is doubtful whether it may be generalised from this that out-of-roundness will decrease the holding ability of a grip.

Surface finish has been examined by several investigators. Sawin<sup>(37)</sup> concludes that the finer the finish the higher the coefficient of friction. Baugher<sup>(1)</sup> came to the opposite conclusion which shows the conflicting nature of some of the reports on this work. It is generally held today that Sawin's results are correct. In railway shop practice larger press-on loads are recorded for ground axles than for turned ones, when the remaining variables are standardised.

#### (iii) Assembly and Dis-assembly Methods

It is a popular belief that shrink fits possess higher coefficients of

friction than force fits. Also the friction coefficient calculated from torsional slip is higher than that from axial slip. Russell<sup>(34)</sup> carried out some tests to clarify these points.

Table VII shows results of 1st and 2nd slip loads for specimens which vary in method of assembly. On a basis of 1st load, the coefficient of friction for shrink fits is much higher than the others. 2nd loads however show a drop in the shrink and expansion fits and a slight rise in the force fit. After the plugs have moved approximately 1/4 inch, the expansion and force assemblies carry comparable loads whereas the shrink fit is 40 % lower. The large difference between 1st and 2nd slip loads in shrink fits is considered characteristic of this method of assembly. The writer has found the ratio of loads to be of the order of 2 although this figure is not consistent. It may be visualized that when the hot ring comes in contact with the cold plug that the high points of the two surfaces tend to weld together and squeeze out the lubricant into the valleys or troughs. Since little relative movement has occurred between the surfaces in contact an absorbed primary film is unlikely to have formed at initial fitting. On 1st slip, however, more favourable conditions of lubrication are envisaged which accounts for the comparatively low 2nd loads. A similar trend is noticed for expansion fits, but the effect is not so serious. Force fits have adequate primary films established on entry and the high 1st and low 2nd loads are not a characteristic with them.

Russell,<sup>(34)</sup> later on in the same article, contradicts himself by stating that coefficients of friction for shrink and force fits are the same. He gives as figures, 0.3, if assemblies are torqued off and 0.263, if pushed out. He does not explain the basis for his calculations.

Wilmore<sup>(47)</sup> showed that coefficients of friction for shrink fits were 2 to 3 times higher than for force fits. He used steel shafts and cast-iron hubs and

Axial Push- Out Loads (Tons)	Method of Assembly		
	Shrink	Expansion	Force
1st	8.5	3.4	3
2nd	2.8	2.1	3.5

TABLE VII - METHOD OF ASSEMBLY - RUSSELL

(Fit Allowance 1 Mil; Lub. - Rape Oil)

Investigator	No. of Specs.	Variation in $\bar{\mu}$
MacGill (22)	20	.096 - .233
Sawin (37), (1) (calculated by Baughner)	Not Known	.054 - .22
Baughner (1)	123	.03 - .25

TABLE VIII - VARIATION IN COEFFICIENTS OF  
FRICTION FOR APPARENTLY STANDARDIZED  
CONDITIONS - MACGILL, SAWIN, BAUGHNER

varied the fit allowance from 1 to 3 mils per inch shaft diameter. For torqued specimens the coefficients were slightly higher than for pushed out ones.

Several other variables have been investigated, but they appear to have little effect. Baugher<sup>(1)</sup> states that hardness of material, its chemical composition, and whether it is cast, forged or rolled have little effect on the coefficient of friction. Werth<sup>(19)</sup> investigated the velocity of assembly. He concludes that the press-on loads are reduced for increase in velocity; the press-out loads remain unaltered.

#### (iv) Variations in $\bar{\mu}$ for Apparently Standardised Conditions

Probably the most important feature of this section of the review is the fact that investigators report large variations in their values of friction coefficients for apparently standardised conditions. This indicates that the friction or more correctly stiction coefficient is extremely sensitive to some variable which is operative and not easily controlled. The writer has been unable to find any reports dealing with stiction under high pressures. Dokos,<sup>(12)</sup> Bowden, Leben, Taylor<sup>(2)</sup> have investigated sliding friction under high pressures, by varying the velocity of sliding. At low velocities ( $10^{-4}$  inches per sec.), the friction conditions are extremely complex and continues according to the "mechanism of stick-slip". It is to be concluded that the nature of stiction is in some way associated with this complex phenomenon.

Table VIII and Fig. 49<sup>(19)</sup> indicate the variations in friction coefficient according to several investigators. Conditions of test are not given but may be found in the references. The figures are self explanatory. It is suggested that if the actual interface pressure were used in the calculation of press fit coefficients of friction, that variations would not be so great. There is no doubt, however, that the variations would not be fully explained and that a more complete knowledge of stiction under high pressure is required for a satisfactory

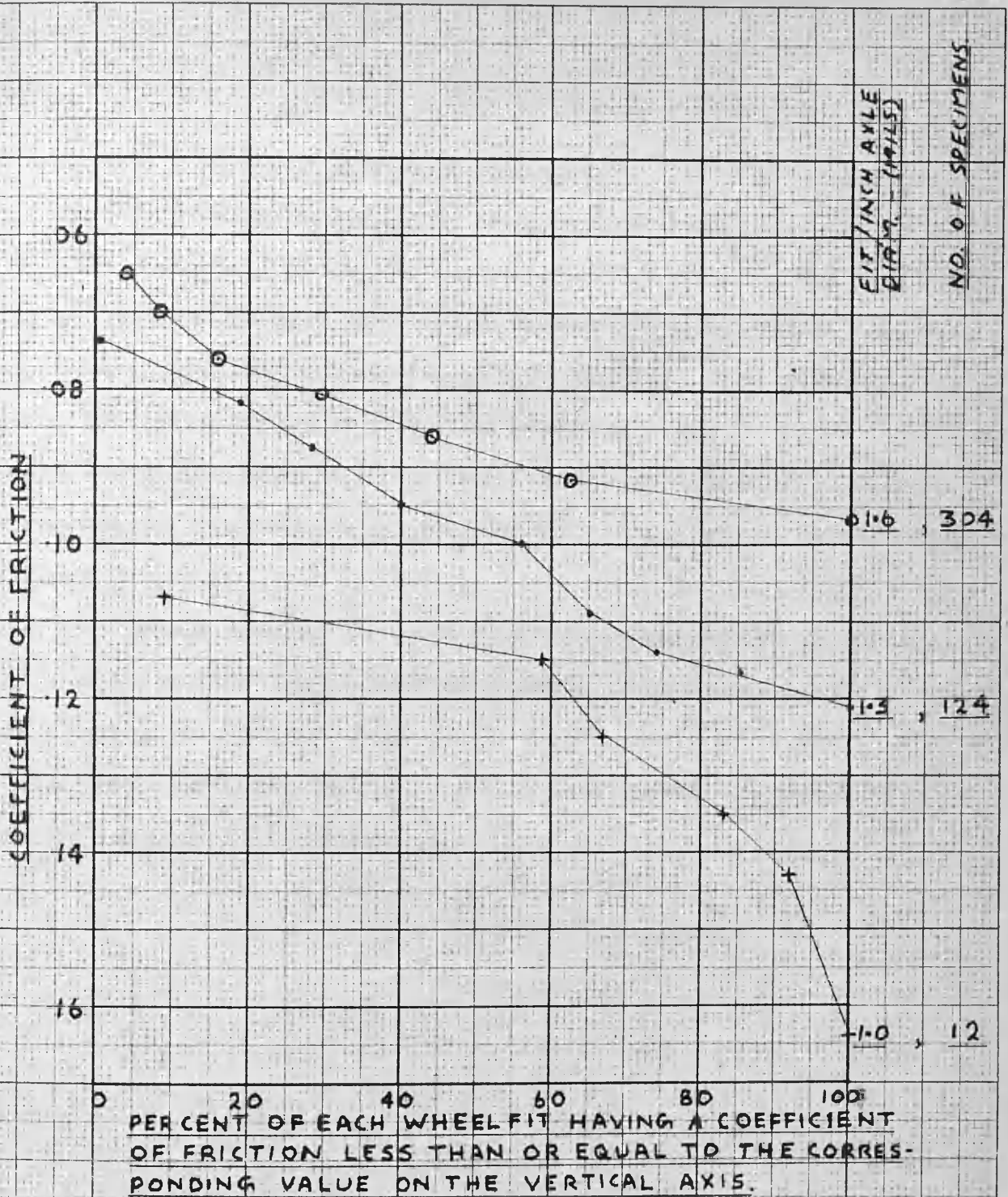


**FIG 49 - VARIATION IN COEFFICIENT OF FRICTION FOR WHEELS HAVING A CERTAIN FIT.**

**N.B. RESULTS ARE FROM PRESS FITS OF AXLES ON ROLLED STEEL WHEELS FOR ROLLER-BEARING FREIGHT-CAR TRUCKS MADE BY TIMKEN ROLLER-BEARING COY., U.S.A.**

solution.

### 3. Conclusions from Work of Previous Experimenters

Three important conclusions may be drawn from the review.

(i) The characteristic shape of the load-fit allowance curve for force fits may be explained using experimental strain measurements and an interference fit theory based on Sopwith's thick-walled cylinder analysis. These statements should at present be limited to mild steel cylinders.

(ii) The optimum value of fit allowance for Russell's results is associated with considerable overstrain in the ring (54 %) and not with an elastic theory of failure.

At this optimum value of fit allowance the interface pressure is only 82.5 % of the maximum elastic interface pressure calculated by neglecting entry forces.

(iii) Large variations in coefficients of friction may be expected for apparently standardised conditions.

## II. AUTHOR'S INVESTIGATIONS

It is the purpose of this section to analyse the effects due to initial fitting, in shrink fits. The major variable is fit allowance and the analysis will include overstrained rings.

A theory is presented which is based on Sopwith's analysis of thick-walled cylinders. The latter is selected in view of the good agreement shown with experiment on mild steel cylinders under internal fluid pressure.

Results from three independent series of shrink fit specimens are presented. They are compared with theory and discrepancies discussed in detail.

Table IX indicates details of the series. Ring outside diameter to bore ( $k$ ) and length to bore  $\frac{L}{d}$  are constant at 2 and 11/12 respectively. Rings and plugs are of mild steel.

### 1. Theory

(i) To facilitate discussion of the subsequent experimental results it is convenient to summarize briefly at this stage the basis of the comparisons between experiment and theory which have been adopted.

(a) No resultant axial force exists on the ring or plug.

(b) The interface pressure is uniform along the entire length of the plug and ring. The members are of equal length.

(c) The plug strains elastically for all fits.

According to the maximum shear stress theory of failure the interface pressure must reach the yield stress in a tension test before inelasticity occurs in the plug. A 2:1 ratio ring will not carry such a high pressure and so it may be assumed that elastic stresses exist in the plug for all fits. No evidence of permanent set was found in any plugs after test.

(d) On dis-assembly the strains are released elastically.

Series No.	No. of Specimens	Nominal Bore Diam. (inches)	Range of Fit Allowances (Mils per inch)	Finish of Ring Bore	Finish on Plug	Lubricant
I	20	1 $\frac{1}{2}$	0 - 3.6	Ground Followed by Honing	Ground Followed by Honing	Sperm Oil
II	30	3	0 - 6	4-Super-Finished Remainder Turned	4-Super-Finished Remainder Ground	Sperm Oil
III	20	1 $\frac{1}{2}$	0 - 6.09	Turned	Ground	Chemically Dry

TABLE IX - SPECIMEN DETAILS

(ii) Relation between Fit Allowance and Interface Pressure

It is conditional that,

$$\Delta' = |\epsilon_{\theta} \text{ ring bore}| + |\epsilon_{\theta} \text{ plug}| \quad \text{-----} \quad (80)$$

From Lamé' elastic theory  $|\epsilon_{\theta} \text{ plug}| = \frac{(1 - \mu) P}{E} \quad \text{-----} \quad (81)$

If the ring is all elastic  $|\epsilon_{\theta} \text{ ring bore}| = \frac{P}{E (k^2 - 1)} [(1 - \mu) + k^2 (1 + \mu)] \quad \text{-----} \quad (82)$

A combination of Eqs. 80, 81, and 82 produce the customary elastic theory based on Lamé' and presented on pages 60 and 61. If the ring is overstrained ( $1 < n < k$ ), then

$$|\epsilon_{\theta} \text{ ring}| = \frac{s}{E} (1 - 2\mu) \left[ \frac{n^2}{k^2} + W_5 + a_0 W_1 \right] \quad \text{-----} \quad (83)$$

and the interface pressure,  $P$ , is given by,

$$P = s \left[ \log n^2 + \frac{k^2 - n^2}{k^2} \right] \quad \text{-----} \quad (84)$$

A combination of Eqs. 80, 81, 83, and 84 give,

$$\frac{E \Delta'}{s} = (1 - 2\mu) \left[ \frac{n^2}{k^2} + W_5 + a_0 W_1 \right] + (1 - \mu) \left[ \log n^2 + \frac{k^2 - n^2}{k^2} \right] \quad \text{-----} \quad (85)$$

Eqs. 84 and 85 enable the unit fit allowance,  $\Delta'$ , to be connected with the interface pressure,  $P$ . Thus for a given fit allowance the stresses and strains existing in the overstrained outer member may be found from the equations and graphs already presented on pages 34 - 39.

Fig. 50 shows a dimensionless plot connecting interface pressure and fit allowance.

(iii) Relation between Fit Allowance and Outside Diameter Circumferential Strain

From Eq. 43 of the thick-walled cylinder investigation,

$$\frac{E \epsilon_{\theta}^{\prime})_{o/d}}{s} = (1 - 2\mu) \left[ \frac{n^2}{k^2} + 2\mu a_o \right] + (1 + \mu) \frac{n^2}{k^2} \quad \text{--- (86)}$$

Eqs. 85, and 86 enable Fig. 51 to be plotted.

It is seen that the complete curve is practically a continuation of Lamé's elastic line. There is a slight tendency for the curve to rise more steeply as the fit allowances approach the fully plastic value.

(iv) Relation between Fit Allowance and Residual Strains

Elastic release of strains from P to zero, are given by,

$$E \epsilon_{\theta}^{\prime})_{o/d} = \frac{2P}{k^2 - 1} \quad \text{--- (87)}$$

$$E \epsilon_{\theta}^{\prime})_{bore} = \frac{P}{(k^2 - 1)} \left[ k^2 (1 + \mu) + (1 - \mu) \right] \quad \text{--- (88)}$$

It is apparent that residual strain is given by original strain less release of strain. Hence: -

$$\frac{E \epsilon_R^{\prime})_{o/d}}{s} = (1 - 2\mu) \left[ \frac{n^2}{k^2} + 2\mu a_o \right] + \frac{(1 + \mu) n^2}{k^2} - \frac{2P}{s (k^2 - 1)} \quad \text{--- (89)}$$

$$\frac{E \epsilon_R^{\prime})_{bore}}{s} = (1 - 2\mu) \left[ \frac{n^2}{k^2} + W_5 + a_o W_1 \right] - \frac{P [k^2 (1 + \mu) + (1 - \mu)]}{s (k^2 - 1)} \quad \text{--- (90)}$$

where P is given by Eq. 84.

From Eqs. 85 and 89, Fig. 52 is plotted.

From Eqs. 85 and 90, Fig. 53 is plotted.

Plots of stress against fit allowance are not given since the graphs of the thick-walled cylinder investigation are available. Figs. 51, 52, and 53 will be

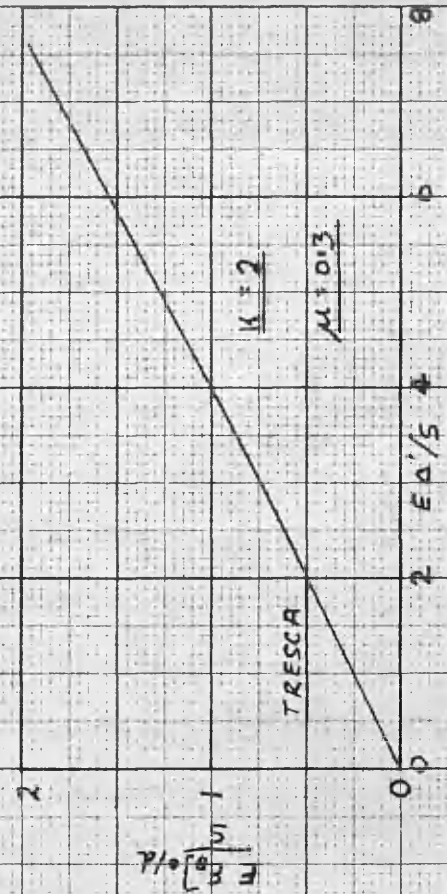


FIG. 50 - INTERFACE PRESSURE AGAINST FIT ALLOWANCE - THEORY

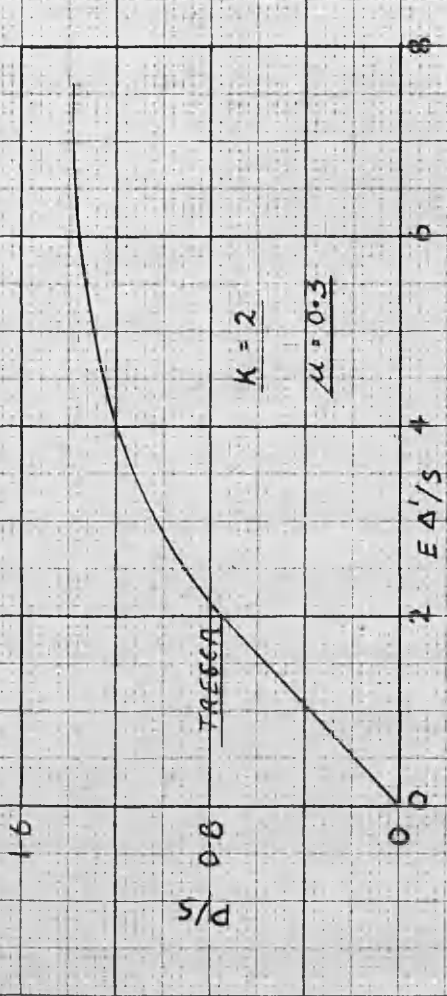


FIG. 51 - OUTSIDE DIAMETER STRAIN AGAINST FIT ALLOWANCE - THEORY

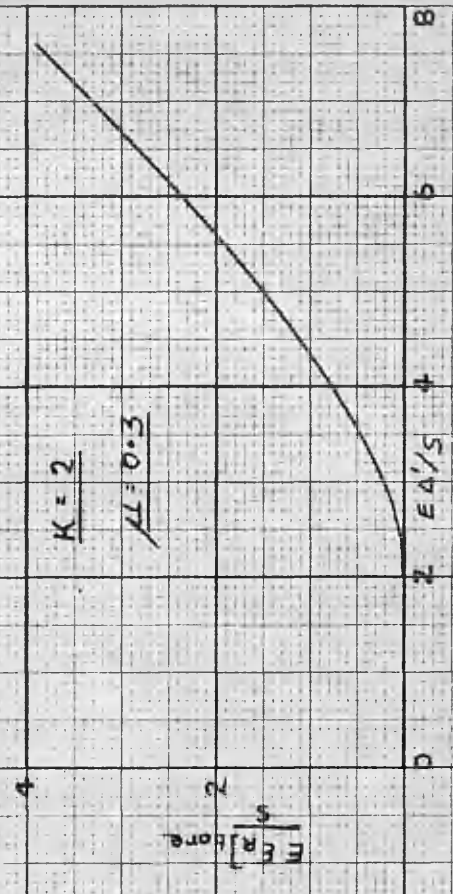


FIG. 52 - OUTSIDE DIAMETER RESIDUAL STRAIN AGAINST FIT ALLOWANCE - THEORY

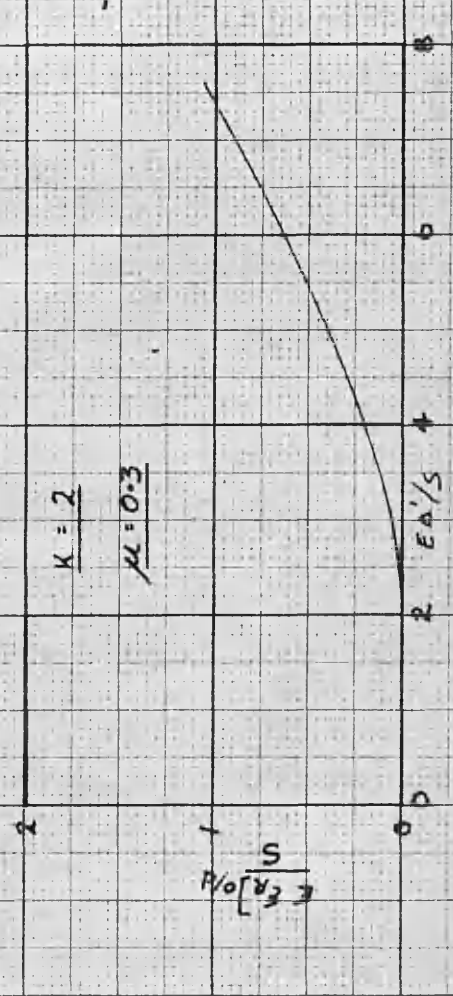


FIG. 53 - BORE RESIDUAL STRAIN AGAINST FIT ALLOWANCE - THEORY

compared with experimental observations.

## 2. Specimens

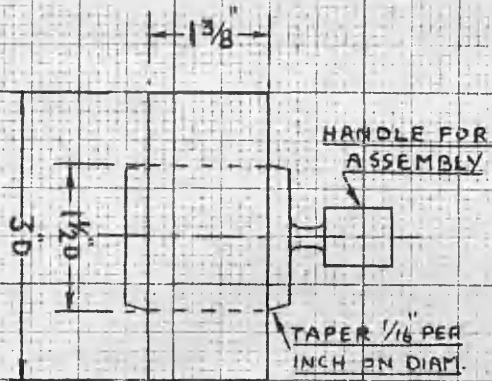
Figs. 54(e), (b), and (c) give sketches of specimens and pertinent information for series I, II, and III.

Specimens were all ordered from standard "28-32 Ton" mild steel and 4 tensile test specimens were supplied with each series. Variations are seen in Young's modulus and the yield stress. The figures given for each series are average values and similar variations may be taken to exist within series. This causes scatter of experimental points but it is thought that sufficient specimens are used to avoid the drawing of erroneous conclusions. No evidence of upper and lower yield point is shown in the tension tests. A sharp bend over in the graph characterises yielding.

Care was taken on machining the specimens to ensure (i) concentricity of bore and outside ring surfaces (ii) roundness and straightness of ring bore and plug diameter (iii) uniformity of mating surface, surface finishes in any one series.

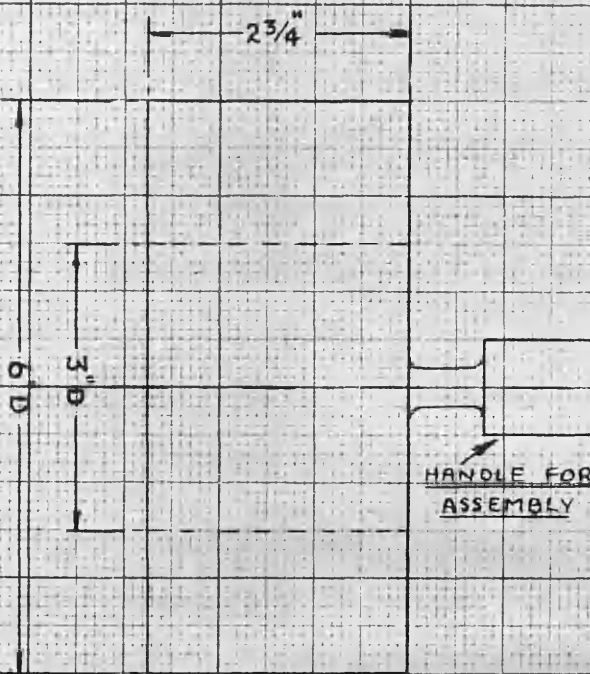
In series I a special attempt was made to eliminate the surface finish variable. Ring bores and plug diameters were ground close to size and then honed. This provided uniformity of surface finish condition. The finish, however, was so good that seizure of the larger fit allowance specimens took place. Adequate lubrication was supplied. A similar series of force fit specimens seized at entry for fit allowances low in the elastic range, and the tests had to be abandoned. This suggests there is a limit to the fineness of finish that can be used for force fits.

It is considered that concentricity, roundness, and straightness are adequately controlled in the tests.



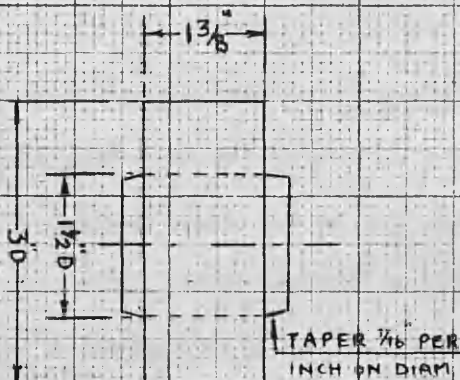
(a) SERIES I

YIELD STRESS ( $\frac{\text{TONS}}{\text{IN}^2}$ )	17.68
ULTIMATE STRESS ( $\frac{\text{TONS}}{\text{IN}^2}$ )	30.15
YOUNG'S MODULUS ( $\frac{\text{TONS}}{\text{IN}^2}$ )	13,400
% REDUCTION IN AREA	52
% ELONGATION	34



(b) SERIES II

YIELD STRESS ( $\frac{\text{TONS}}{\text{IN}^2}$ )	16.7
ULTIMATE STRESS ( $\frac{\text{TONS}}{\text{IN}^2}$ )	29
YOUNG'S MODULUS ( $\frac{\text{TONS}}{\text{IN}^2}$ )	14,000
% REDUCTION IN AREA	49.7
% ELONGATION	36



(c) SERIES III

YIELD STRESS ( $\frac{\text{TONS}}{\text{IN}^2}$ )	14.5
ULTIMATE STRESS ( $\frac{\text{TONS}}{\text{IN}^2}$ )	30.2
YOUNG'S MODULUS ( $\frac{\text{TONS}}{\text{IN}^2}$ )	13,400
% REDUCTION IN AREA	59.6
% ELONGATION	29

FIG. 54 - INTERFERENCE FIT SPECIMENS.

### 3. Measuring Devices

#### (i) Fit Allowance

Fit allowances are measured correct to the nearest  $1/10,000$ th of an inch.

Ring bores are measured by comparators of the John Bull (1-1/2" nominal bore diam.) and Mercer (3" nominal bore diam.) type, set to a ring gauge standard.

Fig. 55 shows a photograph of the Mercer comparator. Bores may be explored by this method and degree of bellmouthing and taper noted. An average of ten readings at least is taken.

Plug diameters are measured by a Sigma vertical comparator ( $\pm .003$  inches) set to Johanssen slip gauges. Fig. 56 shows the instrument measuring the outside diameter of one of the rings. The standard slip gauges are shown along side. Any irregularity in surface generation is noted and an average of at least ten readings taken as the dimension.

#### (ii) Ring Outside Diameter Measurement

As for plug diameters (See Fig. 56).

#### (iii) Records of Fit Surface Finishes

A record is made of all the mating surfaces. They are not used in this thesis but it is believed that in the future, coefficients of friction may be related to physical quantities. The records were made to complete the experimental observations.

A Taylor and Hobson "Talysurf" machine (Fig. 57) is used which gives (a) a trace of surface micro-imperfections and (b) an "average roughness" figure. The stylus covers a surface distance of approximately 0.2 inches in its travel and a trace is obtained with magnification ranges of 2000 - 40,000 times vertically (perpendicular to surface) and 50 or 200 times horizontally (parallel to surface). Average roughness figures are obtained from an electronic integration meter.

A representative "average roughness" figure for a surface is found from the

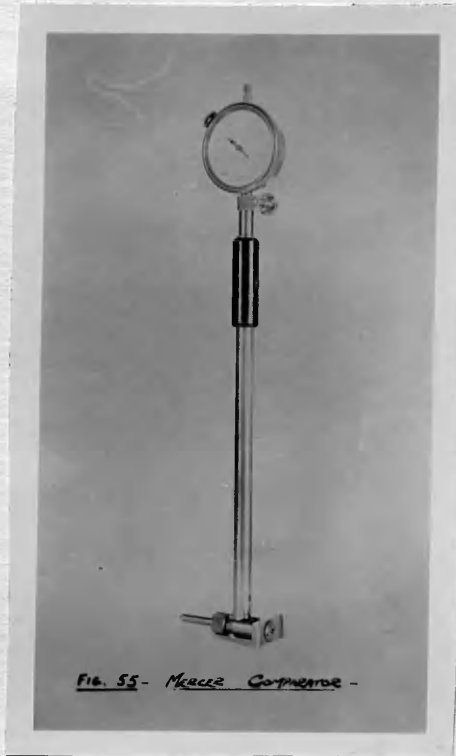


**Fig. 55 - MERCER COMPARATOR.**



Fig. 56 - SIGMA VERTICAL COMPARATOR.

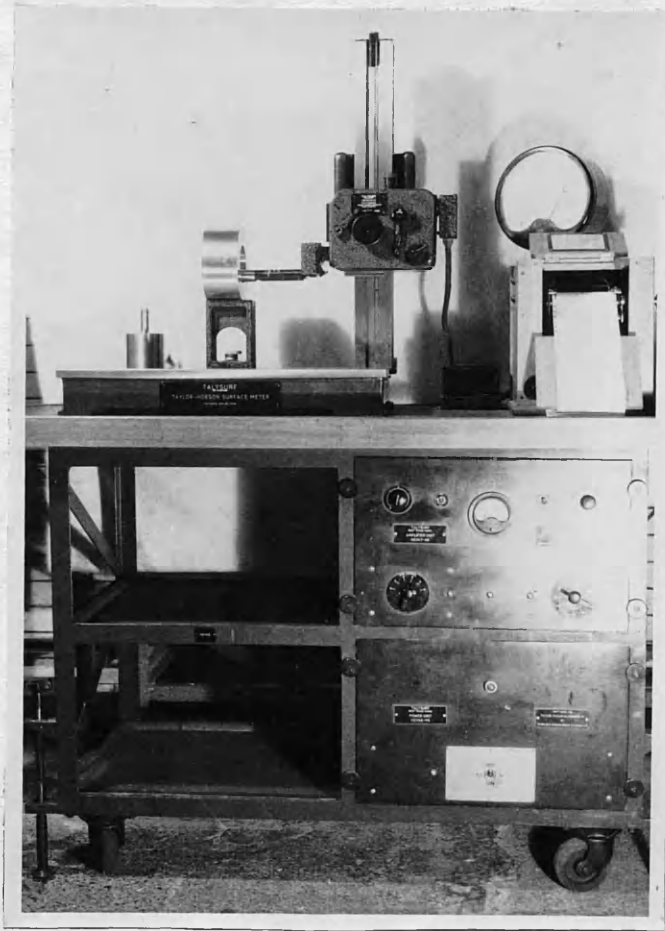


Fig. 57 - TALYSURF SURFACE - FINISH MACHINE.

mean of 10 to 15 runs made at various locations. A typical trace is then recorded and these two observations taken to define the surface.

#### (iv) Shrinking Process

The rings are brought to a uniform heat in a Birlec, thermostatically controlled furnace. The ring surfaces are thoroughly degreased before placing in the furnace. Approximately one hour per inch of metal thickness is allowed for soaking time. When the ring is ready, the plug is degreased, dipped in the lubricant (sperm oil), and immediately inserted in the hot element. Cooling is effected in air.

#### (v) Stripping Process

The holding ability of an assembly is determined by applying an axial load to the plug (Fig. 58). The cylindrical die and plunger are obvious essentials. An Avery 30 Ton electro-hydraulic machine is suitable for the 1-1/2 inch bore diameter specimens. A 100 Ton beam type Avery machine pushed out the 3 inch specimens.

Care is taken to ensure purely axial loading of the grip by placing the assembly centrally on the crosshead. Loads are applied at approximately 2000 lbs. per minute. Slipping, except for very small fits, is accompanied by sharp cracks.

#### 4. Test Procedure

Operations are indicated by the following chronological sequence: -

- (1) Ring bore measurement.
- (2) Plug diameter measurement.
- (3) Ring outside diameter measurement.
- (4) Records of mating surface, surface finishes.
- (5) Shrinking Process.
- (6) Ring outside diameter measurement.

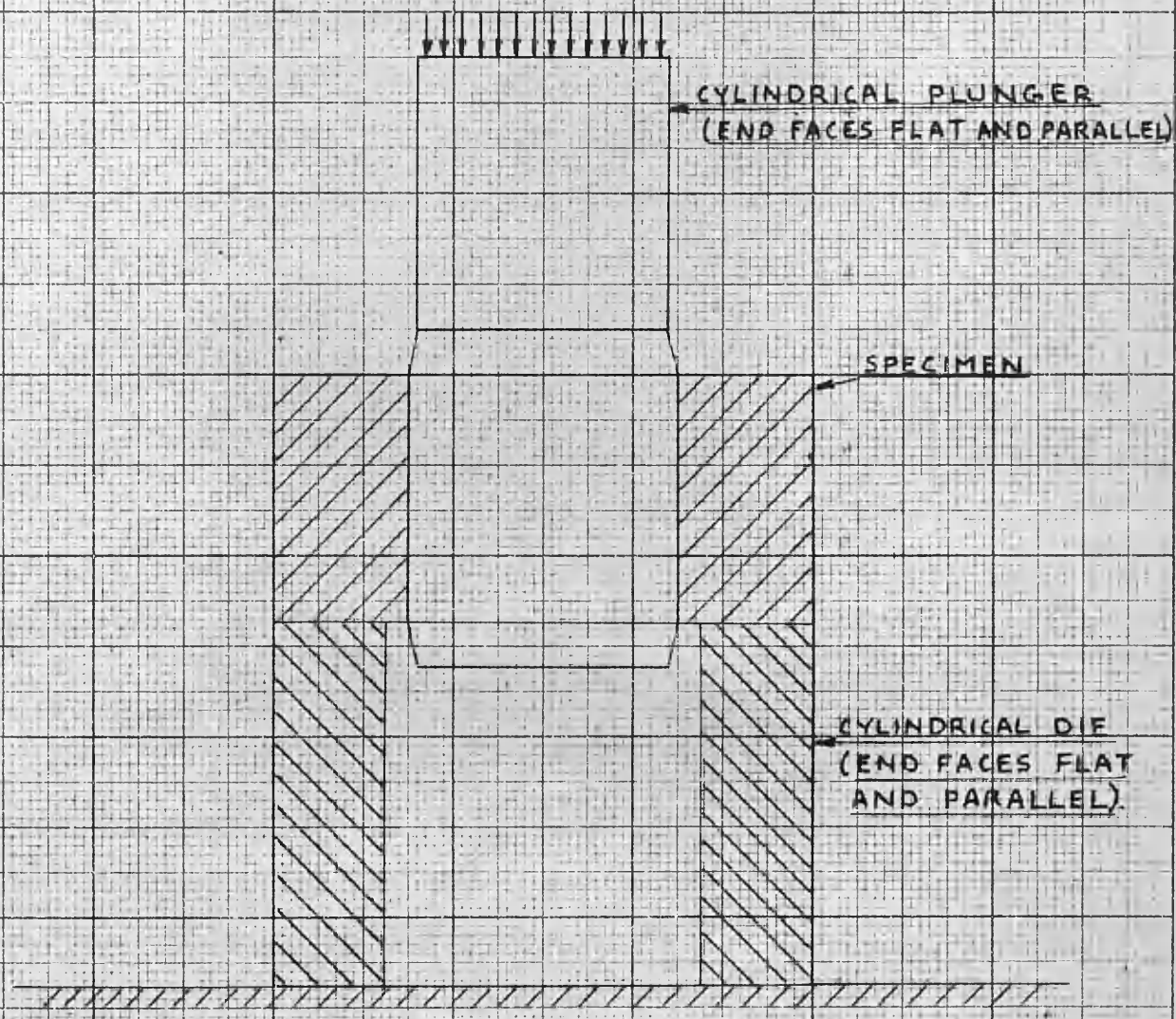


FIG. 58 - DISASSEMBLY BY AXIAL FORCE.

- (7) Stripping Process.
- (8) Ring outside diameter measurement.
- (9) Ring bore measurement.
- (10) Plug diameter measurement.
- (11) Records of mating surface, surface finishes.

Computations may be made as follows: -

Initial Fit Allowance	---	(2) - (1)
Ring o/d change on fitting	---	(6) - (3)
Ring o/d permanent set	---	(8) - (3)
Ring bore permanent set	---	(9) - (1)
Plug diameter permanent set	---	(10) - (3)
Residual fit allowance	---	[(2) - (1)] - [(9) - (1) + (10) - (3)]

The fine measurements presented a problem in patience. It was necessary to develop experience and skill in the use of all the measuring instruments before faith could be placed in the accuracy of the readings. All the rules associated with current metrology practice were rigidly adhered to.

##### 5. Experimental Results

Non-dimensional plots are used in recording the strain results. This reduces the number of graphs and aids in the comparison of the different series.

Fig. 59 shows the results of outside diameter change on fitting to a base of fit allowance. The full line is the theoretical curve of Fig. 51. The dotted line represents the mean curve drawn through the experimental points for series III (dry).

Figs. 60 and 61 record outside diameter and bore permanent sets respectively. Theoretical curves are shown with and without correction for temperature effects. Series III specimens seized on dis-assembly and are not recorded.

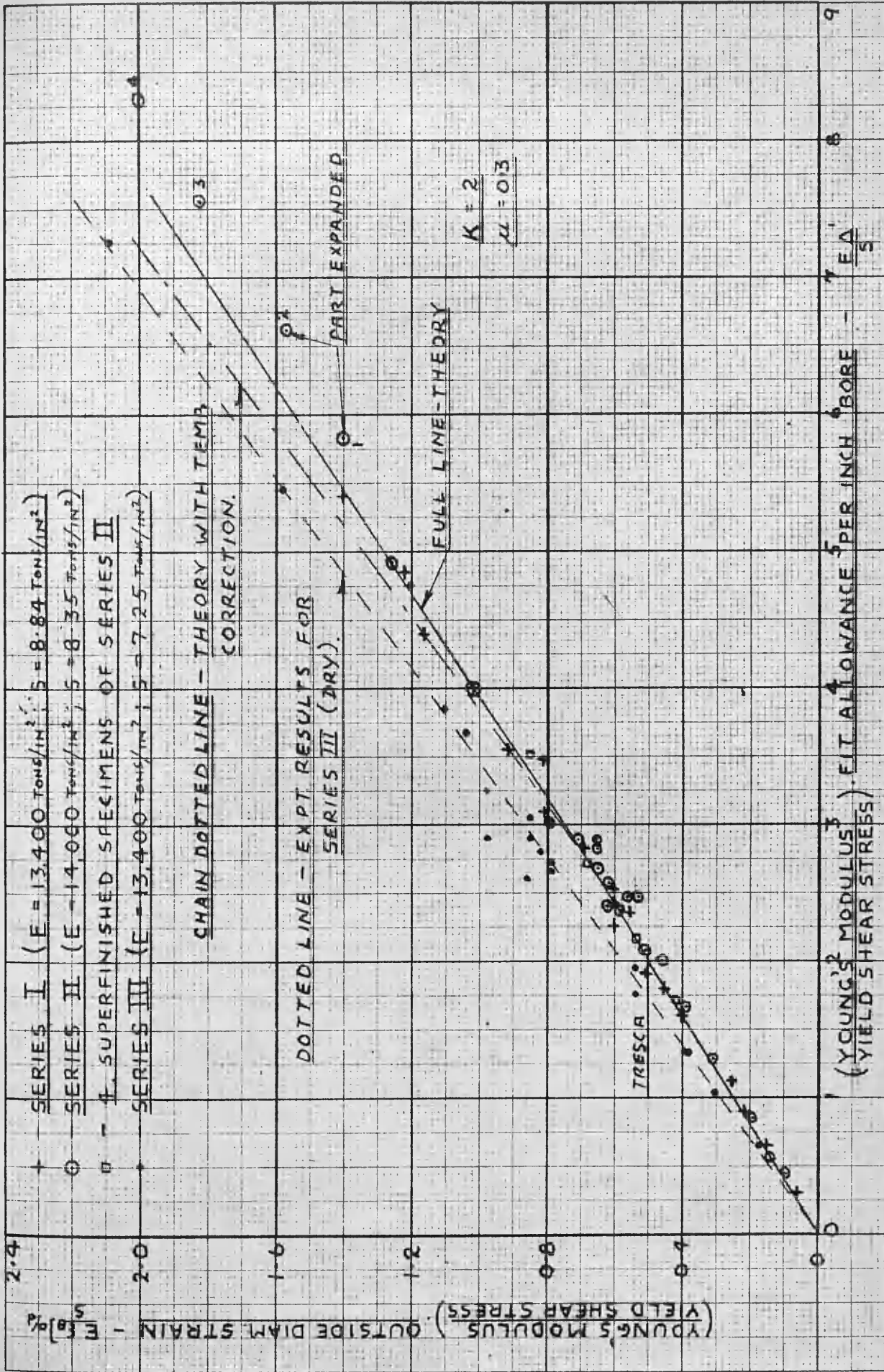


FIG. 59 - EXPERIMENTAL OUTSIDE DIAMETER DEFLECTIONS

20 X 25 PHOTO COPY  
 20 X 25 PHOTO COPY  
 20 X 25 PHOTO COPY

(YOUNG'S MODULUS / 4 RESIDUAL STRAIN -  $\frac{E E_R}{S}$ )  
 (YIELD SHEAR STRESS)

- + - SERIES I (E = 13400 TONS/IN<sup>2</sup>; S = 8.84 TONS/IN<sup>2</sup>)
- o - SERIES II (E = 14,000 TONS/IN<sup>2</sup>; S = 8.35 TONS/IN<sup>2</sup>)
- - SUPERFINISHED SPECIMENS OF SERIES II

0.3

CHAIN DOTTED LINE - THEORY WITH  
 TEMP CORRECTION

$K = 2$

$\mu = 0.3$

PART EXPANDED

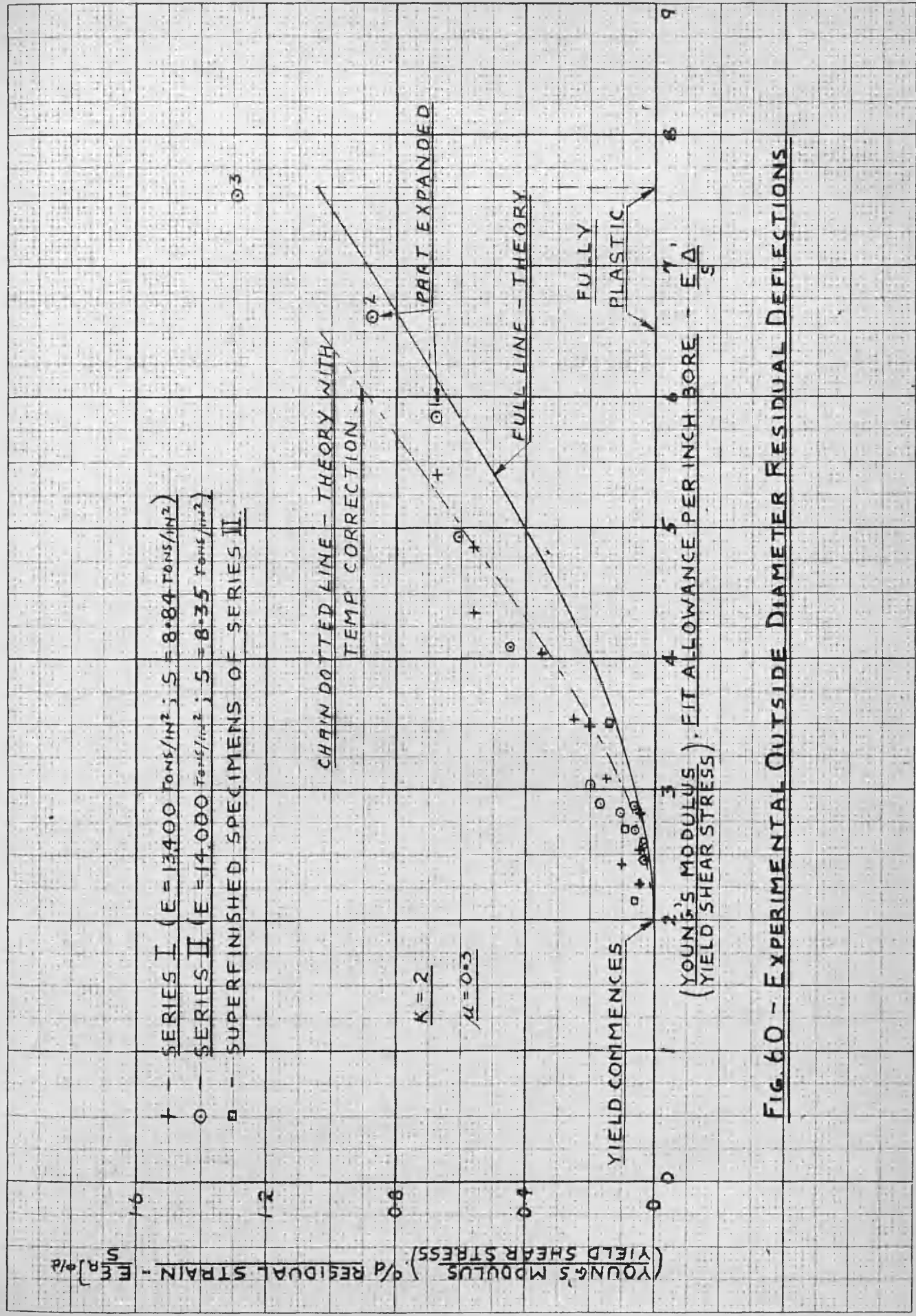
FULL LINE - THEORY

YIELD COMMENCES

FULLY PLASTIC

(YOUNG'S MODULUS / YIELD SHEAR STRESS) FIT ALLOWANCE PER INCH BORE -  $\frac{E \Delta}{S}$

FIG. 60 - EXPERIMENTAL OUTSIDE DIAMETER RESIDUAL DEFLECTIONS



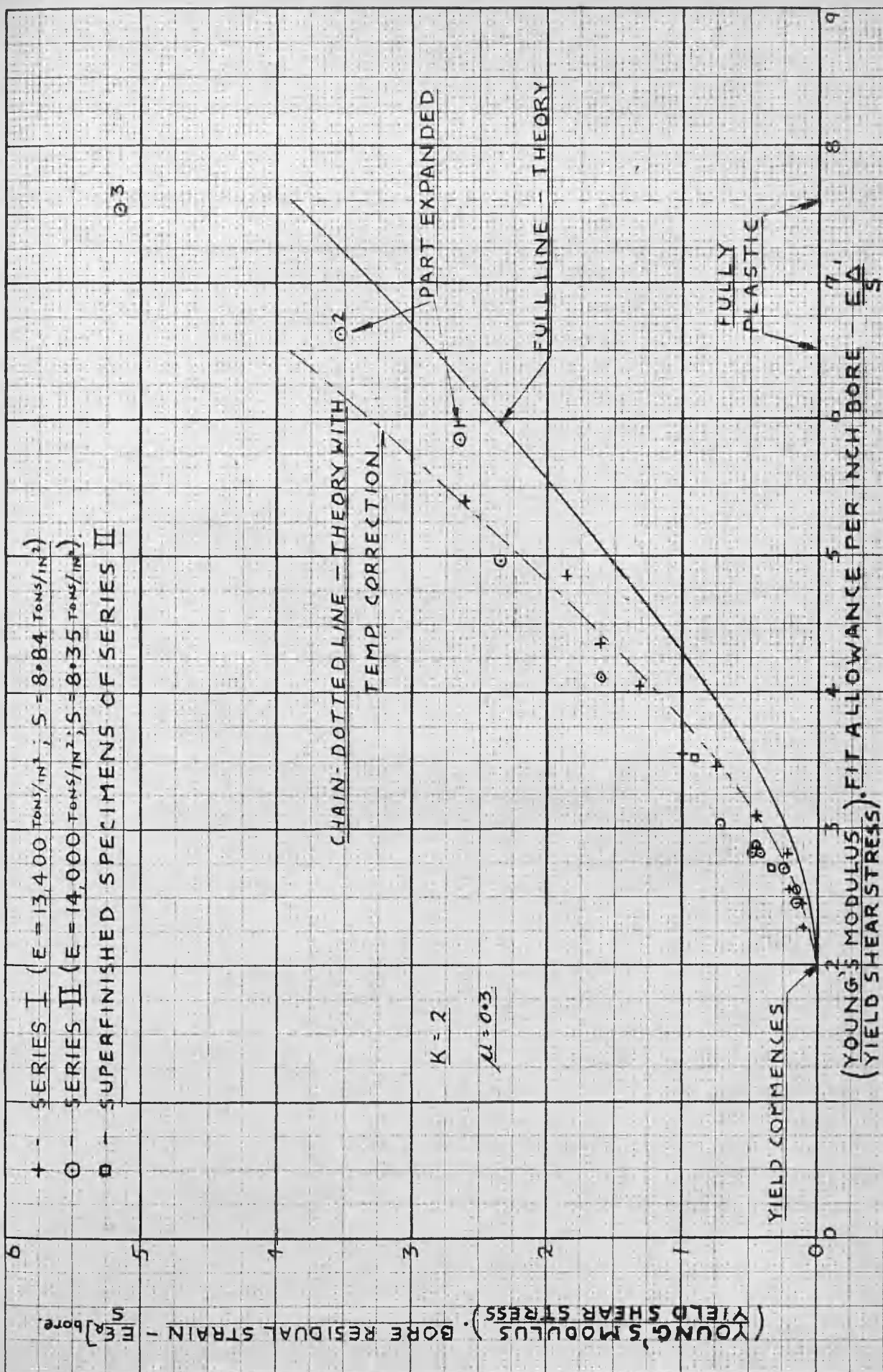
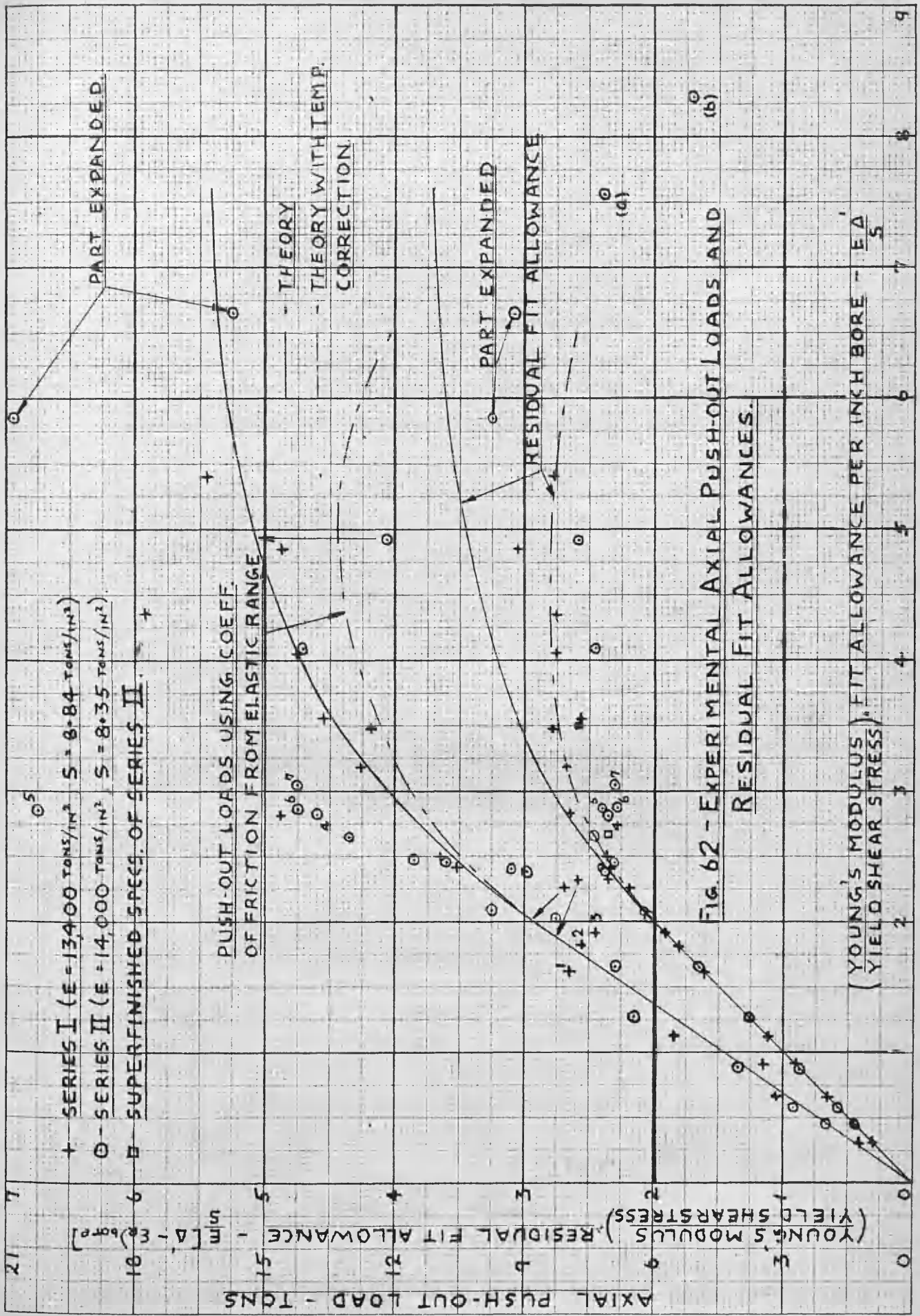


FIG. 61 - EXPERIMENTAL BORE RESIDUAL DEFLECTIONS

REPRODUCED FROM "STRESS AND STRAIN IN METALS" BY R. W. CLIFTON, JOHN WILEY & SONS, INC., 1954

Fig. 62 shows experimental points and theoretical curves for residual fit allowances and axial push out loads. Axial loads for superfinished specimens are given in Table X to avoid ambiguity in Fig. 62.

Table XI records the axial push out first slip and maximum loads for series III specimens.



+ SERIES I (E = 134,000 TONS/IN<sup>2</sup> S = 8.84 TONS/IN<sup>2</sup>)  
 o - SERIES II (E = 14,000 TONS/IN<sup>2</sup> S = 8.35 TONS/IN<sup>2</sup>)  
 B - SUPERFINISHED SPEC. OF SERIES II

PUSH-OUT LOADS USING COEFF. OF FRICTION FROM ELASTIC RANGE

- THEORY  
 - THEORY WITH TEMP. CORRECTION

PART EXPANDED  
 RESIDUAL FIT ALLOWANCE

FIG. 62 - EXPERIMENTAL AXIAL PUSH-OUT LOADS AND RESIDUAL FIT ALLOWANCES.

(YOUNG'S MODULUS) RESIDUAL FIT ALLOWANCE  
 (YOUNG'S MODULUS) FIT ALLOWANCE PER INCH BORE - EA

$\frac{E \Delta'}{s}$	1st Slip Load	% Decrease from Mean of Series I and II Loads.
1.71	18.2	37
2.14	26.1	30
2.69	29.5	34
3.5	29.4	45

TABLE X - 1ST SLIP LOADS - SERIES II -

SUPERFINISHED SPECIMENS

Fit Allowance per inch bore diameter (mils/in.)	1st Slip (Tons)	Maximum Load (Tons)
0.56	9.56	30
0.97	20.3	56.1
0.97	22.1	63.6
1.06	15	54.8
1.44	14	52.7
1.41	18.25	55.6
1.52	14.6	56.85
1.47	15.3	53.8
1.57	13	55.5
1.57	17	54.8
1.77	18.1	57.9
1.67	14.3	58.15
2.00	15.9	57.8
2.08	15.56	49.5
2.58	16	56.2
2.97	10.7	55.7
3.93	28	57
6.09	58.3	58.3

TABLE XI - 1ST SLIP AND MAXIMUM LOADS FOR DRY SPECIMENS - SERIES III

### III. DISCUSSION OF AUTHOR'S EXPERIMENTAL RESULTS

Results show discrepancies between experimental points and theory. For instance, in Fig. 59 the lubricated specimens (series I and II), in general, show agreement whereas the dry specimens (series III) are decidedly different. Also, the residual strains (Figs. 60 and 61) are higher than those predicted by the analysis.

It is apparent that factors are operative which are not accounted for in the theory. These factors will be introduced and their effects analysed. The experimental observations may then be more conveniently discussed.

#### 1. Axial Friction at the Interface

This problem is discussed in the review by reference to Goodier's work on frictional effects due to cooling. The writer pointed out that frictional effects are also produced due to the nature of straining of the members. The ring tends to contract axially whereas the plug expands, under the action of an interface pressure.

It is evident that the "axial effect" is not constant but will vary with fit allowance and coefficient of friction. As straining commences the mating surfaces grip and slip, depending on the normal force and friction conditions. Gripping tends to increase the fit allowance and hence the interface pressure; slipping produces the opposite effect. It is not known whether slipping is accompanied by a gradual or sudden movement.

The initiation of plastic flow in the ring may produce a change in the axial effect. The complexity of stress conditions prevents an accurate analysis but it is evident that the axial stiffness of the ring bore layers is decreased and a relief of strain in the plug ensues. As plastic flow progresses in the ring, it is expected that the axial effect, interpreted as a fraction of the fit allowance,

will decrease.

Two approximate analyses will indicate the magnitude of the axial effect and present its importance in the correct perspective.

(i) Approximate Analysis for Condition of No Slip

The ring is assumed to be at uniform temperature  $T$  when the cold plug first comes in contact. If the fit allowance is  $\Delta'$  for the assembly then

$$\Delta' = T \alpha \quad \text{-----} \quad (91)$$

Also, assume that on initial contact immediate gripping occurs uniformly along the length of the assembly. On final cooling the plug will be in axial compression ( $\delta L_p$ ) and the ring in axial tension ( $\delta L_R$ ). (It should be emphasised that the analysis covers effects due to cooling only.)

Then,

$$L \alpha T = \delta L_p + \delta L_R \quad \text{-----} \quad (92)$$

It is assumed that the frictional forces are uniformly distributed along the length of the assembly. Also an average value of stress (obtained by dividing total load on section by area of section) is used in the belief that the strains calculated from it will be reasonably accurate (Fig. 63). This stress builds up towards the central cross section of the assembly. In the calculation of average axial strains the stresses at a distant of  $L/4$  from the ends will be used.

Thus, if  $F_A$  is the total axial frictional force, there exists: -

(a) Plug

$$\text{mean stress} = \frac{F_A/2}{\pi/4 d^2}$$

$$\text{mean axial strain} = \frac{2 F_A}{\pi d^2 E}$$

$$\text{mean change in length} = \delta L_p = \frac{2 F_A L}{\pi d^2 E} \quad \text{-----} \quad (93)$$

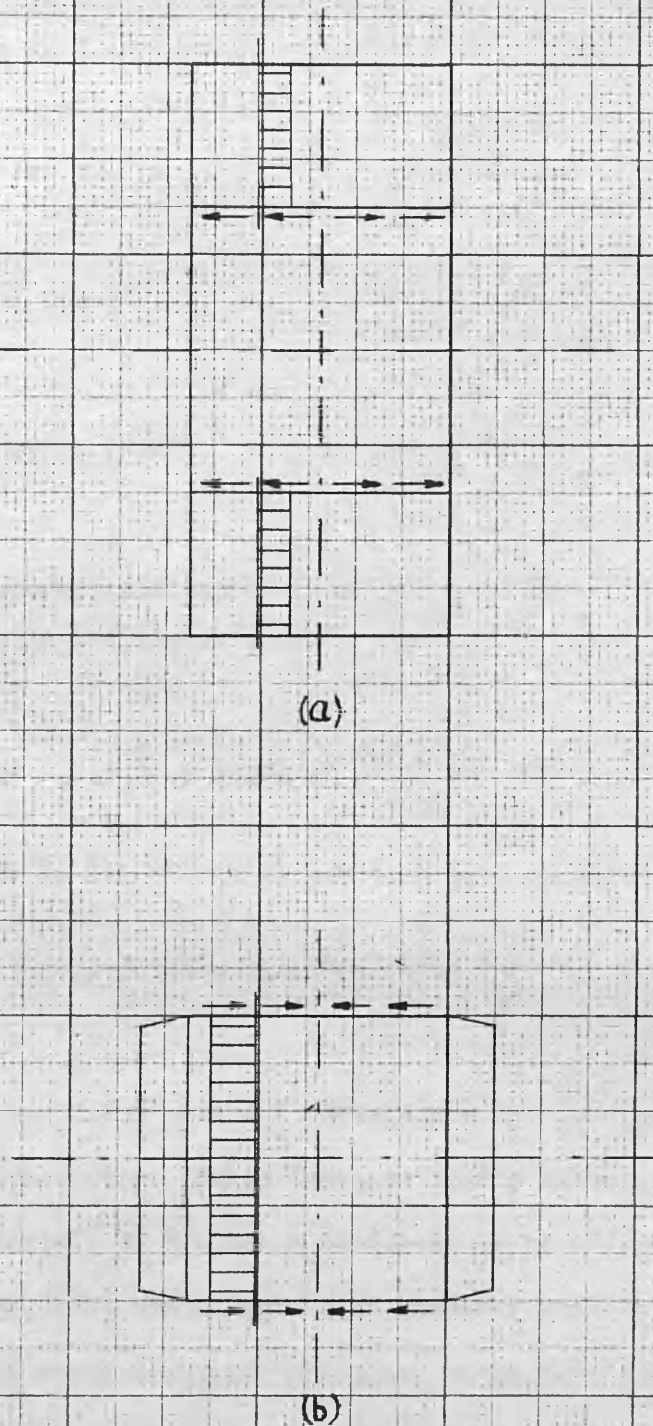


FIG. 63 - ASSUMED LOAD AND STRESS FOR APPROX.  
ANALYSIS OF FRICTIONAL EFFECT.

$$\text{mean circumferential strain} = \frac{2\mu F_A}{\pi d^2 E} \quad \text{----- (94)}$$

(increase in diameter)

(b) Ring

$$\text{mean stress} = \frac{F_A/2}{\frac{\pi}{4} (D^2 - d^2)}$$

$$\text{mean axial strain} = \frac{2 F_A}{\pi (D^2 - d^2) E}$$

$$\text{mean change in length} = \frac{2 F_A L}{\pi (D^2 - d^2) E} \quad \text{----- (95)}$$

$$\text{mean circumferential strain} = \frac{2\mu F_A}{\pi (D^2 - d^2) E} \quad \text{----- (96)}$$

(decrease in diameter of bore)

From Eqs. 91, 92, 93, 95,

$$F_A = \pi E \Delta' d^2 \frac{(k^2 - 1)}{2 k^2} \quad \text{----- (97)}$$

if  $\delta \Delta'$  is increase in fit allowance per inch bore diameter,

$$\delta \Delta' = \mu \Delta' \frac{(k^2 - 1)}{k^2} + \frac{\mu \Delta'}{k^2}$$

$$\delta \Delta' = \mu \Delta' \quad (\text{where } k = 2) \quad \text{----- (98)}$$

$\mu = 0.3$  for steel assemblies. Hence increase in fit allowance per inch bore diameter is approximately 30 % for a condition of no slip at the interface. It is unlikely, however, that the effect in an assembly will be so severe, since some slip is sure to occur even with specimens which have dry surfaces.

(ii) Approximate Analysis Including Coefficient of Friction

The approximations are the same as in the previous analysis. The difference lies in the method of calculating  $F_A$ .

$$\text{It is apparent that } F_A = \bar{\mu} \cdot P \cdot \pi \frac{dL}{2} \quad \text{----- (99)}$$

where  $\bar{\mu}$  is the coefficient of friction.

$$\text{Hence } \delta \Delta' = \frac{\mu \bar{\mu} P}{E} \cdot \frac{L}{d} \cdot \frac{k^2}{(k^2 - 1)} \quad \text{----- (100)}$$

Inserting experimental values: -  $k = 2$ ;  $\frac{L}{d} = \frac{11}{12}$ ;  $\mu = 0.3$ ;  $\bar{\mu} = 0.3$  - - -

a reasonable figure for machined and lubricated surfaces,

$$\delta \Delta' = .11 \frac{P}{E} \quad \text{----- (101)}$$

Eq. 101 may be expressed in terms of  $\Delta'$  also but the relation between  $P$  and  $\Delta'$  is not linear. To compare with previous analysis choose the maximum elastic condition to relate  $P$  and  $\Delta'$ .

$$\frac{E \Delta'}{s} = 1.994 \quad ; \quad \frac{P}{s} = .75$$

$$\frac{P}{E} = .376 \Delta'.$$

Hence  $\delta \Delta' = .041 \Delta'$ .

An increase, for this particular value of  $\Delta'$ , of 4.1 % is to be expected for machined and lubricated specimens.

It may be concluded that these approximate analyses show the following: -

(a) A noticeable axial effect is possible if the mating surfaces have a high coefficient of friction. Such a condition exists if shrink fits are assembled "dry".

(b) For machined and lubricated surfaces, the effect is small and may well be within the limits of experimental error.

(c) Axial effects, interpreted as increase in interface pressure, reduce as plastic flow in the ring progresses.

## 2. Variations in Elastic Constants due to Temperature

There are two stages to be considered in the cooling of an overstrained shrink fit assembly.

(i) Period during which heat is transferred from the hot ring to the cold plug. In this time the total fit is realised and it is important in calculating stresses or strains to use the appropriate value of the elastic constants (notably Young's modulus and the yield shear stress) for the temperature at which straining is accomplished. Overstrain will proceed to a radius given by ' $\bar{n}$ ', which will be larger than the corresponding one calculated at room temperature.

(ii) Period during which the assembly is gradually cooling down to room temperature. It is evident that the elastic constants will regain their room temperature values and that the interface pressure will alter. It will in fact increase and may be calculated from Eq. 80, viz.  $\Delta' = |\epsilon_{\theta \text{ plug}}| + |\epsilon_{\theta \text{ ring}}|$ . The value of  $\epsilon_{\theta \text{ ring}}$  is found by observing that the ring is, in effect, loaded to give a depth of plastic flow ' $\bar{n}$ ' and then partially unloaded.

In the following analysis the overscript ( $\bar{\quad}$ ) denotes values of symbols for temperatures other than ambient.

Consider an assembly of fit allowance per inch bore diameter  $\Delta'$ .

The temperature at which ring meets plug is given by,

$$T = \frac{\Delta'}{\alpha} \quad \text{-----} \quad (102)$$

It can be shown approximately by neglecting radiation that the equilibrium temperature at which the fit is realised is given by,

$$\bar{T} = \frac{(k^2 - 1)}{k^2} T \quad \text{-----} \quad (103)$$

For the cylinders in this thesis,  $k = 2$ , thus  $\bar{T} = \frac{3}{4} T$ .

The values of ' $\bar{E}$ ' and ' $\bar{s}$ ' corresponding to ' $\bar{T}$ ' will be used to determine strains in the initial period.

Depth of overstrain may be found from

$$\frac{\bar{E} \Delta'}{s} = (1 - 2\mu) \left[ \frac{\bar{n}^2}{k^2} + \bar{W}_5 + \bar{a}_0 \bar{W}_1 \right] + (1 - \mu) \left[ \log \bar{n}^2 + \frac{k^2 - \bar{n}^2}{k^2} \right] \quad \text{----- (104)}$$

There is an interface pressure corresponding to ' $\bar{n}$ ' and given by,

$$\bar{P} = s \left[ \log \bar{n}^2 + \frac{k^2 - \bar{n}^2}{k^2} \right] \quad \text{----- (105)}$$

These conditions are assumed to exist in the ring and plug reaching an equilibrium temperature  $\bar{T}$ .

When the assembly cools to room temperature, let pressure  $P'$  exist. Then: -

$$|\epsilon_{\theta} \text{ plug}| = \frac{P'}{E} (1 - \mu)$$

$$|\epsilon_{\theta} \text{ ring}| = \frac{s}{E} \left[ (1 - 2\mu) \left\{ \frac{\bar{n}^2}{k^2} + \bar{W}_5 + \bar{a}_0 \bar{W}_1 \right\} \right] - \frac{(P - P')}{E (k^2 - 1)} \left[ k^2 (1 + \mu) + (1 - \mu) \right]$$

The first term on the right hand side represents the bore strain for a ring under internal pressure ' $P$ ' at room temperature and strained to  $n = \bar{n}$ . The second term gives the elastic release of bore strain when pressure falls to ' $P'$ '. It is seen that,

$$\frac{E \Delta'}{s} = \frac{P' (1 - \mu)}{s} + (1 - 2\mu) \left[ \frac{\bar{n}^2}{k^2} + \bar{W}_5 + \bar{a}_0 \bar{W}_1 \right] - \frac{(P - P') \cdot [k^2 (1 + \mu) + (1 - \mu)]}{s (k^2 - 1)}$$

Substituting from Eq. 104 and rearranging,

$$\frac{(P - P')}{s} = \frac{(k^2 - 1) \Delta'}{2 k^2} \left[ \frac{\bar{E}}{s} - \frac{E}{s} \right] \quad \text{----- (106)}$$

N.B. It should be emphasised that ' $P'$ ' is the interface pressure at room temperature for a ring overstrain condition given by  $n = \bar{n}$ .

Corrections to the four theoretical graphs (Figs. 51 to 53 inclusive) are made using Figs. 64 and 65. Fig. 64 is constructed from available information (21), (32), (46) on mild steel in the range of temperatures under consideration.

Individual authors are in poor agreement as to the specific magnitude of the effect of temperature on Young's modulus and shear stress. The curve of Fig. 64 must be considered approximate. It is sufficient, however, to demonstrate the sensitivity of an overstrained shrink fit assembly to the temperature at which the fit is completed. It should also be noted that  $\bar{T}$  is the minimum temperature of fitting and may be considerably higher in practice. Fig. 65 is constructed from the theory originally presented on pages 132 to 135.

The steps to be noted in the correction are as follows: -

1. Select  $\Delta'$ .
2. From Eqs. 102 and 103 calculate  $T$  and  $\bar{T}$  respectively.
3. From Fig. 64 find  $\bar{E}/s$  for specific  $\bar{T}$ .
4. From Eq. 106, calculate  $\frac{(P - P')}{s}$ .
5. From  $\frac{\bar{E}\Delta'}{s}$  and Fig. 65 estimate  $\bar{n}$ .
6. From ' $\bar{n}$ ' estimate  $\frac{E \epsilon_{\theta} o/d}{s}$  ---- N.B. This is the room temperature calculation for outside diameter strain for a value of  $n = \bar{n}$ .
7. From  $\frac{(P - P')}{s}$  and Fig. 6 estimate elastic release of outside diameter strain.

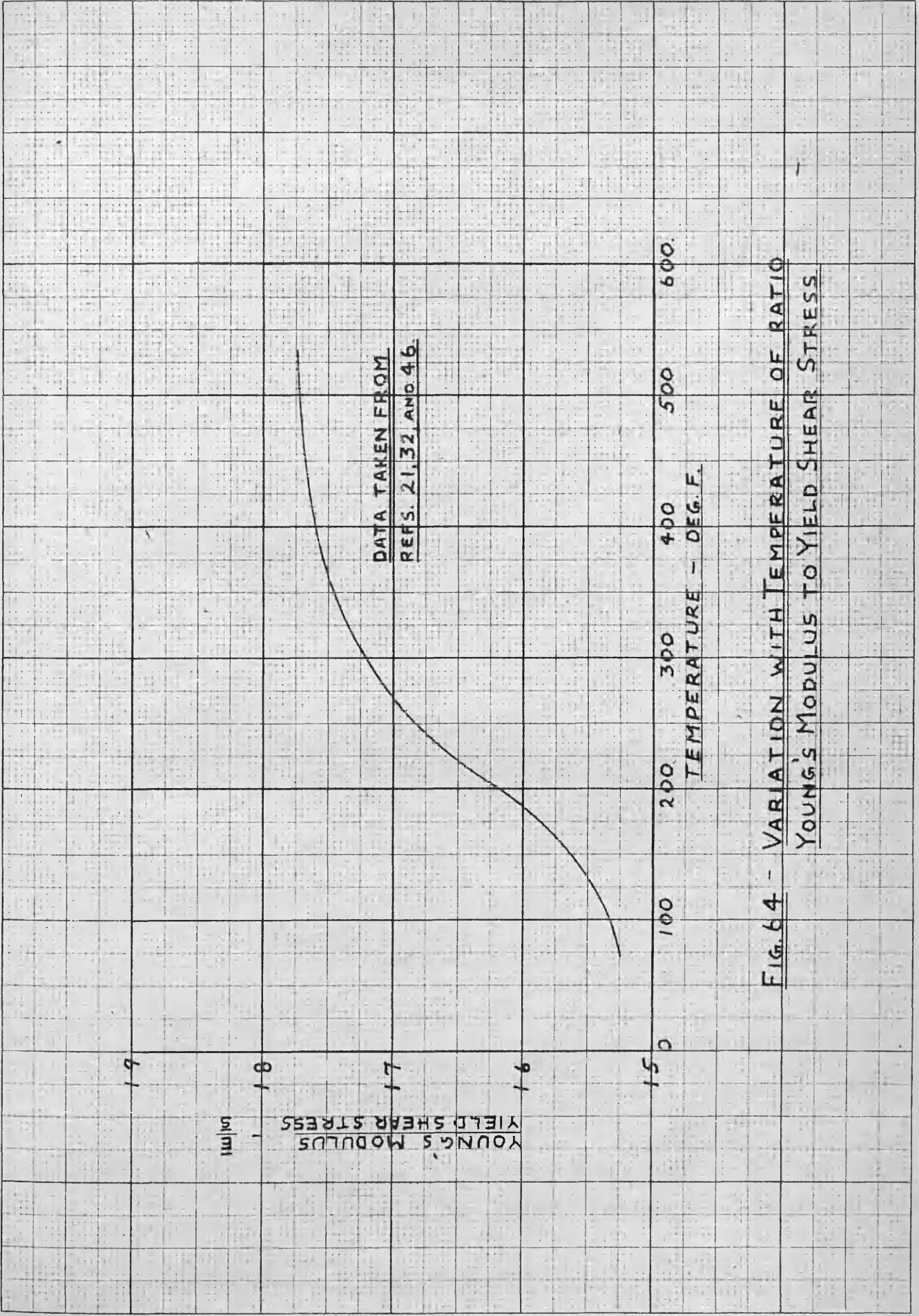
It is evident that the corrected room temperature values of

(a) Outside diameter strain is given by (6) - (7). i.e. the calculated value of  $\frac{E \epsilon_{\theta} o/d}{s}$  for  $n = \bar{n}$ , less the release of  $\frac{E \epsilon_{\theta} o/d}{s}$  due to pressure falling to  $P'$ .

(b) Outside diameter and bore permanent sets are obtained from Fig. 65 and  $n = \bar{n}$ .

(c) Interface pressure ( $P'$ ) is obtained from values of  $\frac{(P - P')}{s}$  and estimation of  $\frac{P}{s}$  at  $n = \bar{n}$ , from Fig. 65.

Elastic constant temperature corrections are shown in Figs. 59, 60 and 61.



DATA TAKEN FROM  
REFS. 21, 32, AND 46.

FIG. 64 - VARIATION WITH TEMPERATURE OF RATIO  
YOUNG'S MODULUS TO YIELD SHEAR STRESS

PHOTOCOPIED FROM THE PROCEEDINGS OF THE AMERICAN SOCIETY OF MECHANICAL ENGINEERS

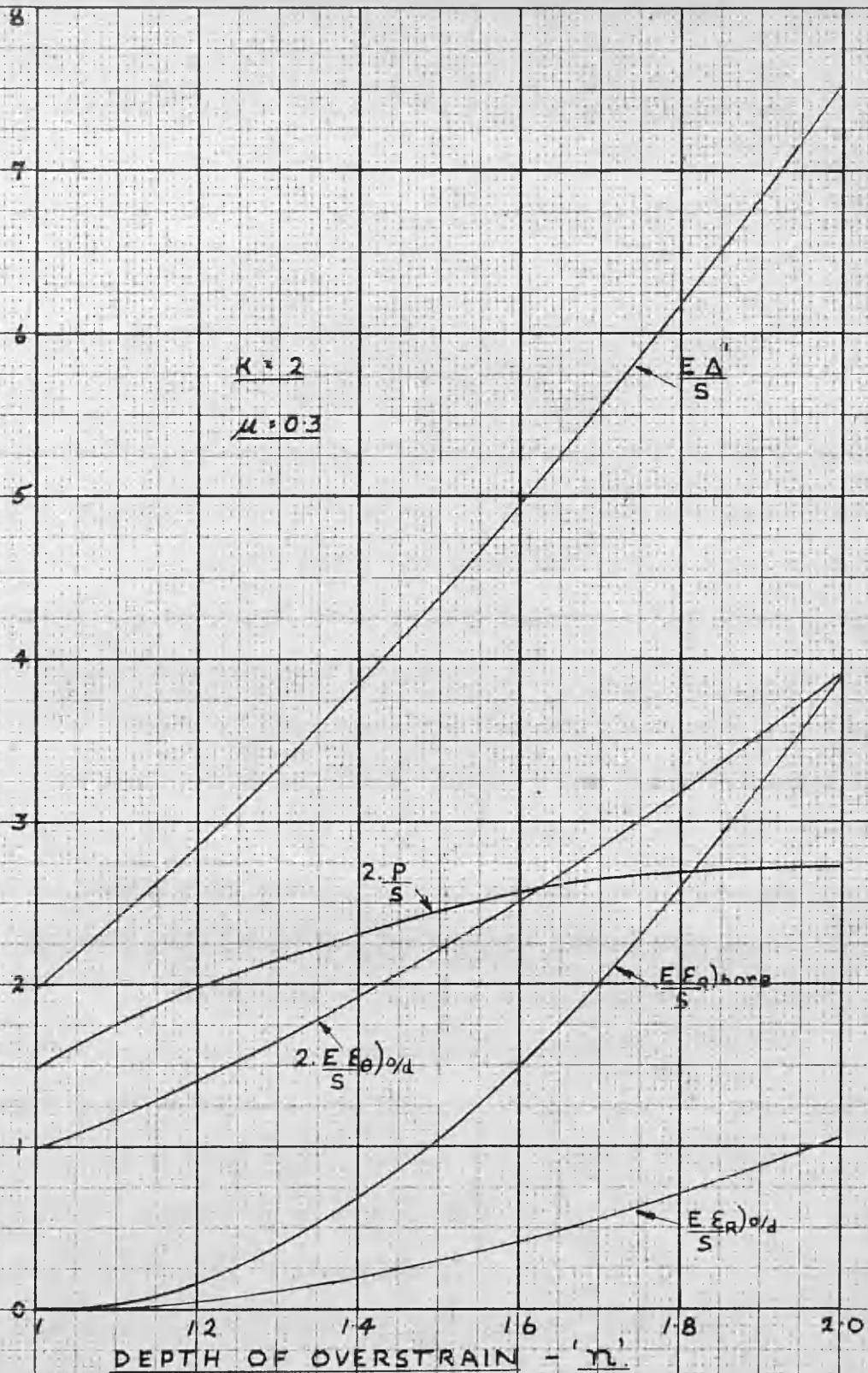


FIG. 65 - RELATION BETWEEN MEASURABLE VARIABLES  
 AND DEPTH OF OVERSTRAIN IN RING WALL.

They will be discussed later. Fig. 66 compares the theoretical interface pressure of Fig. 50 with the corrected values. It can be seen that considerably smaller pressures may be expected in overstrained assemblies if the temperature effect is operative.

### 3. Axial Load Effect

An axial load pushes the plug out of the ring on dis-assembly. It is evident that the load may alter, (i) residual strains, (ii) interface pressure. An analytical determination of this effect is complex and recourse is made to experiment. Electrical strain gauges are placed on the plug end face and ring outside diameter and the effect of axial load recorded. (See Appendix B).

It is apparent that interest lies in,

(i) Actual interface pressure distribution immediately prior to first slip load. This will enable a correct interpretation to be placed on coefficient of friction.

(ii) the possible increase in residual strains due to increased interface pressures, either overall or local. The pressure causing most damage may occur at B only (Fig. 67). The passage of the plug through the ring, however, would subject each section in turn to a high localized value.

Appendix B should be consulted for details concerning the experiments. The effects of applying an axial load prior to first slip are summarised: -

(i) A relief of pressure at A (Fig. 68).

(ii) No change in ring outside diameter.

(iii) A compressive axial stress at the ring outside diameter.

The magnitude of this stress is smaller than the mean calculated from the axial load and cross-sectional area of the ring.

The probable interface pressure distribution changes to that shown in Fig. 68. It is evident that a bending force action on the ring causes the bore at A

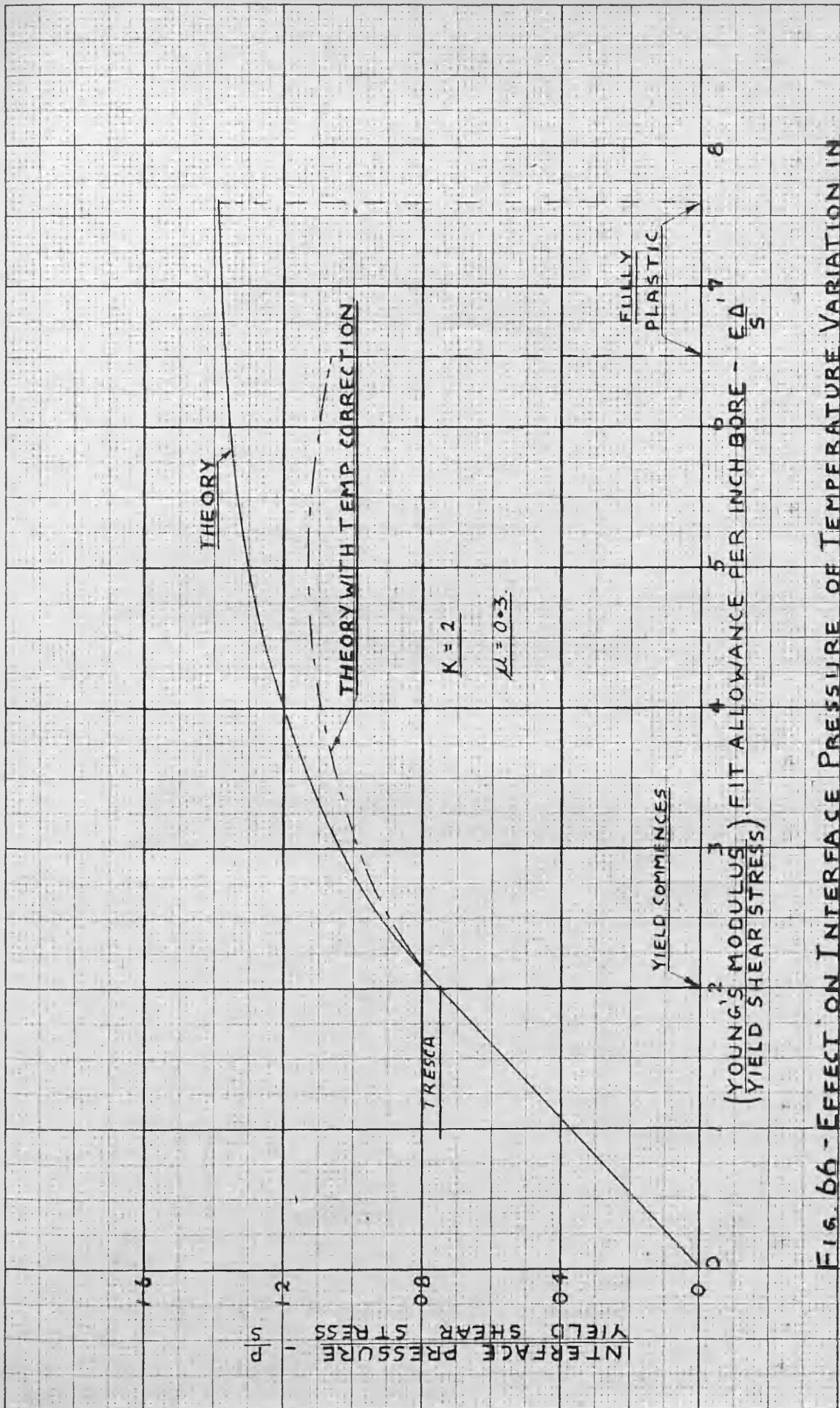


Fig. 66 - EFFECT ON INTERFACE PRESSURE OF TEMPERATURE VARIATION IN MATERIAL CONSTANTS

20 x 25 PER INCH

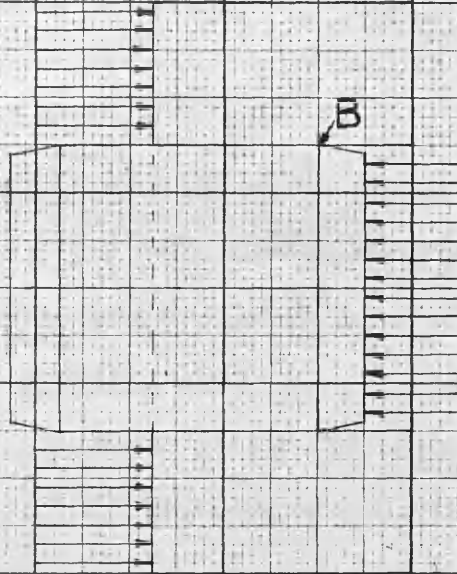


FIG. 67 - HIGH PRESSURE AT B ON PASSAGE  
OF PLUG THROUGH RING.

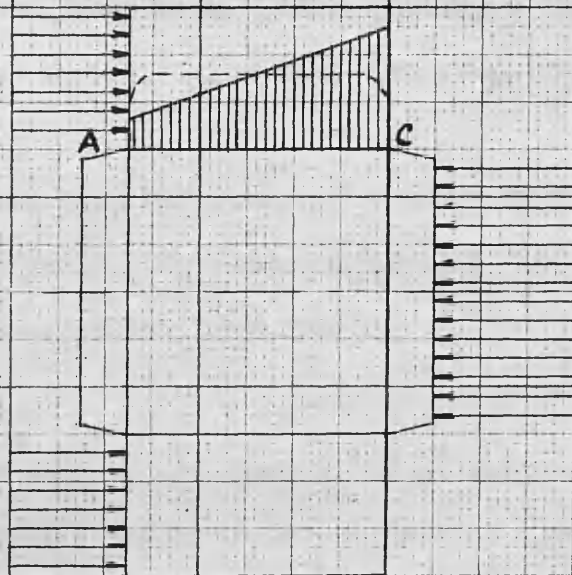


FIG. 68 - PROBABLE INTERFACE PRESSURE  
DISTRIBUTION PRIOR TO FIRST SLIP.

to open up. The effect of such an interface pressure distribution, however, has a negligible influence on the outside diameter. It would appear that the mean interface pressure may correspond closely with the original uniform shrink fit pressure.

An effect on residual strains may be caused by the changed interface pressure distribution of Fig. 68 or by localised pressures, at B, (Fig. 67). The problem is further complicated by bending force actions in the ring which occur when the plug is only partially pushed out. Appendix B shows that axial stresses measured at the outside diameter of the ring change from tensile to compressive (Approximately 1 ton/in.<sup>2</sup> for both) due to this bending force action alone. It is clear that if residual strains are increased by dis-assembly the effect will be larger at end C of the ring (Fig. 68) than end A. This would show up as a taper in the bore. Measurements indicate a taper not exceeding .0001 inches.

In the discussion on temperature effects due to Young's modulus and yield shear stress changing, it was observed that in overstrained rings partial unloading of the interface pressures occurred. Thus an increase in interface pressure, due to an axial load, would behave elastically up to a certain value. This factor is important when the axial load effects on residual strains are considered.

The writer believes that the effect of an axial load on interface pressures and residual strains is small. The tendency for both factors is to increase their values over those calculated from theory.

#### 4. Time Effect - Creep

Creep of the bore strains was observed in the thick-walled cylinder investigation. Referring to Figs. 39 and 40, it is seen that increases of 5 - 10 % in 15 minutes are possible with no apparent increase in outside diameter deflections. Close to the maximum pressure the outside deflections also showed

creep. It is recalled that the increase of bore strain with time takes place under a constant internal pressure.

It is believed that this phenomenon is due to the yielding mechanism of mild steel in which plastic wedges characterise the process. An analogous effect will exist in overstrained mild steel interference fit assemblies. An increase in ring bore deflection with time would cause a relief of interface pressure and some doubt exists as to whether the creep would continue under the lower loading conditions. It is reasoned that the propagation of the plastic wedges approaches a condition of local instability and their arrest would not be affected by reducing the load. The chance of formation of new wedges, however, would be reduced and the overall time effect would be less than that observed in the thick-walled cylinder experiments.

To estimate the effects of creep in an interference fit assembly the graphs of Fig. 69 are used. Curve A gives relation between  $P/s$  and  $\frac{E \Delta'}{s}$  to one scale and  $\frac{E \epsilon_{\theta} o/d}{s}$  to the other. Curve B connects  $P/s$  with  $\frac{E \epsilon_{\theta} \text{ bore}}{s}$ . Curve C shows the plug deflections for specific interface pressures.

It is assumed, (i) that creep produces a 5 % increase in bore strain, (ii) the outside diameter strain is unaffected if the interface pressure remains the same, and (iii) elastic release of strain accompanies drop in interface pressure.

For a selected value of  $\frac{E \Delta'}{s}$ , K gives theoretical interface pressure; D shows corresponding bore strain; FE represents 5 % increase in bore strain; DF represents drop in pressure; GH shows elastic release of outside diameter deflection. In this way percentage decreases in interface pressure and outside deflections are estimated for selected values of  $\frac{E \Delta'}{s}$ . The effects are shown in Table XII.

It is seen from Table XII that small time effects in mild steel assemblies

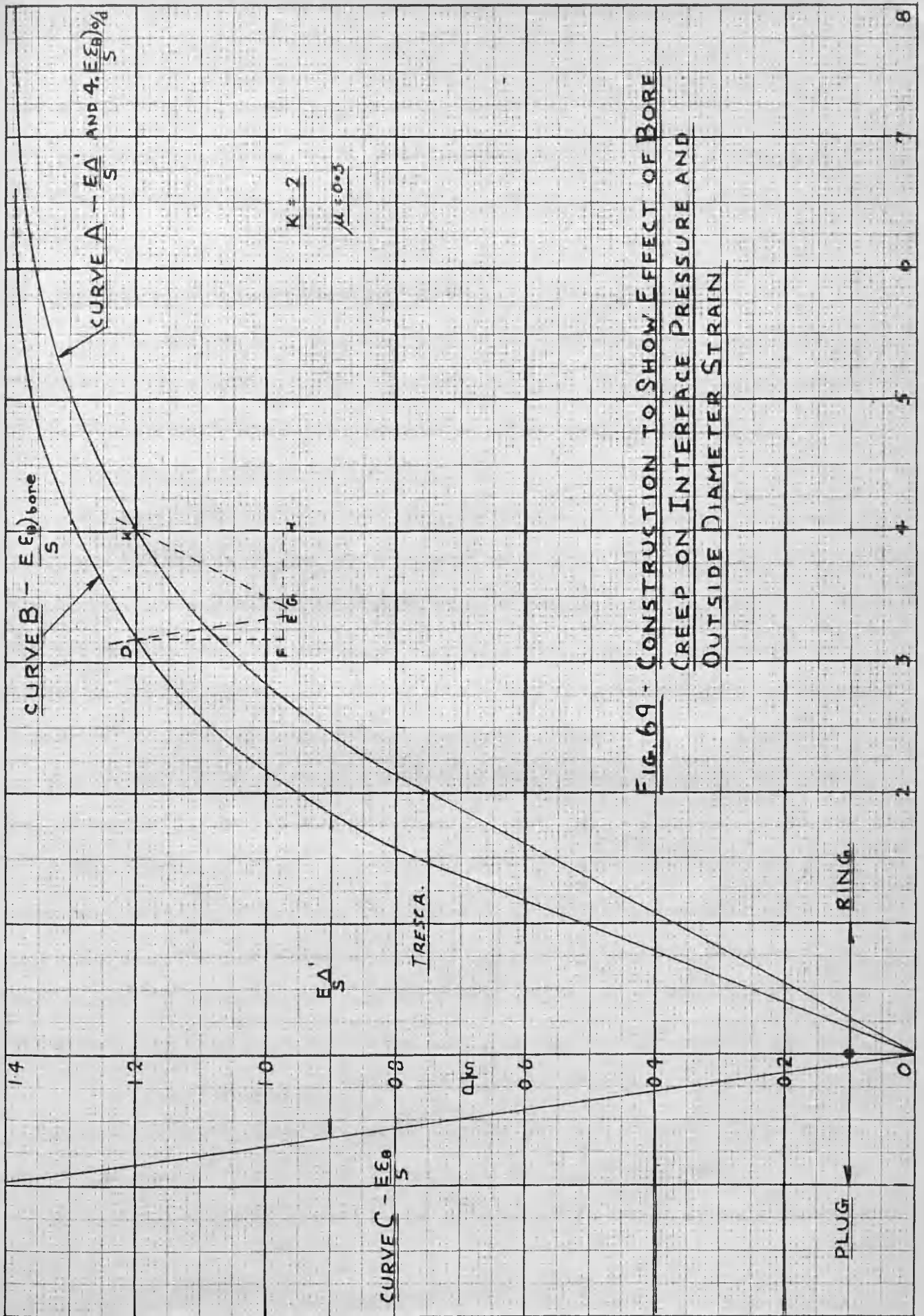


**FIG. 69 - CONSTRUCTION TO SHOW EFFECT OF BORE CREEP ON INTERFACE PRESSURE AND OUTSIDE DIAMETER STRAIN**

KUBINE DIE-CASTING CO.

5000 2000 1000 500 250 125 62.5 31.25 15.625 7.8125 3.90625 1.953125 0.9765625 0.48828125 0.244140625 0.1220703125 0.06103515625 0.030517578125 0.0152587890625 0.00762939453125 0.003814697265625 0.0019073486328125 0.00095367431640625 0.000476837158203125 0.0002384185791015625 0.00011920928955078125 0.000059604644775390625 0.0000298023223876953125 0.00001490116119384765625 0.000007450580596923828125 0.0000037252902984619140625 0.00000186264514923095703125 0.000000931322574615478515625 0.0000004656612873077392578125 0.00000023283064365386962890625 0.000000116415321826934814453125 0.000000582076609129469422265625 0.0000002910383045647347111328125 0.00000014551915228236735556640625 0.000000072759576141183677783203125 0.000000363797880705916888916015625 0.0000001818989403529584444580078125 0.00000009094947017647922222900390625 0.0000004547473508823961111145154296875 0.00000022737367544119805555725771484375 0.000000113686837720599027778628857421875 0.000000568434188602995118893144287109375 0.0000002842170943014975594465721435546875 0.00000014210854715074877972328607177734375 0.000000710542735753743888616430355888671875 0.0000003552713678768719443082151779443359375 0.00000017763568393843597215410758897216796875 0.00000088817841969217986077053529436484484375 0.000000444089209846089930385267647182422421875 0.0000002220446049230449651926338235912112109375 0.00000011102230246152248259631691179560560546875 0.00000055511151230761224129315955847802802734375 0.000000277555756153806120646579779239014013671875 0.0000001387778780769030603232898896195070068359375 0.00000069388939038451530161164944809753503417796875 0.000000346944695192257650805824724048767517088984375 0.0000001734723475961288254029123620243837585444921875 0.0000008673617379806441270114518101219168772224609375 0.00000043368086899032206350572590506095843861123046875 0.000000216840434495161031752862952530479219305615234375 0.0000001084202172475805158764314762652396096528076171875 0.0000005421010862379025793821571812761980482640380859375 0.00000027105054311895128969107859063809902413201904296875 0.000000135525271559475644845539295319049512066009521484375 0.00000067762635779723782222779647659524756014753004696875 0.000000338813178898618911113898238297623780073765023484375 0.0000001694065894493094555569491191488118900368825117421875 0.00000084703294724654727777974559574440945018441255859375 0.000000423516473623273638889872797872204725092206289296875 0.0000002117582368116368194449363989361023625461031446484375 0.00000010587911840581840972246819946805118127307177232421875 0.000000529395592029092048612340997340255906365358861123046875 0.00000026469779601454602430617049867012795318267943056171875 0.0000001323488980072730121530852493350639765913397152809375 0.000000661744490036365060765426246675319877956698556171875 0.00000033087224501818253038271312333765993897834927809375 0.000000165436122509091265191356561668829969489174639046875 0.00000082718061254545513038271312333765993897834927809375 0.000000413590306272727565191356561668829969489174639046875 0.0000002067951531363637825956782828344149847445873195234375 0.00000010339757656818189129783914141720749237229367976171875 0.00000051698788284090945564891720749237229367976171875 0.000000258493941420454727824458603746186138589880889375 0.0000001292469707102273639122293018730930692949404446875 0.000000646234853551136719561117559365470346186138589880889375 0.0000003231174267755683597805587796827351730930692949404446875 0.0000001615587133877841798902793898413675865470346186138589880889375 0.0000008077935669389208994513969491727351730930692949404446875 0.0000004038967834694604497256984745863675865470346186138589880889375 0.0000002019483917347302248628492372931827351730930692949404446875 0.0000001009741958673651124314246186363675865470346186138589880889375 0.0000005048709793368255621571623091727351730930692949404446875 0.0000002524354896684127810785811545863675865470346186138589880889375 0.0000001262177448342063905392905772931827351730930692949404446875 0.000000631088724171031952696452886475863675865470346186138589880889375 0.000000315544362085515976348226443237931827351730930692949404446875 0.0000001577721810427579881741132216189659163675865470346186138589880889375 0.000000788860905213789940870566110594829581827351730930692949404446875 0.0000003944304526068949704352830552974147659163675865470346186138589880889375 0.0000001972152263034474852176415276487329581827351730930692949404446875 0.0000009860761315172374260882076187643675865470346186138589880889375 0.0000004930380657586187130441038093821827351730930692949404446875 0.000000246519032879309356522051904691271363675865470346186138589880889375 0.00000012325951643965467826102595234563675865470346186138589880889375 0.0000006162775821982723913051297617271363675865470346186138589880889375 0.000000308138791099136195652564880863563675865470346186138589880889375 0.000000154069395549568097826282440431827351730930692949404446875 0.00000077034697774784048913014122021563675865470346186138589880889375 0.00000038517348887392024456507061010781827351730930692949404446875 0.0000001925867444369601222825353050539091271363675865470346186138589880889375 0.00000096293372218480061141267652526954563675865470346186138589880889375 0.00000048146686109240030570633826263476827351730930692949404446875 0.0000002407334305462001528531691313173841363675865470346186138589880889375 0.0000001203667152731000764265845656686827351730930692949404446875 0.000000601833576365500382132922827827341363675865470346186138589880889375 0.0000003009167881827501910664614139136716827351730930692949404446875 0.00000015045839409137509553323070695683675865470346186138589880889375 0.0000007522919704568754777664614139136716827351730930692949404446875 0.00000037614598522843773888323070695683675865470346186138589880889375 0.00000018807299261421886944161535347841363675865470346186138589880889375 0.00000094036496307109443472080767673921363675865470346186138589880889375 0.000000470182481535547217360403838369606827351730930692949404446875 0.00000023509124076777360868020191918480341363675865470346186138589880889375 0.000000117545620383886804340100959592401706827351730930692949404446875 0.000000587728101916933602170100959592401706827351730930692949404446875 0.000000293864050958466801085050479596203401363675865470346186138589880889375 0.000000146932025479233400542525239798101706827351730930692949404446875 0.000000734660127396166800271262619596203401363675865470346186138589880889375 0.000000367330063698083400135631309798101706827351730930692949404446875 0.0000001836650318490417000678156548990508506827351730930692949404446875 0.000000918325159224020850033907827449525425341363675865470346186138589880889375 0.000000459162579612010425016953913724762716827351730930692949404446875 0.000000229581289806005212508476956861881363675865470346186138589880889375 0.0000001147906449030026062542384784309406827351730930692949404446875 0.0000005739532245150130312711921917171716827351730930692949404446875 0.0000002869766122575065156355960958585881363675865470346186138589880889375 0.00000014348830612875325781779804792929406827351730930692949404446875 0.000000717441530643766289088990239648470346186138589880889375 0.0000003587207653218831445444951198242351730930692949404446875 0.0000001793603826609415722722475599123675865470346186138589880889375 0.0000008968019133047078613611977995618376827351730930692949404446875 0.00000044840095665235393068059889978091881363675865470346186138589880889375 0.000000224200478326176965340299449890459406827351730930692949404446875 0.00000011210023916308848267014972494522970341363675865470346186138589880889375 0.00000056050119581544241335074862472611881363675865470346186138589880889375 0.000000280250597907721206675374312363559406827351730930692949404446875 0.00000014012529895386060333768715618177970341363675865470346186138589880889375 0.000000700626494769303016675374312363559406827351730930692949404446875 0.00000035031324738465150833768715618177970341363675865470346186138589880889375 0.000000175156623692325754168843578090889375 0.000000875783118461628770844217714454446875 0.000000437891559230814385422108857227341363675865470346186138589880889375 0.0000002189457796154071927110544286171706827351730930692949404446875 0.00000010947288980770359635552721430341363675865470346186138589880889375 0.000000547364449038517798177763607171706827351730930692949404446875 0.00000027368222451925889908888180358585341363675865470346186138589880889375 0.000000136841112259629449544440901792926716827351730930692949404446875 0.00000068420556127814722472222045470346186138589880889375 0.000000342102780639073612361110227351730930692949404446875 0.0000001710513903195368061805551136716827351730930692949404446875 0.0000008552569515976836309027755683585341363675865470346186138589880889375 0.000000427628475798841815451387784171706827351730930692949404446875 0.00000021381423789942090772569389208585341363675865470346186138589880889375 0.000000106907118949710453862846946042926716827351730930692949404446875 0.000000534535594748552269314234730171706827351730930692949404446875 0.00000026726779737427613465711736508585341363675865470346186138589880889375 0.000000133633898687138067328558682542926716827351730930692949404446875 0.00000066816779343569403665711736508585341363675865470346186138589880889375 0.000000334083896717847018328558682542926716827351730930692949404446875 0.000000167041948358923509164279341363675865470346186138589880889375 0.000000835209741794617545821371706827351730930692949404446875 0.00000041760487089730877291068585341363675865470346186138589880889375 0.000000208802435448654386455342926716827351730930692949404446875 0.0000001044012177243271932276714633585341363675865470346186138589880889375 0.000000522006088621635966113356826716827351730930692949404446875 0.0000002610030443108179830566784133585341363675865470346186138589880889375 0.0000001305015221554089915283392066784133585341363675865470346186138589880889375 0.0000006525076107770449576416784133585341363675865470346186138589880889375 0.0000003262538053885224788208392066784133585341363675865470346186138589880889375 0.0000001631269026942612394104196033392066784133585341363675865470346186138589880889375 0.000000815634513471306197052052016784133585341363675865470346186138589880889375 0.000000407817256735653098526026008392066784133585341363675865470346186138589880889375 0.000000203908628367826549263013004196033392066784133585341363675865470346186138589880889375 0.000000101954314183913274631506502098016784133585341363675865470346186138589880889375 0.000000509771570919566373157503253274008392066784133585341363675865470346186138589880889375 0.000000254885785459783186578751626637004196033392066784133585341363675865470346186138589880889375 0.000000127442892729891593289375813318502098016784133585341363675865470346186138589880889375 0.000000637214463649457966578751626637004196033392066784133585341363675865470346186138589880889375 0.000000318607231824728983289375813318502098016784133585341363675865470346186138589880889375 0.000000159303615912364491644687906637004196033392066784133585341363675865470346186138589880889375 0.000000796507231824728983289375813318502098016784133585341363675865470346186138589880889375 0.000000398253615912364491644687906637004196033392066784133585341363675865470346186138589880889375 0.000000199126807956182245822343953318502098016784133585341363675865470346186138589880889375 0.000000995634039780911229111719766592516784133585341363675865470346186138589880889375 0.00000049781701989045561455585988329625839206678413358534136367586547034618613858988088

may account for decreases in interface pressure and outside diameter deflection. The residual bore strains are of course correspondingly increased whereas the residual outside measurements are unchanged, except at the highest interface pressures.

#### 5. Analysis of Strain Observations

Several effects have been discussed in the preceding pages which were not included in the original theory. They will assist in explaining discrepancies which exist between theory and experimental strain observations.

##### (1) Outside Diameter Strains (Fig. 59)

The most important feature of this figure lies in the marked difference between the deflections of dry and lubricated specimens. The full line shows the theoretical curve which the lubricated results (series I and II) follow closely. The dotted line describes results of the dry series III. On the average the latter are 15 % higher than theory. The reason is undoubtedly due to frictional forces at the interface. Increase of 30 % was computed for the assumption of no slip at the interface. Such a condition cannot exist in a practical assembly and the effect is correspondingly reduced.

The frictional effects appear to increase proportionately with fit allowance and overstrain of the ring bore produces no additional complications. Two experimental points (at values of  $\frac{E \Delta'}{s}$  of 2.6 and 2.9) are high relative to the mean curve. It is considered they are within the limits of experimental error. One division on this graph represents less than one ten-thousandth of one inch.

It should be emphasised series III specimens are carefully prepared in a laboratory and the surfaces are chemically dry and free from oil film. In industry the term "dry" applied to a shrink fit has a different meaning. No intentional lubricant is applied to the mating surfaces which are usually wiped

$\frac{E \Delta^i}{s}$	Percentage relief of interface press.	Percentage relief of outside diameter deflection
3	15	14
4	18.7	14.2
5	22.5	15.1

TABLE XII

Effect of 5 % Bore Creep on (i) interface pressure and (ii) outside diameter deflection for various fit allowances.

prior to mounting by the most convenient rag. This gives rise to a surface film of doubtful properties. The tendency will be to reduce frictional effects below the 15 % value.

Points, in the range of  $2 < \frac{E \Delta'}{s} < 3$  are low compared to theory. This is in agreement with the thick-walled cylinder investigation (see Fig. 36). The mechanism of yielding in mild steel thick-walled cylinders is such that transfer of load to the outside elastic layers is not so great as the ordered arrangement of yielding, assumed in the theoretical analysis, would predict.

The temperature effect due to variations in Young's modulus and yield shear stress is shown chain dotted in Fig. 59. It is small and only becomes important at the higher fits. In this range the experimental points are low relative to both theoretical curves. Assemblies for points 1 and 2 are part expanded and the effect of temperature may be altogether eliminated. The ring for 3 was heated to 500° C and scale on the outside surfaces formed, with consequent loss in change of measurement. In addition a small time effect could easily account for the deviation from theory.

#### (ii) Residual Strains (Fig. 60 and 61)

Both time and temperature effects increase the residual strains. This is in contrast to the outside diameter strains for which temperature increases and time decreases the theoretical values.

Figs. 60 and 61 are useful in estimating the fit allowance at which overstrain of the outer member commences. This is especially true of the bore measurements which are twice as sensitive as the outside diameter changes. Theory predicts from the maximum shear stress flow condition that overstrain commences at  $\frac{E \Delta'}{s} = 1.994$  ( $\Delta' = 1.25$ ). This is borne out by experimental results. There is no indication that upper and lower values for the maximum shear stress control the initiation and progression of overstrain.

The correction for temperature effects on 'E' and 's' brings the theoretical curve in line with experimental results. The correction is based on Fig. 64. Values of 'E' and 's' are selected from individual investigations which show poor agreement. A slight change in the E/s versus temperature curve could identify theory even more closely with experiment. It was not, however, the purpose of studying these effects to substantiate experimental points on flimsy evidence. The magnitudes of the E/s ratios of Fig. 64 are conservative and the issue is clearly that residual strains are considerably affected by such variations. Points 1 and 2 are from specimens which were part expanded and the "equilibrium" temperature is correspondingly lower. It is seen that they are relatively close to the basic room temperature curve. Point 3 is from a specimen in which the ring is completely overstrained.

Time effects at the low values of overstrain are likely to be small. Axial load effects, however, will be a maximum and the high points of Figs. 60 and 61 in the range  $2 < \frac{E \Delta^s}{s} < 3$ , may be attributed to the disassembly process. This will be discussed later in connection with the load fit allowance curves.

#### (iii) Residual Fit Allowance (Fig. 62)

The residual fit allowances may be deduced directly from Fig. 61. The experimental points show similar discrepancies from theory. This curve is more useful in discussing load-fit allowance curves. Points (a) and (b) show clearly the effect of using fit allowance which cause complete overstrain of the ring. Either a severe temperature or time effect must be responsible for such low values of residual fit.

### 6. Analysis of Axial Holding Ability of Grip

#### (i) Lubricated Specimens

Series I and II axial loads are plotted on Fig. 62. The ratio of mating surface areas for series II to series I specimens is 4. The scale of series II

loads is reduced by this amount.

The axial loads to cause first slip is the maximum for lubricated specimens. The second slip load is considerably smaller, usually about 1/2 to 1/4 of the initial load. A possible reason for this is discussed in the review. No obvious relation exists between second slip loads and fit allowance.

It is apparent that a wide scatter exists in the axial push out loads. It is the purpose of the discussion to decide whether this is due to (i) differences from theoretically computed interface pressures or (ii) variations in coefficient of friction.

Consider the all elastic range,  $0 < \frac{E \Delta'}{s} < 2$ . Specimens of both series may be taken to define the same straight line. The average value of coefficient of friction based on Lamé' interface pressure is 0.21. The maximum and minimum specimen values are 0.242 and 0.183, respectively. Thus, a variation in apparent coefficient of friction amounting to  $\pm 14\%$  is recorded when the interface pressures are reliably computed.

Points 1, 2, and 3 (Fig. 62) show large relative differences, the reasons for which are not apparent from the strain graphs. Axial friction could not account for such variations even in dry specimens; time and temperature effects must be excluded also. It is possible that a combination of experimental error, axial load, and variations in material properties would explain the differences. It is more likely that the coefficient of stiction, which was shown in the review to be an indeterminate quantity, is responsible.

A theoretical load-fit allowance curve (full line) is drawn, based on theoretical interface pressure and  $\mu = 0.21$  obtained from elastic region. A corresponding curve allowing for temperature correction is also shown. Rough agreement is seen between loads and the former relationship.

Points 4, 5, 6, and 7 will be examined in an attempt to explain their

obvious discrepancies. Reference will be made to Table XIII. The following is noted in connection with 5 and 6.

(i) (5) has lower outside diameter deflection than (6); this might indicate that (5) has a lower interface pressure.

(ii) (5) has a higher push out load. This may be due to a higher mean interface pressure on first slip or due to a higher coefficient of friction. It is interesting that the latter may cause the former. If the axial load effect is so great it will show up in the residual strains.

(iii) From Fig. 62, it is seen that (5) has a higher residual fit allowance than (6). This high first slip load has no apparent effect on residual strains.

It was pointed out in the section dealing with axial loads that the passage of the plug through the ring may produce a more damaging effect than the first slip loads. This means that subsequent loads (2nd, 3rd, 4th slips, etc.) will have more bearing on the residual fit allowances. Table XIII shows that if this is the case, the relative position of 4, 5, 6, and 7 in the residual fit graph is explained.

A similar examination of all the axial load values leads to the same conclusion; namely, that variations in interface pressure due to the several effects already enumerated are not compatible with results. Thus variation in the coefficient of friction must be held responsible for the discrepancies. This is in agreement with previous investigations referred to in the review.

Axial loads indicate that interface pressures between 50 and 70 % higher than the maximum elastic interface pressure exist. Thus in an assembly of similar dimensions, material, etc. shrink fitting can produce maximum interface pressures approximately double those in force fits. This gives rise to considerable increase in efficiency.

Four of series II specimens have superfinished mating surfaces. Experi-

Point on Fig. 61	1st Load (Tons)	2nd Load (Tons)	3rd Load (Tons)
4	55.1	16.7	15.3
5	81	9.4	7.5
6	57	25	20.7
7	57	35	33.4

TABLE XIII - 1st, 2nd, and 3rd Slip Loads for Assemblies 4, 5,  
6, and 7 of Fig. 62.

mental strains are in close agreement with theory. Axial loads, however, show low values compared to the rest of the specimens of series I and II. Table X shows their values and percentage deviation from the theoretical load-fit allowance curve of Fig. 62. It is apparent that the superfinished lubricated specimens have a lower coefficient of friction than the turned rings and ground plugs. This is in contradiction to Sawin who claims that the finer the finish the higher the friction coefficient. It should be noticed that series I specimens are carefully prepared by grinding and honing which gives a fine quality of finish. No noticeable difference in friction coefficient is seen when compared to series II specimens which had the turned ring bores and ground plugs.

(ii) Dry Specimens

Series III specimens were assembled chemically dry and free from oil film. First slip is accompanied by a movement approximately  $1/16$  inch. Thereafter the mating surfaces seize and the axial load increases to a value necessary to shear the material. The grip is so strong that the failure path passes through the plug and ring but never along the grip. Table XI shows the results of first slip and maximum load.

It is considered of the utmost practical significance that measurable slip occurs at loads lower than the maximum. A movement of the magnitude measured could seriously effect alignment in built-up crankshafts. It would be necessary to base design on the first slip load.

#### IV. CONCLUSIONS

##### 1. Agreement of Theory with Experiment

An interference fit theory is developed and supported by experimental results. Stresses and strains depend on second order effects which are operative under certain conditions. These effects are due to (a) axial friction at the interface, (b) variation in Young's modulus and yield shear stress with temperature, (c) axial load and (d) creep with time. When account is taken of the second order effects the theory is considered adequate.

##### 2. Author's Interpretation of Russell's Experiments

A new interpretation is placed on Russell's load-fit allowance curve for force fits and his claim that overstraining of the ring provides no increase in holding ability is refuted. It is shown, using Russell's experimental results and the interference fit theory of this thesis, that, at the optimum value of fit allowance the ring wall is 54 % overstrained.

##### 3. Coefficient of Friction

(i) Axial tractions at the interface are important in shrink fit assemblies with perfectly dry mating surfaces. The effect is to increase the fit allowance by approximately 15 %. Traction produce a negligible effect in specimens with well lubricated surfaces.

(ii) The axial push out loads for 4 specimens with superfinished mating surfaces is 37 - 45 % lower than corresponding loads for ground and honed surfaces. The lubricant in both cases is sperm oil.

(iii) Considerable variation in coefficient of stiction (based on first slips) is apparent especially in the high fit allowance range. This is in agreement with the findings of previous investigators.

##### 4. Maximum Interface Pressures - Shrink and Force Fits

From the author's experimental work on shrink fits it is seen that the maximum interface pressure is in the region of 50 - 70 % higher than the maximum elastic interface pressure. The author showed from his interpretation of Russell's work on force fits that the maximum interface pressure in this case is only 82.5 % of the maximum elastic interface pressure calculated by neglecting entry forces. Thus the maximum pressure in a shrink fit is approximately double that in a force fit for the type of assembly under consideration.

APPENDIX A

Preliminary Investigation of Pressure Effect  
on Electrical Strain Ganges

## General Features

The results of preliminary tests on bakelite electrical resistance strain gauges are recorded. Previous work performed by the writer had shown that paper backed gauges behaved irrationally when subjected to normal pressures. A considerable number of tests were performed on protected and unprotected paper-backed gauges but the results were unreliable.

Apparatus consists of the thick-walled cylinder pressure equipment and a medium-carbon steel cylinder which can withstand pressures up to 25,000 lbs./in.<sup>2</sup> Three bakelite gauges (1/4 inch gauge length) are mounted on a thin metal strip (Fig. 70) according to the technique explained on pages 90 and 93. No protective coating is applied to the gauges. The strip is enclosed in the apparatus and one compensating gauge is located on the outside. Change in resistance is recorded for pressures up to 25,000 lbs./in.<sup>2</sup> It was considered unlikely that a mild steel test cylinder ( $k = 2$ ) would carry a pressure beyond this.

## Results and Discussion

Fig. 70 shows comparative results from two test runs for the three gauges. Fig. 71 shows results from several test runs for one gauge in order to investigate the effect of repeating the pressure cycle.

Three factors are apparent from a study of Figs. 70 and 71: -

(i) Small variations in pressure effect among gauges are possible. The differences and also the total pressure effect are small compared to the circumferential bore strains of a thick-walled cylinder ( $k = 2$ ). It is thought that lack of care in mounting may be the reason for the variations, especially in the case of gauge no. 2.

(ii) In all cases the gauges show linear response, over most of the pressure range. If the effect of pressure is known for  $0 < P < 15,000$  lbs./in.<sup>2</sup>, then a linear extrapolation would suffice for  $15,000 < P < 25,000$  lbs./in.<sup>2</sup> This is

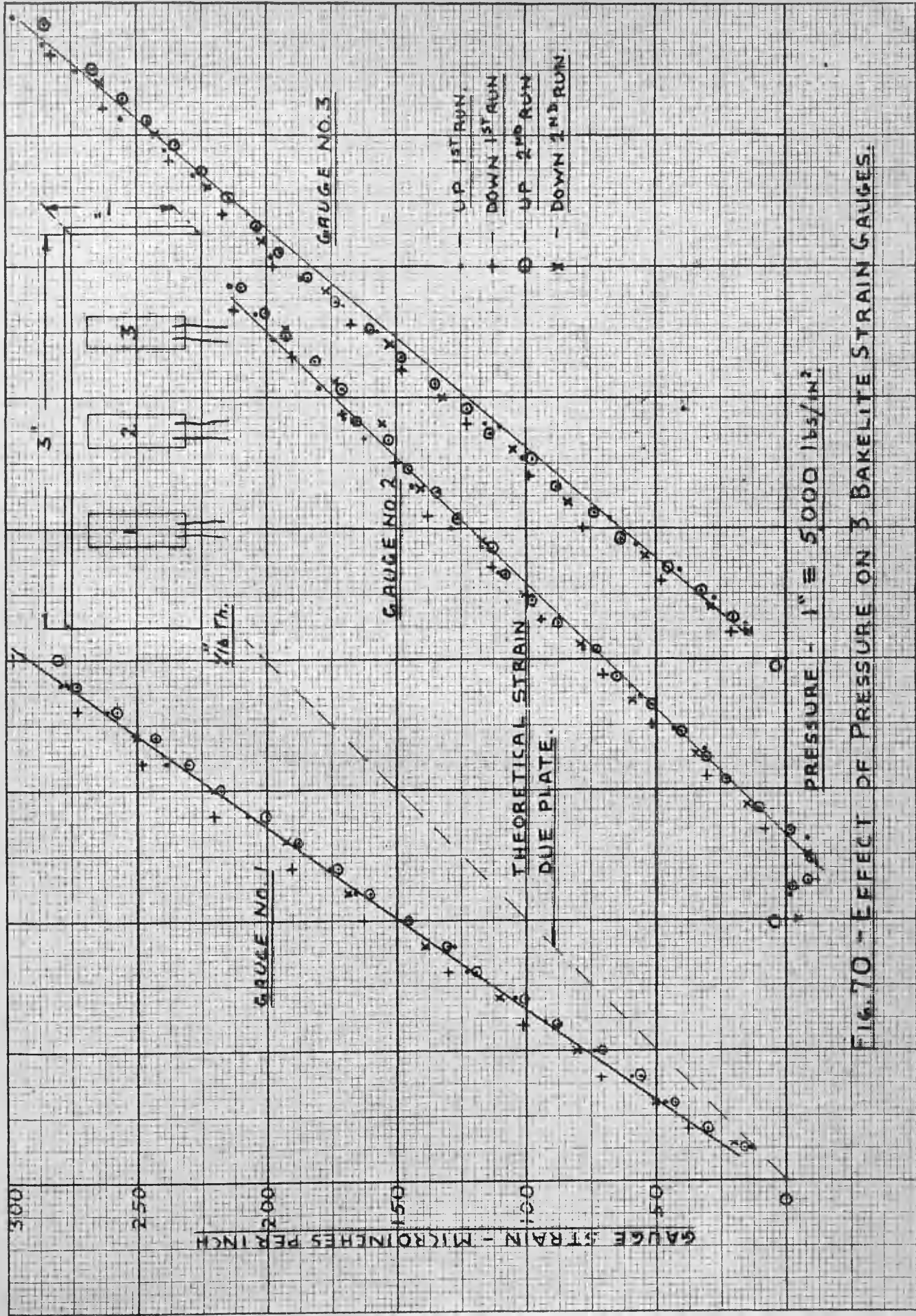


FIG. 70 - EFFECT OF PRESSURE ON 3 BAKELITE STRAIN GAUGES.

COPIED FROM THE REPORT OF THE NATIONAL BUREAU OF STANDARDS, U. S. A.

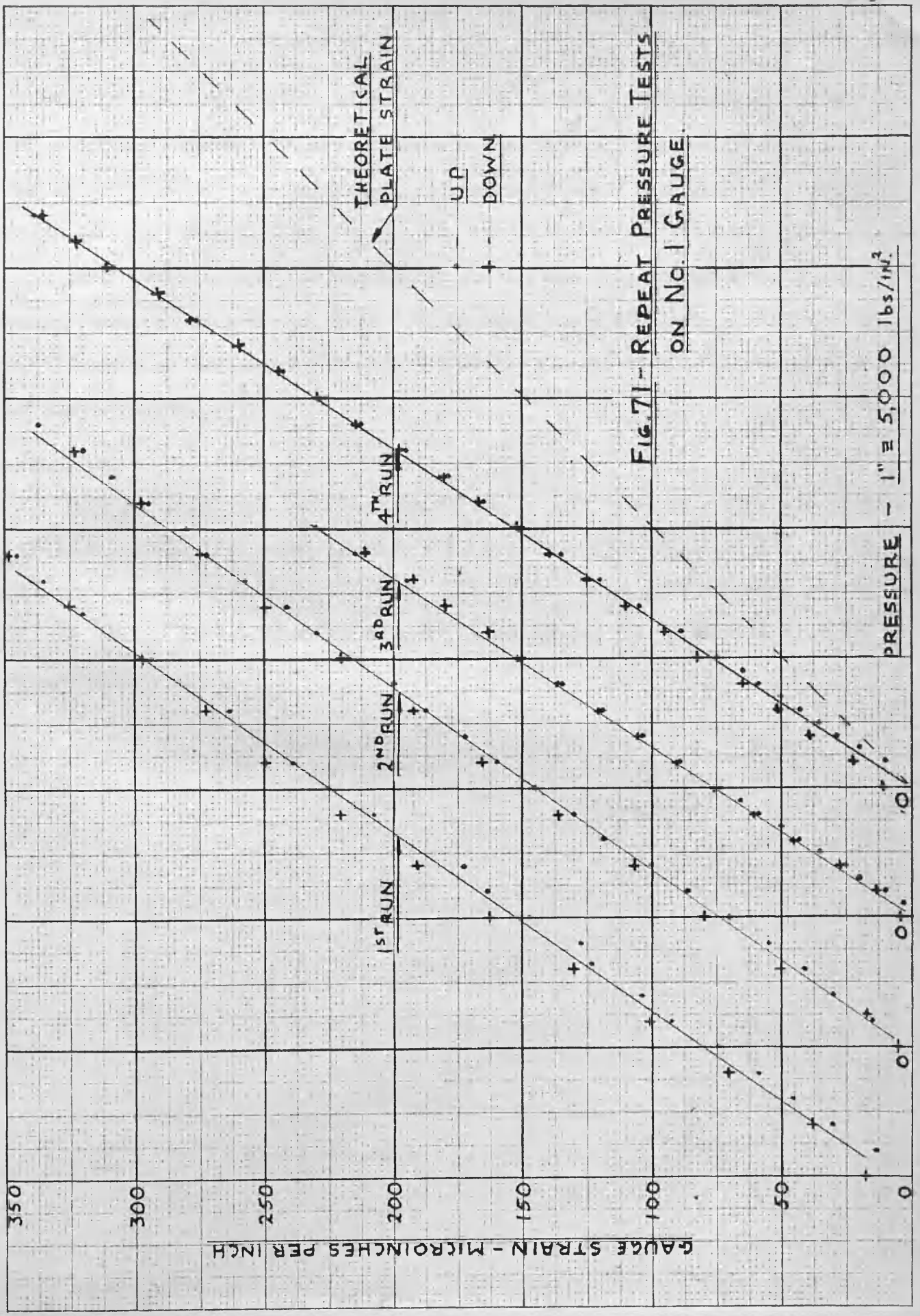


FIG. 71 - REPEAT PRESSURE TESTS ON NO. 1 GAUGE

GAUGE STRAIN - MICROINCHES PER INCH

PRESSURE - 1" = 5,000 lbs/in²

important in that the pressure effect on gauges mounted on the bore of a thick-walled cylinder may be deduced accurately in the elastic range and extrapolated when the cylinder becomes overstrained. This technique is employed in the thick-walled cylinder investigation.

(iii) There is a marked consistency for any one gauge which is subjected several times to the pressure cycle. No permanent set or creep is noticed and it may be concluded that a gauge behaves in a stable and consistent fashion under the fluid pressure.

### Conclusions

Bakelite electrical resistance gauges may be used to measure bore strains in a thick-walled cylinder under internal fluid pressure. The effect of pressure on them may be obtained in the all elastic range of the cylinder by assuming Lamé's theory. Linear extrapolation suffices for pressures giving rise to overstraining in the cylinder wall.

APPENDIX B

Effects of Axial Dis-assembly Force

## General Features

Two of series II specimens are selected to examine the effects of axial load on the initial interference fit stresses. Four axial and four circumferential electrical resistance strain gauges (in pairs) are placed on the outside periphery of each ring, and in the center of the length. Two gauges in the same diameter are located on the face of each plug at the end removed from the axial push out force.

It is convenient to study the effects in two stages: - (i) up to 1st slip load, and (ii) due to various positions of the plug in the ring.

It should be emphasised that the tests are designed to obtain a qualitative idea of the effects of an axial load on (i) outside diameter hoop stress (ii) outside diameter axial stress, and (iii) plug end face stress.

## Results and Discussion

Fig. 72 shows relief of compressive stress on the plug end face up to the second slip load. Points are the mean of two gauges. Fig. 73 indicates the effect of axial, hoop and plug end face stresses of forcing the plug through the ring. The axial and hoop stresses are the mean of 4 gauges equally spaced round the circumference.

### (i) Effects up to 1st slip load

It is clearly seen from Fig. 72 that there is a relief of interface pressure at the end of the assembly remote from the applied load. This is undoubtedly due to bending in the ring. The hoop stresses remain unaffected. A small compressive axial stress proportional to the applied load was observed. It is not recorded and is considered negligible.

The axial load effect on 1st slipping will depend on the interface pressure magnitude and distribution. It is thought that a relief of pressure at one end of the assembly is accompanied by an increase at the other. The overall effect

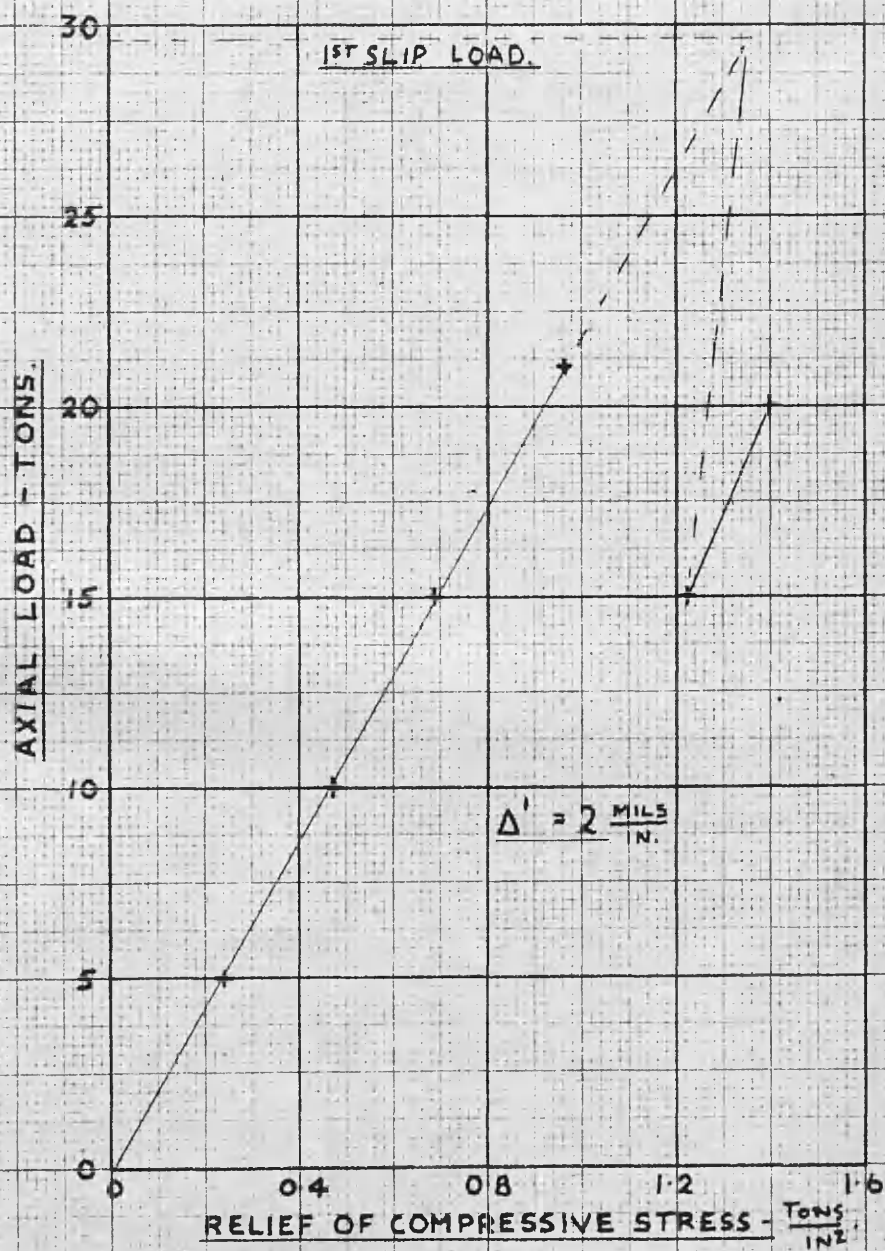


FIG. 72 - RELIEF OF STRESS FROM GAUGES LOCATED ON END FACE OF PLUG REMOTE FROM APPLIED LOAD.

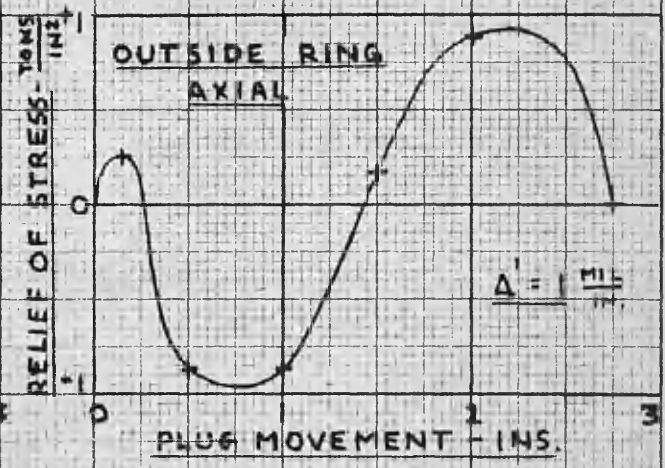
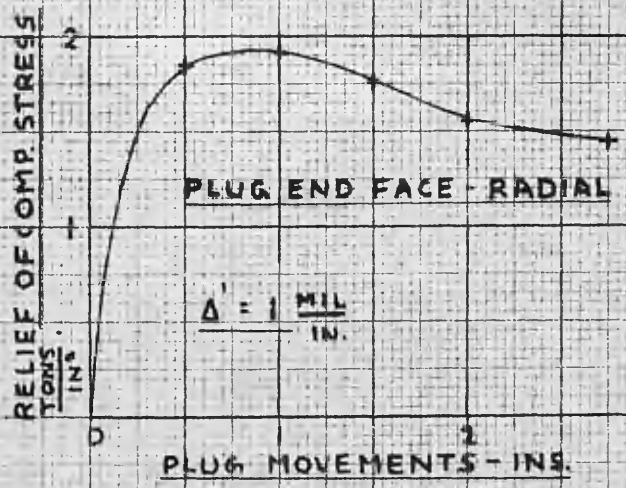
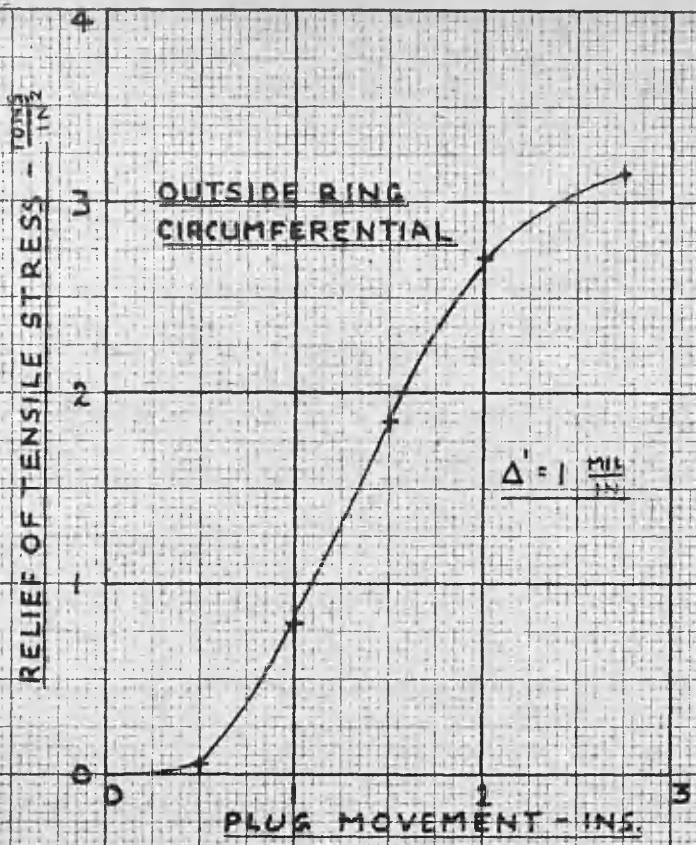


FIG 73 - RELIEF OF STRESSES DUE TO PASSAGE OF PLUG THROUGH THE RING.

may therefore be small.

(ii) Effect due to forcing plug through the ring

Fig. 73 indicates that comparatively large bending stresses are imposed. The overall effect of these is difficult to assess. It is probable that the bending force actions combined with the local high pressure at the applied load end of the plug will be the deciding factors as to whether the dis-assembly process provides additional overstraining.

Conclusions

(i) The overall effect of axial loads prior to first slip is probably small.

(ii) Comparatively large bending stresses occur during the passage of the plug through the ring. It is thought that further overstrain may be produced in the ring. The amount will be small.

APPENDIX C

Quantitative Measurements of  
Surface Finish and Lubricant

Fig. 74 shows traces and average roughness readings for typical rings and plugs from the three series of specimens. It should be noted that the vertical magnification scale is not constant.

Sperm oil is used as mating surface lubricant on all the specimens except the dry series. Viscosity and static friction coefficient are given below.

Viscosity (Redwood Viscometer) at 71° F ----- 0.127 poises.

at 120° F ----- 3.22 poises.

Static Friction Coefficient (Deeley Machine) --- 0.27

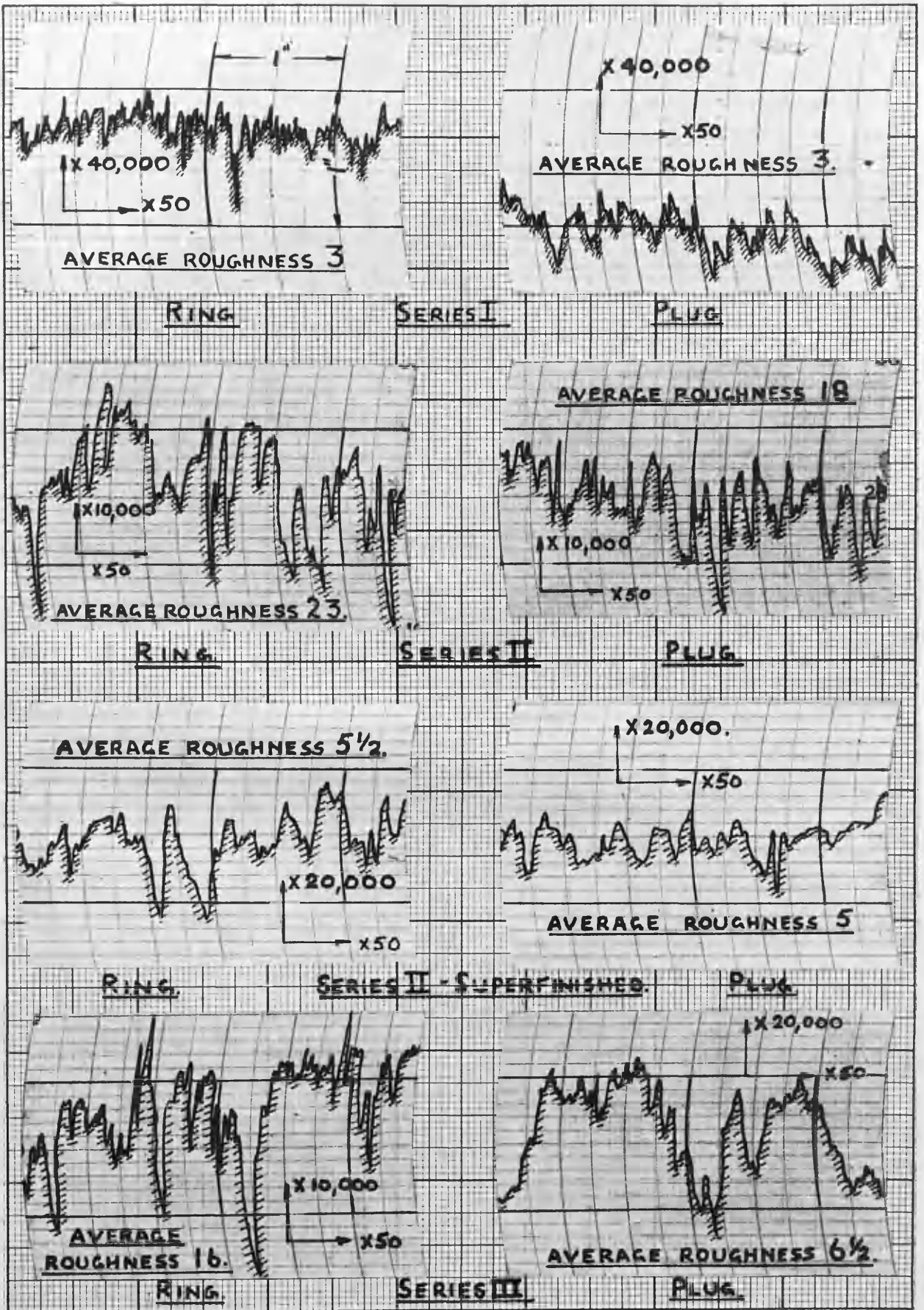


FIG. 74 - SURFACE FINISH (TALYSURF) RECORDS.

**APPENDIX D**

**Bibliography**

1. Baughner, J. W. - 1931, "Transmission of Torque by Means of Press and Shrink Fits", - T.A.S.M.E., Vol. 53, MSP-53-10.
2. Bowden, F. P., Leben, L., and Tabor, D. - 1939, "The Sliding of Metals, Frictional, Fluctuations and Vibrations of Moving Parts", The Engineer, Vol. 168, pp. 214-217.
3. Bridgman, P. W. - 1931, "The Physics of High Pressure" - The Macmillan Corp., New York.
4. Buckwalter, T. V. and Horger, O. J. - 1937, "Investigation of Fatigue Strength of Axles, Press Fits, Surface Rolling, and Effect of Size", - T.A.S.M.E., Vol. 25, p. 229.
5. Coker, E. G. and Levi, E. - 1934, "Force Fits and Shrinkage Fits in Crank Webs and Locomotive Driving Wheels", - Proc. I. Mech. E., London, Vol. 127, p. 249.
6. Cook, G., and Robertson, A. - 1911, "Strength of Thick Hollow Cylinders under Internal Pressure", - Engineering, Vol. 92, p. 786.
7. Cook, G., and Robertson, A. - 1913, "Transition from the Elastic to the Plastic State in Mild Steel", - Proc. Royal Soc., Series A, Vol. 88, p. 462.
8. Cook, G. - 1931, "Yield Point and Initial Stages of Plastic Strain in Mild Steel Subjected to Uniform and Non-uniform Stress Distributions", - Phil. Trans. Royal Soc., Series A, Vol. 230, p. 103.
9. Cook, G. - 1934, "The Stresses in Thick-walled Cylinders of Mild Steel Overstrained by Internal Pressure", - Proc. Inst. Mech. Engrs., Vol. 126, p. 407.
10. Cook, G. - 1938, "Some Factors Affecting the Yield Point in Mild Steel", - Trans. Inst. Eng. and Shipbuilders in Scotland, Vol. 81.
11. Cox, E. S. - 1935, "Locomotive Wheels, Tyres and Axles", - Journal of the Institution of Locomotive Engineers in Great Britain, Vol. 25, No. 128, p. 761.
12. Dokos, S. J. - 1946, "Sliding Friction under Extreme Pressures", Journal of Applied Mechanics, June, Vol. 13, No. 2, p. A148.
13. Gleyzal, A. - 1946, "General Stress-Strain Laws of Elasticity and Plasticity", - T.A.S.M.E., Vol. 13, No. 4, p. A261.
14. Goodier, J. N. - 1938, "Frictional Effects in Shrink Fits", - Stephen Timoshenko 60th Anniversary Volume, Macmillan, New York.
15. Hausner, H. H. - 1946, Editor of "Plastic Deformation Principles and Theories", - David W. Taylor Model Basin, U.S.N. N.B. Translation from the Russian, of papers by L. N. Kachanow, N. M. Beliaev, A. A. Ilyushin, W. Mostow, and A. N. Gleyzal.

16. Hill, R., Lee, E. H., and Tupper, S. J. - 1947, "The Theory of Combined Plastic and Elastic Deformation with Particular Reference to a Thick Tube under Internal Pressure", - Proc. Royal Soc., Series A, Vol. 191, p. 278.
17. Hodge, P. A. and White, G. N. - 1949, "A Quantitative Comparison of Flow and Deformation Theories of Plasticity", - Bulletin from Brown University, Providence, U.S.A.
18. Horger, O. J. and Nelson, C. W. - 1937, "Design of Press and Shrink-Fitted Assemblies - Part I", - T.A.S.M.E., Vol. 59, A-183.
19. Horger, O. J. and Nelson, C. W. - 1938, "Design of Press and Shrink-Fitted Assemblies - Part II", - T.A.S.M.E., March, p. A-32
20. Horger, O. J. and Cantley, W. I. - 1946, "Design of Crank Pins for Locomotives", - T.A.S.M.E., Vol. 13.
21. Hoyt, S. L. - 1943, "Metals and Alloys Data Book", - Reinhold Publishing Corporation, New York.
22. MacGill, C. F. - 1913, "A Record of Press Fits", - A.S.M.E. Journal - Nov., p. 1657.
23. MacGregor, C. W. - 1931, "Yield Point of Mild Steel", - Trans. Am. Soc. Mech. Eng., Vol. 53, p. Apr 187.
24. MacGregor, C. W., Coffin, L. F., Jr. and Fisher, J. C. - 1948, "Partially-Plastic Thick-walled Tubes", - Journal Franklin Inst., Vol. 245, p. 155.
25. Macrae, A. E. - 1930, "Overstrain of Metals", - H. M. S. O.
26. Morrison, J. L. M. - 1948, "The Criterion of 'Yield' of Gun Steels", Proc. Inst. Mech. Eng., Vol. 159.
27. Morrison, J. L. M. - 1939, "The Yield of Mild Steel with Particular Reference to the Effect of Size of Specimen", - Proc. Inst. Mech. Eng., Vol. 142, p. 193.
28. Morrison, J. L. M. and Shepherd, W. M. - 1949, "An Experimental Investigation of Plastic Stress-Strain Relations", - Proc. I. Mech. E. (advance copy).
29. Nadai, A. L. - 1931, "Plasticity. A Mechanics of the Plastic State of Matter", - McGraw Hill Book Corp., New York.
30. Peterson, R. E. and Wahl, A. M. - 1935, "Fatigue of Shafts at Fitted Members with a Related Photoelastic Analysis", T.A.S.M.E., Vol. 57, A-1.
31. Rankin, A. W. - 1944, "Shrink Fit Stresses and Deformations", T.A.S.M.E., Vol. 66, A-77.
32. Roberts, M. H. and Northcliffe, J. - 1947, "Measurements of Young's Modulus at High Temperatures", - Journal of the Iron and Steel Institute, Nov., p. 345.

33. Russell, R. and Shannon, J. F. - 1930, "The Limit of Grip Due to Force Fits and Its Increase by Cold-working", - J.R.T.C., Vol. 2, Part 2.
34. Russell, R. - 1933, "Factors Affecting the Grip in Force, Shrink and Expansion Fits," - Proc. I. Mech. E., Vol. 125, p. 493.
35. Russell, R. - 1935, "Contact Film Resistance in Rail Wheel Force Fits", - J.R.T.C., Vol. 3, Part 3.
36. Russell, R. - 1937, "Influence of Film and Time on Force and Shrink Fits", - Inst. of Eng. and Shipbuilders in Scotland, Vol. 80.
37. Sawin, N. N. - 1928, "Research in Force Fits", - American Machinist, May 31, p. 889.
38. Schmaltz, G. - 1936, "Technische Oberflachenkunde", Julius Springer, Berlin.  
Reviewed by Abbot, E. J. and Goldschmidt, E. - 1937, "Surface Quality", - Mechanical Engineer, Vol. 59, p. 813.
39. Seely, F. B. - 1946, "Advanced Mechanics of Materials", - John Wiley and Sons, Inc., New York.
40. Shepherd, W. M. - 1948, "Plastic Stress-Strain Relations", Proc. Inst. Mech. Eng., Vol. 159.
41. Sopwith, D. G. - 1948, "The Stresses and Strains in a Partly-Plastic Thick Tube under Internal Pressure and End Load", - Presented at the IXth International Congress of Applied Mechanics in England.
42. "Tables of Lagrangian Interpolation Coefficients", - Mathematical Tables Project, National Bureau of Standards, U.S.A.
43. Tables of MacGregor's Numerical Solution for Open-end Cylinders. - Bureau of Ordnance, Project G2, United States Navy.
44. Taylor, G. I. and Quinney, H. - 1931, "The Plastic Distortion of Metals", - Phil. Trans. Roy. Soc., Series A, Vol. 230, p. 323.
45. Taylor, Sir G. I. - "Faults in a Material which Yields to Shear Stress while Retaining its Volume Elasticity", - Proc. Royal Soc. A., 1934, Vol. 145, p. 1.
46. Timoshenko, S. and Lessells, J. M. - 1925, "Applied Elasticity", - Westinghouse Technical Night School Press, Pa.
47. Wilmore, O. J., Jr. - 1899, "Shrink and Force Fits" - American Machinist, Feb. 16.